

TECHNISCHE UNIVERSITÄT MÜNCHEN

Lehrstuhl für Entwicklungsgenetik

Molecular mechanisms that govern the establishment of sensory-motor networks

Rosa-Eva Hüttl

Vollständiger Abdruck der von der Fakultät Wissenschaftszentrum Weihenstephan für Ernährung, Landnutzung und Umwelt der Technischen Universität München zur Erlangung des akademischen Grades eines

Doktors der Naturwissenschaften

genehmigten Dissertation.

Vorsitzender: Univ.-Prof. Dr. E. Grill
Prüfer der Dissertation: 1. Univ.-Prof. Dr. W. Wurst
2. Univ.-Prof. Dr. H. Luksch

Die Dissertation wurde am 08.12.2011 bei der Technischen Universität München eingereicht und durch die Fakultät Wissenschaftszentrum Weihenstephan für Ernährung, Landnutzung und Umwelt am 27.02.2012 angenommen.

Erklärung

Hiermit erkläre ich an Eides statt, dass ich die der Fakultät Wissenschaftszentrum Weihenstephan für Ernährung, Landnutzung und Umwelt der Technischen Universität München zur Promotionsprüfung vorgelegte Arbeit mit dem Titel „Molecular mechanisms that govern the establishment of sensory-motor networks“ am Lehrstuhl für Entwicklungsgenetik unter der Anleitung und Betreuung durch Univ.-Prof. Dr. Wolfgang Wurst ohne sonstige Hilfe erstellt und bei der Abfassung nur die gemäß § 6 Abs. 5 angegebenen Hilfsmittel benutzt habe.

Ich habe keine Organisation eingeschaltet, die gegen Entgelt Betreuerinnen und Betreuer für die Anfertigung von Dissertationen sucht, oder die mir obliegenden Pflichten hinsichtlich der Prüfungsleistung für mich ganz oder teilweise erledigt.

Ich habe die Dissertation in dieser oder ähnlicher Form keinem anderen Prüfungsverfahren als Prüfungsleistung vorgelegt.

Ich habe den angestrebten Dokortitel noch nicht erworben und bin nicht in einem früheren Promotionsverfahren für den angestrebten Doktorgrad endgültig gescheitert.

Die Promotionsordnung der Technischen Universität München ist mir bekannt.

München, den _____

Rosa-Eva Hüttl

ABSTRACT

During the development of the vertebrate nervous system, motor projections that activate muscles in the extremities and sensory afferents delivering feedback to the motor neurons about posture and other sensations need to be assembled to precisely integrated circuitries. Only then, the initiation, execution and completion of complex locomotor behaviors are feasible. Projections to peripheral targets are established in a stepwise process that is spatially and temporally tightly controlled, however, while some basic principles of axon guidance are well established, the molecular mechanisms and cues governing sensory-motor co-extension, inter-axonal communication and axon-glia interactions are not well understood.

The goal of my PhD project was to investigate the molecular mechanisms that govern the establishment of sensory-motor networks. I used cell-type specific ablation of the axon guidance receptor Neuropilin-1 (*Npn-1*) in spinal motor neurons or sensory neurons in the dorsal root ganglia (DRG) to explore the contribution of this signaling pathway to the correct innervation of the limb. We show that *Npn-1* controls fasciculation of both motor and sensory projections, as well as communication between sensory and motor trajectories at crucial choice points during axon extension. Removal of *Npn-1* from sensory neurons lifts the tight coupling of sensory axon growth on previously extended motor axons, thus resulting in sensory axons leading the spinal nerve projection. Interestingly, defasciculation of sensory axons is accompanied by defasciculation of motor axons before and after the plexus region. Deletion of *Npn-1* from motor neurons leads to severe defasciculation of motor axons in the distal limb and errors in the dorsal-ventral guidance decision, while pre-plexus fasciculation, as well as patterning and fasciculation of sensory projections in the distal limb remain unaffected. Thus, we found that motor and sensory axons are dependent on each other for the generation of their trajectories and partially interact through *Npn-1* to mediate axon coupling and fasciculation of spinal nerves before and within the plexus region of the limb.

Also at cranial levels, *Npn-1* is expressed in motor neurons and sensory ganglia. Loss of *Sema3A-Npn-1* signaling leads to defasciculation of the superficial projections to the head and neck. However, as these are mixed sensory-motor

projections, it was unclear whether Npn-1 is required in both neuronal populations for proper distal nerve assembly and fasciculation. Furthermore, the molecular mechanisms that govern the initial fasciculation and growth of the pure motor projections of the hypoglossal and abducens nerves in general, and the role of Npn-1 in these processes in particular were unclear. We show here that ablation of *Npn-1* specifically from cranial neural crest and placodally derived sensory tissues recapitulates the distal defasciculation of the trigeminal, facial, glossopharyngeal and vagal projections, that was observed in *Npn-1^{-/-}* mutants and in mice where binding of Npn-1 to all class 3 Semaphorins was abolished (*Npn-1^{Sema-}*). Selective removal of *Npn-1* from somatic motor neurons impairs the initial fasciculation and assembly of hypoglossal rootlets and leads to reduced numbers of abducens and hypoglossal fibers. Surprisingly, assembly and fasciculation of the hypoglossal nerve that consists exclusively of somatic motor axons are also impaired when *Npn-1* was ablated in sensory tissues. The defects in initial fasciculation are accompanied by a decrease of neural crest derived Schwann cells migrating along hypoglossal rootlets. These findings were corroborated by partial genetic elimination of cranial neural crest and embryonic placodes: we found aberrant growth patterns of the hypoglossal nerve after the loss of neural crest derived Schwann cell precursors. Interestingly, rostral turning of hypoglossal axons is not perturbed in any of the investigated genotypes. Our results therefore emphasise the crucial role of Sema3A-Npn-1 signaling for selective fasciculation of motor and sensory projections during cranial nerve extension. Furthermore, our data suggest that somatic motor nerve fasciculation at cranial levels depend on *Npn-1* expression and axon-Schwann cell interactions in developing vertebrates.

Several ligand-receptor interactions have been identified that critically contribute to the establishment of neuronal projections to the limb and mediate the stereotypic dorsal-ventral guidance decisions of growing motor axons at the base of the limb. However, these interactions cannot explain exhaustively how correct wiring of the motor system is achieved during development, as single or compound mutant embryos do not show a complete deregulation of motor axon guidance. For sensory neurons of the DRG, no guidance cues facilitating dorsal or ventral sensory axon guidance decisions have been identified so far. Classical ablation experiments in chicken suggested that sensory axons only depend on correctly laid out motor projections for proper guidance to peripheral targets. However, we showed that

sensory axons are capable to establish correct growth patterns even when distal motor projections are severely defasciculated or absent. These findings implicate specific guidance also of sensory axons. Our group employed a genome wide expression profiling using microarray technique to identify novel molecules involved in the guidance of motor and sensory axons to the dorsal or ventral limb. Using *in situ* hybridization and immunohistochemistry, we validated the expression patterns of four candidate genes that were predicted to be differentially expressed in brachial motor neurons at E12.5. The functions of the candidate genes *Arhgap29* and *Ccdc3* during development have not been characterized until now. However, these genes show a patterned expression already between E10.5 and E11.5, when motor axons navigate the dorsal-ventral choice point, and might therefore contribute to the topographic organization of motor projections. The ETS transcription factor *Elk3* is expressed differentially in ventrally projecting motor neurons only at E12.5. At E11.5, the transcription factor is expressed uniformly in both dorsally and ventrally projecting motor neurons, and shows no expression at E10.5. Therefore, differential expression of *Elk3* was only found at a time when the dorsal-ventral decision point has already been navigated. Still, as a close relative to genes of the ETS gene family, it might nevertheless have a function in the definition of motor neuron pools innervating the same target musculature. *Fgfr2*-signaling is essential for early rostro-caudal motor neuron patterning and limb bud induction, however, its role in motor nerves innervating the extremities has not been assessed up to now. I confirmed the predicted differential expression with higher expression levels in ventrally projecting LMC neurons and employed a conditional approach to selectively remove *Fgfr2* from spinal motor neurons. We found that *Fgfr2* expression in spinal motor neurons is dispensable for fasciculation, distal advancement and general growth patterns of motor axons to the distal limb.

As mentioned above, up to now, no markers exist to distinguish sensory neurons according to their topographic projections in the periphery. We confirmed the predicted differential expression for five genes and found them to be predominantly, but not exclusively expressed in dorsally projecting sensory neurons that were retrogradely labeled from dorsal limb mesenchyme: *Cux2*, *Gnb4*, *Ift172*, *Nek1* and *PLCd4*. Further investigations of their expression patterns at earlier developmental time points, as well as their potential assignment to nociceptive or proprioceptive classes of sensory neurons will help to define the function of these genes in sensory

axon growth and guidance. This might result in the identification of the first molecular markers for a subset of dorsally projecting sensory neurons. Further investigations will contribute to our knowledge of the molecular mechanisms that govern the establishment of sensory-motor circuits. This work, therefore, has the potential to offer a starting point for the development of new treatments to re-build neuronal circuits after neurological diseases or trauma, which impair function of the spinal sensory-motor system.

ZUSAMMENFASSUNG

Um komplexe Bewegungsabläufe zu ermöglichen, müssen motorische Nervenfasern, welche die Muskeln in den Extremitäten aktivieren, und sensorische Afferenzen, die Rückmeldung über Muskelstellung und andere Sinneswahrnehmungen liefern, bereits während der Entwicklung des peripheren Nervensystems von Wirbeltieren zu präzise verschalteten Netzwerken verknüpft werden. Während jedoch die grundlegendsten Prinzipien, die zur schrittweisen Etablierung dieser Nervenprojektionen in enger zeitlicher und räumlicher Nachbarschaft führen, gut untersucht sind, weiß man nur wenig über die molekularen Mechanismen und Wegfindungsfaktoren, die für das gleichzeitige Auswachsen sensorischer und motorischer Fasern, und die Interaktion von Axonen untereinander und mit Gliazellen eine Rolle spielen.

Das Ziel dieser Doktorarbeit war es, molekulare Mechanismen zu untersuchen, die zum Aufbau sensorisch-motorischer Netzwerke beitragen. Zellspezifische Entfernung des Wegfindungsrezeptors Neuropilin-1 (*Npn-1*) von spinalen Motorneuronen oder sensorischen Neuronen in den Spinalganglien diente dazu, den Beitrag dieses Rezeptors zur korrekten Innervierung der Gliedmaßen zu untersuchen. Dabei zeigte sich, dass *Npn-1* die Faszikulierung sowohl von motorischen als auch von sensorischen Nervenfasern kontrolliert und zusätzlich die Kommunikation an kritischen Entscheidungspunkten zwischen den beiden Fasersystemen vermittelt. Ablation von *Npn-1* von sensorischen Nervenzellen hebt die Wachstumskopplung sensorischer Axone an früher ausgewachsene, motorische Axone auf, sodass sensorische Fasern den auswachsenden Spinalnerv anführen. Interessanterweise geht die Defaszikulierung sensorischer Axone hierbei mit defaszikulierten motorischen Projektionen vor und nach der Plexusregion einher. Entfernung von *Npn-1* von motorischen Nervenzellen führt zu schwerwiegender Defaszikulierung motorischer Axone im distalen Beinchen und Fehlern in der dorsal-ventralen Wachstumsentscheidung. Die Faszikulierung der Spinalnerven vor der Plexusregion, sowie das Wachstumsmuster und die distale Faszikulierung von sensorischen Nervenfasern werden in diesem Fall jedoch nicht beeinflusst. Wir zeigen, dass motorische und sensorische Axone in Abhängigkeit voneinander

Nervenbahnen in die Extremitäten bilden. Dabei interagieren die unterschiedlichen Fasertypen zum Teil über Npn-1, um die Faszikulierung und die Wachstumskopplung der Axone aneinander innerhalb der Spinalnerven vor und innerhalb der Plexusregion aufrecht zu erhalten.

Auch im Hirnstamm wird *Npn-1* von Motorneuronen und Nervenzellen in sensorischen Ganglien exprimiert. Der Verlust des Sema3A-Npn-1 Signalwegs führt zur Defaszikulierung der oberflächennahen Nervenprojektionen zu Kopf und Hals. Die molekularen Mechanismen, welche die Faszikulierung und das Wachstum der rein motorischen Fasern der Hypoglossal- und Abduzensnerven nach dem Verlassen des Hirnstammes steuern, sowie die Rolle, die Npn-1 bei diesen Ereignissen spielt, sind bisher jedoch unbekannt. Wir zeigen hier, dass die Entfernung von Npn-1 von sensorischen Zellen, die von Vorgängern aus der Neuralleiste oder embryonalen ektodermalen Verdickungen (Placoden) abstammen, die distale Defaszikulierung der gemischt sensorisch-motorischen Trigemini-, Fazialis-, Glossopharyngeus- und Vagusnerven rekapituliert, welche bereits in *Npn-1^{-/-}* Mutanten und in Mäusen, deren Npn-1 keine Klasse 3 Semaphorine mehr binden kann (*Npn-1^{Sema}-*) beobachtet wurde. Selektive Ablation von *Npn-1* von somatischen Motorneuronen beeinträchtigt die initiale Faszikulierung der Axone, die zusammen den Hypoglossalnerv bilden, und führt zu einer Reduzierung der Anzahl der Nervenfasern von Hypoglossal- und Abduzensnerven. Überraschenderweise sind die Faszikulierung und der initiale Aufbau des rein motorischen Hypoglossalnervs ebenfalls beeinträchtigt, wenn *Npn-1* in sensorischem Gewebe eliminiert wurde. Diese Defizite gehen einher mit einer verringerten Anzahl an Schwannzellen, die entlang der defaszikulierten Fasern wandern. Diese Ergebnisse werden von Beobachtungen in Embryonen, deren Neuralleiste und Placoden genetisch eliminiert wurden, unterstützt: Nach dem Verlust von Schwannzellen wurden ebenfalls aberrante Wachstumsmuster von Fasern, die den Hypoglossalnerv bilden, entdeckt. Interessanterweise wird die spätere Änderung der Wachstumsrichtung des Hypoglossalnervs in Richtung Zunge in keinem der untersuchten Genotypen in Mitleidenschaft gezogen. Unsere Daten unterstreichen daher die entscheidende Rolle des Sema3A-Npn-1 Signalweges in der selektiven Faszikulierung motorischer und sensorischer Projektionen der Hirnnerven. Desweiteren weisen unsere Ergebnisse darauf hin, dass die frühe Bildung und Faszikulierung des Hypoglossalnervs, jedoch nicht spätere

Wachstumsentscheidungen, von der *Npn-1*-Expression und Axon-Schwanzzell-Interaktionen abhängen.

Bisher wurden mehrere Ligand-Rezeptorinteraktionen identifiziert, die wesentlich zur Bildung neuronaler Projektionen in die Extremitäten beitragen, und die stereotypen dorsal-ventralen Wachstumsentscheidungen motorischer Axone in der Plexusregion an der Basis der Beine kontrollieren. Bislang bekannte Interaktionspartner können jedoch nicht allumfassend erklären, wie die korrekte Vernetzung des motorischen Nervensystems während der Entwicklung erreicht wird: Embryonen mit Mutationen in einzelnen oder mehreren dieser Wegfindungssysteme zeigen keine absolute Deregulierung der Wachstumsentscheidungen motorischer Axone. Für sensorische Nervenzellen in den Spinalganglien wurden bislang noch keine Wegleitungsmoleküle entdeckt, die spezifisch die dorsal-ventrale Wachstumsentscheidung definieren. Klassische Ablationsexperimente in Hühnerembryonen deuteten bisher darauf hin, dass sensorische Axone auf korrekt etablierte motorische Projektionen angewiesen sind, um ihre Ziele in der Peripherie zu finden. Wir konnten jedoch zeigen, dass sensorische Axone selbst dann korrekte Wachstumsmuster ausbilden, wenn motorische Fasern schwerwiegend defaszikuliert sind, oder sogar fehlen. . Diese Ergebnisse deuten daher auch auf spezifische Wegfindungsmechanismen für sensorische Nervenfasern hin. Daher etablierte unsere Arbeitsgruppe einen genomweiten Screen, um mittels Microarray Analyse Expressionsprofile neuer Moleküle zu erstellen, welche für die dorsal-ventrale Wachstumsentscheidung von sensorischen und motorischen Axonen eine Rolle spielen könnten. Durch *in situ* Hybridisierung und immunhistochemische Methoden war es mir möglich, das vorhergesagte Expressionsmuster von vier Kandidatengenen in brachialen Motorneuronen zum Embryonalzeitpunkt E12.5 zu bestätigen. Die Funktionen der beiden Kandidatengene *Arhgap29* und *Ccdc3* während der Entwicklung sind bisher weitgehend unbekannt, jedoch weist ihr Expressionsmuster bei E10.5 und E11.5, also genau zu der Zeit, in der die dorsal-ventrale Entscheidung gefällt wird, auf eine mögliche Rolle während dieser Entscheidung hin. Der ETS-Transkriptionsfaktor *Elk3* zeigt erst bei E12.5 eine differenzielle Expression in ventral projizierenden Motorneuronen. Zuvor ist der Transkriptionsfaktor bei E11.5 gleichmäßig in dorsal oder ventral projizierenden Motorneuronen exprimiert, und zeigt keine Expression im ventralen Horn bei E10.5. Dies bedeutet, dass *Elk3* erst differenziell exprimiert wird, wenn die dorsal-ventrale

Wachstumsentscheidung bereits getroffen wurde. Aufgrund seiner Verwandtschaft zur ETS Genfamilie hat der Transkriptionsfaktor möglicherweise dennoch eine Bedeutung in der Definition von Motorneuronen, welche dieselben Ziele innervieren. Bei der rostro-caudalen Verteilung von Motorneuronen im Rückenmark, und bei der Einleitung des Wachstums von Extremitäten ist *Fgfr2* von entscheidender Wichtigkeit, über die Rolle des Rezeptors bei der Innervierung der Vorderbeine ist jedoch nichts bekannt. Wir konnten die differenzielle Expression von *Fgfr2* in ventral projizierenden Motorneuronen nachweisen, und eliminierten den Rezeptor konditional in motorischen Nervenzellen zur genaueren Untersuchung der motorischen Projektionen. Anhand dieser Untersuchungen zeigen wir, dass die Expression von *Fgfr2* in spinalen Motorneuronen für Faszikulierung, distales Wachstum und die generelle Bildung von Wachstumsmustern von motorischen Axonen ins Vorderbein keine offensichtliche Bedeutung hat.

Wie bereits erwähnt, existieren bislang keinerlei molekulare Marker, anhand deren Expression man dorsal von ventral projizierenden sensorischen Nervenzellen unterscheiden kann. Uns gelang es, die vorhergesagte Expression fünf brachialer sensorischen Kandidatengene, nämlich *Cux2*, *Gnb4*, *ift172*, *Nek1* und *PLCd4*, hauptsächlich, jedoch nicht ausschließlich, in dorsal projizierenden Nervenzellen mittels retrograder Markierung der sensorischen Neurone zu bestätigen. Tiefgehende Untersuchungen des Expressionsmusters dieser Gene zu früheren Zeitpunkten, und in propriozeptiven und nozizeptiven Subpopulationen sensorischer Neuronen werden dazu beitragen, die Rolle dieser Gene für die differentiellen Wachstumsentscheidungen sensorischer Axone zu definieren. Dies führt möglicherweise zur Entdeckung des ersten Markergens für dorsal projizierende sensorische Nervenfasern. Weitere Forschungen werden zum grundlegenden Verständnis molekularer Mechanismen, die am Aufbau sensorisch-motorischer Netzwerke beteiligt sind, beitragen. Diese Arbeit hat daher das Potential, einen Ansatzpunkt für die Entwicklung neuer Behandlungsmethoden zur Wiederherstellung neuronaler Netzwerke nach Krankheiten oder Traumata zu bieten.

TABLE OF CONTENTS

Abstract	1
Zusammenfassung	5
Table of contents	9
Table of figures	13
Table of tables	15
I. Introduction	16
1. Formation of motor and sensory neurons in the vertebrate hindbrain and spinal cord.....	16
2. Pathway selection, fasciculation and axon guidance	19
2.1 Subtype specification and topographic markers	19
2.2 The establishment of peripheral projections – a stepwise process.....	22
2.2.1 Definition of motor axon exit points and pioneering of pathways.....	22
2.2.2 Selective fasciculation and contact mediated guidance.....	23
2.2.3 Signaling pathways that regulate cranial nerve extension and dorsal-ventral guidance decisions in the developing limb.....	24
2.2.3.1 Netrin - DCC.....	24
2.2.3.2 Slit - Roundabout (Robo).....	25
2.2.3.3 Hepatocyte growth factor - Met proto-oncogene tyrosine kinase	25
2.2.3.4 Glial cell line-derived neurotrophic factor – Ret.....	26
2.2.3.5 Class 3 Semaphorins - Neuropilins	26
2.2.3.6 ephrins and Eph receptors	28
2.2.4 Target selection and neurotrophic support	29
3. Identification of novel cues mediating the dorsal-ventral guidance decision	30
4. Aim of this study	32
4.1 <i>Npn-1</i> contributes to axon-axon interactions that differentially control sensory and motor innervation of the limb.....	32
4.2 Cranial nerve fasciculation and Schwann cell migration are impaired after loss of <i>Npn-1</i>	34
4.3 Identification of novel guidance cues	35
4.3.1 Candidate genes – selection criteria.....	35
4.3.2 Candidate genes – brachial motor neurons	36
4.3.3 Candidate genes – brachial sensory neurons.....	40
II. Materials and Methods	43
1. Ethics statement.....	43
2. Mouse embryo preparation	43

3. Immunohistochemistry.....	44
4. Retrograde labeling of neurons.....	45
5. RNA isolation and cDNA synthesis.....	46
6. Probe synthesis.....	46
7. In situ hybridization.....	47
8. LacZ staining.....	48
9. Quantification of motor and sensory defasciculation in the E12.5 limb.....	48
10. Quantification of distal advancement of motor projections to the limbs.....	49
11. Quantification of misprojecting LMC neurons.....	49
12. Quantification of pre-plexus defasciculation at E10.5 and E12.5.....	49
13. Quantification of <i>Npn-1</i> expression in the trigeminal ganglion of <i>Npn-1^{cond-/-};Ht-PA-Cre⁺</i> mutant embryos.....	50
14. Quantification of abducens nerve thickness and proportions.....	50
15. Quantification of hypoglossal rootlet length and number.....	50
16. Quantification of hypoglossal nerve proportions.....	51
17. Quantification of somatic motor neurons in hypoglossal and abducens nuclei.....	51
18. Quantification of Schwann cells.....	51
19. Quantification of candidate gene expression and guidance errors.....	52
III. Results.....	53
1. Conditional ablation of <i>Npn-1</i> : Axon-axon interactions control sensory-motor innervation of the limb.....	53
1.1 Fasciculation of spinal motor axons is controlled by <i>Npn-1</i> expressed in motor neurons.....	53
1.2 <i>Npn-1</i> in spinal motor neurons is required for accurate dorsal-ventral guidance of LMC axons..	62
1.3 Ablation of <i>Npn-1</i> from spinal motor neurons does not affect fasciculation of sensory projections into the periphery.....	63
1.4 Ablation of <i>Npn-1</i> from sensory neurons causes defasciculation of sensory projections to the body and extremities.....	66
1.5 Ablation of <i>Npn-1</i> in sensory neurons leads to defasciculation of motor projections.....	69
1.6 Fasciculation of motor axons before the plexus region determines fasciculation in the distal limb.....	72
2. Conditional ablation of <i>Npn-1</i> : roles in cranial nerve fasciculation and Schwann cell migration.....	79
2.1 <i>Npn-1</i> in cranial neural crest and placodally derived sensory neurons controls peripheral cranial nerve fasciculation.....	79
2.2 <i>Npn-1</i> is required in somatic motor neurons for correct fasciculation and outgrowth of the abducens nerve.....	81
2.3 Loss of <i>Npn-1</i> signaling in somatic motor neurons impairs initial fasciculation of hypoglossal nerve rootlets.....	85

2.4 Loss of <i>Npn-1</i> in somatic motor neurons leads to a reduction and defective assembly of the hypoglossal nerve.....	86
2.5 Elimination of <i>Npn-1</i> from cranial sensory neurons and partial loss cranial neural crest and placodally derived tissues impairs hypoglossal nerve assembly.....	88
2.6 Sox10-positive Schwann cells facilitate initial hypoglossal nerve fasciculation.....	89
3. Identification of novel guidance factors that govern the dorsal-ventral guidance decision of motor and sensory axons.....	92
3.1 Validation of candidate genes for brachial motor axon guidance.....	93
3.1.1 Rho GTPase activating protein 29 - <i>Arhgap29</i>	95
3.1.2 Coiled coil domain containing 3 – <i>Ccdc3</i>	97
3.1.3 ETS domain-containing protein Elk-3.....	98
3.1.4 Fibroblast growth factor receptor 2 – <i>Fgfr2</i>	100
3.1.4.1 Conditional ablation of <i>Fgfr2</i> in motor neurons does not alter fasciculation and growth patterns of motor nerves in the embryonic forelimb.....	101
3.1.4.2 Dorsal-ventral guidance of motor axons is normal in embryos that lack <i>Fgfr2</i> in motor neurons.....	102
3.2 Validation of candidate genes for sensory axon guidance.....	104
3.2.1. Cut like homeodomain transcription factor 2 - <i>Cux2</i>	105
3.2.2. Guanine nucleotide binding protein beta 4 – <i>Gnb4</i>	107
3.2.3 Intraflagellar transport homolog 172 – <i>Ift172</i>	107
3.2.4 Never in mitosis gene a (NIMA) related kinase 1 – <i>Nek1</i>	108
3.2.5 Phospholipase C delta 4 – <i>PLCd4</i>	109
3.2.6 Outlook.....	109
IV. Discussion.....	111
1. <i>Npn-1</i> governs axon-axon interactions during innervation of the vertebrate limb.....	111
1.1 Fasciculation of motor axons and their role in the establishment of peripheral sensory trajectories.....	112
1.2 <i>Npn-1</i> governs dorsal-ventral guidance decisions of motor axons.....	114
1.3 Maintenance of motor phenotypes after ablation of <i>Npn-1</i> in motor neurons.....	114
1.4 <i>Npn-1</i> on sensory axons mediates fasciculation of sensory and motor axons.....	115
1.5 Ablation of <i>Npn-1</i> from sensory neurons does not influence the dorsal-ventral guidance decision of motor axons.....	119
1.6 Conclusions.....	120
2. <i>Npn-1</i> mediates cranial nerve fasciculation and Schwann cell migration.....	122
2.1 <i>Npn-1</i> on neural crest and placodally derived sensory tissues governs distal fasciculation of cranial nerve projections.....	122

2.2 Npn-1 on somatic motor axons governs initial fasciculation of abducens and hypoglossal projections.....	123
2.3 Neural crest derived Schwann cell progenitors facilitate initial hypoglossal nerve fasciculation	125
2.4 Conclusions.....	128
3. Identification of novel guidance cues predicted by a differential microarray screen.....	129
3.1 <i>Arhgap29</i> is expressed in ventrally projecting motor neurons of the brachial LMC	132
3.2 The ETS transcription factor <i>Elk3</i> is expressed in the medial aspect of the brachial LMC.....	134
3.3 <i>Ccdc3</i> is expressed in ventrally projecting brachial motor neurons	136
3.4 Specific expression of <i>Fgfr2</i> in ventrally projecting brachial motor neurons plays no role for motor axon growth and guidance.....	137
3.5 <i>Cux2</i> is expressed in dorsally projecting brachial sensory neurons	140
3.6 A subset of dorsally projecting brachial sensory neurons expresses <i>Gnb4</i>	141
3.7 <i>Ift172</i> is differentially expressed in sensory neurons at brachial levels.....	142
3.8 <i>Nek1</i> is expressed predominantly in dorsally projecting sensory neurons of the brachial DRG	144
3.9 <i>PLCd4</i> is predominantly expressed in dorsally projecting sensory neurons	145
3.10 Conclusions.....	146
Abbreviations.....	150
Bibliography.....	153
Acknowledgements	167

TABLE OF FIGURES

Figure 1: Developmental origin of motor and sensory neurons of the central nervous system.....	17
Figure 2: Mechanisms of axon guidance at cranial and limb levels	21
Figure 3: Semaphorins and their receptors.....	27
Figure 4: Schematic illustration of the global differentiation screen for novel guidance cues	31
Figure 5: Schematic illustrating tissue specific ablation of <i>Npn-1</i>	34
Figure 6: Functional categories of candidate genes in the differentially projecting neuronal populations.....	37
Figure 7: Quantification of Cre recombinase efficiency.....	54
Figure 8: <i>Npn-1</i> is required in motor neurons for proper fasciculation of LMC projections to the forelimb.....	55
Figure 9: <i>Npn-1</i> is required in motor neurons for proper fasciculation of LMC projections to the hindlimb	57
Figure 10: Fasciculation and distal advancement of motor projections are impaired after ablation of <i>Npn-1</i> from motor or sensory neurons.....	59
Figure 11: Defasciculation of MMC projections after cell type specific removal of <i>Npn-1</i>	61
Figure 12: LMC projections are misrouted when <i>Npn-1</i> is removed from motor neurons.....	62
Figure 13: Quantification of sensory defasciculation after ablation of <i>Npn-1</i> in either motor or sensory neurons..	64
Figure 14: Late ablation of <i>Npn-1</i> in sensory neurons does not affect fasciculation of sensory innervation of the limbs	66
Figure 15: Removal of <i>Npn-1</i> from sensory neurons leads to defasciculation of sensory and motor projections to the limbs	68
Figure 16: Defasciculation of motor fibers is accompanied by defasciculation of TrkA- and TrkC-positive fibers in <i>Npn-1^{cond-/-};Ht-PA-Cre⁺</i> , but not in <i>Npn-1^{cond-/-};Olig2-Cre⁺</i> mutant embryos	71
Figure 17: Fasciculation before the plexus determines the fasciculation in the distal limb	72
Figure 18: Ablation of <i>Npn-1</i> in sensory neurons impairs pre-plexus fasciculation sensory-motor axon coupling. 74	74
Figure 19: Sensory axons break sensory-motor axon coupling after removal of <i>Npn-1</i> from sensory neurons.....	75
Figure 20: Assessment of DRG segmentation, Schwann cell progenitors, boundary cap cell formation and blood vessel formation in <i>Npn-1^{cond-/-};Ht-PA-Cre⁺</i> mutant embryos.....	77
Figure 21: <i>Npn-1</i> in sensory neurons is required for distal fasciculation of cranial projections.....	80
Figure 22: Absence of <i>Olig2</i> leads to loss of somatic motor projections.....	82
Figure 23: Loss of <i>Npn-1</i> in somatic motor neurons reduces abducens projections.....	84
Figure 24: Initial fasciculation, but not final targeting is impaired by loss of <i>Npn-1</i> in somatic motor and/or cranial neural crest and placodally derived sensory neurons.....	87
Figure 25: Defasciculation of the hypoglossal nerve in <i>Npn-1^{cond-/-};Ht-PA-Cre⁺</i> , <i>Ht-PA-Cre⁺;DT-A^{flxed}</i> and <i>Npn-1^{Sema-}</i> mutant embryos is accompanied by loss of Sox10 positive Schwann cells	90
Figure 26: Expression analysis of <i>Arhgap29</i>	96

Figure 27: Expression analysis of <i>Ccdc3</i>	98
Figure 28: Expression analysis of <i>Elk3</i>	99
Figure 29: Expression analysis of <i>Fgfr2</i>	101
Figure 30: Conditional ablation of <i>Fgfr2</i> does not affect motor axon growth, fasciculation and guidance.....	103
Figure 31: Validation of candidate genes for dorsal-ventral guidance of brachial sensory neurons	106
Figure 32: Npn-1 mediated axon-axon and axon-environment interactions.....	121

TABLE OF TABLES

Table 1: Primary antibodies and concentrations used for wholemount antibody staining and fluorescent immunohistochemistry	45
Table 2: Probe generation and synthesis	47
Table 3: Candidate genes in brachial motor neurons	94
Table 4: Candidate genes in brachial sensory neurons	105

I. INTRODUCTION

To enable the initiation, execution and completion of complex locomotor behaviors, motor projections that activate muscles in the extremities and sensory afferents delivering feedback to the motor neurons about posture and other sensations need to be assembled to precisely integrated circuitries during the development of the vertebrate nervous system. The establishment of these heterotypic projections to their distal targets in the extremities is achieved in a stepwise process in close spatial and temporal vicinities. In the past decades, a variety of ligand-receptor interactions have been discovered that govern precise guidance of axons to their targets in the periphery. The molecular mechanisms underlying the communication between heterotypic axon bundles during their outgrowth, or axon-glia interactions in the process of peripheral nervous system development and sensory-motor network formation, however, are not well understood.

1. FORMATION OF MOTOR AND SENSORY NEURONS IN THE VERTEBRATE HINDBRAIN AND SPINAL CORD

The origin of the vertebrate central nervous system can be traced back to processes during gastrulation, when the dorsal ectoderm changes fate from epidermal to neural, initiated by signals from the underlying notochord, which induces the formation of the floorplate (reviewed in Ruiz i Altaba, 1993; Cleaver and Krieg, 2001). Form-shaping events modify the morphology of the neural plate: the plate borders, or neural folds, are brought together, forming the neural plate to a tube that will differentiate into the three vesicles forming the fore-, mid-, and hindbrain, as well as the spinal cord. Fusion of the neural folds leads to a detachment of the epidermis and formation of the roofplate of the spinal cord. At hindbrain level (*sinus rhomboidalis*), the neural plate does not form a tube, but a rather broad, mediolaterally elongated structure (Fig. 1A; Smith and Schoenwolf, 1997). Graded expression of bone morphogenic protein (*BMP*), as well as signaling by members of the wingless-type MMTV integration site family (*Wnt*), or Fibroblast Growth Factors (*FGF*) in the dorsal part of the embryo induce the formation of pluripotent neural crest

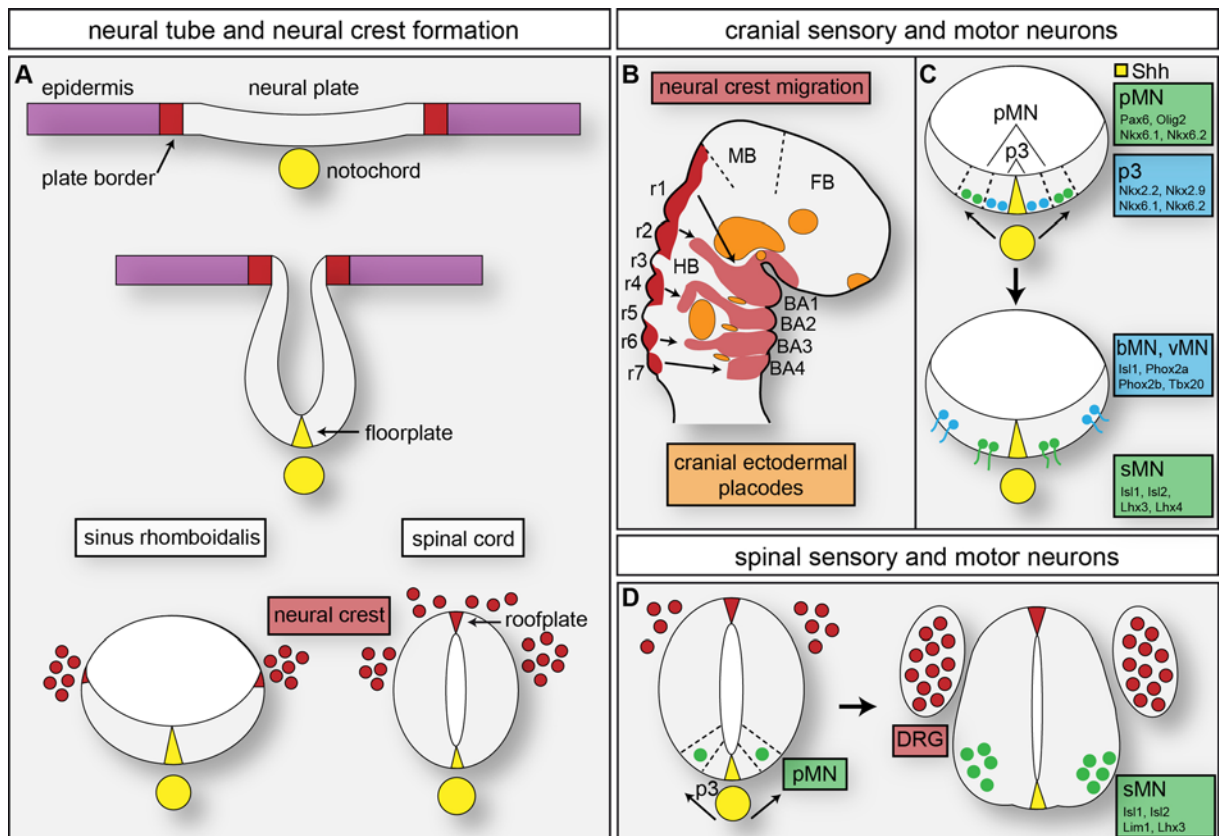


Figure 1: Developmental origin of motor and sensory neurons of the central nervous system.

(A) Schematic overview of the process of neurulation, leading to the formation of the brain (not shown), *sinus rhomboidalis*, and spinal cord. Form-shaping events due to signaling from the notochord lead to formation of the floorplate and bring the plate borders of the neural plate together to build the neural tube and the roofplate. Neural crest cells delaminate from the former neural plate borders. **(B)** Neural crest migration within the hindbrain to position where bones, muscles, or, in cooperation with cranial ectodermal placodes, sensory ganglia are established. **(C)** Graded Shh signaling from notochord and floorplate leads to motor neuron development in the sinus rhomboidalis: somatic motor neurons from the pMN domain arise in response to Pax6, Nkx6.1, Nkx6.2 and Olig2 signaling, and their axons exit the neural tube ventrally. Branchiomotor and visceromotor neurons derive from the p3 domain under the control of Nkx2.2 and Nkx2.9 instead of Pax6 and Olig2. Their axons exit the brainstem at more dorsal positions. **(D)** At spinal levels, all motor neurons develop under the control of Pax6, Olig2, Nkx6.1 and Nkx6.2 from progenitors in the pMN domain and migrate to ventro-lateral positions in the neural tube, while interneurons arise in the p3 domain. Sensory neurons derive from segmentally migrating neural crest cells in the somites that condense to dorsal root ganglia (DRG). The figure was adapted from Smith and Schoenwolf, 1997; Guthrie, 2007; Donoghue et al., 2008. Abbreviations: r=rhombomere, BA=branchial arch, FB=forebrain, HB=hindbrain, MB=midbrain, bMN=branchiomotor neurons, vMN=visceromotor neurons, sMN=somatic motor neurons.

cells that delaminate from the former plate borders (Fig. 1A) and migrate throughout the embryo (Bronner-Fraser, 1994; Meulemans and Bronner-Fraser, 2004). During early embryogenesis, anterior-posterior patterning mechanisms initiated by the differential expression of homeobox genes lead to a segmentation of the vertebrate hindbrain and embryonic body into rhombomeres (r) and somites, respectively (Alexander et al., 2009). While somites will give rise to vertebrae and ribs, muscles and skin of the trunk, positional information and cell-cell interactions within distinct

rhombomeres at hindbrain levels contribute to a compartmentalization of cranial neural crest cells migrating to the branchial arches. One of the most fascinating characteristics of neural crest cells is their ability to generate multiple cell lineages. Within the branchial arches they will, for example, develop into bones of the skull, muscles of the face and neck, Schwann cell precursors, or culminate in the differentiation and migration of neuronal cells that form, together with neuronal cells from the cranial ectodermal placodes, sensory ganglia at characteristic locations within the brainstem (Fig. 1B; Cordes, 2001; Huang and Saint-Jeannet, 2004; McCabe and Bronner-Fraser, 2009). At spinal cord level, progeny of neural crest cells that migrate unsegmentedly along a dorsal pathway underneath the ectoderm become pigment cells, while those taking a more ventral pathway, migrating in a segmental fashion through the rostral part of the somites of the vertebrate embryo, give rise to sensory neurons of dorsal root ganglia (DRG, Figs. 1D, 2C) and sympathetic ganglia (Rickmann et al., 1985; Kuan et al., 2004; Le Douarin, 2004).

Motor neuron identity within the hindbrain and spinal cord is assigned through the stepwise activity of transcription factors whose expression is fine-tuned to the graded expression of inductive factors such as Sonic Hedgehog (Shh) or retinoic acid that are expressed in the floorplate and notochord, or the paraxial mesoderm and a subset of spinal motor neurons, respectively (Jessell, 2000; Wilson and Maden, 2005). These signals lead to the expression of homeodomain transcription factors and trigger the formation of genetically distinct progenitor domains within the neural tube. At spinal cord level, all motor neurons arise from the pMN domain that is marked by the expression of *Pax6*, *Nkx6.1*, *Nkx6.2* and *Olig2*, providing motor innervation to axial musculature or muscles in the extremities (Fig. 1D; Jessell, 2000; Lee and Pfaff, 2001). Within the hindbrain, motor neurons arise from two adjacent, yet genetically distinct, progenitor domains: somatic motor neurons that will innervate target muscles of the tongue or the eye derive from the pMN domain in response to the same set of transcription factors as at spinal cord level, and their axons leave the neural tube at ventral positions. A second set of motor neurons is exclusively generated in the p3 domain adjacent to the floorplate. Within the spinal cord, this domain, which is characterized by the expression of *Nkx2.2* and *Nkx2.9*, gives rise to V3 interneurons, while at hindbrain level, branchio- and visceromotor neurons are generated. These motor neurons migrate to more dorsal positions within the neural tube (Fig. 1C; Pabst et al., 2003). Most dorsally exiting motor neurons are found in

the hindbrain, and their axons innervate neural crest-derived targets in the head, throat and heart (Cordes, 2001; Guthrie, 2007). This distinction of motor neurons leaving the brainstem either dorsally or ventrally might be a remnant from the way motor neurons evolved: dorsally exiting motor neurons are found in primitive chordates like *Amphioxus*, while ventrally exiting motor neurons coincide with the appearance of additional types of muscles for locomotion in vertebrates (Fritzschn and Northcutt, 1993).

2. PATHWAY SELECTION, FASCICULATION AND AXON GUIDANCE

2.1 SUBTYPE SPECIFICATION AND TOPOGRAPHIC MARKERS

In the vertebrate nervous system, where a huge variety of neuronal subtypes is required to form a working neuronal network, establishing the appropriate connections with peripheral targets presents a very challenging endeavor. Motor and sensory neuron localization and identity are defined already at early embryonic stages by detailed dorso-ventral, medial-lateral, and rostro-caudal patterning mechanisms of the neural tube. Subsequent combinatorial activation of segment-specific transcription factors further defines neuron identity. The specification of neuronal subtypes in the spinal cord becomes evident with the appearance of distinct cell types at defined positions along the neural tube. Motor neuron subclasses that innervate different anatomical targets are also diverse on a molecular basis and can be defined by the restricted expression pattern of transcription factors. Intersegmental codes of different homeobox transcription factor genes (*Hox*) along the rostro-caudal axis specify columnar identities of spinal motor neurons or cranial motor nuclei. *Hoxa2*, for example, is expressed exclusively in rhombomere 2 (r2), facilitating the generation of trigeminal (V) motor neurons (Keynes and Krumlauf, 1994; Prince and Lumsden, 1994; Jungbluth et al., 1999), while confined expression of *Hoxb1* together with *Hoxa1* in r4 drives differentiation of facial (VII) branchiomotor neurons (Hunt et al., 1991). Branchio- and visceromotor neurons of the brainstem express *Islet1* (*Isl1*), but activate expression of paired-like homeobox 2 (*Phox2*) transcription factors instead of homeodomain proteins like *Lhx3* and *Lhx4* during the initial phase of axon extension (Fig. 1C, D, Fig. 2C; Sharma et al., 1998; Guthrie,

2007). Paralogues of the *Hox3* gene have been shown to promote generation of somatic motor neurons in the vertebrate brainstem (Manzanares et al., 1997; Manzanares et al., 1999) by induction of transcription factors that promote generation of somatic motor neurons (Gaufo et al., 2003). Induction of somatic motor neurons from progenitor cells in the pMN domain critically depends on activation of *Olig2* in response to graded Shh hedgehog signaling. In mice, where the function of the homeobox gene *Pax6* is ablated, the *Nkx2.2* positive p3 domain is enlarged, and in the brainstem branchio- and visceromotor neurons are produced instead of somatic motor neurons (Ericson et al., 1997b). *Olig2* function is dispensable for the establishment of the border between these two progenitor domains, but of critical importance for the induction of somatic motor neuron specification by genes like *Hb9* (Arber et al., 1999; Lu et al., 2002). Thus, coordinate activity of different sets of transcription factors collaborate to differentiate and organize cranial motor neurons in target-specific nuclei (Fig. 2B).

Neural cells of the spinal cord initially resemble forebrain neuronal cells on a molecular basis, however, secreted signals derived from the primitive streak at the gastrula stage further characterize neuronal tissues of the mid- and hindbrain, as well as the spinal cord (Muhr et al., 1999; Harland, 2000). As mentioned above, many secreted factors have been implicated in the rostro-caudal patterning of the nervous system. The differentiation of cells of spinal cord character, however, requires the action of retinoic acid-mediated signals provided by the prospective caudal paraxial mesoderm (Niederreither et al., 1997; Muhr et al., 1999). At brachial levels, expression of members of the Hox5, Hox6 and Hox8 proteins in response to graded FGF signaling represent aldehyde dehydrogenase 1 family, member A2 (*Raldh2*) positive motor neurons of the lateral motor columns (LMC), which will innervate the vertebrate limb. *Hox9* expression coincides with thoracic motor neurons of the medial motor column (MMC, Fig. 2C; Dasen et al., 2003; Bottcher and Niehrs, 2005; Dasen et al., 2005). LIM homeodomain protein function is required to establish both the generic and columnar identities of motor neurons: *Isl1* function, for example is required for the generation of all motor neurons (Pfaff et al., 1996), while *Lhx3* and *Lhx4* have more selective roles in the specification of motor neuron columnar identity (Sharma et al., 1998). At spinal cord levels, for example, only MMC neurons innervating axial musculature retain expression of *Lhx3* and *Lhx4* (Kania et al., 2000). Next to molecular features, also differences in cell cycle exit further determine

the sub-columnar identities of motor neurons: motor neurons that will form the medial aspect of the LMC (LMCm) leave the cell cycle before motor neurons that will form the lateral LMC (LMCI) and that have to migrate past the LMCm neurons to their final positions in the lateral ventral spinal cord. Secretion of Raldh2 by the early born motor neurons initiates down-regulation of *Lhx3* and *Isl1* in motor neurons of the LMCI, and activates *Lim1* that controls growth of LMCI axons towards dorsal limb musculature. In the medial LMC, *Isl1* expression in the absence of *Lhx3* and *Lhx4* marks motor neurons that innervate targets in ventral musculature (Fig. 2C; Kania et al., 2000).

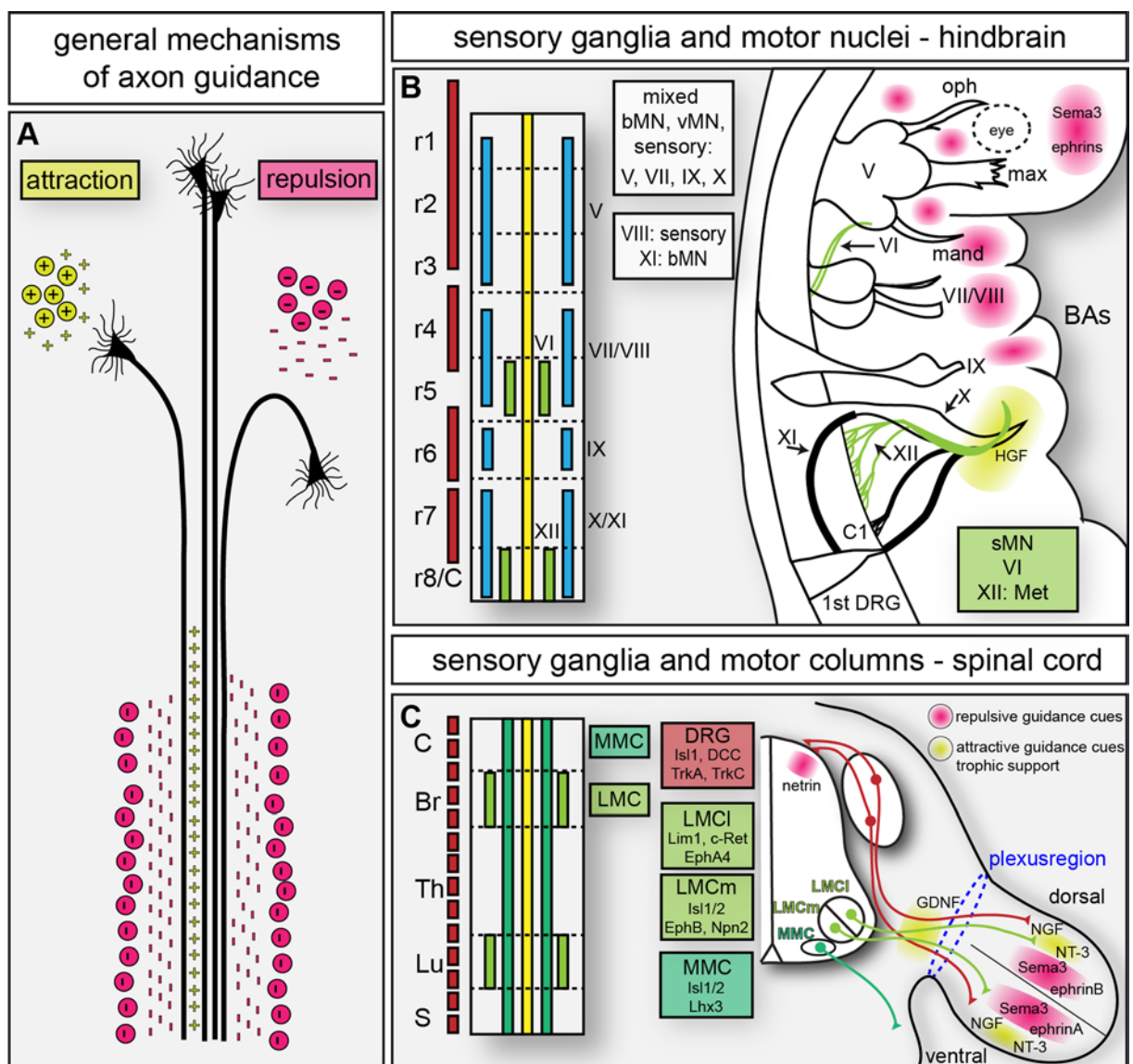


Figure 2: Mechanisms of axon guidance at cranial and limb levels.

(A) Schematic overview of general mechanisms of axon guidance. Contact mediated mechanisms provide adhesive and permissive substrates for axon growth. Interactions of axonally expressed receptors with attractive or repulsive guidance cues lead growth cones into permissive tissues, or drive

them away, respectively. **(B)** Left side: Organization of cranial motor and sensory neurons in rhombomere-specific nuclei (green and blue) and ganglia (red), respectively. Right side: Cranial projections to the head and branchial arches. Repulsive and attractive guidance cues interact with receptors on motor and sensory axons, leading them to their distinct targets. V, VII, IX, and X build mixed sensory-motor projections, VIII provides sensory connections to the ear, XI consists only of bMN fibers, while VI and XII contain exclusively somatic motor fibers. **(C)** Left side: Organization of motor neurons in columns in the spinal cord and sensory neurons in segmented ganglia. Lateral motor columns (LMC) are formed by neurons innervating limb musculature at brachial and lumbar levels, while the medial motor columns (MMC) formed by neurons innervating axial musculature are present over the entire length of the spinal cord. Right side: Topographic projections of axons from lateral (*Lim1*⁺) and medial LMC (*Isl1*⁺) to dorsal and ventral targets in the embryonic limb in response to guidance cue-receptor interactions. For DRG neurons, no markers to distinguish dorsally and ventrally projecting neurons have been identified so far. Large diameter TrkC⁺ neurons that project to muscles (proprioceptive) are dependent on trophic support by NT-3. Small diameter TrkA⁺ neurons innervate the skin (nociceptive) and are dependent on NGF in their target regions. Figure was adapted from Huber et al., 2003; Guthrie, 2007. Abbreviations and nomenclature: r=rhombomeres, BA=branchial arch, bMN=branchiomotor neurons, Br=brachial spinal cord (sc), C=cervical sc, C1= cervical segment 1, Lu=lumbar sc, mand=mandibular branch of V, max=maxillary branch of V, NGF= nerve growth factor, NT-3= neurotrophin 3, oph=ophthalmic branch of V, Th=thoracic sc, S=sacral sc, V=trigeminal, VI=abducens, VII=facial, VIII=vestibulocochlear, IX=glossopharyngeal, X=vagus, XI=spinal accessory, XII=hypoglossal.

2.2 THE ESTABLISHMENT OF PERIPHERAL PROJECTIONS – A STEPWISE PROCESS

The establishment of distinct projections into the periphery is achieved in a stepwise process: Axons derived from specific rhombomeres in the brainstem or the motor columns in the spinal cord have to exit the neural tube at correct positions, they have to be correctly bundled with other sensory and motor axons, and guided to their targets.

2.2.1 DEFINITION OF MOTOR AXON EXIT POINTS AND PIONEERING OF PATHWAYS

Branchio- and visceromotor neurons that exit the neural tube at dorsal positions are found exclusively at hindbrain levels and typically innervate targets derived from neural crest cells. Neural crest derived boundary cap cells at the ventral exit points of somatic motor projections allow somatic motor axons situated in the hindbrain and the spinal cord to pierce the neuroepithelium, but hinder inappropriate translocation of motor neurons along their extending axons into the periphery (Vermeren et al., 2003). Expression of the G-protein coupled receptor *Cxcr4* enables these somatic motor axons to identify exit points from the neural tube by interaction with its cytokine ligand *Cxcl12* that is secreted by mesenchymal cells flanking the spinal cord and caudal hindbrain (Lieberam et al., 2005). Structures like nerve exit

points, sensory ganglia, glial cells and target muscles provide essential guideposts during axon elongation into the periphery. Pioneer axons in the grasshopper leg, or the murine telencephalon, for example, follow distinct pathways pre-patterned on critical positions by so called guidepost cells to their targets in muscles or the olfactory bulb, respectively (Keshishian and Bentley, 1983; Palka et al., 1992; Sato et al., 1998; Tomioka et al., 2000). These first axons that navigate to specific targets in the developing embryo lay down pioneer pathways, which are then travelled by later developing axons.

2.2.2 SELECTIVE FASCICULATION AND CONTACT MEDIATED GUIDANCE

Contact-mediated mechanisms provide an adhesive and permissive substrate for axon growth, permitting selective fasciculation of axon tracts growing to the same targets (Raper et al., 1983). Cadherins have been shown to mediate fasciculation and targeting of cranial sensory axons in zebrafish (LaMora and Voigt, 2009). In chicken and mouse embryos, cadherins facilitate axon branching and guidance of branchiomotor axons, or axon sorting within the olfactory nerve, respectively (Akins and Greer, 2006, Barnes et al., 2010). Neural cell adhesion molecule (NCAM) and polysialic acid (PSA) contribute to motor axon sorting and selective fasciculation before the nerves grow into the limb. Interaction of NCAM and PSA allows for selective defasciculation of nerves in regions where PSA is present, whereas regroupment of the axons takes place where no PSA is secreted (Tang et al., 1992; Tang et al., 1994). Only recently, reverse signaling through ephrinAs expressed on epaxial sensory axons by interaction with EphA receptors on epaxial motor projections was shown to promote sensory axon tracking along pre-extending epaxial motor axons (Wang et al., 2011). Loss of the reverse signal resulted in a repulsion of sensory axons by epaxial motor projections, providing a new concept of mediation of selective fasciculation and contact mediated guidance by other ligand-receptor systems than cell adhesion molecules.

2.2.3 SIGNALING PATHWAYS THAT REGULATE CRANIAL NERVE EXTENSION AND DORSAL-VENTRAL GUIDANCE DECISIONS IN THE DEVELOPING LIMB

Over the past 20 years, interactions of axonally expressed receptors with secreted and membrane-bound proteins, the so called guidance cues, have been identified to regulate axon growth both temporally and spatially. Attractive and repulsive long- and short-range signaling of these ligand-receptor systems lead growth cones into permissive mesenchyme, or drive them away, respectively. Thus, axon growth can be channeled by a corridor of permissive or repulsive cues (Fig. 2A). Several families of guidance cues and their corresponding receptors have been identified in the past.

2.2.3.1 NETRIN - DCC

The first diffusible guidance cues identified were the netrins, which belong to the family of laminin-related small secreted proteins and can act both as attractive and repulsive cues by binding to different receptor complexes (Culotti and Kolodkin, 1996; Tessier-Lavigne and Goodman, 1996). Netrins have an evolutionarily conserved role in attracting commissural axons that express deleted in colorectal cancer (DCC) over long distances towards the ventral midline (Serafini et al., 1996; Fazeli et al., 1997). Similar interactions were shown for the establishment of peripheral motor axon pathfinding in *Drosophila melanogaster* (*Drosophila*) (Harris et al., 1996; Mitchell et al., 1996) as well as for guidance of retinal axons during the formation of the visual system in mammals (Deiner et al., 1997). Quite contrary to these attractive roles, netrin expression in the floorplate at cranial and spinal levels provides an additional repulsive signal for guidance of trochlear and spinal motor axons that express the unc-5 homolog (*unc-5*; Burgess et al., 2006; Kennedy et al., 2006; Cirulli and Yebra, 2007). A similar function of netrin-unc5 interaction was observed in the dorsal spinal cord, where netrin expression prevents sensory axons from entering the neural tube at aberrant positions, steering them ventrally to join motor axons and form spinal nerves, or to the dorsal root entry zone (Fig. 2C; Masuda et al., 2009). Intriguingly, in zebrafish lack of either netrin or DCC function impaired not only motor axon outgrowth, but also vascular pathfinding, arguing for

the employment of similar mechanisms during the formation of the nervous and the vascular systems.

2.2.3.2 SLIT - ROUNDABOUT (ROBO)

Also the secreted Slit proteins have a bi-functional role in axon guidance: on the one hand they mediate growth cone repulsion, on the other hand they can stimulate axonal branching and elongation (Wang et al., 1999, Kramer et al., 2001). The repulsive role in axon guidance was first studied in *Drosophila*, where Slit is expressed at the ventral midline and prevent ipsilateral axons that express Robo receptors from crossing the midline, and prohibit re-crossing of commissural axons that also express Robo (Battye et al., 1999, Kidd et al., 1999). Interestingly, in *Drosophila*, Slit also has a function not only in neuronal cell migration, but also in positioning of mesodermal cells for correct positioning and insertion of muscles in the body wall (Kramer et al., 2001). In vertebrates, expression of the axon guidance cue in the floorplate at hindbrain level was shown to govern repulsion of dorsally exiting branchio- and visceromotor neurons, but not of ventrally exiting somatic motor axons (Hammond et al., 2005).

2.2.3.3 HEPATOCYTE GROWTH FACTOR - MET PROTO-ONCOGENE TYROSINE KINASE

During peripheral pathfinding of cranial projections, axon-axon and axon-environment interactions are involved to establish precise connectivity and promote fasciculation of motor and sensory trajectories. Attraction of hypoglossal nerve fibers expressing the Met tyrosine receptor kinase by hepatocyte growth factor (HGF) expressed in the branchial arches is crucial for rostral navigation of the hypoglossal nerve (Fig. 2B; Caton et al., 2000). At spinal levels, a similar system of HGF-Met attractive signaling in the rostral parts of the somites in combination with expression of repulsive cues in the caudal parts of the somites contribute to the establishment of fasciculated growth and metameric patterning of motor and sensory axons from the spinal cord and DRGs, respectively (Kuan et al., 2004). Distinct expression of HGF in the mesoderm of the developing limbs attracts axons emanating from a specific

subset of Met-positive motor neurons towards the plexus region, and at later stages to specific targets in the limbs (Ebens et al., 1996).

2.2.3.4 GLIAL CELL LINE-DERIVED NEUROTROPHIC FACTOR – RET

Limb-derived growth factors such as glial cell line-derived neurotrophic factor (GDNF) play a role during target specific innervation of the distal limbs. GDNF is expressed at the base of the limb when LMC axons are selecting their dorsal-ventral trajectory into the limb bud. LMC axons express EphA receptors as well as the GDNF receptor and are therefore guided to the dorsal limb by action of repulsive ephrinA signals in the ventral limb and attractive GDNF signals (Fig. 2C; Kramer et al., 2006). Activation of the ETS transcription factor *PEA3* by GDNF signaling further contributes to cell body positioning and muscle innervation of specific motor neuron pools (Haase et al., 2002; see section 1.2.2.4).

2.2.3.5 CLASS 3 SEMAPHORINS - NEUROPILINS

Over the past two decades, the receptors of the Neuropilin (Npn, Fig. 3B) family and their ligands, the secreted class 3 Semaphorins (Sema3, Fig. 3A) were shown to play a role in multiple features of peripheral spinal and cranial nerve guidance, including regulation of the timing of growth, selective fasciculation, and mediation of sensory-motor axon interactions. Secreted Sema3s exert their chemorepulsive effects through receptor complexes consisting of one of four class A Plexins as the signal transducing subunit and one of two Npns as the binding subunit (He and Tessier-Lavigne, 1997; Kolodkin et al., 1997; He et al., 2002). Npns are type 1 transmembrane proteins with a small cytoplasmic domain that lacks any known signaling motif, which explains the need for the Plexins as co-receptors. The extracellular domains can interact with various structurally distinct proteins such as vascular endothelial growth factor (VEGF) or the cell adhesion and pathfinding molecule L1 (Fujisawa et al., 1997; Castellani, 2002). At cranial levels, fasciculation and guidance decisions are governed by Sema3-Npn interactions (Fig. 2B): Sema3F-Npn-2 signaling mainly facilitates pathfinding and fasciculation of oculomotor, trochlear and trigeminal axons (Chen et al., 2000; Gammill et al., 2007). *Npn-1* is

expressed by most sensory and motor neurons within the brainstem, except for oculomotor, trochlear and vestibulocochlear (acoustic) ganglia (Kawakami et al., 1996; Kitsukawa et al., 1997). Loss of the Sema3A-Npn-1 signaling pathway severely affects fasciculation of distal trigeminal, facial, glossopharyngeal and vagus projections to the head and neck projections (Kitsukawa et al., 1997; Taniguchi et al., 1997; Gu et al., 2003; Schwarz et al., 2008a).

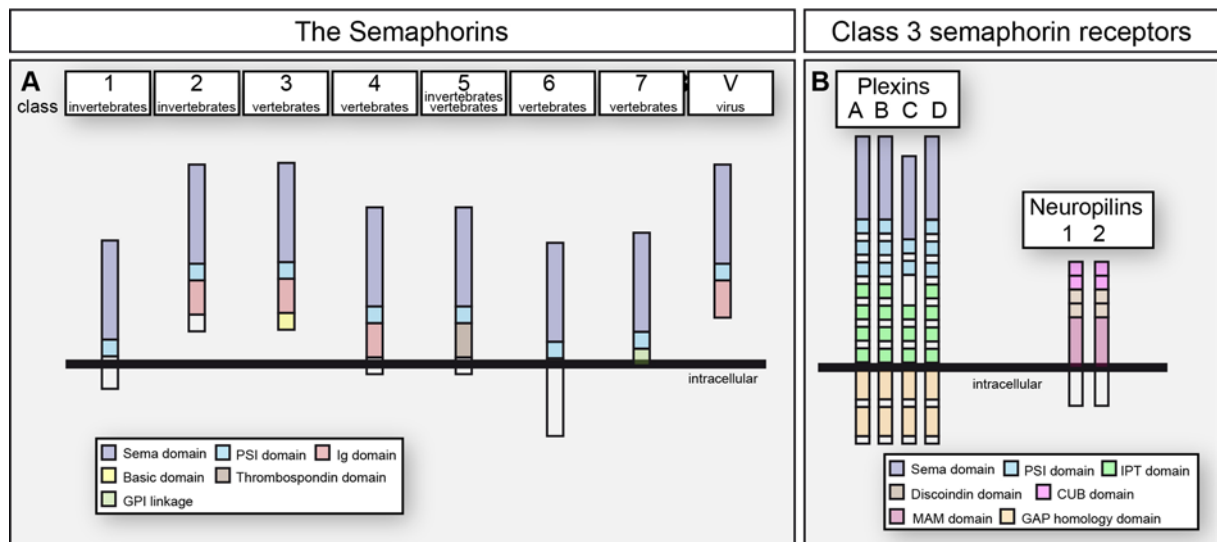


Figure 3: Semaphorins and their receptors.

(A) The Semaphorins: Class 1 Semaphorins (1a and 1b) are invertebrate transmembrane proteins and structurally very similar to vertebrate class 6 Semaphorins (6A-6D). Invertebrate class 2 Semaphorins (2a and 2b) are secreted and structurally similar to vertebrate class 3 Semaphorins (3A-3G). Class 4 (4A-4G), 6 (6A-6C), and 7A transmembrane Semaphorins have been identified only in vertebrates. Class 5 Semaphorins are present in both vertebrates (Sema5A, Sema5B) and invertebrates (Sema5c). Class V Semaphorins (VA and VB) are found in DNA viruses and are very similar to the class 7 Semaphorins. **(B) Receptors for class 3 Semaphorins:** Members of the plexin protein family are organized in four classes (A, B, C, and D); plexins are known to bind to Semaphorins from all classes except class 2, whose receptors are unknown. Secreted class 3 Semaphorins interact with a receptor complex consisting of one of two neuropilins and one of four plexinA's to initiate signaling cascades that are important for axon guidance. Figure was adapted from Yazdani and Terman, 2006.

Motor neurons of the LMC at brachial and lumbar levels innervate limb musculature. Within the plexus region at the base of the limbs, spinal nerves of different segments of the spinal cord meet and exchange fibers to form new bundles that grow specifically towards their targets (Lance-Jones and Landmesser, 1981a, b; Tosney and Landmesser, 1985a; Wang and Scott, 2000). Sema3F is secreted in dorsal limb mesenchyme, while its receptor Npn-2 is expressed by motor neurons of the LMCm. Repulsive interaction of this ligand-receptor system guides motor axons from the LMCm towards the ventral limb. Elimination of Sema3F-Npn2-signaling

leads to pathfinding errors of LMCm axons into dorsal limb mesenchyme while fasciculation and timing of growth remain unaffected (Fig. 2C; Huber et al., 2005). At E10.5, Sema3A is expressed in the entire limb mesenchyme and prevents both motor and sensory axons from prematurely entering limb mesenchyme. Patterned expression of Sema3A at later stages exerts a surround repulsion on nerves growing into the limb, thus channelling their growth. Elimination of Sema3A-Npn-1 signaling results in defasciculation of peripheral motor and sensory projections into trunk and dorsal and ventral limbs. Motor neurons from both LMCm and LMCI show guidance deficits, and, next to premature ingrowth into the limb, the coupling of sensory axon growth on motor axons is lifted (Huber et al., 2005).

2.2.3.6 EPHRINS AND EPH RECEPTORS

As mentioned above, expression of LIM homeodomain transcription factors contributes to the generation of motor neuron diversity of LMC neurons (reviewed in Bonanomi and Pfaff, 2010). Expression of *Lim1* in the LMCI and *Is1* in the LMCm, respectively, confers the ability to motor neurons to select specific axonal pathways to innervate target musculature in different regions of the limb. *Lim1* expression mediates the expression of the EphA4 receptor on axons of the lateral aspect of the LMC. Repulsive interaction of these receptors with ephrinAs in the ventral limb mesenchyme whose expression is controlled by the LIM homeodomain transcription factor *Lmx1b* promotes a dorsal trajectory of LMCI axons (Fig. 2C; Chen et al., 1998; Helmbacher et al., 2000; Kania and Jessell, 2003). Absence of *Lim1* in dorsally projecting motor neurons was shown to cause a random dorsal-ventral choice of LMCI axons at the choice point in the plexus region at the base of the limb (Kania et al., 2000). In a similar mechanism, *Is1* controls expression of the EphB1 receptor on the surface of axons from LMCm neurons. Repulsive interaction with ephrinBs in dorsal limb mesenchyme forces these axons to project to ventral target musculature (Fig. 2C; Luria et al., 2008). Intriguingly, Eph receptors and ephrins are co-expressed in motor neurons of the LMC (Gallarda et al., 2008; Luria et al., 2008): ephrinB2 expression was detected in neurons of the LMCI, while ephrinA5 was expressed by neurons of the LMCm (Kao and Kania, 2011). The authors showed that knockdown of ephrin expression in the lateral or medial LMC, in chick embryos leads to errors in

the dorsal-ventral guidance decision of motor axons. Misexpression of ephrinB in the LMCm, or ephrinA in the LMCI induced rerouting of LMCm axons to dorsal limb musculature, and of LMCI axons to ventral limb musculature, respectively. Ephrins expressed by motor neurons were shown to attenuate the levels of their corresponding receptors on the respective growth cones, therefore contributing to a fine-tuning of motor axon sensitivity to ephrin expression in the mesenchyme (Kao and Kania, 2011).

2.2.4 TARGET SELECTION AND NEUROTROPHIC SUPPORT

Neurotrophins are essential regulators of neuronal survival and morphology, as well as plasticity in the adulthood (Huang and Reichardt, 2001). TrkA-positive cutaneous sensory axons of the DRG innervate distinct targets in the skin, while TrkC-positive proprioceptive sensory neurons project to muscle targets in the limb musculature. The expression of these specific tyrosine receptor kinases on the different types of sensory fibers enables interaction with distinct neurotrophins, i.e. NGF or NT-3, respectively, on the way to the target regions for promotion of axonal growth, or maintenance of cell survival by retrograde trophic support (Fig. 2C; Lindsay, 1996; Gallo et al., 1997; Farinas, 1999). It has been shown that neurotrophins also regulate the expression of transcription factors implicated in motor axon targeting decisions and sensory-motor connectivity: *PEA3* and *Er81*, for example, which are both members of the ETS transcription factor family, are expressed both in proprioceptive sensory neurons and specific pools of motor neurons that innervate the same targets (Lin et al., 1998; Arber et al., 2000). *PEA3* mutant mice show mispositioned motor neurons within the LMC, whose axons fail to correctly innervate their target muscles (Livet et al., 2002). Mice mutant for *Er81* showed deficits in motor coordination and muscle spindle differentiation, and a loss of monosynaptic connections between sensory afferents and motor neurons. Loss of *Er81* and *PEA3* function does, however, not influence generation and early axon pathfinding decisions, indicating that target derived signals influence later targeting and sensory-motor connectivity of specific neurons (Arber et al., 2000).

3. IDENTIFICATION OF NOVEL CUES MEDIATING THE DORSAL-VENTRAL GUIDANCE DECISION

In a typical vertebrate limb, more than 50 muscle groups and the skin require precise innervation from corresponding motor neurons in the LMC and sensory neurons of the DRG at brachial and lumbar levels (Sullivan, 1962; Hollyday and Jacobson, 1990). The LIM homeodomain proteins *Lim1* and *Isl1* define medial and lateral sub-columns of the LMC, from where motor neurons project axons either to the dorsal or ventral limb, respectively (Fig. 2C; Jessell, 2000). These transcription factors code for guidance receptors of the Eph receptor family, which interact with their corresponding ephrin ligands in the limb mesenchyme and thus govern guidance fidelity of growing motor axons (Kania and Jessell, 2003; Luria et al., 2008). Absence of ephrinA-EphA4 and ephrinB-EphB1 signaling misroutes only a subset of motor axons from the LMCI or LMCm, respectively (Helmbacher et al., 2000; Luria et al., 2008). In double-mutant mice where both GDNF-Ret signaling, which attracts LMCI axons to dorsal musculature, and repulsive ephrinA-EphA4 signaling was eliminated, the aberrant ventral pathway selection is enhanced, however, some motor axons still project to dorsal targets (Kramer et al., 2006). Repulsive interaction of the axon guidance receptor Npn-2 which is expressed in medial LMC neurons with Sema3F in the dorsal limb mesenchyme promotes a ventral trajectory of these LMCm axons. Absence of this signaling pathway increases the percentage of LMCm axons misprojecting to the dorsal limb, but also does not completely de-regulate ventral pathfinding of motor axons (Huber et al., 2005). Even when the function of the LIM homeodomain transcription factors *Lim1* and *Isl1* which confer the ability for dorsal-ventral guidance decisions to motor axons of the LMC was abolished, only 30% of the respective axons were misrouted (Kania et al., 2000; Luria et al., 2008). Therefore, the known ligand-receptor interactions cannot explain exhaustively how the correct establishment of dorsal-ventral guidance decisions in the plexus region is achieved during development.

In contrast to motor neurons in the LMC, sensory neurons are not organized topographically according to their peripheral targets, but their cell bodies are rather dispersed throughout the whole DRG. Indeed, up to now, no guidance cues facilitating dorsal or ventral sensory axon guidance have been identified.

In order to determine additional cues that specifically govern the dorsal-ventral guidance decision of motor and sensory axons that project from the spinal cord to their targets in the limbs, Elisa Bianchi, a former PhD student in the Huber Brösamle laboratory established a whole genome expression screen to identify differentially expressed genes in motor and sensory neurons (Fig. 4). Neurons were retrogradely labeled by injection of dextran-conjugated fluorescent dyes into dorsal and ventral limb musculature of E12.5 embryos. After extraction and dissociation, the labeled neurons were separated by fluorescence activated cell sorting (FACS), and RNA of differentially projecting motor and sensory neuron pools was prepared for microarray analysis. Evaluation of this microarray analysis predicts genes that are differentially expressed in either dorsally or ventrally projecting neurons at spinal fore- and hindlimb levels.

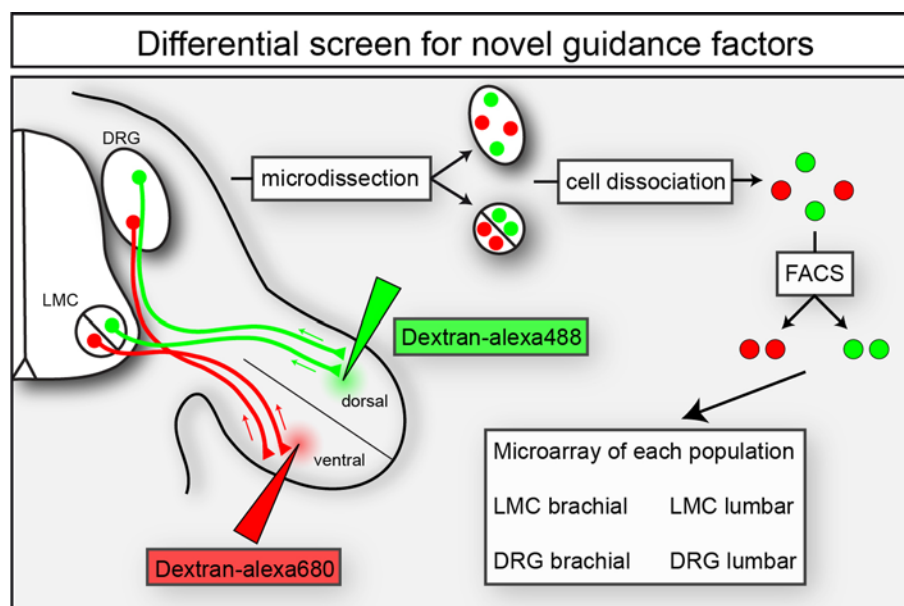


Figure 4: Schematic illustration of the global differentiation screen for novel guidance cues. Injection of dextran-alexa488 and dextran-alexa680 into dorsal and ventral limb musculature of E12.5 embryos, respectively, leads to retrograde labeling of motor and sensory neurons. DRG or LMC were microdissected, motor or sensory neurons were dissociated, and cells were sorted according to their fluorescence by FACS. RNA of either dorsally or ventrally projecting neurons of the LMC and DRG of brachial and lumbar levels was then prepared for microarray analysis.

4. AIM OF THIS STUDY

How are precise connectivity to peripheral targets and corresponding sensory-motor networks established during development and innervation of the vertebrate extremities? The combination of different molecular mechanisms such as communication between heterotypic fiber systems, axon-environment or axon-glia interactions ensures proper fasciculation and accurate pathfinding to distal targets. We investigated the role of the axon guidance receptor Npn-1 selectively in somatic motor neurons and neural crest derived tissues such as Schwann cells and sensory neurons for limb innervation and the establishment of cranial projections to the head and neck. Characterization and expression profiling of genes that were previously predicted by our microarray analysis of differentially projecting sensory and motor neurons further identified candidates that might be involved in the pathfinding decisions of axons at the dorsal-ventral choice point in the plexus region at the base of the limb.

4.1 *NPN-1* CONTRIBUTES TO AXON-AXON INTERACTIONS THAT DIFFERENTIALLY CONTROL SENSORY AND MOTOR INNERVATION OF THE LIMB

Over the past two decades, a number of molecular cues and corresponding receptors on the axonal growth cones that govern axon guidance have been identified (O'Donnell et al., 2009). Classical surgical ablation experiments in chicken shaped the view that spinal motor fibers penetrate the developing extremities first, while sensory axons follow these established trajectories: Early surgical removal of motor neurons resulted in abnormal patterning of sensory trajectories. Elimination of motor neurons in the embryonic chick after neural crest cells have coalesced into DRG and formed spinal nerves, however, had no obvious impact on the formation of sensory projections to limb musculature. (Hamburger et al., 1966; Narayanan and Malloy, 1974; Landmesser and Honig, 1986; Wang and Scott, 1999). While guidance cues like Sema3A mediating the fasciculation and timing of growth of sensory axons have been identified previously (Huber et al., 2005), mechanisms governing interaction of and communication between co-extending sensory-motor fiber systems are only sparsely investigated. Only recently, reverse signaling through eprinAs

expressed on epaxial sensory axons growing along previously extending, EphA4 positive motor axons was reported to mediate sensory fiber tracking (Wang et al., 2011).

The guidance receptor *Npn-1* is expressed in motor neurons of the LMC at brachial and lumbar levels, as well as in sensory neurons of the DRG (Fig. 5; Kitsukawa et al., 1997; Taniguchi et al., 1997). Its capability to form homodimers, or bind to other cell surface molecules like L1 or vascular endothelial growth factor (VEGF; Castellani, 2002; Geretti et al., 2008) puts *Npn-1* in a position to mediate not only axon-environment, but also axon-axon interactions during the formation of sensory-motor circuits in the developing embryo. Using a genetic approach to conditionally ablate *Npn-1* in either sensory or motor neurons by tissue specific activation of Cre-recombinase (Fig. 5) we examined the interactions of the two different projections as they navigate to their targets in the limbs and trunk (Huettl et al., 2011). Investigation of whole embryo preparations revealed that removal of *Npn-1* from motor neurons caused prominent defasciculation of their axons in the plexus region and further distally with a severe defect in distal axonal advancement. Retrograde tracing of motor neurons from the dorsal or ventral limb mesenchyme showed errors in the stereotypical dorsal-ventral guidance decision of motor neurons in the LMCm and LMCl. In contrast to findings in chick embryos where motor neurons were surgically removed, genetic ablation of *Npn-1* in motor neurons and subsequent severe defasciculation of motor axons in the limb does not affect establishment and patterning of distal sensory projections. Surgical removal of neural crest precursors in chicken embryos was reported to impair the ability of the animals to react to environmental stimuli, however, no alteration of motor innervation was observed (Hamburger et al., 1966; Narayanan and Malloy, 1974). Quite unexpectedly, elimination of *Npn-1* from sensory neurons caused defasciculation of both sensory and motor projections before and after the plexus region, and the tight coupling of sensory axon-growth to pre-extending motor axons was lifted. We therefore provide evidence that *Npn-1*-mediated inter-axonal contacts and fasciculation of sensory axons in specific regions are crucial for the correct establishment of the innervation of the vertebrate limb.

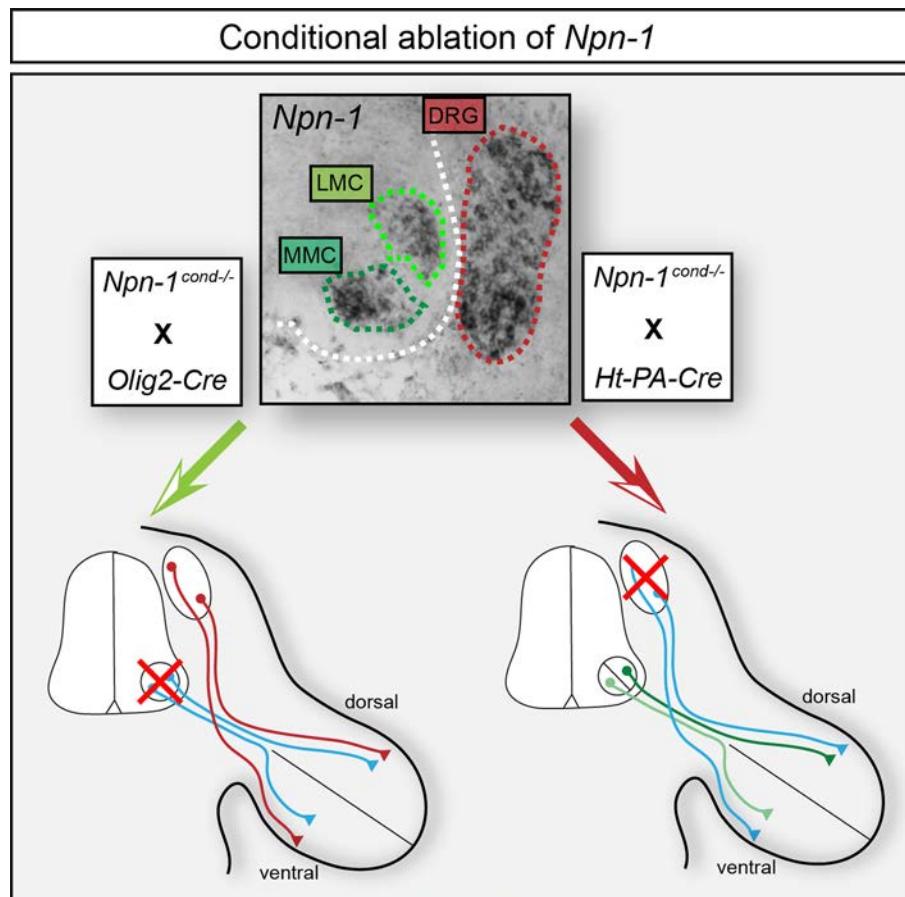


Figure 5: Schematic illustrating tissue specific ablation of *Npn-1*.

In situ hybridization against *Npn-1* shows expression in motor neurons of the LMC and MMC, and in sensory neurons of the dorsal root ganglia. Left side: Tissue specific activation of Cre recombinase driven by the *Olig2-Cre* promoter ablates *Npn-1* in motor, but not in sensory neurons. Right side: Activation of Cre recombinase driven by the *Ht-PA-Cre* promoter eliminates *Npn-1* expression from sensory neurons in the DRG, while motor neurons in the ventral horn are not targeted.

4.2 CRANIAL NERVE FASCICULATION AND SCHWANN CELL MIGRATION ARE IMPAIRED AFTER LOSS OF *NPN-1*

At cranial levels, defined peripheral nerves are formed from either primarily sensory, purely motor, or mixed populations of axons to innervate in precisely defined trajectories targets of the vertebrate head and neck. Disruption the Sema3-*Npn-1* signaling pathway has been shown to result in defasciculation of the distal projections of the cranial trigeminal, facial, glossopharyngeal and vagus nerves. However, as these projections contain both motor and sensory axons, it was unclear whether *Npn-1* is required in both neuronal populations for proper distal assembly and fasciculation. Furthermore, a possible function of *Npn-1* for the establishment of

the purely somatic motor projections of the cranial abducens and hypoglossal nerves or in accompanying glia cells has not yet been investigated.

We explored the role of Npn-1 in the assembly, guidance and fasciculation of cranial nerve projections by using tissue specific loss-of-function mutants in whole embryo preparations (Huettl and Huber, 2011). Loss of *Npn-1* in sensory neurons recapitulates the distal defasciculation of trigeminal, facial, glossopharyngeal and vagus projections, and aberrant axons between trigeminal and facial ganglia that were observed in *Npn-1*^{-/-} mutant embryos and in embryos where the binding site for all class 3 Semaphorins was mutated (*Npn-1*^{Sema-}; Taniguchi et al., 1997; Gu et al., 2003; Schwarz et al., 2008a). Interestingly, removal of *Npn-1* from sensory neurons and placodally derived tissue also leads to defects in fasciculation of the hypoglossal nerve, which is a pure somatic motor projection. These initial fasciculation defects are accompanied by a decrease of neural crest derived Schwann cells migrating along hypoglossal rootlets. Our results therefore emphasise the crucial role of Sema3A-Npn-1-signaling for selective fasciculation of motor and sensory trajectories during proximo-distal axon guidance. Furthermore, our data underscore the hypothesis that somatic motor nerve fasciculation at cranial levels depends on axon-Schwann cell interactions in developing vertebrates.

4.3 IDENTIFICATION OF NOVEL GUIDANCE CUES

4.3.1 CANDIDATE GENES – SELECTION CRITERIA

As nerves project to their targets in the periphery, the growth cones at the leading edge of the axons sense and respond to secreted, i.e. long-range, and membrane-bound, i.e. short-range cues presented in surrounding tissues and on other axons. Genes for receptor proteins, but also for molecules secreted by navigating axons therefore pose interesting candidates to influence guidance decisions as guidance cues or guidance receptors during axon pathfinding. Typically, guidance signalling pathways and subsequent growth cone turning events involve activation of signaling pathways via GTP binding proteins, and subsequent re-organization of the cytoskeleton within the filopodia and lamellipodia of the growth

cone (Hall, 1998; Dickson, 2001; Luo, 2002). Genes encoding proteins in the signaling cascades which lead to actin polymerization or depolymerisation therefore are also likely candidates for mediation of specific guidance events during axon elongation. Also neurotrophins play critical roles for neuronal survival, growth, branching and plasticity. Whether these factors directly influence primary axonal dorsal-ventral pathfinding into the target regions still needs to be elucidated. However, it was shown that the factors of the neurotrophin family NGF, BDNF, NT-3 and NT-4 function as chemoattractants for growth cones *in vitro* and promote formation of axonal filopodia during axon branching events (Gallo et al., 1997; Ming et al., 1999; Ketschek and Gallo, 2010). Neurotrophins have been suggested as axonal guidance molecules during growth and regeneration of nerves by stimulation of polymerization and accumulation of F-actin in growth cones and axon shafts via G-Protein signaling pathways (Yamashita et al., 1999; Nusser et al., 2002). Furthermore, activation of the MAP kinase pathway leads to activation of genes promoting axon extension, cell proliferation and survival (Huang and Reichardt, 2001), rendering genes within this specific signaling pathway possible candidates facilitating dorsal and ventral guidance decisions. Among the candidates identified by the microarray analysis, various representatives of gene families that are in a position to mediate guidance events during axonal growth were found (Fig. 6).

We selected ten candidates for differentially projecting brachial motor neurons and five for differentially projecting brachial sensory neurons based on literature recherche that suggested a potential role in axon guidance according to the above mentioned selection criteria. Expression patterns in the embryonic spinal cord that were assembled in the GenePaint database (www.genepaint.org) provided additional information for the selection process.

4.3.2 CANDIDATE GENES – BRACHIAL MOTOR NEURONS

In the microarray screen, 124 genes were predicted to be differentially expressed in either dorsally or ventrally projecting motor neurons in the brachial LMC. Among these predicted genes previously identified differentially expressed motor neuron markers were found, such as *Lim1* and *EphA4* in dorsally projecting neurons, and *Isl1* and *Npn-2* in ventrally projecting motor neurons, which further confirms the reliability of the screening approach (Kania et al., 2000; Huber et al.,

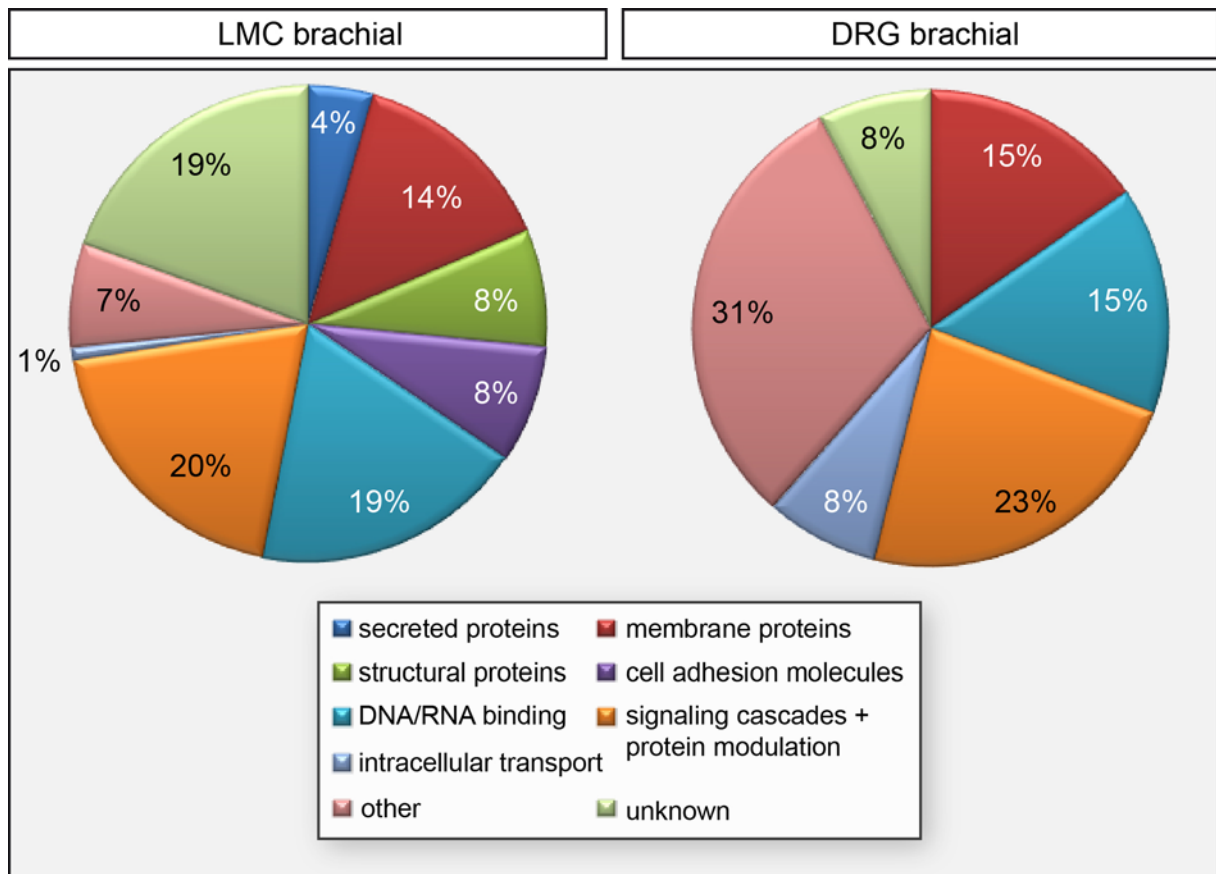


Figure 6: Functional categories of candidate genes in the differentially projecting neuronal populations.

The pie charts represent the main functions of the genes differentially expressed in brachial motor and DRG neurons according to gene ontology analysis.

2005; Elisa Bianchi, unpublished data). We chose four of the candidate genes based on the above mentioned selection criteria for a more detailed investigation. We confirmed their predominant expression in ventrally projecting motor neurons by *in situ* hybridization and briefly introduce the candidates here:

Like all small GTP-binding proteins, Rho GTPases cycle between active and inactive conformation through the binding of guanine nucleotides. GTP activating proteins (GAP) turn off Rho GTPase signalling by promotion of hydrolysis of bound GTP to GDP. As these molecules can be directly or indirectly be linked to guidance receptor signalling, Rho-GTPase activating protein 29 (*Arhgap29*; Myagmar et al., 2005) may therefore play a significant role in Rho-GTPase signaling and actin filament assembly or disassembly during axon pathfinding events.

In order to correctly navigate to peripheral targets, nerve fiber tracts and blood vessels employ similar molecular mechanisms and also show morphological analogies: just as growth cones at the tip of extending axons, specialized motile tip

cells express receptors of the Eph receptor, Neuropilin or Plexin families and guide growing blood vessel in response to ephrins or Semaphorins in the surrounding tissue (Adams and Eichmann, 2010). Coiled coil domain containing 3 (*Ccdc3*) is a hormonally and nutritionally regulated novel secretory protein that was found to be expressed in endothelial cells of the vascular system and in mature adipocytes (Kobayashi et al., 2010). Specific secretion of *Ccdc3* by ventrally projecting motor axons might affect pathway selection and/or fasciculation of axons growing to the same target regions.

Expression analysis by *in situ* hybridization against *Arhgap29* and *Ccdc3* at earlier time points revealed that they develop a distinct expression in LMCm neurons at the time point when dorsal-ventral guidance decisions are made. While the distinct function of *Arhgap29* in the Rho signaling pathway still remains to be elucidated, its ability to activate GTP-hydrolysis by Rho-GTPases was already shown to influence cytoskeletal rearrangements in blood cells (Xu et al., 2011) and thus displays an interesting candidate for mediation of motor axon pathfinding. The novel secretory factor *Ccdc3* was originally detected in a screen for genes specifically expressed in the murine aorta and is expressed and secreted by cells of the vascular system. Therefore, it might not only play a role in axon pathfinding, but also in co-extension and communication of vasculature and nerve fibers. Up to now, no mice with mutations for these two genes are available. Expression analysis on chicken embryos will help to elucidate conserved expression patterns between species, while gain- and loss of function approaches by *in ovo* electroporation will provide further insight in the function of the two genes in axon growth and guidance.

Early removal of the limb prevents the onset of ETS gene expression, which indicates that target derived signaling is required for the expression of these genes in motor pools (Lin et al., 1998). The late onset of ETS gene expression also raises the possibility that these genes control the patterning of motor projections (Arber et al., 2000). *Elk3*, like all ETS family members is a protein that is involved in transcriptional regulation of genes that are critical for cell differentiation and proliferation (Buchwalter et al., 2005). *Elk1*, a close relative to *Elk3* already has been proposed to have a role in neuronal function based on its expression pattern including the soma, dendrites and axon terminals of striatal neurons (Sgambato et al., 1998). Its relations to other ETS genes that already have been shown to play a role in motor neuron differentiation and motor-sensory connectivity rendered *Elk3* a likely candidate for

mediation of distinct guidance events. The expression analysis confirmed the differential expression of *Elk3* at E12.5, but not at earlier time points, when the dorsal-ventral guidance decisions are taking place. However, as a close relative to ETS genes, *Elk3* might also be involved in the definition of motor pools projecting the same peripheral targets. Expression analysis and retrograde tracing of motor neurons at later stages during embryonal development might help to understand target derived induction of motor pool specification.

Tightly regulated FGF-FGF receptor (FGFR) signaling plays important roles in neural induction and patterning of the developing embryo. Graded FGF expression along the spinal cord, for example, leads to activation of different Hox genes defining the columnar identity of motor neurons within the ventral horn (Dasen et al., 2003; Bottcher and Niehrs, 2005; Dasen et al., 2005). Furthermore, FGF signaling has been shown to promote synapse formation within the hippocampus (Terauchi et al., 2010). Ablation of isoforms of the FGF receptor 2 (*FGFR2*) leads to impaired limb bud induction and malformations of the skeleton (Lizarraga et al., 1999; De Moerlooze et al., 2000; Coumoul and Deng, 2003). During early embryonic development, *FGFR2* is co-localized with neural cell adhesion molecule (NCAM), a modulator of axonal growth and fasciculation in the developing brain which was observed to activate *FGFR2* signaling and its downstream pathways (Vesterlund et al., 2011). To further investigate the role of *FGFR2* in motor axon guidance decisions, we employed a genetic approach to conditionally ablate *FGFR2* in motor neurons of mouse embryos. Intriguingly, we found no deficits in the general growth pattern and distal extension of motor projections into the distal limb. Motor nerves were correctly fasciculated and extended to appropriate distal positions. Investigation of the guidance fidelity of LMCm neurons by dorsal retrograde labeling showed no increase in errors in the dorsal-ventral guidance decision of ventrally projecting motor axons. Thus, *FGFR2* function is dispensable for distal positioning and guidance fidelity during extension of motor axons into the forelimbs.

4.3.3 CANDIDATE GENES – BRACHIAL SENSORY NEURONS

In the microarray screen, 13 genes were predicted to be differentially expressed in sensory neurons in brachial DRG. Based on literature recherche and the criteria mentioned in 4.3.1, we chose five candidate genes, which will be briefly presented here, for further investigation. In contrast to motor neurons of the LMC, no genetic markers for dorsally or ventrally projecting sensory neurons have been found so far. Therefore, we used the retrograde tracing method employed for the microarray screen to label differentially projecting neurons before performing *in situ* hybridization to validate the expression pattern of the candidate genes predicted by the microarray screen.

Proliferation and differentiation of neural progenitor cells are precisely regulated processes during the formation of the vertebrate nervous system. In *Drosophila* embryos, the homeodomain transcription factor Cut is expressed in sensory precursor cells that later form mechanosensory or chemosensory external sensory organs (Blochinger et al., 1990). In vertebrates, two members of the cut-like homeodomain transcription factor family were identified: *Cux1* regulates cell cycle progression by inhibition of the cyclin kinase p27 (Ledford et al., 2002). *Cux2* is expressed in various tissues in the developing vertebrate embryo such as the branchial arches and limb bud, or the olfactory epithelium and neurons in the brain, spinal cord and DRG (Iulianella et al., 2003). Mutant mice in which *Cux2* function was abolished show deficits in the differentiation of neuronal precursor cells and formation of dendrites and synaptic spines (Iulianella et al., 2008). Behavioural analyses of these *Cux2*^{-/-} mutant animals demonstrated a hypersensitivity to mechanical stimuli, indicating miswiring of a specific subset of nociceptor projections to the skin (Bachy et al., 2011).

Guanine nucleotide binding proteins confer signals from a large variety of cell surface receptors to intracellular effectors. The alpha subunit of large G proteins is believed to confer receptor and effector specificity, however, compared to the large variety of receptors, only 16 different alpha subunits have been identified (Simon et al., 1991). While the alpha subunit hydrolyzes GTP, beta and gamma subunits play a role in activation of ion channels (Logothetis et al., 1987; Krapivinsky et al., 1995). Mice deficient in the *Gnb1* gene showed deficits in neural tube closure, neural

progenitor cell proliferation, and neonatal development. Furthermore, abnormal actin organization was observed (Okabe and Iwakura, 2010). In the microarray screen, a close relative of *Gnb1*, guanine nucleotide binding protein (G-protein), beta4 (*Gnb4*), was predicted to be expressed predominantly in dorsally projecting sensory neurons. Features of large G-protein beta subunits in actin polymerization and signal transduction classify *Gnb4* as an interesting candidate.

Multimeric protein complexes facilitating ciliary transport along microtubules between the cell body and external cell organelles are composed of intraflagellar transport (IFT) proteins. Mutations that compromise the function of these cilia lead to various diseases and congenital syndromes like *situs inversus*, retinal degeneration or polydactyly (Kulaga et al., 2004, Pan et al., 2005, Bisgrove and Yost, 2006). The intraflagellar transport homolog 172 (*Ift172*) was found in a screen for proteins binding to LIM homeodomain factors (Howard and Maurer, 2000). Disruption of the gene causes embryonal lethality, patterning defects of nervous system, the neural tube fails to close, Shh signaling is blocked, and regulation of early FGF signaling at the mid-hindbrain boundary is disrupted (Huangfu et al., 2003; Gorivodsky et al., 2009). Whether these defects also affect sensory axon guidance, however, still needs to be assessed.

Members of the never in mitosis gene A (NIMA)-related kinase (Nek) family, are defined by their similarity in their kinase domain mainly to that of the essential *Aspergillus nidulans* cell cycle kinase NIMA (Hiesberger et al., 2006). Ablation of never in mitosis gene A (NIMA) related kinase 1 (*Nek1*) which also is expressed in spinal sensory neurons, was shown to impair cilia formation and proper activation of checkpoint kinases (Arama et al., 1998; Chen et al., 2008; White and Quarumby, 2008). As *Nek1* also cycles through the nucleus, it might also be capable of carrying signals affecting ciliary transport and influencing growth cone reaction to external signals (Hilton et al., 2009).

Spatio-temporally regulated turnover of phosphoinositides enables eukaryotic cells to induce various functions such as cell signaling, cytoskeletal re-organization, phagocytosis, membrane traffic, and ion channel activity. Phospholipase C hydrolyzes phosphatidylinositol-4,5-bisphosphate to generate second messengers (Rhee and Bae, 1997). The delta type of PLC (PLC- δ) contains a pleckstrin homology domain for membrane association and is thought to be evolutionarily the oldest form in the mammalian PLC family. *PLCd4* is expressed in brain and testes,

and so far has been shown to be required for the induction of sustained Ca^{2+} increases, cell growth and DNA synthesis onset, as well as the acrosome reaction of murine sperm (Fukami et al., 2001; Fukami et al., 2003; Akutagawa et al., 2006). Features like generation of second messengers and control of DNA synthesis make *PLCd4* a possible guidance factor governing reactions to extracellular signals or synapse formation.

Investigation of new guidance cues and specific markers for neurons is essential to further our understanding of the underlying mechanisms of axon guidance, interaction between developing fiber tracts and eventually the formation of complex neuronal circuitry. This will take research one step closer to solve the mystery of re-establishing those networks after disease or injury. Expression analysis at earlier time points will show whether the sensory candidate genes are already expressed in sensory neurons before or right when dorsal-ventral pathway selection is established. Analyses of whole embryo preparations will provide insight in the function of the candidate genes for fasciculation and axon growth. Further investigations of the expression in either nociceptive or proprioceptive sensory neurons will help to define the function of these genes in sensory axon growth and guidance, and probably result in finding the first marker for a subset of dorsally projecting sensory neurons.

II. MATERIALS AND METHODS

1. ETHICS STATEMENT

Animals were handled and housed according to the federal guidelines for the use and care of laboratory animals, approved by the Helmholtz Zentrum München Institutional Animal Care and Use Committee and the Regierung von Oberbayern.

2. MOUSE EMBRYO PREPARATION

DNA was obtained from mouse tail samples which were incubated for 30 minutes (min) in 100µl 50mM NaOH (Carl Roth) at 100°C. After addition of 30µl 1M Tris (Sigma) pH 7.0, DNA-solution was directly used for polymerase chain reaction (PCR). The genotype of mouse embryos was determined as described for *Npn-1^{cond}* and *Npn-1^{Sema-}* (Gu et al., 2003), *Hb9::eGFP* (Wichterle et al., 2002), *DT-A* (Brockschneider et al., 2006) and *LacZ-Reporter* (Soriano, 1999), or using the following primers to detect the Cre allele in *Hb9-Cre* (Arber et al., 1999), *Ht-PA-Cre* (Pietri et al., 2003), *Isl1-Cre* (Srinivas et al., 2001), *Ncx-Cre* (Neil Shneider, unpublished mouse line), and *Olig2-Cre* (Dessaud et al., 2007): Forward (GTG TCC AAT TTA CTG ACC GTA CAC) and Reverse (GAC GAT GAA GCA TGT TTA GCT GG) primers (Metabion) were used with the following cycling parameters: 5 min preheating to 94°C, 35 cycles of denaturation at 94°C for 1 min, 1 min annealing of the primers at 59,5°C, and 30 sec polymerization at 72°C. The conditional allele of *FGFR2* (Blak et al., 2007) was identified with the forward primer (CCT CCT ACT ACA ATT CCA CC) and reverse primer (CCA GAG GGA ATA TGT GTT TT) with the following cycling parameters: 5 min preheating at 94°C, 35 cycles of denaturation at 94°C for 30 seconds, annealing of the primers at 51°C for 40 seconds and 1 min polymerization at 72°C. In all experiments, mutant mice (*Npn-1^{Sema-}*, *Npn-1^{cond/-};Cre⁺* or *DT-A^{floxed};Cre⁺*, *FGFR2^{cond/-}; Cre⁺*) were compared to control littermates (*wt*, *Npn-1^{cond+/+};Cre⁺* or *Npn-1^{cond+/- or -/-};Cre⁻*, *DT-A^{wt};Cre⁺* or *DT-A^{floxed};Cre⁻*, *FGFR2^{cond+/+};Cre⁺* or *FGFR2^{cond+/- or -/-};Cre⁻*). n=3 for all analyzed genotypes, if not stated differently.

3. IMMUNOHISTOCHEMISTRY

The protocols for wholemount embryo staining and immunohistochemistry have been described previously (Huber et al., 2005). For wholemount antibody staining, mouse embryos from E10.5 to E12.5 were prepared in DMEM/F12 medium, fixed for 24 hours in 4% Paraformaldehyd (PFA) in phosphate buffered saline (PBS) at 4°C, bleached for 24 hours at 4°C in Dent's bleach (1 part H₂O₂ [AppliChem] : 2 parts Dent's Fix) and stored until further use for at least 24 hours in Dent's Fix (1 part dimethyl sulfoxide (DMSO [Sigma]), 4 parts Methanol [Merck]). After washing 3 hours with PBS, primary antibodies (Table 1) were applied in blocking solution (5% heat inactivated normal horse serum [PAA Laboratories], 75% PBS, 20% DMSO) for 5 days rotating at room temperature. Fluorochrome-conjugated secondary antibodies were incubated after 5 hours washing in PBS in blocking solution for 24 to 48 hours at room temperature in the dark. For wholemount imaging, embryos were cleared using BABB (1 part benzyl alcohol [Sigma] : 2parts benzyl benzoate [Sigma]) and imaged using a LSM510 Zeiss confocal microscope. Confocal stacks through the entire extent of the region of interest were acquired and collapsed on a single plane for further investigation. Fluorescent immunohistochemistry was performed on fixed sections of E10.0 to E12.5 embryos without or directly after *in situ* hybridization. Frozen sections were dried 30 min at room temperature before further use. Sections were washed 10 min in PBS before blocking for 30 min in PBST (PBS + 0.1% TritonX-100 [AppliChem]) containing 10% normal horse serum. Slides were incubated with primary antibodies in PBST containing 10% serum overnight in a humified chamber at 4°C. Secondary antibodies in PBST containing 10% serum were applied for one hour at room temperature in the dark and slides were mounted with mowiol after three final wash steps in PBS. The primary antibodies that were used for fluorescent immunohistochemistry are shown in table 1. Antibody staining was visualized using fluorochrome-conjugated secondary antibodies (1:250 [Invitrogen, Jackson Dianova]).

Primary antibody		Concentration
Goat anti-FoxP1	R&D Systems	1:500
Goat anti-Sox10	Santa Cruz Biotechnology	1:100 (wholemout) 1:250 (slides)
Goat anti-TrkC	R&D Systems	1:250
Mouse anti-Isl1/2 39.4D5	DSHB	1:50
Mouse anti-Neurofilament 2H3	DSHB	1:50
Rabbit anti-GFP	Invitrogen	1:2000
Rabbit anti-Krox20	Covance	1:100
Rabbit anti-Lim1	Kindly provided by T.M. Jessell	1:10000
Rabbit anti-Npn-1	A generous gift from Alex Kolodkin	1:100
Rabbit anti-TrkA	A generous gift from Lou Reichardt	1:500
Rat anti-endomucin	Santa Cruz Biotechnology	1:100
Rat anti-PECAM	Clone Mec13.3, BD Pharmigen	1:400

Table 1: Primary antibodies and concentrations used for wholemount antibody staining and fluorescent immunohistochemistry.

Mouse anti-Isl1/2 39.4D5 and mouse anti-Neurofilament 2H3 were obtained from the Developmental Studies Hybridoma Bank (DSHB) developed under the auspices of the NICHD and maintained by The University of Iowa, Department of Biological Sciences, Iowa City, IA 52242).

4. RETROGRADE LABELING OF NEURONS

To retrogradely label dorsally and ventrally projecting sensory neurons, dextran-conjugated Alexa488 (3000MW [Invitrogen]) and dextran-conjugated Rhodamine (3000MW [Invitrogen]) were injected into dorsal or ventral limb musculature of E12.5 embryos. To investigate guidance mistakes in mutant embryos, dextran-conjugated Rhodamine was injected into either dorsal or ventral limb musculature. Preparations were incubated for 4 hours in DMEM/F12 (Gibco) aerated with 5% CO₂ in 95% O₂ (Carbogen [Linde]) prior to 1 hour of fixation in 4% PFA in PBS and cryoprotection in 30% sucrose (Carl Roth) in PBS.

5. RNA ISOLATION AND cDNA SYNTHESIS

For RNA isolation from E10.5 and E12.5 wildtype embryos, mirVana miRNA isolation kit (Ambion) was used and obtained RNA was used as template for cDNA synthesis using superscript reverse transcriptase (Invitrogen). cDNA was subsequently used as template for generation of plasmids for *in situ* hybridization.

6. PROBE SYNTHESIS

5 to 10 µg of the DNA template were cut with a restriction enzyme (Fermentas) leaving 5' sticky ends or blunt ends to avoid transcription of undesirable sequences in a 50µl reaction mix. The mix was incubated for two hours at 37°C, purified by chloroform/phenol extraction and EtOH precipitation and linearized plasmids were stored at – 20°C after eluting the DNA in 1x Tris-Ethylenediaminetetraacetic acid (EDTA, 1xTE, 100mM Tris, 10mM EDTA [Sigma]). Riboprobes identical (sense) and complementary (antisense) to the coding region mRNA were obtained by in vitro transcription. A 20µl reaction mix was set up containing 1 – 2µg of linearized DNA template using T3, T7, or Sp6 RNA polymerases (Fermentas). After 2 hours of incubation at 37°C, transcription was terminated on ice and RNA was precipitated by adding 0.1x Volume LiCl (Sigma) and 2.5x Volumes 100% Ethanol (Merck). The mix was kept for 30 min at –80°C and the precipitated RNA was washed in 70% ethanol and eluted in 20µl diethylpyrocarbonate- treated (DEPC [Serva]) H₂O. The cDNA fragments for probe synthesis of *Npn-1* spanning exon 1 to 4, *Ift172*, *PLCd4*, *Nek1* and *Gnb4* were obtained from E10.5 murine embryonal cDNA with the primers in table 2 using accu prime taq (Invitrogen) and cloned into the PCR II topo vector (Invitrogen). Plasmids containing cDNA of *Arhgap29* (IRAVp968D0653D), *Ccdc3* (IRAVp968H03113D) and *Elk3* (IRAVp968G11108D) were purchased at imagenes (www.imagenes-bio.de). The *Cux2* containing plasmid was a generous gift from Magdalena Götz, and the *FGFR2* containing plasmid was a kind gift from Clive Dickson. Antisense probes were created using the restriction enzymes (RE) and RNA polymerases (RNA pol) as indicated in table 2.

	Sense Primer	Antisense Primer	RE	RNA pol
Arhgap29	-	-	SmaI	T7
Ccdc3	-	-	EcoRI	T3
Cux2	-	-	NotI	T3
Elk3	-	-	NotI	T7
FGFR2	-	-	BamHI	T7
Gnb4	TGT GGC ATT ACT TCT GTG GC	TTA ACA GCA AGG TCC AAT GG	BamHI	T7
Ift172	GAA GGA CTT TCA GAA GGC AGA A	CAG ATC GCG TAG CGT AGT AAT G	KpnI	T7
Nek1	CAG GTG ACG AAT ACA GTG AGG A	TGC AGA ATC TTG GCA TAG AG	XhoI	Sp6
Npn-1 ^{cond}	AGG ATT TTA TGG TTC TTA GG	TTG AAG ATT TCA TAG CGG AT	XhoI	Sp6
Plcd4	AGT TGT TGC GCT ATC TGG TG	CCC CAC TAG GTA GGT GTT GT	NotI	Sp6

Table 2: Probe generation and synthesis.

Primers were used to obtain cDNA fragments by accu prime PCR for subsequent cloning into the PCR II topo vector. Vectors were linearized with restriction enzymes, and linearized plasmid DNA was used as template for RNA polymerases for antisense probe synthesis.

7. IN SITU HYBRIDIZATION

In situ hybridization was performed as described (Huber et al., 2005). Slides were thawed for 30 min, fixed for 15 min in 4% PFA in PBS, rinsed in PBS and incubated for 7 min in PBS containing 5µg/ml Proteinase K (Roche) and 0,1% Triton X-100. Slides were re-fixed in 4% PFA in PBS for 10 min before 3 wash steps for five min in PBS and 10 min acetylation in 0,25% acetic anhydride (Sigma) in 1% triethanolamin (TEA [AppliChem]). After two wash steps for 5 min in PBS and one wash step for 5 min in 2x standard saline citrate (2x SSC), slides were pre-hybridized for 3 hours in a humidified chamber in hybridization solution (50% formamide [Sigma], 5x Denhardt's solution, 250ng/ml baker yeast tRNA [Sigma] and 5x SSC) at room temperature. 200ng of DIG-labeled cRNA probes were dehybridized in hybridization solution for 5 min at 90°C and then incubated for 5 min on ice before applying the mix to the slides, covering them with Nescofilm (Carl Roth), and hybridizing the slides in a humidified chamber at 60°C over night. On the following day, sections were washed for

5 min in 5x SSC, 1 min in 2x SSC, and 30 min in 50% formamide containing 0,2x SSC at 60°C followed by a wash step of 5 min in 0.2x SSC at room temperature. Slides were washed for 5 min in Buffer 1 (100mM Tris, 150mM NaCl [Carl Roth]) before blocking for 1 hour in 1% blocking reagent in Buffer 1. This was followed by 1 – 3 hours of antibody incubation with anti-DIG-Fab-fragments in blocking solution (1:5000) in a humified chamber. Sections were washed two times for 15 min in Buffer 1 and one time for 5 min in Buffer 2 (100mM Tris, 10mM NaCl, 5mM MgCl₂ [Carl Roth]), followed by the light sensitive color reaction at room temperature (340mg/ml nitrobluetetrazolium [NBT, Roche] and 175 mg/ml 5-bromo-4-chloro -3 indolylphosphate [BCIP, Roche] in Buffer 2) in a humified chamber in the dark. The color reaction was stopped by washing the slides for 10 min in 1x TE and sections were either further treated by immunohistochemistry or coverslipped with mowiol mounting medium (Calbiochem).

8. LacZ STAINING

Tissue specific activation of Cre recombinase expression eliminates a stop codon flanked by loxP sites blocking expression of β -galactosidase in the *ROSA26R-LacZ* reporter mouse strain (Soriano, 1999). β -galactosidase catalyzes the hydrolysis of X-Gal producing a blue precipitate. E10.5 and E11.5 embryos were prepared in PBS and fixed for 2 hours in 4% PFA in PBS before 3 wash steps of 20 min in PBS and then incubated in staining buffer (2 mM MgCl₂, 5mM K₄Fe(CN)₆, 5mM K₃Fe(CN)₆ [AppliChem] in PBS) containing 0,5mg/ml X-Gal (AppliChem) at 37°C. Staining was stopped by fixation for 10 min in 4% PFA in PBS followed by 3 wash steps of 5 min in PBS.

9. QUANTIFICATION OF MOTOR AND SENSORY DEFASCICULATION IN THE E12.5 LIMB

To visualize motor defasciculation in wholmount embryos a perpendicular virtual line of 150 pixel length was placed over a projection picture of confocal planes of the entire limb of Hb9::eGFP positive nerve branches in fore- and hindlimbs. A plot profile was calculated, resulting in a peak where a gray value above background

level crossed that line. To quantify motor defasciculation, the thickness of the four major projections in the forelimb was measured and summarized in control and mutant embryos. In the hindlimb, measurements were performed at the position where tibial and peroneal nerves split up into two branches. Significance was calculated using the two-tailed Student's t-test. To quantify sensory defasciculation neurofilament positive pixels above background level (without HB9::eGFP) were counted in a 100x100 pixel area (region of interest, ROI) using the imageJ program and significance was calculated using the two-tailed Student's t-test.

10. QUANTIFICATION OF DISTAL ADVANCEMENT OF MOTOR PROJECTIONS TO THE LIMBS

To quantify the distance of ingrowth of motor axons into the fore- and hindlimb of E12.5 embryos, the length of the distal-most motor fiber was measured starting from the reference point and normalized with the length of the forelimb (see Fig. 10 for a schematic showing of the reference point and the lengths measured). Significance was calculated using the two tailed Student's t-test.

11. QUANTIFICATION OF MISPROJECTING LMC NEURONS

To quantitate misprojecting neurons, backfilled Rhodamin⁺ neurons were counted, and the percentage of aberrantly projecting neurons was calculated based on immunohistochemical stainings against Lim1 or Isl1 by a person blind to the genotype of the evaluated embryos. Significance was calculated using the two-tailed student's *t* test.

12. QUANTIFICATION OF PRE-PLEXUS DEFASCICULATION AT E10.5 AND E12.5

To quantify defasciculation of motor and sensory fibers before the plexus region in E10.5 and E12.5 wholemount embryos, the individual thickness of the 6 spinal nerves contributing to the forelimb-plexus was measured by a person blinded to the genotype of the analyzed embryos ("a" in Fig. 18I), summarized, and

normalized to the length of the spinal cord from which these 6 projections originate (“b” in Fig. 18I) to determine a fasciculation coefficient. Significance was calculated using the two-tailed Student’s t-test.

13. QUANTIFICATION OF *NPN-1* EXPRESSION IN THE TRIGEMINAL GANGLION OF *NPN-1^{COND-/-};HT-PA-CRE⁺* MUTANT EMBRYOS

For quantification of *Npn-1* expressing neurons within the trigeminal ganglion, the area of Isl-1 positive pixels was measured using the ImageJ program, *Npn-1* expressing cells within this area were counted and normalized to the measured area. There was no difference in number/area of Isl-1 positive cells between control and mutant embryos (data not shown). Significance was calculated using the two-tailed Student’s t-test.

14. QUANTIFICATION OF ABDUCENS NERVE THICKNESS AND PROPORTIONS

To quantify the number of abducens fibers projecting to the eyecup at E11.5, the thickness of the abducens nerve was measured at the point, where all projections from the neural tube re-fasciculated (Fig. 23K, JP) and normalized to the length of the entire abducens projection. Proportions of the abducens nerve were analysed by normalizing the length of the abducens projection to the distance from the neural tube to the joining point (JP). Significance was calculated using the two-tailed Student’s t-test.

15. QUANTIFICATION OF HYPOGLOSSAL ROOTLET LENGTH AND NUMBER

To quantify the length of hypoglossal rootlets before they coalesce into one nerve a rootlet coefficient was determined: the individual length of the rootlets was measured from the point where they emerge from the neural tube (white dashed lines in Fig. 24) to the point where they connect with a neighbouring projection and normalized to the distance between neural tube and the point, where all projections

contributing to the hypoglossal nerve have joined (Fig. 24M, a and b, respectively). The number of rootlets was quantified by counting the projections leaving the neural tube blind to the genotype of the analysed embryos (white dashed lines in Fig. 24). Significance was calculated using the two-tailed Student's t-test.

16. QUANTIFICATION OF HYPOGLOSSAL NERVE PROPORTIONS

To investigate whether proportions of the hypoglossal nerve have shifted due to elongated growth of hypoglossal rootlets, the distance of the rootlet convergence point (CP) to the neural tube was measured and normalized to the distance between the neural tube and the point where hypoglossal fibers turn rostrally (TP, Fig. 24M) by a person blind to the genotype of the analysed embryos. Significance was calculated using the two-tailed Student's t-test.

17. QUANTIFICATION OF SOMATIC MOTOR NEURONS IN HYPOGLOSSAL AND ABDUCENS NUCLEI

To quantify the number of somatic motor neurons in the hypoglossal nucleus, the neural tube of E11.5 control and *Npn-1^{cond-/-};Olig2-Cre⁺* mutant embryos was flat-mounted, embedded in Tissue Tek (Sakura) and cryosectioned at 14µm. After immunohistochemistry, sections were imaged using a LSM510 Zeiss confocal microscope and the number of Isl1 positive, Hb9::eGFP positive somatic motor neurons of the hypoglossal ganglion was counted. To quantify the number of somatic motor neurons in the abducens nucleus, Hb9::eGFP positive neurons were counted on images of E10.5 and E11.5 wholemount embryos by a person blind to the genotype of the analysed animals. Significance was calculated using the two-tailed Student's t-test.

18. QUANTIFICATION OF SCHWANN CELLS

For quantification of migrating Schwann cell progenitors, the number of Sox10-positive cells was counted along the entire length of the rootlets and normalized to the number of projections contributing to the hypoglossal nerve to obtain the average

number of Schwann cells per rootlet. The number of Schwann cells at the tip of the hypoglossal projection was counted using the ImageJ program. Significance was calculated using the two-tailed Student's t-test.

19. QUANTIFICATION OF CANDIDATE GENE EXPRESSION AND GUIDANCE ERRORS

Expression of candidate genes for motor axon pathfinding was quantified by a person blind to the experimental setup and prediction by the microarray by counting the total number of FoxP1⁺/Isl1⁺ (LMCm), and FoxP1⁺/Isl1⁻ (LMCI) cells and correlation of the number of cells with a positive *in situ* hybridization signal to them. Expression of candidate genes for sensory axon guidance was performed on cross sections of retrogradely labeled mouse embryos. The number of ventrally back labeled cells positive for *in situ* hybridization signal was quantified blindly and correlated to the total number of neurons retrogradely labeled by injection of dextran-conjugated Rhodamine into ventral limb musculature. The same correlation was done for dorsally projecting neurons.

III. RESULTS

1. CONDITIONAL ABLATION OF *NPN-1*: AXON-AXON INTERACTIONS CONTROL SENSORY-MOTOR INNERVATION OF THE LIMB

1.1 FASCICULATION OF SPINAL MOTOR AXONS IS CONTROLLED BY *NPN-1* EXPRESSED IN MOTOR NEURONS

The establishment of a functional nervous system requires highly appropriate temporal and spatial regulation of axon growth and interaction during the formation of sensory-motor circuits. The axon-guidance receptor Npn-1 has been in the focus of various studies investigating binding specificities, possible ligands and its tasks within the developing organism. Absence of Npn-1 leads to embryonal death midway through gestation due to severe cardiovascular defects (Kitsukawa et al., 1997) and resulted also in impairments in nervous system development. To dissect the effects induced by the two structurally distinct ligands *Sema3A* and *VEGF*, the *Sema3*-binding domain of Npn-1 was mutated and knock-in mice were generated (*Npn-1^{Sema}*; Gu et al., 2003): These mice express normal levels of the receptor, *VEGF* still binds to Npn-1, and therefore, the cardiovascular system develops normally. Neurons expressing the mutated receptor, however, are completely unresponsive to *Sema3A* and its repulsive effects. Absence of *Sema3A*-Npn-1 signaling in motor and sensory neurons results in defasciculation of peripheral sensory and motor projections, defects in timing of axon growth to the limbs and dorsal-ventral guidance errors (Huber et al., 2005). Since Npn-1 is expressed on both sensory and motor projections, it might be responsible not only for transmitting environment-axon signals, but might also mediate direct interaction between these two axonal populations.

To elucidate whether Npn-1 is required cell-autonomously in motor neurons for motor axon growth and fasciculation, we utilized a conditional approach (*Npn-1^{cond}*;

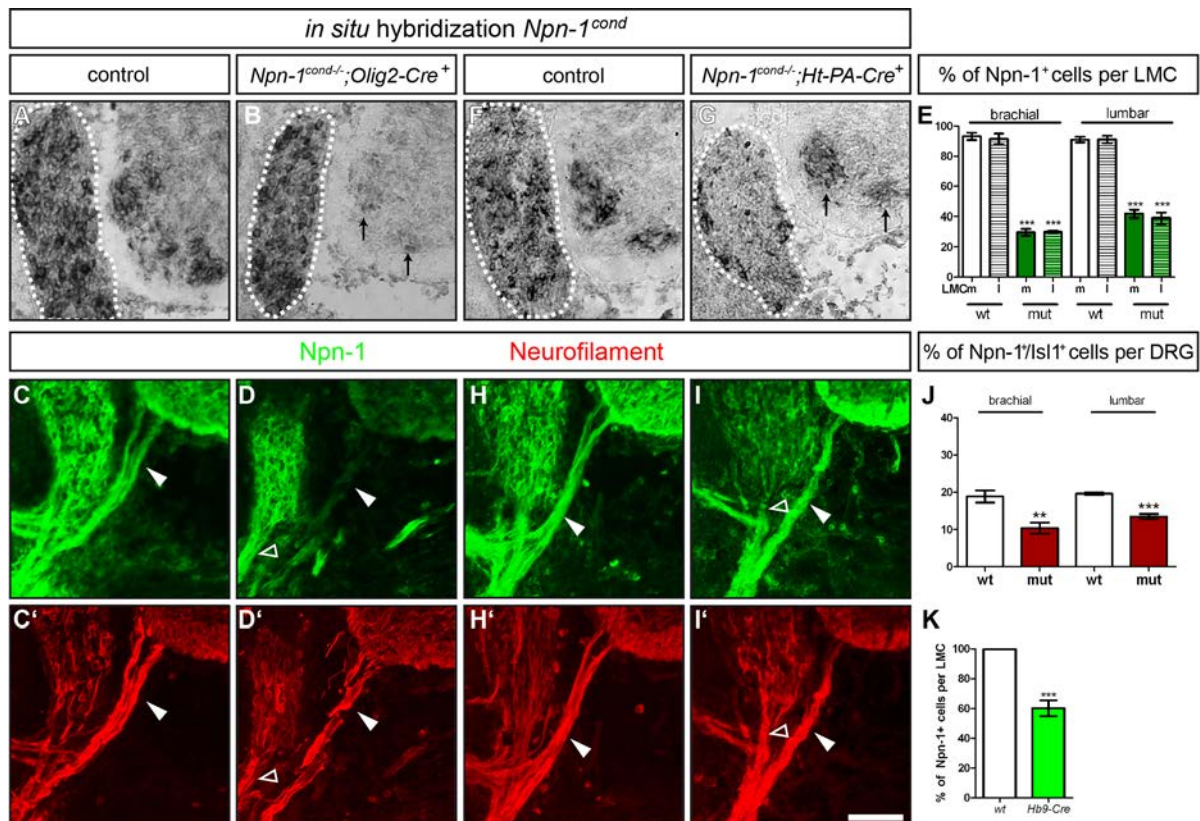


Figure 7: Quantification of Cre recombinase efficiency.

(A) Littermate control. (B) *In situ* hybridization against the floxed exon 2 of *Npn-1* demonstrates ablation of *Npn-1* from motor neurons (arrows) but not from DRG (outlined with a white dashed line) in *Npn-1^{cond/-};Olig2-Cre⁺* mutant embryos. (E) Quantification reveals that mRNA of *Npn-1* was strongly reduced in motor neurons of the LMC at brachial and lumbar levels. (C) Npn-1 protein is visualized by immunohistochemistry against Npn-1 in a wildtype littermate. (D) In *Npn-1^{cond/-};Olig2-Cre⁺* mutant embryos Npn-1 is absent from motor nerve branches (arrowhead), whereas Npn-1 expression is not affected in sensory trajectories (empty arrowhead). (F) Littermate control. (G) *In situ* hybridization on *Npn-1^{cond/-};Ht-PA-Cre⁺* mutant embryos reveals ablation of *Npn-1* selectively from DRG (white line), but not from motor neurons (arrows). (J) Quantification shows a twofold decrease in the numbers of *Npn-1* expressing sensory neurons (positive for Is1-1) in mutant embryos to 10.4% +/- 0.8 at brachial and 13.5% +/- 0.4 at lumbar levels ($p^{\text{brachial}} < 0.005$; $p^{\text{lumbar}} \leq 0.001$). (H) Littermate control. (I) In *Npn-1^{cond/-};Ht-PA-Cre⁺* mutant embryos Npn-1 protein expression is unchanged in motor projections (arrowheads), whereas its presence in sensory fibers is markedly reduced (empty arrowheads). (K) Quantification of Npn-1 positive motor neurons in the LMC of *Npn-1^{cond/-};Hb9-Cre⁺* mutant embryos shows a reduction to 62,14 % +/- 5,24 SEM at brachial levels when compared to controls (= 100%, $p \leq 0,001$). Scale bar in (I') equals 50 μ m in all panels (n=3 for all genotypes).

Gu et al., 2003) to selectively remove the axon guidance receptor from this cell type using the *Olig2-Cre* line (Dessaud et al., 2007). Olig2 is a basic helix-loop-helix transcription repressor that is expressed the pMN domain where motor neurons and oligodendrocytes are generated. At the embryonic time points analyzed, *Olig2*-expression is specific for motor neurons in the spinal cord, while its expression at later time points is of critical importance for the development of oligodendrocytes as well (reviewed in Rowitch et al., 2002). While in control embryos nearly 100% of medial and lateral LMC neurons (positive for Is1-1 and Lim-1, respectively) at brachial

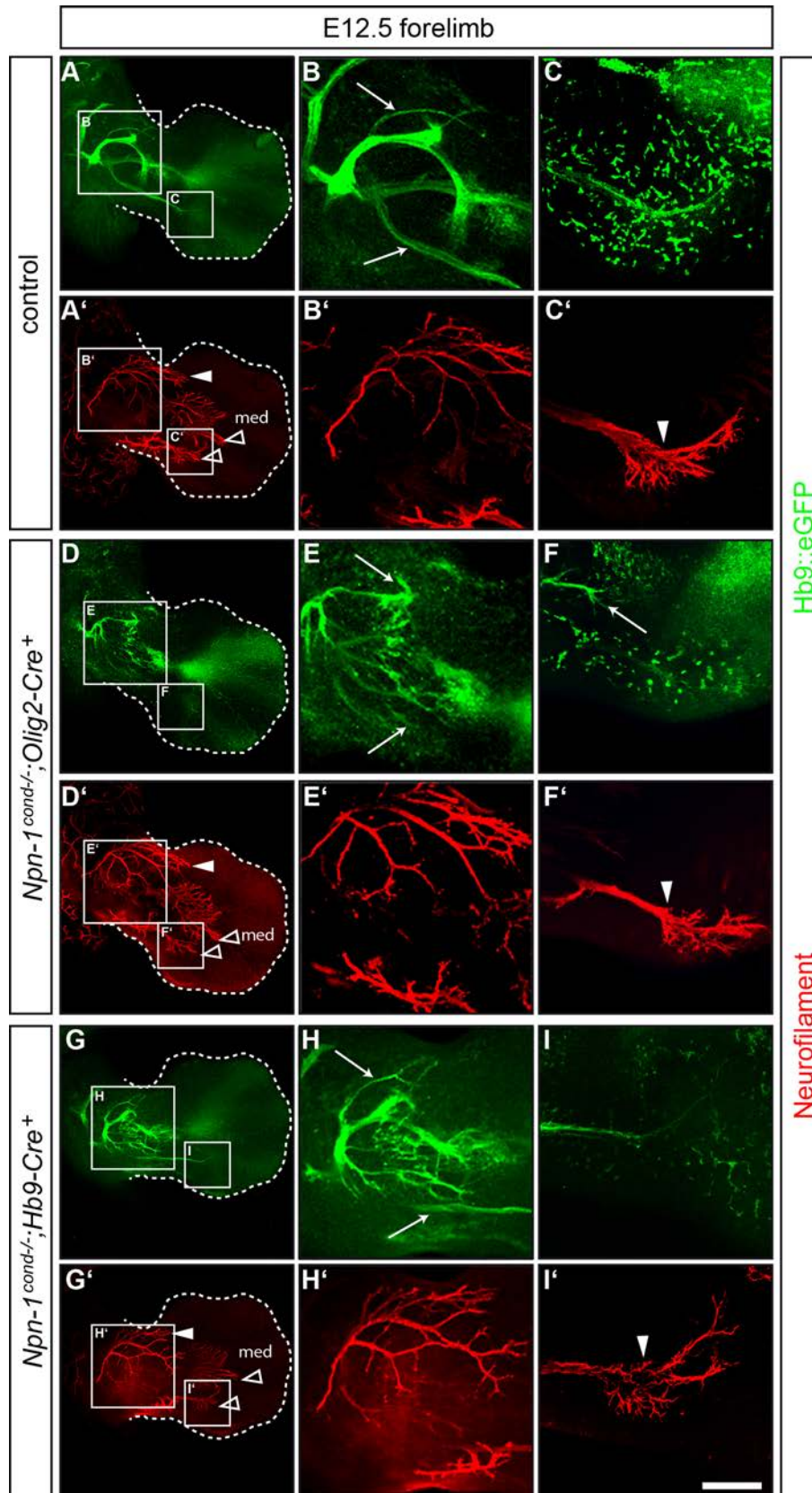


Figure 8: Npn-1 is required in motor neurons for proper fasciculation of LMC projections to the forelimb.

Wholemout antibody staining of E12.5 embryos against GFP (green, motor nerves) and neurofilament (red, motor and sensory nerves). **(A, A')** Littermate control. **(B, B', C, C')** higher magnification of the boxed areas in **(A)**. **(D, E)** Ablation of *Npn-1* from motor neurons leads to severe defasciculation of motor projections to the forelimb in *Npn-1^{cond-/-}; Olig2-Cre⁺* mutant embryos. A higher

magnification reveals that the severe defasciculation of motor nerves in the forelimb is accompanied by absence of several major rami. (**D'**, **E'**) Even though the motor projections are severely defasciculated and reduced in numbers, the general appearance, positioning, and fasciculation pattern of the sensory trajectory appears normal in *Npn-1^{cond/-};Olig2-Cre⁺* mutant embryos (arrowheads and empty arrowheads). (**F**, **F'**) A high magnification shows normal growth of the sensory compartment of the ulnar nerve (arrowhead) in absence of motor projections in mutant embryos when compared to controls (**C**, **C'**). The open arrowhead marks an ectopic motor nerve observed in all mutant embryos. $n^{\text{mutant}} = 10$, $n^{\text{control}} = 7$. (**G**, **H**) Ablation of *Npn-1* from motor neurons using the *Hb9-Cre* line leads to defasciculation of the radial and median nerves but not the ulnar nerve (arrows). (**G'**, **H'**) Fasciculation and distal positioning of sensory nerves is not affected by defasciculation of motor trajectories (empty arrowheads and arrowheads). (**I**, **I'**) High magnification of the ulnar nerve shows normal development of motor and sensory components in *Npn-1^{cond/-};Hb9-Cre⁺* mutants (arrowhead). $n=6$. Scale bar in (**I'**) equals 400 μm for panels (**A**, **D**, **G**), 100 μm for (**B**, **E**, **H**), and 80 μm for (**C**, **F**, **I**).

and lumbar levels express *Npn-1*, in *Npn-1^{cond/-};Olig2-Cre⁺* mutant embryos a decrease to 29.8% +/- 2.3 SEM in medial, 30.1 % +/-0.8 SEM in lateral (Fig. 7E, $p \leq 0,001$) brachial LMC neurons, and to 41.8 % +/-2.6 SEM in medial and 39 % +/-3.6 SEM in lateral (Fig. 7E, $p \leq 0,001$) lumbar neurons was observed. Also motor neurons in the MMC showed reduced expression of *Npn-1* in mutant embryos (control in Fig. 7A, arrows in Fig. 7B). Furthermore, motor axons leaving the spinal cord showed reduced *Npn-1* protein levels in embryos where *Npn-1* was ablated from motor neurons (arrowhead in Fig. 7D), while sensory axons express comparable levels of the axon guidance receptor as in wildtype controls (Fig. 7C, empty arrowhead in D).

The formation of motor and sensory projections innervating peripheral targets was observed in wholemount preparations. Motor axons were identified by crossing the *Npn-1^{cond}* mutant line to an *Hb9::eGFP* line (Wichterle et al., 2002) that selectively labels motor neurons and their projections. Sensory axons were revealed by expression of neurofilament in the absence of GFP fluorescence. At E12.5, motor and sensory projections have traversed the plexus region at the base of the extremities and entered the distal fore- and hindlimb, forming individual nerve branches in wildtype embryos (Figs. 8A, 8B, 9A, 9B). In embryos where *Npn-1* was ablated from motor neurons by *Olig2-Cre* expression, motor axons were found to be so severely defasciculated that hardly any fasciculated motor bundle reached the distal forelimb. Several motor branches, for example the ulnar nerve appeared to be missing altogether (Fig. 8D, E, arrows). Within the hindlimb, the peroneal and tibial branch of the sciatic nerve were defasciculated and fanned throughout the entire hindlimb (Fig. 9C, D) instead of branching in two target specific bundles as in control embryos (Fig. 9A, B). These findings were corroborated by using an alternative Cre

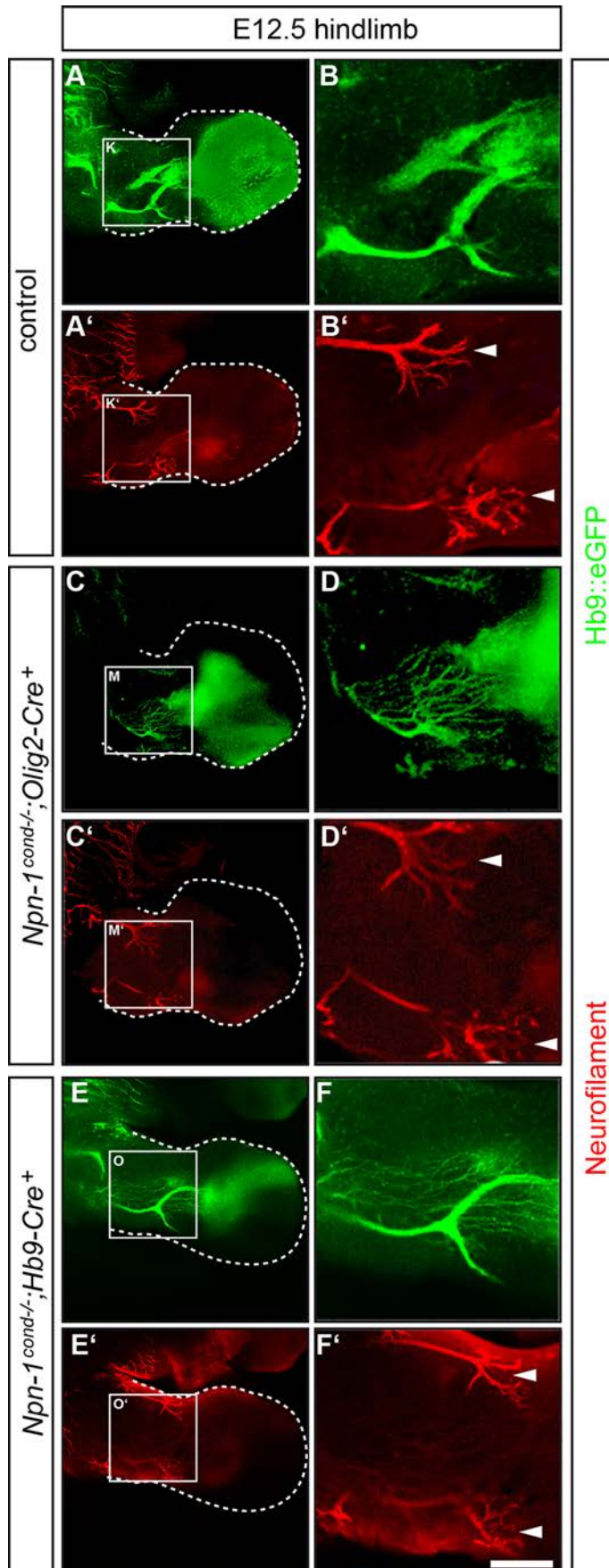


Figure 9: *Npn-1* is required in motor neurons for proper fasciculation of LMC projections to the hindlimb. Wholemount antibody staining of E12.5 embryos against GFP (green, motor nerves) and neurofilament (red, motor and sensory nerves). **(A, A')** Control hindlimb. **(B, B')** Higher magnification of the area boxed in **(A)**. **(C-F)** Analysis of GFP immunofluorescence in wholemount E12.5 embryos reveals that motor axons of the sciatic nerve (peroneal branch) are severely defasciculated and fanned out in *Npn-1^{cond-/-};Olig2-Cre⁺* (n=10) and *Npn-1^{cond-/-};Hb9-Cre⁺* (n=6) mutant embryos instead of forming distinct nerve trunks. **(C'-F')** Wholemount antibody staining against neurofilament shows that defasciculation of motor projections and lack of major rami does not affect fasciculation and distal positioning of sensory nerves in the hindlimb in *Npn-1^{cond-/-};Olig2-Cre⁺* and *Npn-1^{cond-/-};Hb9-Cre⁺* mutant embryos (arrowheads). Scale bar in **(F')** equals 400 μ m for panels **(A, C, E)** and 100 μ m for **(B, D, F)**.

line, *Hb9-Cre* (Arber et al., 1999), to selectively remove *Npn-1* from motor neurons. Motor axons innervating fore- and hindlimbs showed pronounced defasciculation (Figs. 8G, 8H, 9E, 9F), although not as severe as in *Npn-1^{cond/-};Olig2-Cre⁺* mutant embryos. These findings might result from a lower efficiency of the Cre recombinase driven by the *Hb9* promoter. While *Olig2-Cre* removed *Npn-1* from about 70% of the motor neurons in the LMC at brachial levels, *Hb9-Cre* ablated *Npn-1* expression only from 40 % of all motor neurons innervating the embryonic forelimb (Fig. 7E, K).

To visualize the degree of motor defasciculation in embryos where *Npn-1* was ablated in motor neurons, we measured the pixel intensity along a perpendicular line crossing the 4 major projections of the forelimb, and the peroneal and tibial (1 and 2, respectively, in Fig. 10I, J) branches of the sciatic nerve at hindlimb levels. In embryos mutant for *Npn-1^{cond}* and heterozygous for *Olig2-Cre*, all four nerves innervating the forelimb were heavily defasciculated, and only the radial nerve (number 2 in Fig. 10C, D) could still be identified in the generated plot profile. The same holds true for the hindlimb levels, where the peroneal nerve could not be assigned to the plot profile. The tibial branch, however, was identified in the plot profile, even though it was heavily defasciculated as visualized by several peaks in fluorescence along the perpendicular line (Fig. 10K). In *Npn-1^{cond/-};Hb9-Cre⁺* mutant embryos, the median nerve (3 in Fig. 10E, F) was found to be affected most severely, not forming one distinct branch but being defasciculated over almost the entire area between radial (2) and ulnar nerves (4). At hindlimb level, both nerve branches of the sciatic nerve could be identified, however, also here, motor fibers defasciculated from the major nerve trunk in embryos where *Npn-1* was ablated in motor neurons by *Hb9-Cre* (Fig. 10M, N).

To quantify the defasciculation of motor fibers, we measured the individual thickness of the four major nerve branches in the forelimb, and of the peroneal and tibial nerve branches in the hindlimb. In *Npn-1^{cond/-};Olig2-Cre⁺* and *Npn-1^{cond/-};Hb9-Cre⁺* mutant embryos the values were increased significantly due to fibers defasciculating from all nerve branches, broadening the area these nerves are occupying within the developing limbs (Fig. 10S). These findings corroborate the qualitative analysis, where defasciculated fibers are indicated as a peak along a perpendicular line in a plot profile. Note that the increased thickness of hindlimb nerves in *Npn-1^{cond/-};Hb9-Cre⁺* mutant embryos does not indicate a more severe degree of defasciculation, but rather a wider spread of defasciculated nerve fibers.

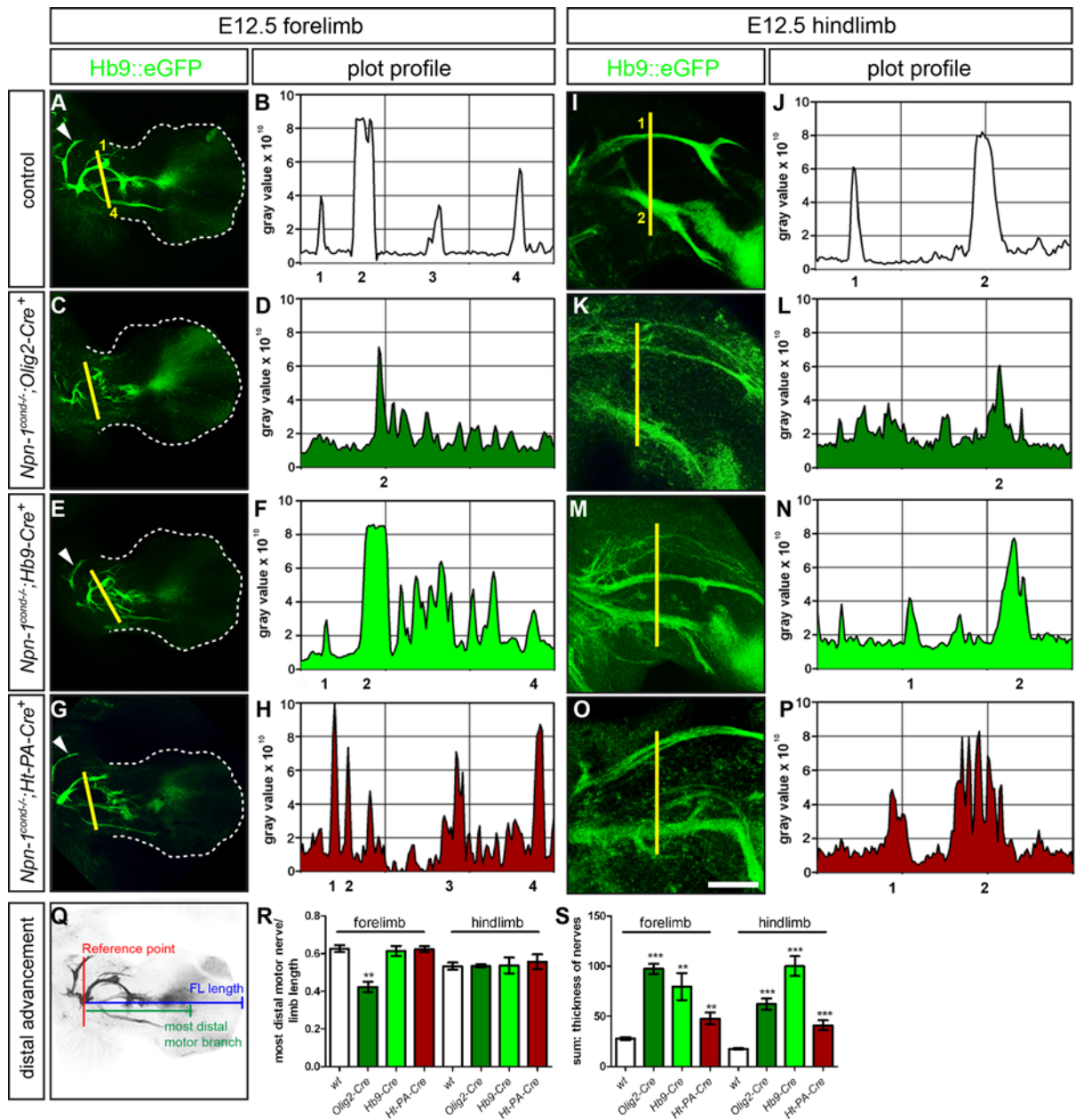


Figure 10: Fasciculation and distal advancement of motor projections are impaired after ablation of *Npn-1* from motor or sensory neurons.

Defasciculation of motor nerves was assessed by calculating a plot profile of Hb9::eGFP positive motor projections crossing a virtual line. **(A, B)** In control embryos four major projections were present (1= branch of n. radialis, 2= n. radialis, 3= n. medianus, 4= n. ulnaris, arrowhead = n. musculocutaneous). **(C, D)** In *Npn-1^{cond/-};Olig2-Cre⁺* mutant embryos only the n. radialis (2) could be assigned to the plot profile, whereas all other motor projections were heavily defasciculated, leading to many peaks along the virtual line. **(E, F)** In *Npn-1^{cond/-};Hb9-Cre⁺* mutant embryos, (1), (2) even though it is defasciculated more distally, and (4) can be assigned to the peaks in the plot profile, whereas the median nerve is heavily defasciculated. **(G, H)** All four nerve branches were found in *Npn-1^{cond/-};Ht-PA-Cre⁺* mutant embryos, however, at slightly inappropriate positions relative to each other, with defasciculated fibers in between major nerve branches. **(I, J)** In control embryos the two major projections of the sciatic nerve are present (1 = n. peroneus, 2 = n. tibialis). **(K, L)** In *Npn-1^{cond/-};Olig2-Cre⁺* mutant embryos, (2) can be assigned to the plot profile, even though smaller fibers are defasciculated from the main branch. (1) is split up into many small projections that did not merge to a fascicle when growing into the distal limb. **(M, N)** In *Npn-1^{cond/-};Hb9-Cre⁺* mutant embryos, (1) shows many small fibers that are separated from the main nerve trunk, whereas (2) appears normal. **(O, P)** Ablation of *Npn-1* from sensory neurons by *Ht-PA-Cre* causes defasciculation of motor projections,

shown in the plot profile to result particularly in defasciculation of (2). **(Q, R)** At forelimb level, distal advancement of motor fibers was significantly reduced in *Npn-1^{cond/-};Olig2-Cre⁺* mutant embryos while it was unchanged when *Npn-1^{cond/-}* mice were crossed to the *Hb9-Cre* line (0.61 +/- 0.03), or the *Ht-PA-Cre* line (0.62 +/- 0,016). At hindlimb level, distal advancement was not altered in any of the analyzed genotypes. **(S)** Quantification of motor fiber defasciculation: Measurement of the thickness of motor nerve branches in the forelimb was found to be significantly increased values in *Npn-1^{cond/-};Olig2-Cre⁺* (97.4 +/-5.0 SEM, p≤0.001), *Npn-1^{cond/-};Hb9-Cre⁺* (79.7 +/-13.4 SEM, p<0.005) and *Npn-1^{cond/-};Ht-PA-Cre⁺* mutant embryos (47,9 +/- 5,98 SEM, p≤0,001), when compared to wildtype embryos (27,8 +/- 1,4 SEM). At hindlimb level, quantification of the defasciculation by summarizing the thicknesses of tibial and peroneal nerves revealed increased defasciculation in *Npn-1^{cond/-};Olig2-Cre⁺* (62.3 +/-5.5 SEM, p≤0.001), *Npn-1^{cond/-};Hb9-Cre⁺* (100.1 +/-9.7 SEM, p≤0.001), and *Npn-1^{cond/-};Ht-PA-Cre⁺* (41.1 +/-4.9 SEM, p<0.005) mutants when compared to wildtype littermates (17.7 +/-0.8 SEM). Both limbs were quantified. Scale bar in **(O)** equals 400µm for panels **(A, C, E, G)**, and 100µm for **(I, K, M, O)**.

In addition to the fasciculation, in *Npn-1^{cond/-}; Olig2-Cre⁺* embryos the distal advancement of motor axons into the forelimb also appeared to be impaired. We therefore measured the length of the distal-most motor nerve fiber and correlated it to the length of the forelimb (Fig. 10Q, R): Advancement of motor axons into the distal forelimb was significantly reduced in embryos where *Npn-1* was ablated in motor neurons by *Olig2-Cre* (0,42 +/- 0,03 SEM), when compared to littermate controls (0,63 +/- 0,02 SEM; p<0,005). Distal advancement of motor nerves in the hindlimbs of *Npn-1^{cond/-}; Olig2-Cre⁺* mutant embryos, and into fore- and hindlimbs of embryos, where *Npn-1* was ablated by *Hb9-Cre* was unaffected.

Interestingly, not only projections from the LMC innervating targets in the fore- and hindlimbs were affected by selective removal of *Npn-1* from motor neurons. Motor neurons from the lateral aspect of the MMC innervate the intercostal musculature at thoracic levels. In wildtype embryos these intercostal nerves are tightly bundled without fibers crossing between the main bundles (Fig. 11A, A'). In mice, where *Npn-1* was ablated from motor neurons by *Olig2-Cre* or *Hb9-Cre*, we found aberrant crossings between the main nerve trunks: 14,17 +/- 4.1 SEM axons were crossing between the main fascicles in *Npn-1^{cond/-};Olig2-Cre⁺* mutant embryos (Fig. 11B, B' arrowheads, p<0,005) and 16.00 +/- 2.86 SEM crossings in *Npn-1^{cond/-};Hb9-Cre⁺* mutant embryos (Fig. 11C, C' arrowheads, p=0,005) versus 0,5 +/- 0,5 crossings per embryo in controls.

These data indicate that *Npn-1* is required in spinal motor neurons for adequate fasciculation of motor trajectories to the distal limbs and trunk musculature.

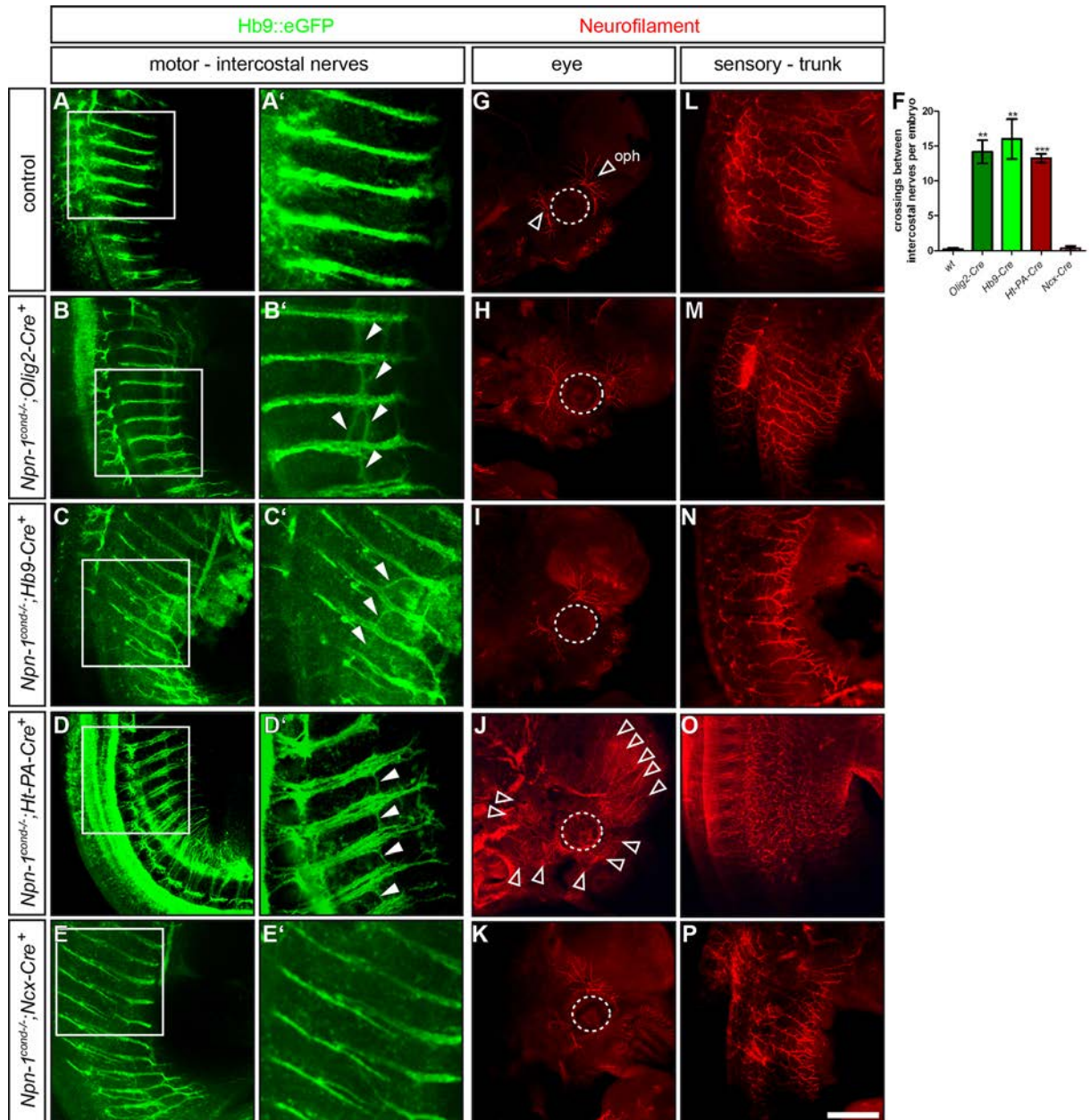


Figure 11: Defasciculation of MMC projections after cell type specific removal of *Npn-1*.

(A, A') Intercostal innervation of an E12.5 embryo stained against Hb9::eGFP (motor nerves). (B, B') Elimination of *Npn-1* from motor neurons using the *Olig2-Cre* line leads to misprojections of MMC nerve branches innervating intercostal muscles with axons crossing between the main nerve bundles (arrowheads, n=6). (C, C') Also in *Npn-1^{cond/-};Hb9-Cre⁺* mutant embryos, crossings between main intercostal nerve fascicles were observed (arrowheads, n=4). (D, D') Ablation of *Npn-1* from sensory neurons by *Ht-PA-Cre* leads to defasciculation of motor projections at thoracic levels. Motor axons cross frequently between major nerve bundles. (E, E') In *Npn-1^{cond/-};Ncx-Cre⁺* mutant embryos, no intercostal crossings were observed. (F) Quantification of the number of crossings between intercostal nerves per embryo (G) Ophthalmic sensory innervation (empty arrowheads) of the eye (circled dashed line) in a control embryo at E12.5 is visualized by neurofilament staining. (H, I, K) Ophthalmic innervation of the eye is not altered in embryos where *Npn-1* was ablated in motor neurons, or in *Npn-1^{cond/-};Ncx-Cre⁺* mutant embryos. (J) In *Npn-1^{cond/-};Ht-PA-Cre⁺* mutant embryos, ophthalmic innervation is severely defasciculated and growing exuberantly around the eye (arrowheads), or into the eye (circled dashed line). (L) Sensory innervation of the skin of the trunk of a control embryo. (M, N, P) Sensory innervation of the skin of the trunk is not altered in *Npn-1^{cond/-};Olig2-Cre⁺*, *Npn-1^{cond/-};Hb9-Cre⁺* and *Npn-1^{cond/-};Ncx-Cre⁺* mutant embryos. (O) Severe defasciculation of sensory trunk innervation of *Npn-1^{cond/-};Ht-PA-Cre⁺* mutant embryos. Scale bar in (P) equals 500µm for panels (A-E) and (G-P), and 200µm for (A'-E').

1.2 *NPN-1* IN SPINAL MOTOR NEURONS IS REQUIRED FOR ACCURATE DORSAL-VENTRAL GUIDANCE OF LMC AXONS

The stereotypical dorsal-ventral guidance decisions of LMC axons at the base of the limb could be impaired by the pronounced defasciculation of motor projections. To examine whether cell-type specific removal of *Npn-1* from motor neurons affected this guidance decision, we retrogradely labeled motor neuron cell bodies by injection of dextran-coupled Rhodamine into either the dorsal or ventral limb musculature of E12.5 embryos. We then assessed the presence of retrogradely transported fluorescent tracer in the cell bodies of dorsally projecting, *Lim1* positive motor neurons of the LMCI, or ventrally projecting, *Isl1* positive motor neurons of the LMCm. In control embryos, only very few motor neurons that were retrogradely

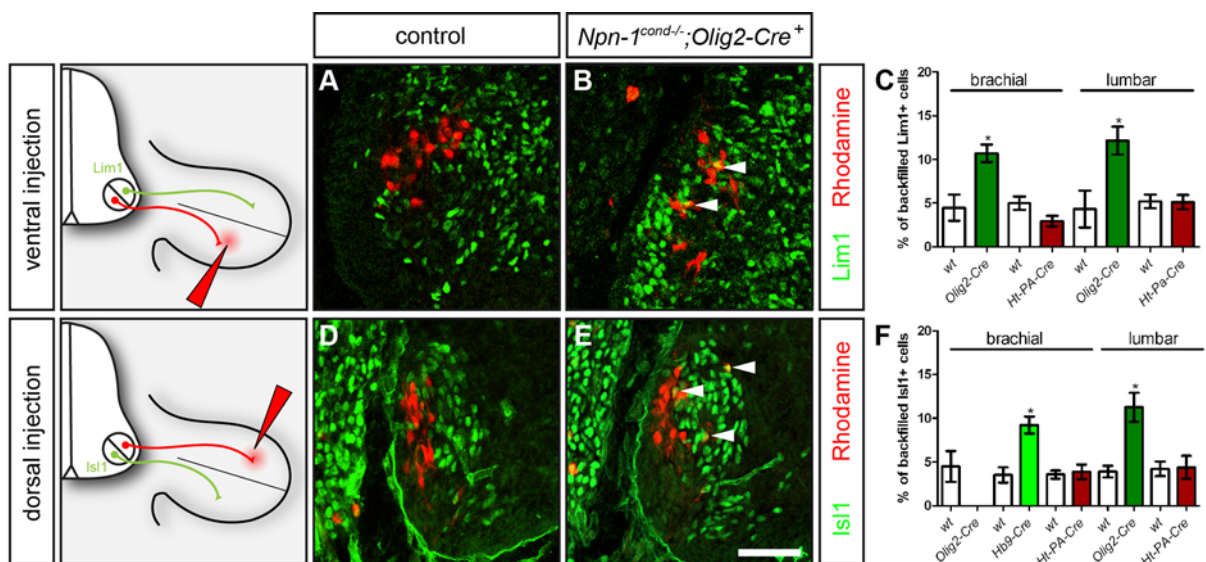


Figure 12: LMC projections are misrouted when *Npn-1* is removed from motor neurons. Retrograde tracing of ventrally and dorsally projecting LMC neurons by injection of dextran-coupled Rhodamine into the limb musculature of E12.5 embryos. **(A)** After ventral injection of the fluorescent tracer, backfilled motor neurons are not *Lim1* positive neurons in control embryos. **(B, C)** Injection of fluorescent tracer into the ventral musculature of *Npn-1^{cond/-}; Olig2-Cre⁺* mutant embryos showed a significant increase of aberrantly projecting *Lim1* positive neurons of the LMCI at lumbar ($p=0.03$, $n=4$) and brachial levels ($p=0.01$, $n=4$, arrowheads) when compared to controls (4.33% ± 2.11 and $n=4$, 4.48% ± 1.5, respectively). **(D)** Dorsal injection of fluorescent tracer leads to no backfilled, *Isl1* positive neurons in control embryos. **(E, F)** In *Npn-1^{cond/-}; Olig2-Cre⁺* mutant embryos increased numbers of dorsally backfilled misprojecting neurons were found at lumbar levels ($p=0.01$, arrowheads) compared to only 3.9% ± 0.65 in littermate controls. Dorsal backfill of *Npn-1^{cond/-}; Hb9-Cre⁺* mutant embryos shows increased misprojection of LMCm neurons at brachial levels. **(C, F)** Retrograde tracing from ventral and dorsal limb mesenchyme of *Npn-1^{cond/-}; Ht-PA-Cre⁺* mutant embryos did not show an increase of pathfinding errors at brachial (2.95% ± 0.59 SEM and 3.86% ± 0.84 SEM, respectively) nor lumbar levels (5.1% ± 0.82 SEM and 4.33% ± 1.31 SEM, respectively) when compared to wildtype littermate embryos (forelimb^{ventral} = 4.99% ± 0.76 SEM., forelimb^{dorsal} = 3.56% ± 0.47 SEM; hindlimb^{ventral} = 5.19% ± 0.77 SEM, hindlimb^{dorsal} = 4.21% ± 0.84 SEM). Scale bar in **(E)** equals 45µm for all panels.

labeled from the ventral fore- or hindlimb expressed Lim1 (Fig. 12A, C). In contrast, the number of Lim1-positive LMCI cells that were retrogradely labeled from the ventral limb and thus identified as misprojecting, was significantly increased to 10.71% +/- 0,99 SEM at brachial levels and 12,16% +/- 1,59 SEM at lumbar levels in embryos, where *Npn-1* was ablated in motor neurons by *Olig2-Cre* (arrowheads in Fig. 12B, C). A similar analysis of motor neurons backfilled from dorsal limb musculature revealed that 11.25 % +/- 1,66 SEM LMCm motor neurons misprojected their axons to the dorsal half of the hindlimbs in *Npn-1^{cond/-};Olig2-Cre⁺* mutant embryos (arrowheads in Fig. 12E, F). At brachial levels, the dorsal injections did not result in any retrogradely labeled neurons, which is due to the reduced ingrowth of motor axons into the forelimb in *Npn-1^{cond/-};Olig2-Cre⁺* mutant embryos (Figs. 8E, 10R, 12F). We therefore assessed the guidance fidelity of LMCm motor neurons in *Npn-1^{cond/-};Hb9-Cre⁺* mutant embryos where motor axons are defasciculated, but are found at roughly comparable distal positions in the forelimbs as in control littermates (Fig. 8A, B, G, H). Retrograde tracing from the dorsal limb revealed that 9.21 % +/- 0.97 SEM of *Isl1* positive LMCm neurons misprojected their axons to dorsal limb musculature in mutant embryos when compared to control littermates (3.51 % +/- 0.88 SEM, $p=0,012$).

Taken together, these data show that cell type specific ablation of *Npn-1* from motor neurons not only leads to defasciculation of motor projections, but also to impairments in the pathfinding fidelity of motor axons at the dorsal-ventral choice point.

1.3 ABLATION OF *NPN-1* FROM SPINAL MOTOR NEURONS DOES NOT AFFECT FASCICULATION OF SENSORY PROJECTIONS INTO THE PERIPHERY

To establish peripheral innervation of the limb, sensory axons from the DRG and motor axons from the ventral horn of the spinal cord form conjoined trajectories on the way to their respective targets. To what extent the later born sensory axons depend on the correctly laid out motor projections in the formation of their peripheral projection patterns, however, is not clear. In *Npn-1^{cond/-}; Hb9-Cre⁺* mutant embryos, motor axons in the limb arrive at roughly appropriate distal positions (Fig. 8G, H), while in *Npn-1^{cond/-};Olig2-Cre⁺* mutant embryos, motor innervation is severely

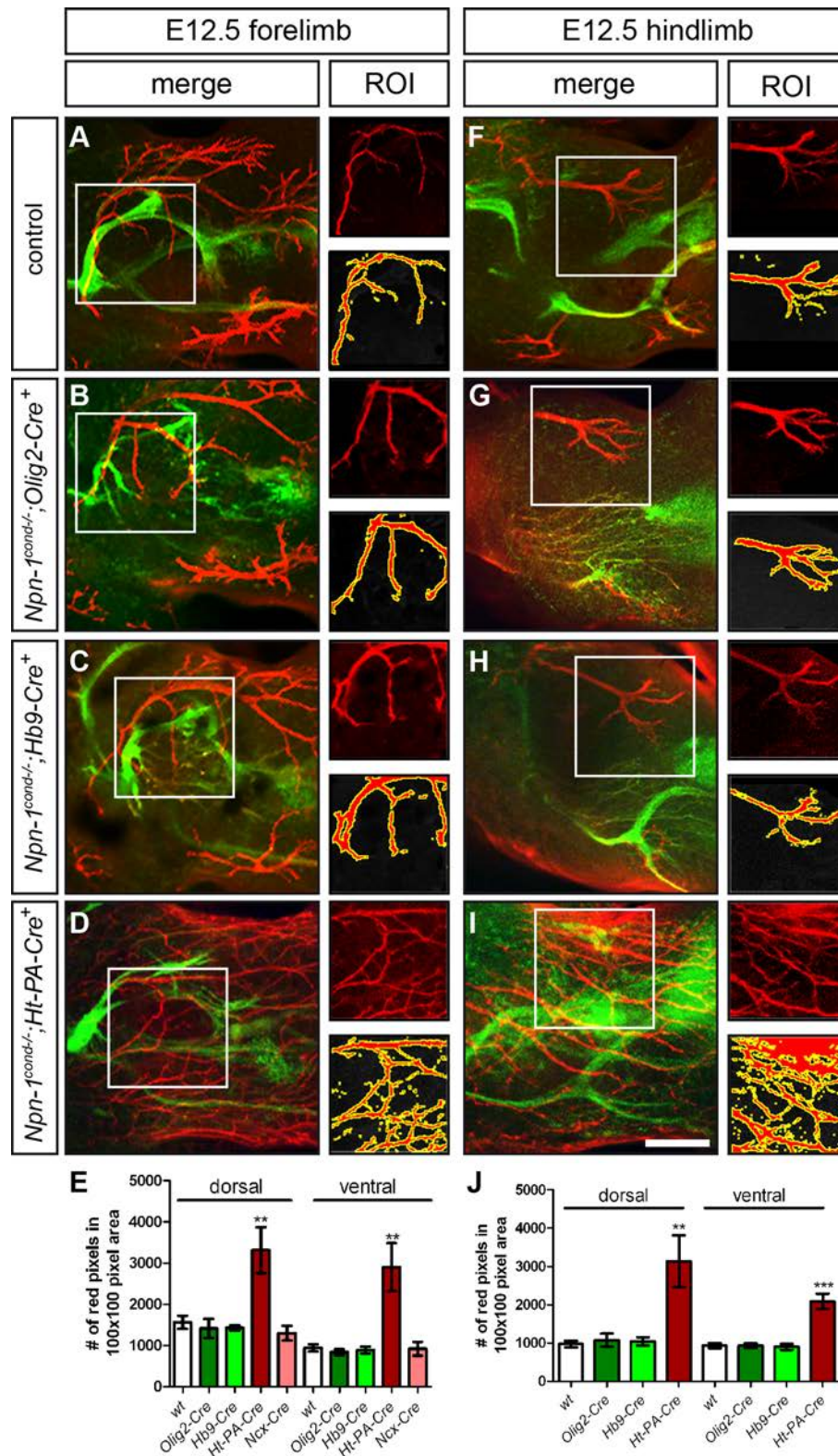


Figure 13: Quantification of sensory defasciculation after ablation of *Npn-1* in either motor or sensory neurons.

Defasciculation of cutaneous sensory nerves was assessed by calculating the number of neurofilament positive red pixels in a given 100x100 pixel region of interest (ROI, white squares in (A-D) and (F-I)). (A) Control forelimb. (B, C, E) Sensory innervation was not altered in *Npn-1^{cond-/-};Olig2-Cre⁺*, *Npn-1^{cond-/-};Hb9-Cre⁺* and *Npn-1^{cond-/-};Ncx-Cre⁺* mutant embryos in the forelimb. (D) Number of neurofilament positive pixels is significantly increased in *Npn-1^{cond-/-};Ht-PA-Cre⁺* mutant embryos. (E) Quantification of sensory defasciculation in the dorsal and ventral forelimb, both limbs were quantified,

$p^{Ht-PA-Cre \text{ dorsal}} \leq 0.005$, $p^{Ht-PA-Cre \text{ ventral}} \leq 0.005$. **(F)** Control hindlimb. **(G, H, J)** Quantification of sensory defasciculation in the hindlimb does not show differences in $Npn-1^{cond-/-}; Olig2-Cre^+$ and $Npn-1^{cond-/-}; Hb9-Cre^+$ mutant embryos. **(I)** Significant increase of defasciculated sensory innervation in $Npn-1^{cond-/-}; Ht-PA-Cre^+$ mutant embryos at hindlimb level. **(J)** Quantification of sensory defasciculation in the dorsal and ventral hindlimb, both limbs were quantified, $p^{Ht-PA-Cre} \leq 0,005$, $p^{Ht-PA-Cre \text{ ventral}} \leq 0,001$. Scale bar in **(I)** equals 100 μ m for all panels.

defasciculated and stunted (Fig. 8D, E). Surprisingly, the formation of cutaneous sensory trajectories to the skin (Fig. 8E', H') and proprioceptive projections along motor nerves to the muscles (open arrowheads in Fig. 8D', G') were unaffected by the deficits in motor axon growth and fasciculation in both mutant mouse lines. Sensory nerves reached appropriate distal positions within the embryonic forelimb when compared to control embryos (arrowheads and open arrowheads in Fig. 8D', G'). Sensory axons growing along the median nerve to innervate the palm form a normally patterned, fan-like structure ("med" in Fig. 8A', D', G'). Also sensory innervation along the ulnar nerve developed normally in $Npn-1^{cond-/-}; Hb9-Cre^+$ mutant embryos (Fig. 8I, arrowhead in I'). This was even the case in $Npn-1^{cond-/-}; Olig2-Cre^+$ mutant embryos, where the ulnar nerve did not extend as far as in control embryos, and only an ectopic motor branch was detected (arrow in Fig. 8F, arrowhead in Fig. 8F'). In the hindlimb of embryos where $Npn-1$ was removed by either $Olig2-Cre$ or $Hb9-Cre$, we observed a similar phenotype: motor projections were defasciculated, while the sensory branching patterns were established normally when compared to littermate controls (arrowheads in Fig. 9B', D', F'). Furthermore, no alteration of cutaneous sensory projections of the trunk, or ophthalmic projections towards the eye were observed in $Npn-1^{cond-/-}; Olig2-Cre^+$ and $Npn-1^{cond-/-}; Hb9-Cre^+$ mutant embryos (Fig. 11H, I, M, N). To quantify the defasciculation of sensory projections in the limbs we counted the number of neurofilament positive pixels in a defined region of interest of cutaneous sensory innervation to the dorsal and ventral limb. When compared to littermate controls (Fig. 13A, F), we found no difference in the fasciculation of sensory innervation to fore- and hindlimbs of $Npn-1^{cond-/-}; Olig2-Cre^+$ (Fig. 13B, E, G, J) and $Npn-1^{cond-/-}; Hb9-Cre^+$ mutant embryos (Fig. 13C, E, H, J).

These data indicate that peripheral sensory projections are established correctly, even though motor projections to fore- and hindlimbs are severely defasciculated due to loss of $Npn-1$ signaling in motor neurons.

1.4 ABLATION OF *NPN-1* FROM SENSORY NEURONS CAUSES DEFASCICULATION OF SENSORY PROJECTIONS TO THE BODY AND EXTREMITIES

To assess the consequences of ablation of *Npn-1* from sensory neurons we crossed *Npn-1^{cond}* mice with a mouse line expressing Cre recombinase under the control of the neural crest homeobox protein (*Ncx*, Neil Shneider, unpublished data), which is expressed in tissues derived from neural crest cells, particularly in neurons of the DRG, enteric nerve ganglia and parasympathetic ganglia of the heart (Hatano et al., 1997, Shirasawa et al., 1997). In E12.5 *Npn-1^{cond/-};Ncx-Cre⁺* mutant embryos, we did not find alterations in motor or sensory innervation of the limbs (open arrowheads and arrowheads, respectively in Fig. 14D), nor of cutaneous innervation of the trunk (Fig. 11P) or ophthalmic projections to the eye (Fig. 11K) when compared to control embryos. Also motor intercostal innervation was not altered in embryos, where *Npn-1* was ablated in sensory neurons by *Ncx-Cre* (Fig. 11E, E').

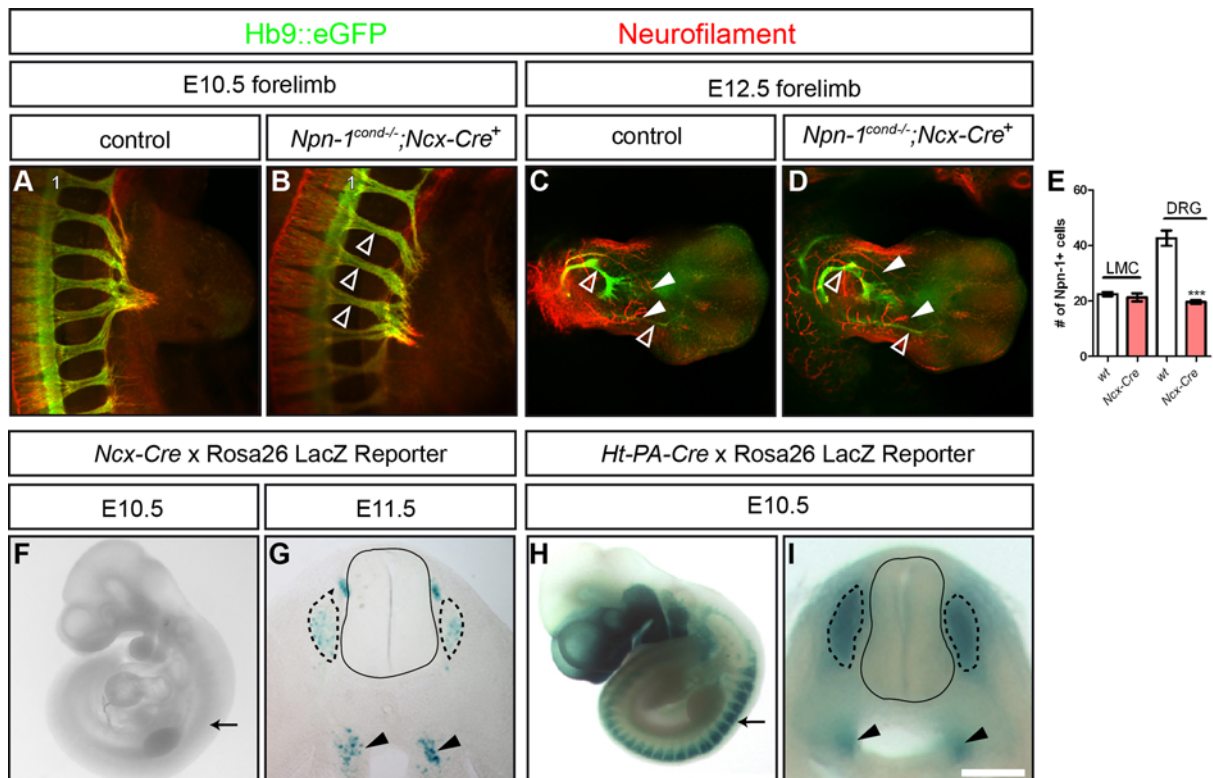


Figure 14: Late ablation of *Npn-1* in sensory neurons does not affect fasciculation of sensory innervation of the limbs.

(A-D) Wholemount antibody staining of E10.5 and E12.5 embryos against Hb9::eGFP (green, motor nerves) and neurofilament (red, motor and sensory nerves). (A) Plexus region of an E10.5 control embryo. (B) Fasciculation of spinal nerves (empty arrowheads) and plexus formation is not impaired in

Npn-1^{cond/-};Ncx-Cre⁺ mutant embryos. **(C)** Motor and sensory innervation of an E12.5 control forelimb. **(D)** Formation of sensory nerve growth patterns (arrowheads) and motor innervation (empty arrowheads) are not affected by ablation of *Npn-1* in sensory neurons by *Ncx-Cre*. **(E)** Quantification of *Npn-1* positive cells shows no alteration in the LMC, but a decrease in the DRG at brachial levels in *Npn-1^{cond/-};Ncx-Cre⁺* mutant embryos at E12.5 (n=3, $p^{Ncx-Cre\ DRG} \leq 0,001$). **(F, G)** Activation of the LacZ Reporter by *Ncx-Cre* in DRG (black dashed lines) and enteric ganglia (arrowheads) occurs only at E11.5, while at E10.5 no β -galactosidase staining was observed. **(H, I)** *Ht-PA-Cre* robustly activates the LacZ Reporter already at E10.5 in DRG (arrow, black dashed lines) and enteric ganglia (arrowheads). Scale bar in **(I)** equals 500 μ m for **(A, B)**, 400 μ m for **(C, D)**, 2,5mm for **(F, H)**, 1mm for **(G)**, and 1,3mm for **(I)**.

Quantification of *Npn-1* positive cells by *in situ* hybridization on cross sections of E12.5 embryos showed a significant down-regulation of *Npn-1*-positive cells in the DRG, while the number of *Npn-1* positive motor neurons was normal in *Npn-1^{cond/-};Ncx-Cre⁺* mutant embryos (Fig. 14E, $p \leq 0,001$). We therefore employed an expression analysis to define the onset of Cre-recombination by crossing the Cre line to a *ROSA26R-LacZ* reporter strain (Soriano, 1999), where expression of β -galactosidase is activated upon onset of Cre-expression. We found that the *Ncx-Cre* line activates the *LacZ* gene in DRG and enteric ganglia, but leads to a weak β -galactosidase staining only at E11.5 (Black dashed line and arrowheads in Fig. 14G, respectively). At E10.5, when spinal nerves reach the plexus region at the base of the limb, no activation of β -galactosidase was observed (Fig. 14F).

To determine whether the late onset of Cre recombination is responsible for the wildtype-like appearance of *Npn-1^{cond/-};Ncx-Cre⁺* mutant embryos, we utilized another transgenic line, expressing Cre recombinase under the *human tissue plasminogen activator* promoter (*Ht-PA-Cre*; Pietri et al., 2003). This line targets neural crest cells and the same structures within the sensory nervous system, vasculature and cephalic tissues as the *Wnt1-Cre* line (Danielian et al., 1998), but is not expressed in cells of the dorsal neural tube. Crossed to the LacZ-reporter strain, activation of the *LacZ* gene could be observed already at E8.5 (data not shown). At E10.5, the *Ht-PA-Cre* line showed robust expression of β -galactosidase in the DRG (arrow in Fig. 14H, black dashed lines in I) and enteric ganglia (arrowheads in Fig. 14I). In *Npn-1^{cond/-};Ht-PA-Cre⁺* mutant embryos we found reduced levels of *Npn-1* mRNA in sensory neurons of the DRG (Fig. 7G, J), and reduced levels of *Npn-1* protein in sensory axons (empty arrowheads in Fig. 7I), while motor neurons and axons expressed normal amounts of mRNA and protein (arrows and arrowheads, respectively, in Fig. 7G, I). Interestingly, sensory fibers contributing to the cutaneous innervation to the fore- and hindlimbs of E12.5 *Npn-1^{cond/-};Ht-PA-Cre⁺* mutant

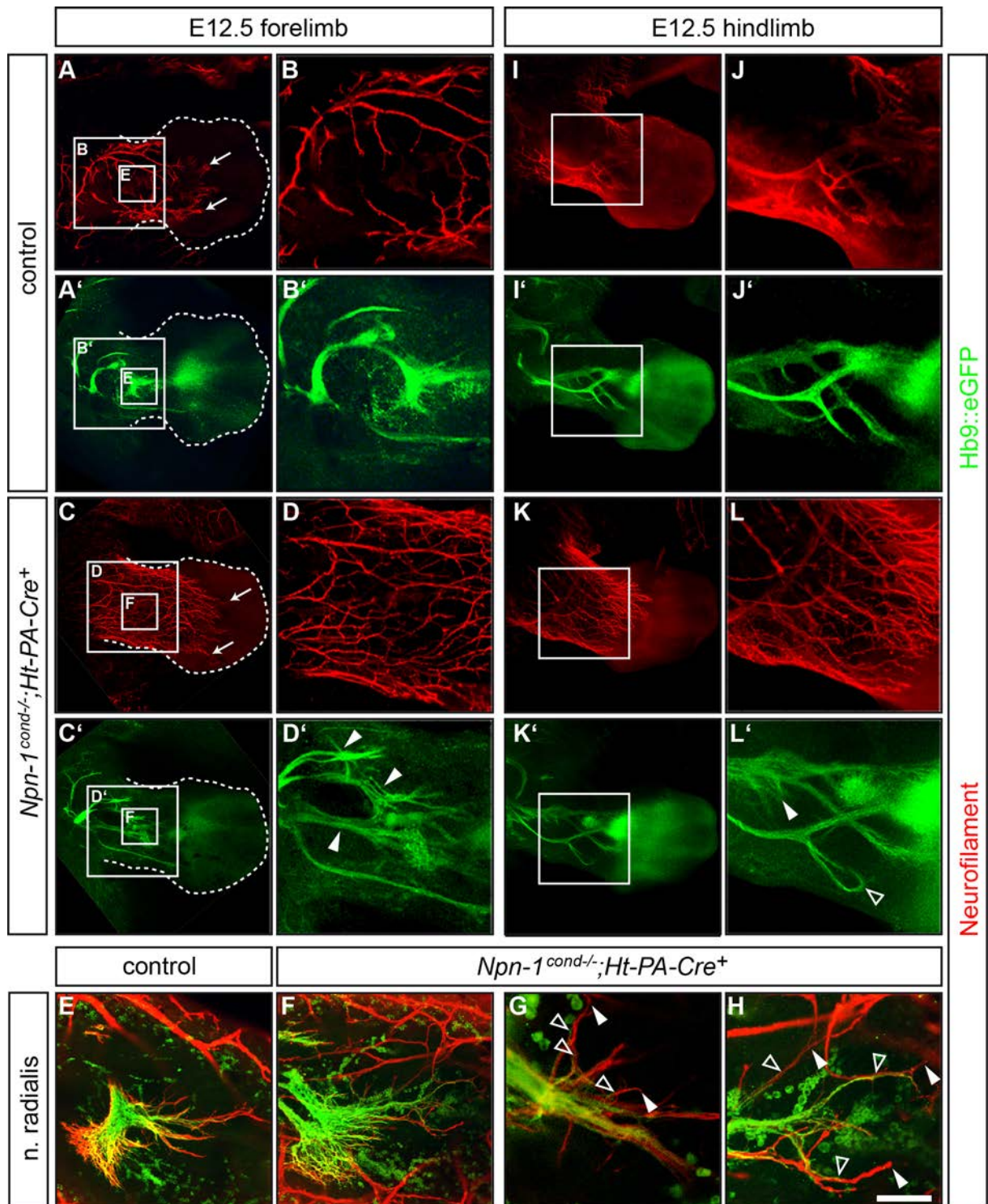


Figure 15: Removal of *Npn-1* from sensory neurons leads to defasciculation of sensory and motor projections to the limbs.

Wholemount antibody staining of E12.5 embryos against GFP (green, motor nerves) and neurofilament (red, motor and sensory nerves). **(A, A')** Control forelimb. **(B, B')** Higher magnification of the area boxed in **(A)**. **(C, D)** Ablation of *Npn-1* from sensory neurons leads to severe defasciculation and exuberant growth of sensory projections to the forelimb in *Npn-1^{cond-/-};Ht-PA-Cre⁺* mutant embryos (arrows). **(C', D')** A higher magnification of the boxed area in **(C')** reveals that the severe defasciculation of sensory projections is associated with defasciculation of major motor nerve trunks in the forelimb (arrowheads). **(E-H)** A high magnification of the radial nerve shows aberrant projections of motor axons (open arrowheads) that are always preceded by an aberrantly projecting sensory axon (arrowheads). $n^{\text{mutant}} = 7$, $n^{\text{control}} = 8$. **(I, I')** Control hindlimb. **(J, J')** Higher magnification of

the boxed areas in **(I)**. **(K, L)** Elimination of Npn-1 from sensory neurons causes strong defasciculation and exuberant growth of sensory nerves in *Npn-1^{cond/-};Ht-PA-Cre⁺* mutant animals. **(K', L')** Motor projections in *Npn-1^{cond/-};Ht-PA-Cre⁺* mutant embryos show defasciculation of the tibial nerve (arrowhead) and loop formation of the superficial branch of the peroneal nerve (empty arrowhead). n=5. Scale bar in **(H)** equals 400µm for **(A, C, I, K)**, 100µm for **(B, D, J, L)**, 25µm for **(E, F)** and 10 µm for **(G, H)**.

embryos did not form distinctly patterned branches as in control embryos (Fig. 15A, B, I, J), but were profoundly defasciculated and showed aberrant, exuberant growth (arrows in Fig. 15C, D, K, L). When we quantified the degree of defasciculation of sensory projections to both dorsal or ventral fore- and hindlimbs we found a significant increase of neurofilament positive pixels in a defined region of interest (Fig. 13D, E, I, J), when compared to littermate controls (Fig. 13A, F). Furthermore, we observed severe defasciculation of the cutaneous innervation of the trunk in *Npn-1^{cond/-};Ht-PA-Cre⁺* mutant embryos at the thoracic level (Fig. 11O), and also ophthalmic projections to the eye were defasciculated, growing in very thin projections all over the head and into the eye area (open arrowheads and dashed circle in Fig. 11J, respectively).

These findings suggest that timing of *Npn-1* expression plays a crucial role for fasciculation of sensory projections to the body and extremities: Early removal of the axon guidance receptor from sensory neurons impairs peripheral growth and patterning of sensory nerves. Ablation at a time point, when spinal nerves have reached or already transversed the plexus region at the base of the limb does not alter peripheral sensory projections.

1.5 ABLATION OF *NPN-1* IN SENSORY NEURONS LEADS TO DEFASCICULATION OF MOTOR PROJECTIONS

Surprisingly, the severe defasciculation of sensory axons in the limbs of E12.5 *Npn-1^{cond/-};Ht-PA-Cre⁺* mutant embryos was accompanied by defasciculation of motor projections: in the forelimb, the radial and median nerves showed deficits in fasciculation (arrowheads in Fig. 15D'). At hindlimb level, the tibial nerve was defasciculated before the branching point (arrowhead in Fig. 15L'). In addition to defasciculation, we also observed errors in axonal growth: in two out of five embryos, one branch of the peroneal nerve was observed to form a loop (empty arrowhead in Fig. 15L'), a behavior that was never observed in wildtype controls (Fig. 15I', J'). We

quantified the degree of motor defasciculation by measuring the intensity of Hb9::eGFP along a perpendicular line positioned over the 4 major motor projections of the forelimb, and the two main projections of the hindlimb. While motor nerves grew to roughly appropriate distal positions and also the distal advancement of motor nerves was not affected in *Npn-1^{cond/-};Ht-PA-Cre⁺* mutant embryos (Fig. 10R), defasciculated nerve fibers were observed in the plot profile in between the major projections to the distal fore-and hindlimbs (Fig. 10G, H, O, P) when compared to control embryos (Fig. 10A, B, I, J,). Measurement of the thickness of the individual motor nerve branches revealed an increased value in embryos where *Npn-1* was eliminated in sensory neurons by *Ht-PA-Cre*, albeit to a less severe degree than that caused by ablation of *Npn-1* in motor neurons (Fig. 10S). Not only motor projections to the limbs, but also intercostal nerves were affected by loss of *Npn-1* in sensory neurons: In *Npn-1^{cond/-};Ht-PA-Cre⁺* mutant embryos, intercostal nerve branches were defasciculated; 13,25 +/- 0,63 SEM axons were frequently crossing between the main fascicles (arrowheads in Fig 11D', F, $p \leq 0,001$) when compared to control littermates (0,40 +/- 0,24 SEM).

When we observed the motor branches in the forelimbs at a higher magnification, we found that defasciculated motor fibers, for example of the radial nerve, were always accompanied and preceded by sensory axons (empty arrowheads and arrowheads, respectively, in Fig. 15G, H). We therefore distinguished proprioceptive innervation to the muscles (TrkC-positive sensory fibers) from nociceptive cutaneous innervation (TrkA-positive sensory axons) by immunohistochemistry (Fig. 16B). While expression of *Npn-1* by nociceptive sensory neurons already has been confirmed (Fu et al., 2000), we found that also 19% +/- 1,9 SEM proprioceptive sensory neurons at brachial levels and 16,5% +/- 0,8 SEM at lumbar levels co-expressed *Npn-1* at E12.5 (Fig. 16A, arrows, and data not shown), which therefore is in a position to mediate sensory axon fasciculation. We found that in *Npn-1^{cond/-}; Ht-PA-Cre⁺* mutant embryos, defasciculated motor axons always coincided with TrkA or TrkC positive sensory fibers at the base of the limb, where nerve branches turn either to the dorsal or ventral limb (arrowhead, empty arrowhead and double arrowhead in Fig. 16C). These findings were in stark contrast to what we observed in embryos, where *Npn-1* was ablated in motor neurons: motor axons are defasciculated (arrows in Fig. 16D), however, proprioceptive and nociceptive fibers

are fasciculated and do not follow defasciculated, *Hb9::eGFP* positive motor branches (open arrows in Fig. 16D).

To address whether the defasciculation of motor projections caused by the loss of *Npn-1* from sensory neurons is also accompanied by errors in the pathfinding decision of motor axons, we retrogradely labeled dorsally and ventrally projecting motor neurons in E12.5 embryos. We found no significant increase of misprojecting neurons from the LMCm and LMCI to the dorsal or ventral limb mesenchyme, respectively, at brachial and lumbar levels of *Npn-1^{cond/-};Ht-PA-Cre⁺* mutant embryos (Fig. 12C, F).

These data suggest that defasciculation of sensory axons by removal of *Npn-1* from sensory neurons impairs motor axon fasciculation but not dorsal-ventral guidance fidelity at the choice point at the base of the limbs.

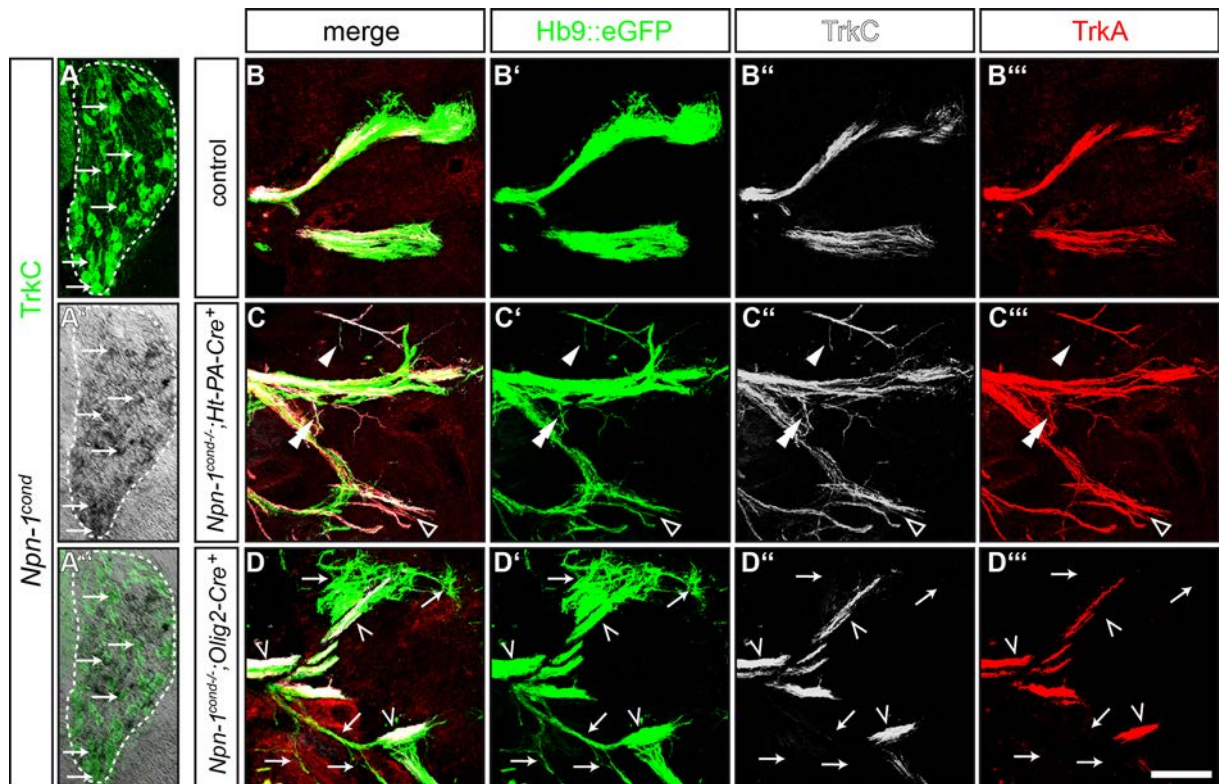


Figure 16: Defasciculation of motor fibers is accompanied by defasciculation of TrkA- and TrkC-positive fibers in *Npn-1^{cond/-};Ht-PA-Cre⁺*, but not in *Npn-1^{cond/-};Olig2-Cre⁺* mutant embryos. (A) Anti-TrkC staining and *in situ* hybridization show that *Npn-1* is expressed in TrkC-positive neurons (arrows). (B) Control embryo, fluorescent immunohistochemistry shows that nociceptive TrkA positive (red) and proprioceptive TrkC positive (white) fibers accompany motor nerves (*Hb9::GFP*, green) on their way into the distal limb. (C) In *Npn-1^{cond/-};Ht-PA-Cre⁺* mutant embryos, defasciculation of motor projections is only observed in combination with severe defasciculation of sensory trajectories, either axons positive for TrkA or TrkC (empty arrowhead and arrowhead, respectively), or fibers positive for both TrkA and TrkC (double arrowhead). (D) In *Npn-1^{cond/-};Olig2-Cre⁺* mutant embryos, no defasciculated sensory axons were observed even in areas with clear defasciculation of motor projections (arrows). Sensory axons grow rather fasciculated and do not seem to be affected by

defasciculation of motor pathways (open arrowheads). Scale bar in (C'') equals 15µm for (A) and 100µm for (B-D).

1.6 FASCICULATION OF MOTOR AXONS BEFORE THE PLEXUS REGION DETERMINES FASCICULATION IN THE DISTAL LIMB

During the establishment of sensory-motor innervation to the extremities of the developing vertebrate limb, the plexus region at the base of the limb is of critical importance. At different axial levels, motor axons from the spinal cord and sensory axons from the DRG grow together as fasciculated spinal nerves towards this region, where they are sorted into new, target specific bundles and are guided towards dorsal and ventral targets within the limbs (Lance-Jones and Landmesser, 1981a, b, Tosney and Landmesser, 1985b, Wang and Scott, 2000). We therefore carefully investigated the effects that loss of *Npn-1* in either motor or sensory neurons might have on the establishment of the plexus. At E12.5, distal motor projections of embryos where *Npn-1* was ablated in motor neurons by either *Olig2-Cre* or *Hb9-Cre* showed pronounced defasciculation (red arrowheads in Fig. 17B, C), and motor nerves appear thinner or stunted (red arrowheads in Fig. 17B).

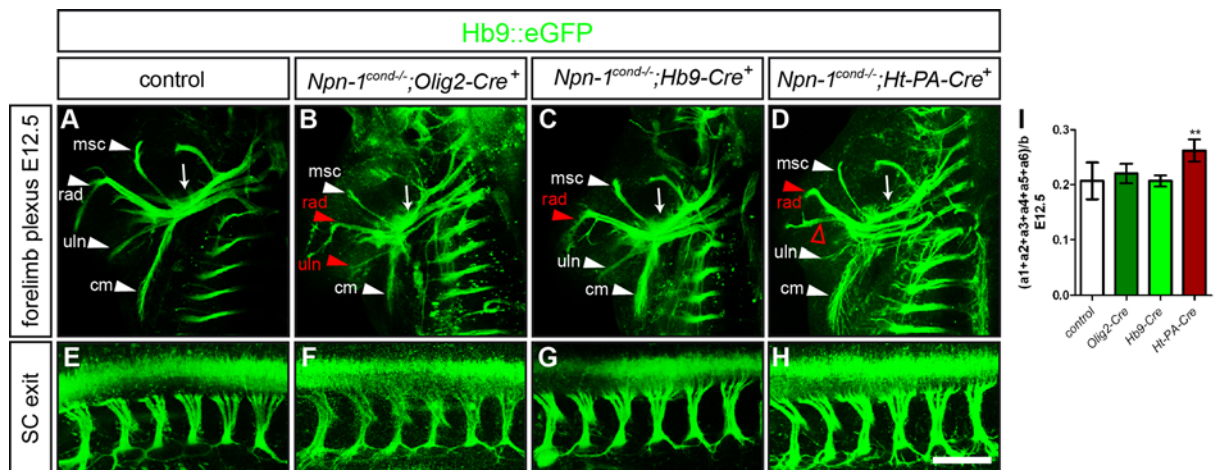


Figure 17: Fasciculation before the plexus determines the fasciculation in the distal limb.

(A, E) Control embryo, dorsal view of the plexus region and exit of brachial spinal nerves from the spinal cord at E12.5. N. musculocutaneous (msc), n. radialis (rad), n. ulnaris (uln), and n. cutaneous maximus (cm) can be identified. (B, F) Spinal nerves are fasciculated from their exit of the spinal cord until they reach the plexus in *Npn-1^{cond-/-};Olig2-Cre⁺* mutant embryos, however, after the plexus motor nerves are thinner, defasciculated (e.g. radial nerve) or stunted (e.g. ulnar nerve). (C, G) Defasciculation after the plexus was also observed in *Npn-1^{cond-/-};Hb9-Cre⁺* mutant embryos, while the spinal nerves were fasciculated from the spinal cord to the plexus. (D, H) In *Npn-1^{cond-/-};Ht-PA-Cre⁺* mutant embryos spinal nerves arrived at the plexus in a slightly defasciculated manner. Motor nerves were also disorganized after the plexus region (red arrowhead and red empty arrowhead) (I)

Quantification of pre-plexus defasciculation shows significantly higher values only in *Npn-1^{cond/-};Ht-PA-Cre⁺* mutant embryos at E12.5 ($p^{Olig2-Cre} = 0,92$, $p^{Hb9-Cre} = 0,84$, $p^{Ht-PA-Cre} < 0,01$, both sides were quantified). Please view the Material and Methods section and Fig. 17I for an explanation of the quantification method. Scale bar in **(H)** equals 200 μ m for **(A-D)** and 100m for **(E-H)**.

Before the plexus region (arrow in Fig. 17A-D), however, spinal nerves grew in a fasciculated manner and showed no enhanced defasciculation after exiting the spinal cord (Fig. 17B, C, F, G, J). In contrast, in embryos where *Npn-1* was ablated from sensory neurons by *Ht-PA-Cre* expression, growth of motor nerves was disorganized before, within, and beyond the plexus region: Sorting of target specific bundles appeared to be impaired, as the small branch of the radial nerve (red arrowhead in Fig. 17D, view also Fig. 15D') was thicker than in control embryos (Fig. 17A). Within the plexus region, motor fibers of the spinal nerves are defasciculated (arrow in Fig. 17F). When we quantified the individual thickness of the six spinal nerves contributing to the brachial plexus after they exited the spinal cord (Fig. 17E-H) and normalized the sum to the length of the spinal cord segment from where these projections originate, we found a significant increase of the fasciculation coefficient only in *Npn-1^{cond/-};Ht-PA-Cre⁺* mutant embryos (Fig. 17I). Embryos, in which *Npn-1* was ablated from motor neurons, did not show alterations in the fasciculation before the plexus region at E12.5 (Fig. 17I).

We next investigated the formation of spinal projections to the plexus region of the forelimb at earlier stages: At E10.5, motor and sensory axons have reached the dorsal-ventral choice point at the base of the limb in wildtype embryos, but have not yet navigated through it (Fig. 18A, A'). In *Npn-1^{cond/-};Olig2-Cre⁺* mutant embryos we observed pronounced defasciculation of motor axons in the plexus region (circled area in Fig. 18B). All these defasciculated axons were stained for Hb9::eGFP, indicating their motor origin (empty arrowheads in Fig. 18B'). Interestingly, defasciculation in *Npn-1^{cond/-};Olig2-Cre⁺* mutant embryos was limited to the plexus region, while spinal nerves projected towards the plexus in a fasciculated manner (arrowheads in Fig. 18B'). Contrary to that, ablation of *Npn-1* from sensory axons by *Ht-PA-Cre* resulted in defasciculation of both motor and sensory projections already before the plexus (arrowheads in Fig. 18C, C'), as well as in the plexus region. Interestingly, mixed sensory-motor spinal nerves are spread over a wider area before they reach the plexus in *Npn-1^{cond/-};Ht-PA-Cre⁺* mutant embryos than in control embryos or embryos where *Npn-1* was ablated from motor neurons (perpendicular view of spinal nerves in Fig. 18E-H). To quantify the degree of pre-plexus

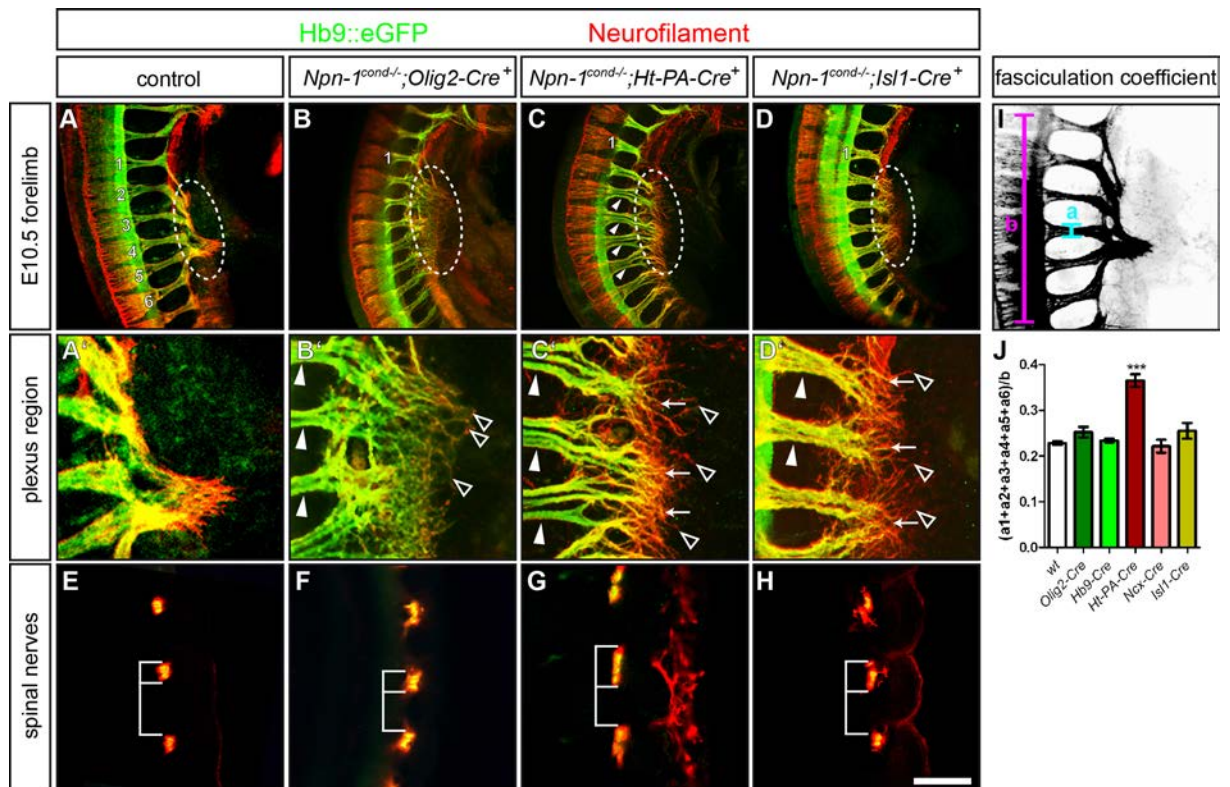


Figure 18: Ablation of *Npn-1* in sensory neurons impairs pre-plexus fasciculation sensory-motor axon coupling.

(A, A') Side view of forelimb plexi of a control E10.5 wholemount embryo stained against GFP (green, motor nerves) and neurofilament (red, motor and sensory nerves), numbers 1-6 mark the spinal nerves contributing to the forelimb plexus, plexus region is encircled with a white dashed line. (E) Perpendicular view of control spinal nerves growing towards the brachial plexus. (B, B', F) Elimination of *Npn-1* selectively from motor neurons (*Olig2-Cre*) leads to defasciculation of motor nerves in the plexus region. Note that all defasciculated and disorganized axons in the plexus region are positive for Hb9::GFP, indicating that these are motor axons (empty arrowheads). (I, J) Quantification of the fasciculation of spinal nerves before the plexus region showed no significant differences in embryos where *Npn-1* was ablated in motor neurons (n=4, arrowheads, $p^{Olig2-Cre}=0,27$). (C, C', G, J) In *Npn-1^{cond-/-};Ht-PA-Cre⁺* mutant embryos, motor and sensory axons are defasciculated in the plexus region and sensory projections are further advanced than motor axons (empty arrowheads and arrows, respectively). Motor and sensory trajectories are defasciculated already before the plexus region (n=6, arrowheads, $p^{Ht-PA-Cre}\leq 0,001$). (D, D', H, J) When *Npn-1* is ablated from both motor and sensory neurons (*Npn-1^{cond-/-};Isl1-Cre⁺*), mutant embryos showed an intermediary phenotype with sensory and motor projections defasciculated in the plexus region and broken sensory-motor axon coupling (arrowheads and arrows, respectively), however, only 2/3 of the mutant embryos exhibit pre-plexus defasciculation (n=6, arrowheads, $p^{Isl1-Cre}=0,23$). (S) For the fasciculation coefficient animals were analyzed for both forelimb regions. Scale bar in (H) equals 500 μ m for (A-D), 150m for (A'-D') and (E-H).

defasciculation, we calculated a fasciculation coefficient measuring the thickness of the six spinal nerves contributing to the brachial plexus at their narrowest point and correlated the results to the total length of the analyzed spinal cord segment (Fig. 18I). Corresponding to what we found at E12.5, the value of the fasciculation coefficient was significantly higher only when *Npn-1* was ablated from sensory neurons by *Ht-PA-Cre* (Fig. 18J). Within the plexus region, we found that sensory axons are further advanced than motor axons (empty arrowheads and arrows,

respectively, in Fig. 18C') in *Npn-1^{cond/-};Ht-PA-Cre⁺* mutant embryos, thus breaking the coupling of sensory axon growth on pre-extending motor axons. This was never observed in *Npn-1^{cond/-};Olig2-Cre⁺* mutant embryos, and also no difference in the value of the fasciculation coefficient was observed in embryos, where *Npn-1* was ablated in motor neurons (Fig. 15S, $p^{Olig2-Cre}=0,27$, $p^{Hb9-Cre}=0,48$). Later ablation of *Npn-1* in sensory neurons by *Ncx-Cre* did not affect the fasciculation of spinal nerves before the plexus region (empty arrowheads in Fig. 14F), nor the formation of the plexus at the base of the limb at E10.5.

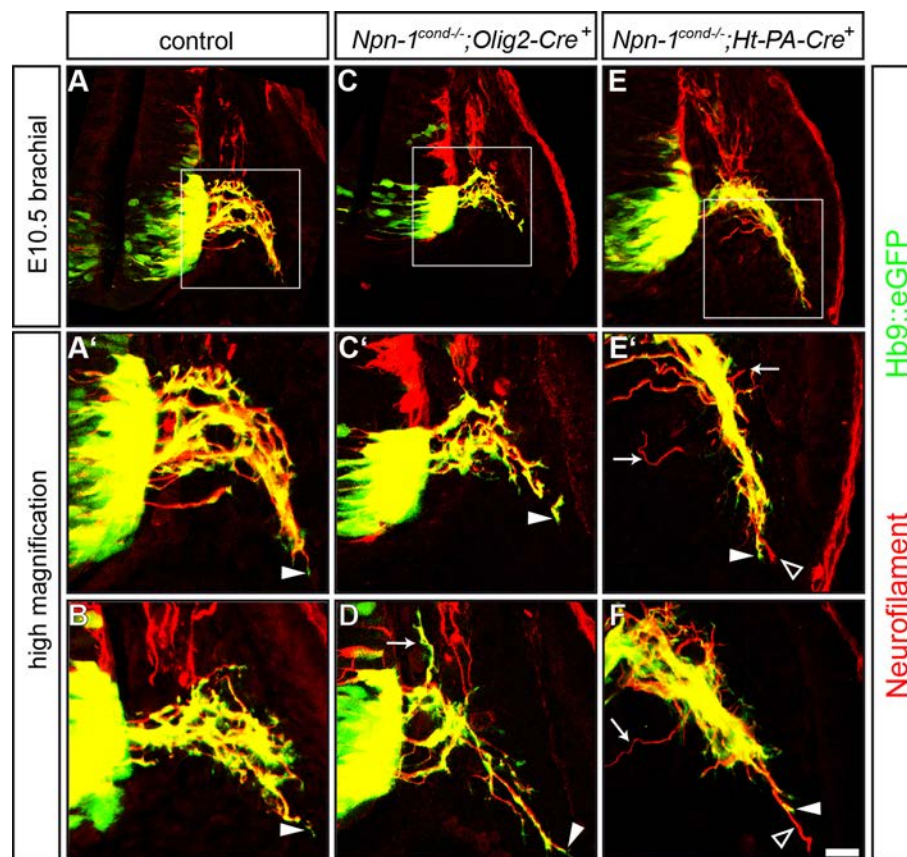


Figure 19: Sensory axons break sensory-motor axon coupling after removal of *Npn-1* from sensory neurons.

Coronal sections of E10.0 (Theiler stage 16, 30-32 somites) embryos, staining against Hb9::eGFP and neurofilament. **(A, A', B)** In control embryos, GFP expression was found all along motor axons into the distal-most tips of outgrowing trajectories (arrowheads), indicating that motor axons lead the spinal nerve projection. **(C, C', D)** In *Npn-1^{cond/-};Olig2-Cre⁺* mutant embryos, some motor axons choose an aberrant trajectory, turning dorsally into the DRG (arrow). GFP-positive motor axons are observed at the tips of the nerves growing towards the limb (arrowheads). **(E, E', F)** In *Npn-1^{cond/-};Ht-PA-Cre⁺* mutant embryos, sensory axons defasciculate from the forming spinal nerve (arrows, note the missing GFP expression in those nerves, therefore classified as sensory axons). Sensory axons are further advanced than motor axons (empty arrowheads and arrowheads, respectively), indicating that sensory nerves overtake motor axons already on the way towards the plexus. Scale bar equals 20 μ m for **(A, C, E)**, and 10 μ m for **(A', B, C', D, E', F)**.

Therefore, also calculation of the fasciculation coefficient revealed no changes in spinal nerve thickness before the plexus region at this age (Fig. 18J, $p^{Ncx-Cre}=0,95$). Deletion of *Npn-1* from both motor and sensory neurons by an *Isl-1-Cre* transgenic line (Srinivas et al., 2001) resulted in an intermediary phenotype: fasciculation before the plexus region was not affected significantly (arrowheads in Fig. 18D', H, J), however, sensory and motor axons within the plexus region were defasciculated, and sensory axons did break the sensory-motor coupling (Fig. 18D, empty arrowheads in Fig. 18D'').

These data suggest that within the mixed sensory-motor spinal nerves, the state of fasciculation of sensory axons before the plexus at the base of the limb can influence fasciculation of motor axons before, within and after the plexus region.

To test whether the defasciculation of motor fibers might result from a break in sensory-motor axon coupling, we analyzed sensory and motor projections on cross sections of E10.0 embryos by immunohistochemistry against *Hb9::eGFP* and neurofilament. At this time point, sensory and motor axons have just left the DRG and the ventral horn of the spinal cord, respectively, and have joined to form spinal nerves, but did not yet reach the plexus region. We found that in *Npn-1^{cond/-};Olig2-Cre⁺* mutant embryos and in control embryos, *Hb9::eGFP* positive fibers exit the spinal cord fasciculated and lead the growing spinal nerve after joining with sensory axons from the DRG (Fig. 19A, C, arrowheads in Fig. 19A', B, C', D). In a small number of embryos where *Npn-1* was ablated in motor neurons by *Olig2-Cre*, aberrantly, dorsally towards the DRG turning motor axons could be observed (arrow in Fig. 19D). Interestingly, in embryos where *Npn-1* was ablated in sensory neurons, already at the early time point of E10.0, sensory axons were observed to defasciculate from the main projection (neurofilament positive, in the absence of *Hb9::eGFP*, arrows in Fig. 19E', F). Most strikingly, we found sensory axons further advanced than motor axons in the spinal nerves projecting towards the limb, taking the lead in the growing spinal nerve (empty arrowheads and arrowheads in Fig. 19E', F).

When *Npn-1* is ablated by *Ht-PA-Cre*, neural crest cells might be impaired in their migration pattern and condensation to DRG, which later on might influence segmentation of the embryo, positioning of neurons and initial fasciculation of sensory axons as it was observed in compound *Npn-1^{Sema-}/Npn-2^{-/-}* mutant embryos (Schwarz et al., 2009).

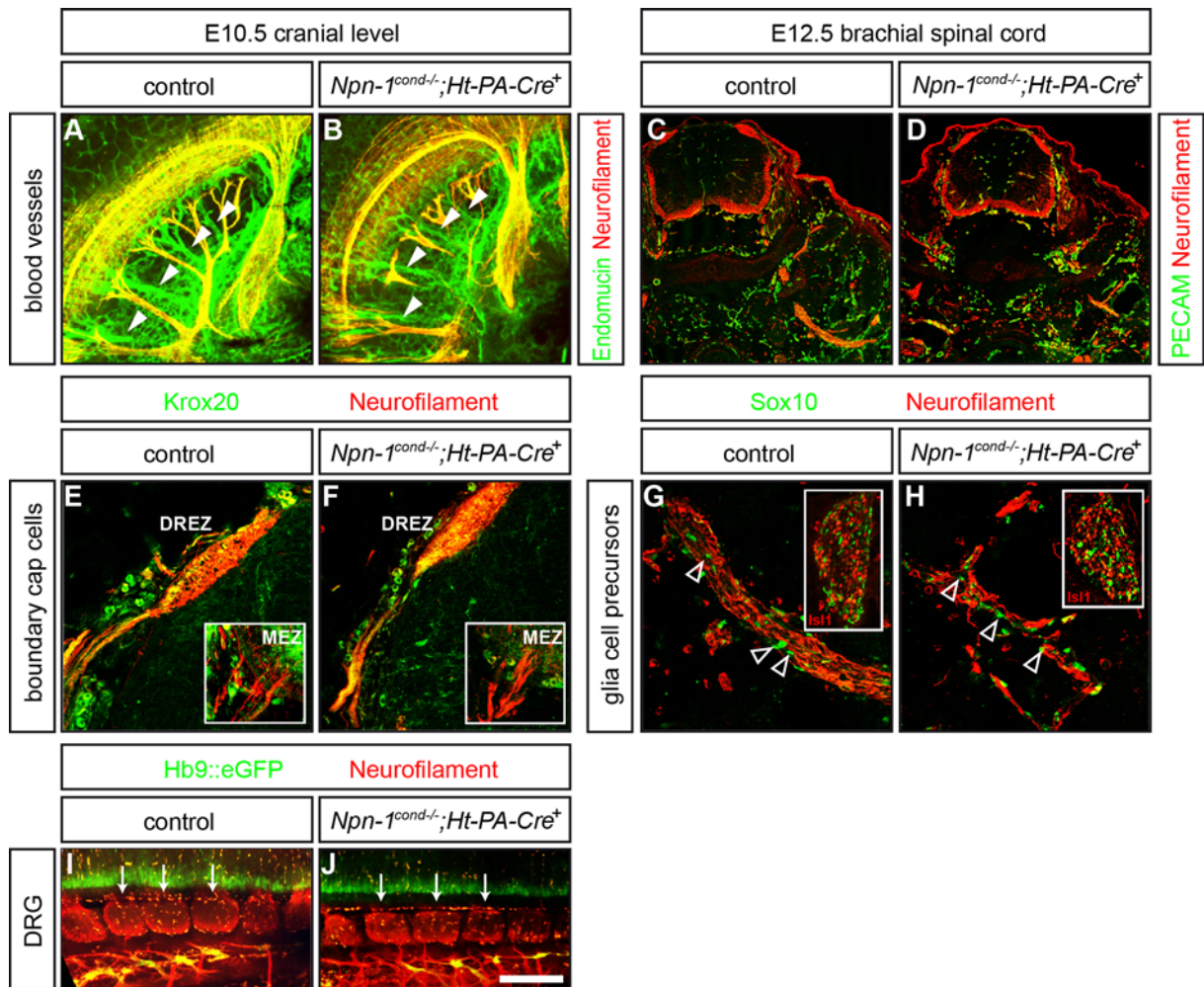


Figure 20: Assessment of DRG segmentation, Schwann cell progenitors, boundary cap cell formation and blood vessel formation in *Npn-1^{cond/-};Ht-PA-Cre⁺* mutant embryos.

(A, B) Fluorescent immunolabeling against endomucin (green) shows no gross abnormalities in blood vessel formation and patterning at the level of the hypoglossal nerve in E10.5 wholemount embryos lacking *Npn-1* in neural crest and placodally derived tissue when compared to control littermates (arrowheads). (C, D) The formation of blood vessels at spinal levels was assessed by staining with anti-PECAM antibody and revealed no obvious differences between mutant and control embryos. (E, F) The formation of boundary cap cells (KROX20⁺) at the dorsal root entry zone (DREZ) and motor entry zone (MEZ) is not impaired in *Npn-1^{cond/-};Ht-PA-Cre⁺* mutant embryos when compared to littermate controls. (G, H) Schwann cell progenitor formation was assessed by Sox10 immunohistochemistry and showed Sox10⁺ progenitor that cells follow a defasciculated distal nerve branch in the forelimb and in DRG (inlay) of mutant embryos. (I, J) Dorsal view of the spinal cord and DRG of E12.5 wholemount embryos revealed that the segmentation of DRG is normal in *Npn-1^{cond/-};Ht-PA-Cre⁺* mutant embryos, in particular, no fusions or aberrant morphology was observed when compared to littermate controls. Scale bar in (J) equals 200µm for (A, B), 150µm for (C, D), 20µm for (E, F), 40µm for (G, H) and 80µm for inlays in (G, H), and 100µm for (I, J).

A horizontal view of the DRG of E12.5, however, showed normally segmented DRG and no aberrantly positioned sensory neurons were observed (Fig. 20J). In *Npn-1^{-/-}* mutant embryos, blood vessel formation was affected by the loss of *Npn-1* signaling in the whole organism (Gu et al., 2003). While in *Npn-1^{Sema-}* mutant embryos this phenotype was averted by only mutating the Sema binding domain, in *Ht-PA-Cre* conditional mutant embryos the entire receptor is missing in neural crest derived

tissues. As blood vessels and nerve fibers co-extend to similar targets, using similar mechanisms of guidance signals during their development, we analyzed blood vessel formation in cross sections of E12.5 *Npn-1^{cond-/-};Ht-PA-Cre⁺* embryos using an antibody against platelet/endothelial cell adhesion molecule 1 (PECAM). We found no obvious alteration in the formation of the blood vessel system, or enhanced tracking of axons along misprojecting blood vessels or vice versa in mutant embryos when compared to littermate controls (Fig. 20C, D). Neural crest cell derived boundary cap cells, which allow motor axons to exit the spinal cord, but prevent cell bodies from doing so, were found to be developed normally (Fig. 20E, F). Loss of neural crest derived Schwann cells was reported to cause defasciculation of motor nerves before (Finzsch et al., 2010). When we investigated migration of Sox10 positive Schwann cell precursors we found no obvious alteration in the number of Schwann cells migrating along defasciculated nerves in the distal embryonic limb (Fig. 20G, H, arrowheads). While an effect of loss of *Npn-1* in other neural crest derived tissues cannot be completely excluded, it seems unlikely that mispatterned neural crest cells affect motor axon growth in *Npn-1^{cond-/-};Ht-PA-Cre⁺* mutant embryos.

We therefore conclude that elimination of *Npn-1* from sensory neurons breaks the tight coupling of sensory and motor axons. Thereby, defasciculated sensory axons overtake motor fibers and take the lead in the growing spinal nerve, providing a permissive substrate for motor axons to track along.

2. CONDITIONAL ABLATION OF *NPN-1*: ROLES IN CRANIAL NERVE FASCICULATION AND SCHWANN CELL MIGRATION

2.1 *NPN-1* IN CRANIAL NEURAL CREST AND PLACODALLY DERIVED SENSORY NEURONS CONTROLS PERIPHERAL CRANIAL NERVE FASCICULATION

At cranial levels, where most sensory and motor neurons express Neuropilins, fasciculation and guidance decisions are governed by *Sema3-Npn* interactions: while *Sema3F-Npn-2* signaling mainly facilitates pathfinding and fasciculation of oculomotor, trochlear and a subset of trigeminal axons (Chen et al., 2000; Gammill et al., 2007), loss of the *Sema3A-Npn-1* signaling pathway severely affects fasciculation of distal trigeminal, facial, glossopharyngeal and vagus projections to the head and neck (Kitsukawa et al., 1997; Taniguchi et al., 1997; Gu et al., 2003; Schwarz et al., 2008a). In the *Npn-1^{-/-}* and the *Npn-1^{Sema-}* lines, however, projections from branchiomotor and visceromotor neurons, as well as sensory axons that form these projections lack expression of the Semaphorin receptor, or cannot bind class 3 Semaphorins, respectively. Thus, it is unclear which projection contributes to what extent to peripheral cranial nerve fasciculation. To determine whether *Npn-1* is required in sensory axons exclusively for proper peripheral fasciculation of the mixed sensory-motor projections of the trigeminal, facial, glossopharyngeal and vagus nerves, we analysed axonal projections in wholemount embryos stained for neurofilament. We ablated *Npn-1* from neural crest and placodally derived cells by tissue specific expression of Cre recombinase under the control of the *human tissue plasminogen activator* promoter (*Ht-PA-Cre*; Pietri et al., 2003) and found a significant reduction of neurons in the trigeminal ganglia positive for *Npn-1 mRNA expression* in *Npn-1^{cond-/-};Ht-PA-Cre⁺* mutant embryos when compared to control littermates (Fig. 21A-C). At E10.5, we observed defasciculation of the distal parts of the facial nerve, and the ophthalmic, maxillary and mandibular branches of the trigeminal nerve in *Npn-1^{cond-/-};Ht-PA-Cre⁺* mutant embryos (arrowheads in Fig. 21F). Furthermore, the more caudally situated projections of the glossopharyngeal and vagus ganglia also showed defasciculated peripheral nerve branches (arrowheads in

Fig. 21F'). This phenotype is even more obvious at E11.5, when facial, glossopharyngeal and vagal projections are severely defasciculated distally (Fig. 21I'). Hardly any fasciculated branches were found in ophthalmic and mandibular projections, while the maxillary branch is spread out over the entire nasal area (Fig. 21I).

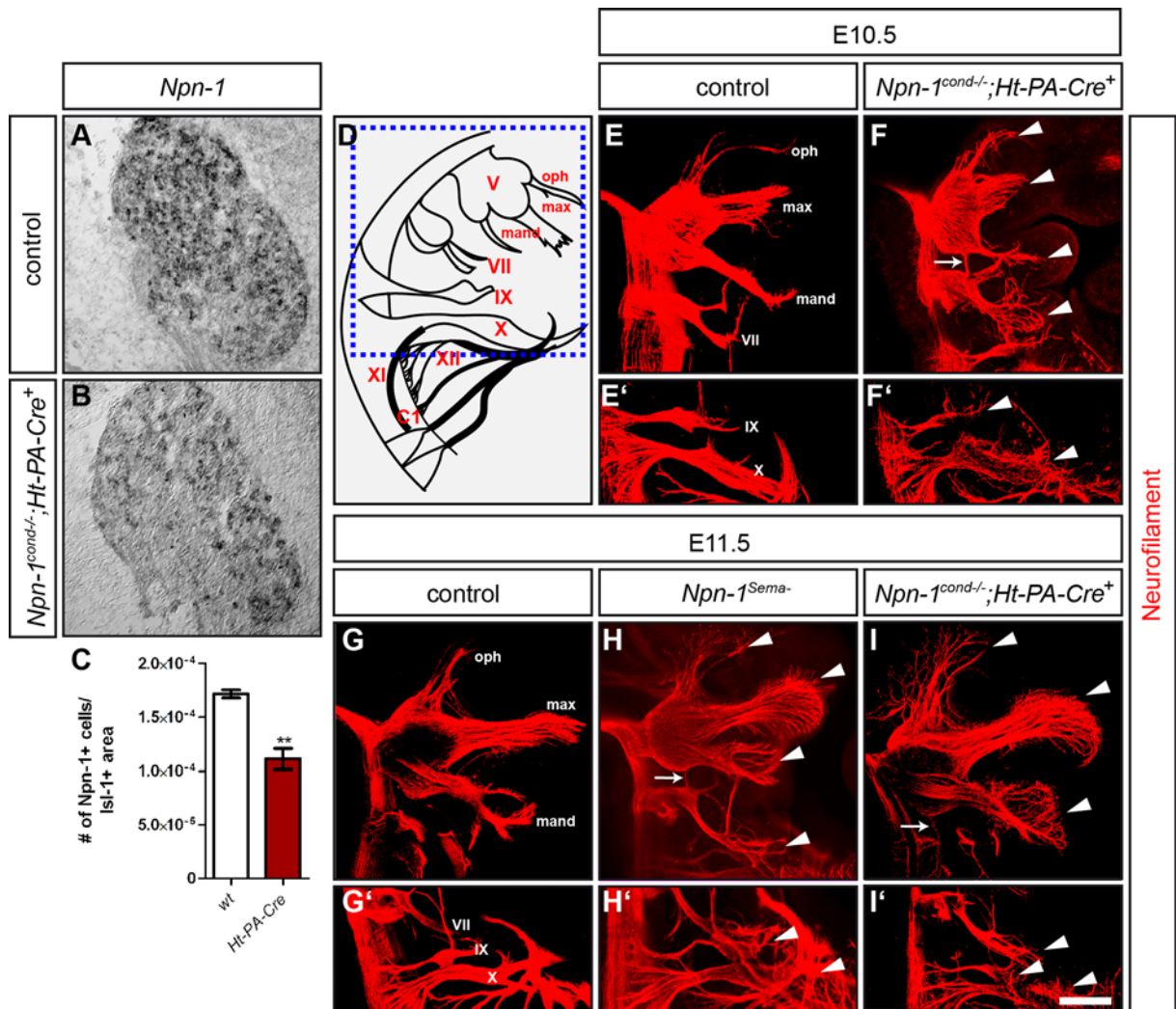


Figure 21: *Npn-1* in sensory neurons is required for distal fasciculation of cranial projections. (A-C) *In situ* hybridization on coronal sections of E11.5 embryos against the floxed exon 2 of *Npn-1* shows reduced expression of *Npn-1* in the neurons of the trigeminal ganglion in *Npn-1^{cond-/-};Ht-PA-Cre⁺* mutant embryos when compared to controls ($p \leq 0,005$). (D) Blue dashed line in the schematic depicts the cranial projections shown in the panels (E-I) with wholemount antibody staining against neurofilament of E10.5 and E11.5 embryos. (E, E', G, G') E10.5 and E11.5 control embryos, respectively. (F, F', I, I') Ablation of *Npn-1* in sensory neurons by *Ht-PA-Cre* leads to distal defasciculation of trigeminal, facial, glossopharyngeal and vagus projections in *Npn-1^{cond-/-};Ht-PA-Cre⁺* mutant embryos (arrowheads) The arrows in (F) and (I) mark aberrant projections between facial and trigeminal ganglia. (H, H') Projections of the trigeminal, facial, glossopharyngeal and vagus nerves are defasciculated in the periphery in *Npn-1^{Sema-}* mutant embryos (arrowheads). Additionally, aberrant projections between trigeminal and facial ganglia are observed in *Npn-1^{Sema-}* mutant embryos (arrow). Abbreviations: V=trigeminal ganglion, oph=ophthalmic, max=maxillary, mand=mandibular branch of the trigeminal nerve, VII=facial nerve, IX=glossopharyngeal nerve, X=vagus nerve, XI=spinal accessory nerve, XII=hypoglossal nerve, C1=first cervical spinal nerve. Scale bar in (I') equals 100 μ m for (A, B, E, F) and 200 μ m for (G-I).

When *Npn-1* was eliminated from sensory neurons, we found ectopic axons between facial and trigeminal ganglia at both E10.5 and E11.5 (arrow in Fig. 21F, I). Schwarz and colleagues showed that in mice, where *Sema3A-Npn-1* signaling is abolished (*Npn-1^{Sema-}*), these ectopic axons project along misguided neural crest cells, which are also targeted by *Ht-PA-Cre* (arrow in Fig. 21H; Schwarz et al., 2008a). Furthermore, phenotypes of distal defasciculation are very reminiscent of the defects observed in *Npn-1^{Sema-}* embryos (arrowheads in Fig. 21H, H'; Gu et al., 2003; Schwarz et al., 2008a).

Thus, our data demonstrate that fasciculation and guidance of peripheral cranial nerves is governed by *Npn-1* expression on sensory cells derived from neural crest and embryonic placodes.

2.2 *NPN-1* IS REQUIRED IN SOMATIC MOTOR NEURONS FOR CORRECT FASCICULATION AND OUTGROWTH OF THE ABDUCENS NERVE

While previous studies have addressed the role of *Sema3A-Npn-1* signaling in the formation of trigeminal, facial, glossopharyngeal and vagus nerves (Kitsukawa et al., 1997, Taniguchi et al., 1997), its role in guidance and fasciculation of the hypoglossal and abducens nerves has not been investigated so far. In contrast to spinal motor neurons that form columns along the entire length of the spinal cord (Jessell, 2000), cranial motor neurons are partitioned into nuclei after differentiation into somatic, branchio- and visceromotor neurons. Knockout of the *Olig2* gene leads to loss of all spinal motor nerves, while at cranial levels only the somatic motor projections of the hypoglossal (arrows in Fig. 22C, F) and abducens nerves (Fig. 22I) are absent. When compared to control embryos (Fig. 22B, E), cranial branchiomotor, visceromotor and sensory projections of the glossopharyngeal, vagus and spinal accessory nerves are not affected by absence of somatic motor trajectories (arrowheads in Fig. 22C, F). When we eliminated somatic motor neurons by crossing *Olig2-Cre* animals with a conditional *diphtheria toxin fragment A (DT-A)* transgenic line (Brockschneider et al., 2006), we observed a similar phenotype: Projections of the hypoglossal nerve are completely absent at E10.5 (empty arrowheads in Fig. 22D) or severely reduced at E11.5 (empty arrowheads in Fig. 22G), and the abducens nerve is missing upon activation of *DT-A* in motor neurons (Fig. 22J).

Branchiomotor, visceromotor and sensory projections develop normal peripheral projections in *Olig2-Cre;DT-A^{flxed}* mutant embryos (arrowheads in Fig. 22D, G).

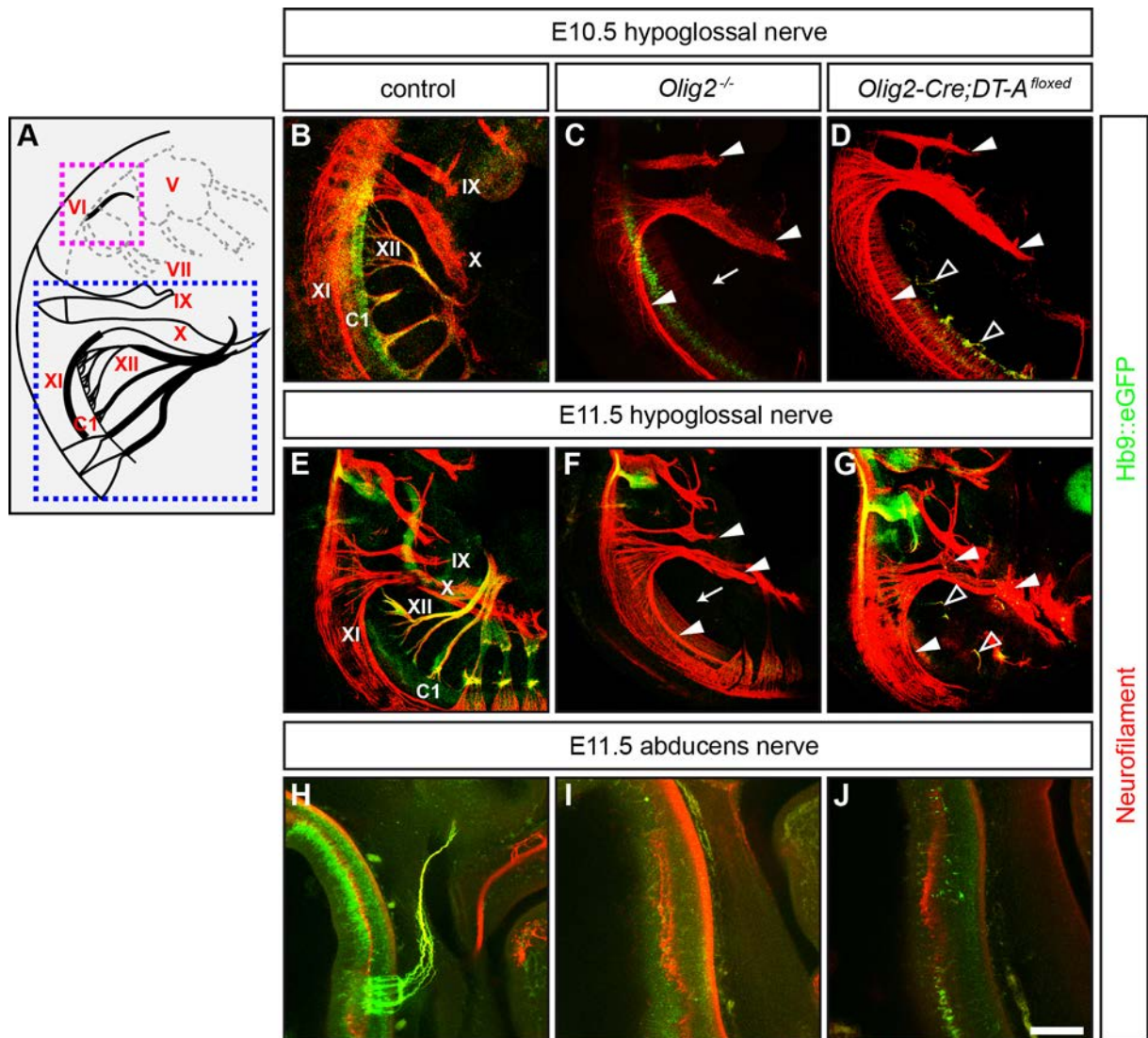


Figure 22: Absence of *Olig2* leads to loss of somatic motor projections.

Wholemount antibody staining against Hb9::eGFP (green, somatic motor axons) and neurofilament (red, motor and sensory axons). **(A)** Blue dashed line in the schematic outlines the cranial projections shown in panels **(B-G)**, magenta dashed box marks the position of the abducens projection **(H-J)**. **(B, E)** Control embryos at E10.5 and E11.5 respectively. **(C, F)** Homozygous *Olig2-Cre* mutant embryos lack the *Olig2* gene. Absence of *Olig2* leads to loss of somatic hypoglossal projections at E10.5 and E11.5 (arrows), while the mixed sensory and branchio-visceromotor projections of glossopharyngeal and vagus nerves are not affected (arrowheads). **(D, G)** Activation of DT-A by *Olig2-Cre* partially eliminates somatic motor neurons at E10.5, and leads to severely reduced somatic motor projections at E11.5. Glossopharyngeal and vagus nerves project normally in *Olig2-Cre;DT-A^{flxed}* embryos (arrowheads). **(H)** Abducens projection of an E11.5 control embryo. **(I)** The somatic motor projections of the abducens nerve are missing in *Olig2* mutant embryos. **(J)** A similar phenotype is observed in embryos where DT-A expression is activated by *Olig2-Cre*: Abducens projections are completely absent. Abbreviations: IX=glossopharyngeal nerve, X=vagus nerve, XI=spinal accessory nerve, XII=hypoglossal nerve, C1=first cervical spinal nerve. Scale bar in **(J)** equals 100µm for **(B-D)** and **(H-J)**, and 200µm for **(E-G)**.

Somatic motor neurons of the abducens nucleus are derived from progenitors in the pMN domain. Projections from these motor neurons innervate the lateral rectus muscle that is responsible for horizontal eye movements (Chilton and Guthrie, 2004). At E11.5, *Npn-1* is expressed in somatic motor neurons of the abducens nucleus (Fig. 23B). At E10.5, when axons of the abducens nucleus leave the brainstem and have not yet fasciculated in wildtype embryos, no differences were observed in *Npn-1^{Sema-}* mutant embryos (data not shown). One day later, re-fasciculation has occurred in control embryos and the abducens nerve grows as a tight fascicle towards the eye (Fig. 23F). In *Npn-1^{Sema-}* embryos, where Sema3A-Npn-1 signaling is abrogated in the entire organism, no differences in thickness or distal growth and proportions of the abducens nerve were observed when compared to littermate controls (Fig. 23G, M, N). However, in one out of three embryos, on one side the abducens projections showed aberrant rostral branching (data not shown).

When *Npn-1* is ablated from somatic motor neurons by *Olig2-Cre*, the abducens nerve shows a reduced number of projections from 11,00 +/- 0,82 SEM in control embryos to 5,00 +/- 0,97 SEM in *Npn-1^{cond-/-};Olig2-Cre⁺* mutant embryos at E10.5 (Fig. 23D, E, L), while the number of somatic motor neurons in the abducens nucleus was not changed in mutant embryos (Fig. 23C). While abducens projections appear defasciculated at E10.5 in control embryos (Fig. 23D), at E11.5 the axons form one fascicle, until they reach the turning point towards the eyecup, where they defasciculate again (Fig. 23F). In *Npn-1^{cond-/-};Olig2-Cre⁺* mutant embryos, nerve fibers appeared diminished in number, however, re-fasciculation of remaining fibers to form a thinner abducens projection was observed in E11.5 mutant embryos (Fig. 23H, M). At E12.5, the remaining abducens projections reach the turning point towards the eye, and seem to turn appropriately to innervate the lateral rectus muscle (data not shown).

Our results therefore show a requirement of *Npn-1* in somatic motor axons for abducens nerve fasciculation and initial outgrowth, while targeting of remaining fibers appears to be governed by alternate factors. Formation of the abducens nucleus is not affected by loss of *Npn-1* in somatic motor neurons.

To assess the role of neural crest and placodally derived cells in the formation, fasciculation and growth of the abducens nerve we analysed *Npn-1^{cond-/-};Ht-PA-Cre⁺* and *Ht-PA-Cre;DT-A^{flxed}* mutant embryos. In *Npn-1^{cond-/-};Ht-PA-Cre⁺* mutant embryos, which lack *Npn-1* expression selectively in cranial neural crest and

placodally derived sensory cells, abducens axons re-fasciculated properly (Fig. 23I). Axonal outgrowth appears delayed after re-fasciculation took place at E11.5 (Fig. 22I, N), however, this phenotype is corrected one day later (data not shown). Also in *Ht-PA-Cre;DT-A^{flox}* mutant embryos this delay of axon outgrowth was observed in one out of three analysed embryos, nevertheless, also when cranial neural crest and placodally derived tissues and neurons are missing, abducens axons still fasciculate appropriately and project towards the eyecup (Fig. 23J, M, N).

These findings indicate a subordinate role for *Npn-1* in sensory tissues for guidance and fasciculation of the abducens nerve.

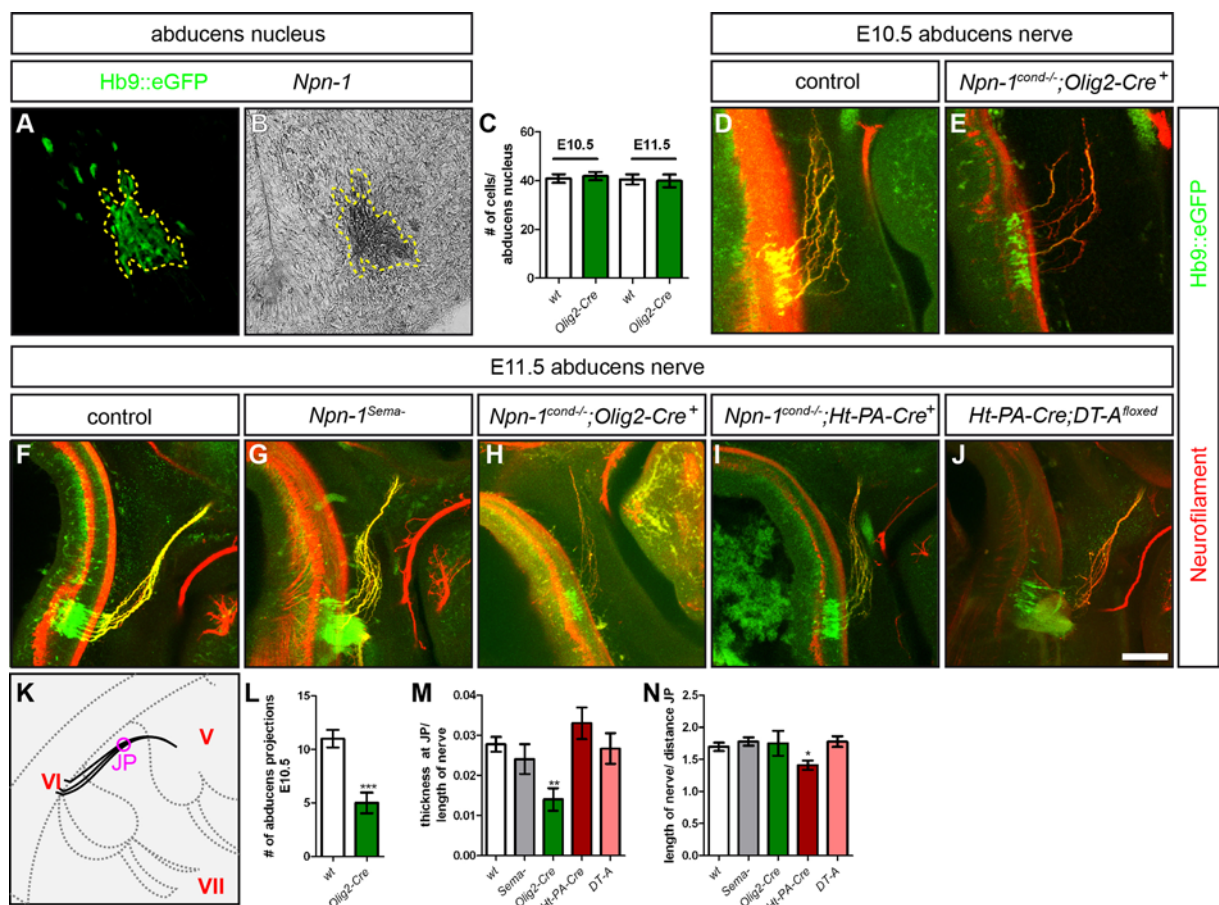


Figure 23: Loss of *Npn-1* in somatic motor neurons reduces abducens projections.

(A, B) *In situ* hybridization demonstrates *Npn-1* expression in the abducens nucleus, that consists of somatic motor neurons that express Hb9::eGFP and hence mark the abducens nucleus. (C) Numbers of somatic motor neurons in the abducens nucleus are unchanged in *Npn-1^{cond-/-};Olig2-Cre⁺* embryos when compared to controls (C, E10.5 control=48,83 +/- 1,76 SEM, mutant = 41,83 +/- 1,70 SEM, $p^{E10.5} = 0,69$). (D, E, L) In E10.5 wholemount embryos stained against Hb9::eGFP (green, somatic motor axons) and neurofilament (red, motor and sensory axons, anterior to the top of the panel), the number of abducens projections is diminished in *Npn-1^{cond-/-};Olig2-Cre⁺* mutant embryos ($p \leq 0,001$). (F) Abducens projection in a control embryo at E11.5. (K) Schematic illustrating the nerves shown in panels (D-J) and the joining point (JP) used for quantification of abducens nerve thickness and proportions in (M) and (N). (G, M, N) At E11.5, the abducens nerve re-fasciculated normally in *Npn-1^{Sema-}* mutant embryos and projected to the eyecup (Thickness at JP/length of nerve, $p^{Sema-} = 0,36$). Also nerve proportions (length of nerve/distance JP) were not affected ($p^{Sema-} = 0,40$) (H, M, N) In *Npn-1^{cond-/-}*

; *Olig2-Cre*⁺ mutant embryos, abducens projections are still thinned (p=0,001) at E11.5, however, rostral turning, fasciculation and advancement of the projection are normal (p=0,77). (I, J, M) Abducens projections of *Npn-1*^{cond^{-/-}}; *Ht-PA-Cre*⁺ and *Ht-PA-Cre*⁺; *DT-A*^{floxed} mutant embryos re-fasciculate properly when compared to control embryos (p^{*Ht-PA-Cre*}=0,23, p^{*DT-A*}=0,79). (I, J, N) Growth is slightly retarded after re-fasciculation in E11.5 embryos where *Npn-1* was ablated from sensory tissues (p^{*Ht-PA-Cre*}=0,01), while distal advancement in *Ht-PA-Cre*⁺; *DT-A*^{floxed} mutant embryos is not impaired (p=0,453). Abbreviations: V=trigeminal ganglion, VI=abducens nerve, VII=facial nerve. Scale bar in (J) equals 50µm for panels (A, B, D, E) and 100µm for (F-J).

2.3 LOSS OF NPN-1 SIGNALING IN SOMATIC MOTOR NEURONS IMPAIRS INITIAL FASCICULATION OF HYPOGLOSSAL NERVE ROOTLETS

The hypoglossal nerve provides somatic motor innervation of the tongue. It arises from an elongated band of motor nuclei in the medulla oblongata and exits the brainstem rostrally to the first cervical spinal nerve (reviewed in Cordes, 2001; Guthrie, 2007). Fibers from the nuclei in the brainstem coalesce to form spinal rootlets that subsequently form roots, and finally fuse to the hypoglossal nerve itself. We investigated the formation of hypoglossal projections in wholemount embryo preparations by *Hb9::eGFP* fluorescence in somatic motor axons (Wichterle et al., 2002) while sensory, branchiomotor and visceromotor projections were visualized by neurofilament staining in the absence of GFP fluorescence. At E11.5, the hypoglossal nerve has connected with the first cervical spinal nerve and turned rostrally towards the tongue in wildtype embryos (empty arrowhead in Fig. 24C). This turning event also takes place in *Npn-1*^{*Sema*⁻} mutant embryos, where binding of all class 3 Semaphorins to Npn-1 is blocked (empty arrowhead in Fig. 24J). However, during assembly of the hypoglossal nerve, the rootlets from the brainstem motor nuclei remain defasciculated over a longer distance before coalescing into the hypoglossal nerve (arrow in Fig. 24J, p<0,005). These findings were quantified by calculating a rootlet coefficient a/b that is significantly higher in *Npn-1*^{*Sema*⁻} mutant embryos (Fig. 24M, N), while total proportions CP/TP of the hypoglossal nerve, and also the number of rootlets exiting the brainstem remain unchanged (Fig. 24M; O, p^{*Sema*⁻}= 0,12; P, p^{*Sema*⁻}=0,80). Furthermore, the formation of the first spinal nerve in the cervical spinal cord is impaired by loss of *Sema3-Npn-1* signaling, leading to thinned and/or aberrant motor projections (double arrowheads in Fig. 24J).

Taken together, these findings demonstrate a role for *Npn-1* in initial fasciculation of the hypoglossal nerve during cranial somatic motor nerve assembly.

2.4 LOSS OF *NPN-1* IN SOMATIC MOTOR NEURONS LEADS TO A REDUCTION AND DEFECTIVE ASSEMBLY OF THE HYPOGLOSSAL NERVE

To investigate the role of *Npn-1* in somatic motor axon fasciculation, we used a genetic approach to remove *Npn-1* selectively from somatic motor neurons using the *Olig2-Cre* line. We found no alteration of glossopharyngeal, vagal and spinal accessory projections that consist of branchiomotor, visceromotor and sensory trajectories (arrowheads in Fig. 24D, E). At E10.5, however, stunted and aberrant projections of the hypoglossal nerve were observed in *Npn-1^{cond/-};Olig2-Cre⁺* mutant embryos (arrow in Fig. 24D). At E11.5, hypoglossal projections form a connection with the first spinal nerve and were found appropriately proportioned (Fig. 24O, $p=0,41$) and positioned within the branchial arches, turning rostrally towards the tongue (empty arrowhead in Fig. 24E). The number of Isl1 positive somatic motor neurons within the hypoglossal nucleus was not altered in *Npn-1^{cond/-};Olig2-Cre⁺* mutant embryos (Fig. 24K, L; ctrl: 175,1 +/- 23,13 SEM, mutant: 180 +/- 12,64 SEM, $p=0,86$). In contrast to control embryos, however, projections from the hypoglossal motor neurons appear markedly thinned, and the number of rootlets exiting the neural tube and contributing to the hypoglossal nerve is decreased from 12.96 +/- 0,57 SEM in control embryos to 7,67 +/- 1,12 SEM in mutants (arrows in Fig. 24E; $P, p\leq 0,001$). In addition, when we quantified the length of the hypoglossal rootlets we found that they remain defasciculated over significantly longer distances before joining together to form the hypoglossal nerve (Fig. 24N). This same phenotype we observed in *Npn-1^{Sema-}* mutant embryos.

Therefore, our findings suggest that loss of *Npn-1* does not impact on the differentiation of somatic motor neurons in the hypoglossal nucleus. *Npn-1* signaling is required in somatic motor axons for proper outgrowth and initial fasciculation of hypoglossal rootlets, while guidance towards the tongue is most likely facilitated by other signaling pathways.

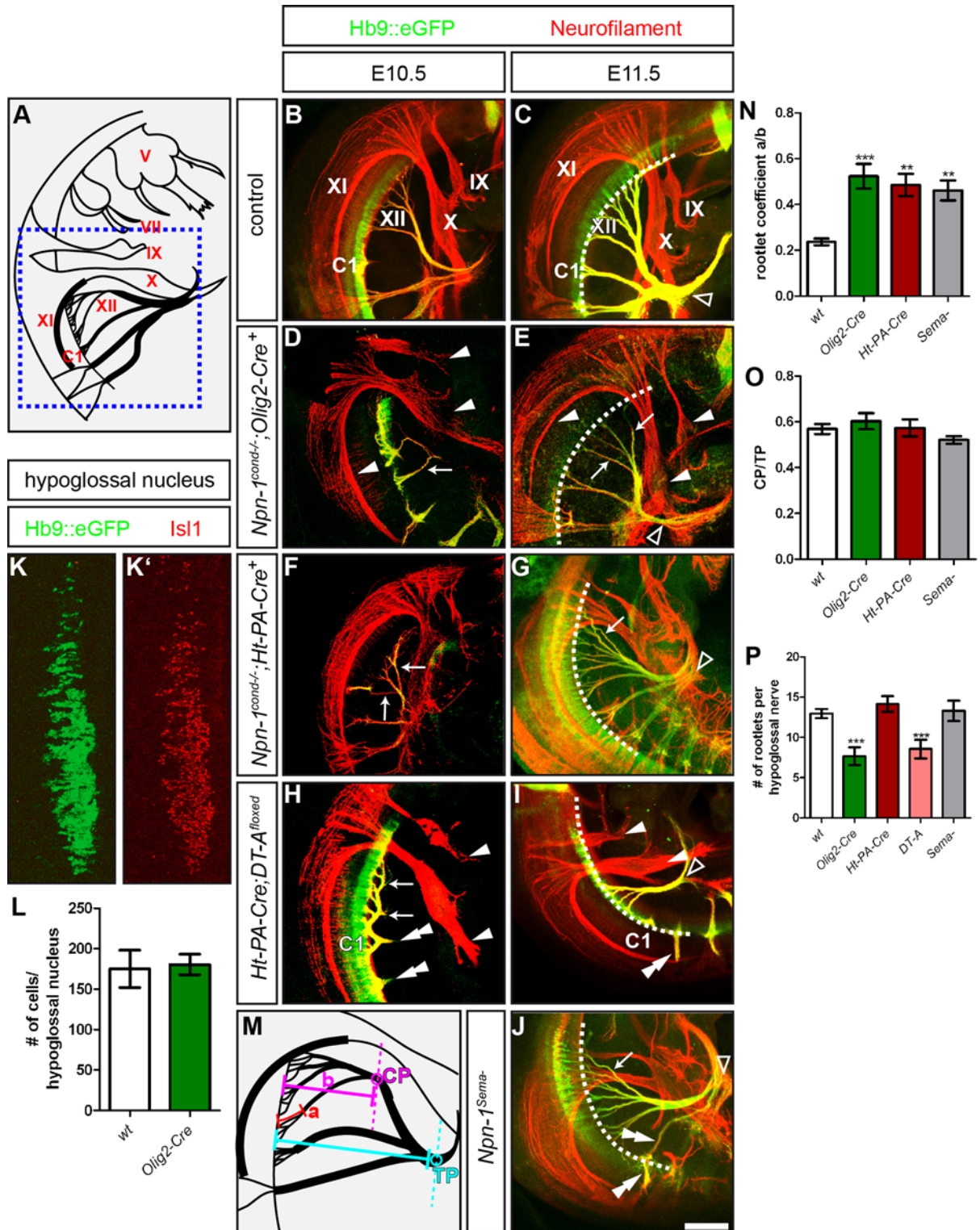


Figure 24: Initial fasciculation, but not final targeting is impaired by loss of *Npn-1* in somatic motor and/or cranial neural crest and placodally derived sensory neurons.

Wholemount antibody staining against Hb9::eGFP (green, somatic motor nerves) and neurofilament (red, motor and sensory axons). (A) Blue dashed line in the schematic frames cranial projections shown in panels (B-J). (B, C) E10.5 and E11.5 control embryos. (M) Schematic illustrating the methods used for quantification of the rootlet coefficient and the proportions of the hypoglossal nerve. (D) At E10.5, hypoglossal projections are reduced and stunted in *Npn-1^{cond/-}; Olig2-Cre⁺* mutant embryos (arrow), while spinal accessory, vagus and glossopharyngeal trajectories are formed normally (arrowheads). (E, N, O, P) At E11.5, the hypoglossal nerve joins with the first cervical spinal

nerve (C1) and projects rostrally in controls and mutants (empty arrowhead). Spinal accessory, vagus and glossopharyngeal projections are formed normally in *Npn-1^{cond/-};Olig2-Cre⁺* embryos (arrowheads). Hypoglossal projections stay defasciculated over a significantly longer distance before they bundle into one nerve trunk (arrows, control = 0,19 +/- 0,02 SEM, mutant = 0,52 +/- 0,06, $p \leq 0,001$). The number of hypoglossal rootlets leaving the neural tube (white dashed line) is reduced, while total proportions of the hypoglossal nerve were normal. **(K, K', L)** The number of Hb9::eGFP⁺/Isl1⁺ motor neurons in the hypoglossal nucleus is not changed in *Npn-1^{cond/-};Olig2-Cre⁺* mutant embryos (anterior to the top, midline to the left of the panel). **(F, H)** At E10.5, hypoglossal projections of *Npn-1^{cond/-};Ht-PA-Cre⁺* mutant embryos appear thinned and project aberrantly (arrows). In embryos where cranial neural crest and embryonic placodes are eliminated by tissue specific activation of DT-A, hypoglossal projections are stunted and form loops (arrowheads) instead of projecting towards the branchial arches. Also projections of the cervical spinal nerves (C1) are stunted (double arrowheads). **(G, N, O, P)** At E11.5, initial fasciculation of hypoglossal projections is disturbed, and rootlets grow significantly longer, before coalescing to one major nerve trunk in *Npn-1^{cond/-};Ht-PA-Cre⁺* mutant embryos (arrow), while the number of hypoglossal rootlets is not altered ($p=0,33$). Connection with the first cervical spinal nerve and rostral turning towards the tongue is not impaired in mutants (empty arrowhead, $p=0,91$). **(I, N, P)** Elimination of cranial neural crest and embryonic placodes by DT-A reduces somatic motor projection contributing to the hypoglossal nerve ($p \leq 0,005$) and leads to aberrant projections of cervical spinal nerves (double arrowhead), but does not impact on rostral turning of hypoglossal projections (empty arrowhead) or development of glossopharyngeal and vagus nerves (double arrowheads). **(J, N, O, P)** In *Npn-1^{Sema-}* mutant embryos, connection of hypoglossal and the first cervical spinal nerve takes place normally (empty arrowhead), while aberrant or thinned projections from the first cervical spinal nerve were observed (double arrowheads) and rootlets forming the hypoglossal nerve are normal in number, but significantly elongated (arrow). Abbreviations: IX=glossopharyngeal nerve, X=vagus nerve, XI=spinal accessory nerve, XII=hypoglossal nerve, C1=first cervical spinal nerve. Scale bar in **(J)** equals 100 μ m for **(B, D, F, H)**, 200 μ m for **(C, E, G, I, J)** and 50 μ m for **(K)**.

2.5 ELIMINATION OF *NPN-1* FROM CRANIAL SENSORY NEURONS AND PARTIAL LOSS CRANIAL NEURAL CREST AND PLACODALLY DERIVED TISSUES IMPAIRS HYPOGLOSSAL NERVE ASSEMBLY

We showed that ablation of *Npn-1* from cranial neural crest and placodally derived sensory tissues is responsible for the distal defasciculation of trigeminal, facial, glossopharyngeal and vagal projections. All these nerves are mixed sensory-motor projections. Surprisingly, we also observed defects in the hypoglossal nerve that is a pure motor projection. While blood vessel formation and patterning at the level of the hypoglossal nerve seemed to be unaffected by loss of *Npn-1* in neural crest and placodally derived sensory tissue at E10.5 (arrowheads in Fig. 20B), hypoglossal projections were markedly thinned and projected aberrantly towards the spinal accessory nerve in *Npn-1^{cond/-};Ht-PA-Cre⁺* mutant embryos (arrows in Fig. 24F). Elimination of cranial neural crest and placodally derived cells due to targeted activation of *DT-A* by *Ht-PA-Cre* leads to even more severe defects in hypoglossal nerve assembly at E10.5. Here, hypoglossal fibers form loops and stall in growth shortly after exiting the brainstem (arrows in Fig. 24H). Additionally, the first spinal

nerves in the cervical spinal cord are stunted in *Ht-PA-Cre;DT-A^{floxed}* animals (double arrowheads in Fig. 24H).

At E11.5, many of these phenotypes have been corrected: hypoglossal projections of embryos that lack *Npn-1* expression in tissues derived from neural crest and placodes have joined the first spinal nerve, are correctly proportioned and project rostrally towards the tongue (empty arrowhead in Fig. 24G; O, $p^{Ht-PA-Cre} = 0,91$). However, while the number of rootlets exiting the neural tube remains unchanged (Fig. 24P, $p=0,33$), *Npn-1^{cond-/-};Ht-PA-Cre⁺* mutant embryos show significantly elongated projections during hypoglossal nerve assembly (arrow in Fig. 24G, N, $p^{Ht-PA-Cre} \leq 0,005$). These data are very reminiscent of the phenotype that we observed in *Npn-1^{Sema-}* and *Npn-1^{cond-/-};Olig2-Cre⁺* mutant embryos. In embryos, where sensory neurons were ablated by tissue specific activation of DT-A, the hypoglossal nerve correctly splits into a rostrally and a caudally turning part (empty arrowhead in Fig. 24I). However, the number of branches contributing to the hypoglossal nerve is dramatically reduced from 11,67 +/- 0,84 SEM in controls to 7,17 +/- 0,60 SEM in mutant embryos (Fig. 24I, P, $p \leq 0,001$). The hypoglossal nerve failed to connect with the first spinal nerve in all analysed embryos due to misprojecting spinal nerves (double arrowheads in Fig. 24I). Glossopharyngeal and vagus nerve developed normally in *Ht-PA-Cre;DT-A^{floxed}* mutant embryos (arrowheads in Fig 24H, I).

Taken together our findings indicate a role for *Npn-1* in neural crest and placodally derived cells for hypoglossal nerve fasciculation and assembly, while guidance towards the tongue is not affected. The presence of these cells targeted by *Ht-PA-Cre* is crucial for correctly laid out somatic motor projections from the brainstem and the rostral cervical spinal cord.

2.6 SOX10-POSITIVE SCHWANN CELLS FACILITATE INITIAL HYPOGLOSSAL NERVE FASCICULATION

We next assessed whether loss of *Npn-1* in cranial neural crest and placodally derived cells affects the migration of Schwann cell precursors along defasciculated hypoglossal nerve rootlets. Wholemount preparations of E11.5 embryos revealed Sox10-positive cells migrating along the entire length of the hypoglossal nerve in

control embryos (Fig. 25B). At the tip of the growing hypoglossal nerve, Schwann cells lag behind the leading axons (arrows and empty arrowheads, respectively, in Fig. 25F). In *Npn-1^{cond-/-};Ht-PA-Cre⁺* mutant embryos, migration of Schwann cells along the axons to the tip of the hypoglossal nerve is not impaired (arrows and empty arrowheads, respectively, in Fig. 25G), and also their number is comparable to what we observed in control embryos, after the hypoglossal projections have joined with the first cervical and the vagus nerve (Fig. 25I). However, along the elongated rootlets, the number of Schwann cells is reduced drastically from 10,94 +/- 0,94 SEM Sox10-positive cells per rootlet in controls to 6,683 +/- 0,57 cells per rootlet in mutant embryos (Fig. 25I). Some projections are even completely devoid of Schwann cells (arrowheads in Fig. 25C).

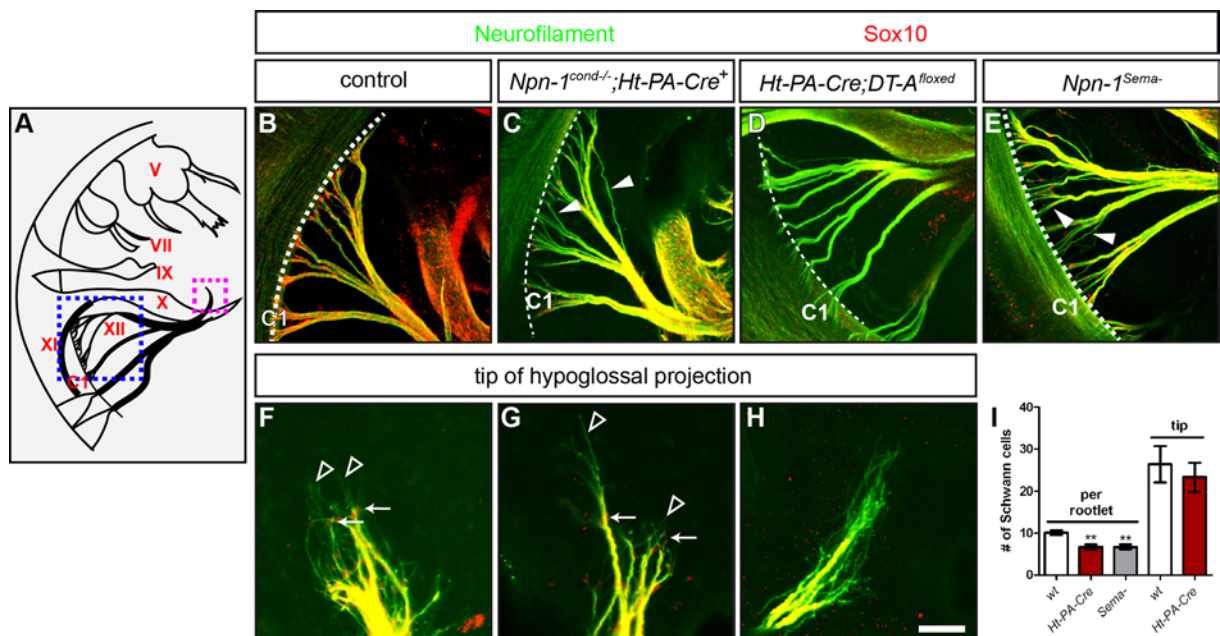


Figure 25: Defasciculation of the hypoglossal nerve in *Npn-1^{cond-/-};Ht-PA-Cre⁺*, *Ht-PA-Cre⁺;DT-A^{floxed}* and *Npn-1^{Sema-}* mutant embryos is accompanied by loss of Sox10 positive Schwann cells. Wholemount antibody staining of E11.5 embryos against Sox10 (red) and neurofilament (green). **(A)** Blue dashed line in the schematic frames cranial projections shown in panels **(B-E)**, magenta dashed line depicts projections shown in **(F-H)**. **(B, F)** Sox10-positive Schwann cells migrate along the hypoglossal nerve. At the leading edge of the hypoglossal projection, tips of the leading axons are found ahead of Sox10-positive cells (empty arrowheads and arrows, respectively). **(C, G, I)** In *Npn-1^{cond-/-};Ht-PA-Cre⁺* mutant embryos, defective fasciculation of initial hypoglossal projections is accompanied by loss of Schwann cells, some rootlets are even devoid of Sox10-positive cells (arrowheads, $p \leq 0,01$). At the tip of the nerve, axons correctly project ahead of Schwann cell progenitors (arrowheads and arrows, $p = 0,59$). **(D, H)** In *Ht-PA-Cre;DT-A^{floxed}* mutant embryos, absence of Schwann cells accompanies defective initial assembly of the hypoglossal nerve, and also the tip of the hypoglossal projection is devoid of Schwann cells. **(E, I)** Wholemount antibody staining for Sox10 in *Npn-1^{Sema-}* mutant embryos shows a reduction of Schwann cells migrating along defasciculated hypoglossal rootlets 8arrowheads from 9,79 +/- 0,68 SEM to 6,72 +/- 0,55 Schwann cells per rootlet ($p \leq 0,005$). Scale bar in **(H)** equals 100 μ m for panels **(B-E)** and 40 μ m for **(F-H)**.

In *Npn-1^{Sema}* mutant embryos, where all Sema3-Npn-1 signaling is abolished in, we observed a similar phenotype of fewer Schwann cells migrating along defasciculated rootlets (Fig. 25E, I). In embryos, where neural crest and placodally derived cells are eliminated by tissue specific activation of *DT-A*, Schwann cell precursors are absent from hypoglossal rootlets and the tip of hypoglossal projections (Fig. 25D, H). In these *Ht-PA-Cre;DT-A^{floxed}* mutant embryos we also found defects in the initial assembly of the hypoglossal nerve, but not in the final targeting of its projections (Fig. 25I, P).

We therefore conclude that *Npn-1* expression by neural crest derived Schwann cells is dispensable for general guidance of hypoglossal projections towards the tongue, but crucial for initial selective fasciculation of the hypoglossal nerve.

3. IDENTIFICATION OF NOVEL GUIDANCE FACTORS THAT GOVERN THE DORSAL-VENTRAL GUIDANCE DECISION OF MOTOR AND SENSORY AXONS

The establishment of precisely wired sensory and motor connections into the periphery requires the correct accomplishment of polarized outgrowth of axons from differentiated neurons and subsequent axon pathfinding towards the target region, and the recognition of the appropriate synaptic partner. Over the past two decades, different adhesion molecules and guidance cues have been identified that are involved in mediating the dorsal-ventral guidance decision of motor axons. Spatio-temporally controlled expression of guidance molecules in the environment and the activation of specific receptors on growth cone at the leading edge of the elongating axon leads to the activation of signal transduction pathways that activate cytoskeletal reorganizations governing axonal elongation, turning, or retraction (reviewed in Huber et al., 2003). In the past years, several cues have been identified that are involved in guiding motor axons to the limbs (reviewed in Bonanomi and Pfaff, 2010). However, while the single or combined deletion of these cues or their receptors and genes mediating their expression caused significant impairments in the development of peripheral projections, the fidelity of dorsal-ventral pathfinding decisions of motor axons was not completely abolished altogether. Surprisingly, to date, nothing is known about how sensory axons navigate the dorsal-ventral decision point, and so far no markers have been found that distinguish sensory neurons based on their projection patterns to the dorsal and ventral limb. In a genome wide screening approach in the Huber Brösamle laboratory motor and sensory neurons were differentially labeled according to their projection patterns. Microarray analysis allowed for expression profiling of the differentially projecting neuronal subgroups to identify candidate genes mediating the dorsal-ventral choice of motor and sensory axons. Expression values of possible candidate genes in dorsally and ventrally projecting neurons were correlated to each other by subtracting the dorsal fold change (FC) from the ventral FC. Therefore, a positive FC predicts a predominant expression in medial LMC neurons projecting to the ventral limb, while a negative

fold change indicates a more prominent expression in lateral LMC neurons projecting dorsally.

3.1 VALIDATION OF CANDIDATE GENES FOR BRACHIAL MOTOR AXON GUIDANCE

Motor neurons projecting their axons to the dorsal and ventral limb mesenchyme are situated in the lateral or medial LMC, respectively. Differentially expressed homeobox transcription factors are markers to identify these distinct sub-columnar populations. Indeed, the microarray analysis correctly predicted previously shown differential expression of markers in dorsally projecting motor neurons, such as the transcription factor *Lim1*, and in ventrally projecting motor neurons, such as the transcription factor *Isl1* (Kania et al., 2000). Also guidance receptors, i.e. EphA4 for the LMCI and Npn2 for the LMCm were found amongst differentially expressed genes (Eberhart et al., 2002; Huber et al., 2005). These findings demonstrate the reliability of differential microarray screens.

Of the 124 genes predicted to be differentially expressed in brachial motor neurons, we chose 10 candidates based on literature recherche that suggested a potential role in axon guidance for a more detailed investigation. The differential expression of seven of these ten candidates was validated by *in situ* hybridization in combination with immunohistochemical stainings against marker proteins differentiating medial and lateral LMC (Table 3). With a FC of -2,6, cellular retinoic acid binding protein 1 (*Crabp1*) was predicted to be predominantly expressed in motor neurons of the LMCI. Expression analysis on coronal section of E12.5 mouse embryos, however, showed that *Crabp1* mRNA was expressed more prominently in *Isl1* positive motor neurons of the LMCm than in *Lim1* positive motor neurons of the LMCI (Table 3 and data not shown). Therefore, *Crabp1* was excluded as a candidate to govern specific dorsal-ventral guidance decisions of brachial motor axons. The POU domain, class 6, transcription factor 1 (*Pou6f1*) and transmembrane glycoprotein Prominin1 (*Prom1*) were predicted by the microarray analysis to be differentially expressed in the LMCI, or the LMCm, respectively. Expression analysis of these two genes showed an even mRNA distribution in motor neurons of the medial and lateral aspect of the LMC (Table 3, data not shown), thus *Pou6f1* and

Prom1 also were excluded as candidates mediating pathfinding decisions of motor axons.

Based on the selection criteria explained before and literature recherche (I. 4.3.1), we chose four of the seven candidates that showed an *in situ* hybridization signal in the predicted subpopulation of the LMC for a more detailed expression analysis from 10.5 to E12.5, covering the developmental period when motor axons execute the dorsal-ventral guidance decision. For her bachelor thesis that was supervised by me, Teresa Hähl validated the predicted expression patterns of *Arhgap29* (III. 3.1.1), *Ccdc3* (III. 3.1.2) and *Elk3* (III. 3.1.3) at E12.5 (Haehl et al., 2011). The role of FGFR2 in motor axon growth, fasciculation and guidance was investigated in detail using a conditional genetic approach to selectively eliminate *FGFR2* in motor neurons (III. 3.1.4.1).

Name	FC	Predicted in	E12.5 ISH	Function
Arhgap29	+4,0	LMCm	LMCm	Rho GTPase activating protein
Ccdc3	+4,3	LMCm	LMCm	Function unknown, secreted protein
Crabp1	-2,6	LMCl	LMCm	cellular retinoid acid binding protein 1
Elk3	+2,3	LMCm	LMCm	Transcription factor
FGFR2	+2,2	LMCm	LMCm	Fibroblast growth factor receptor
Gbx2	-2,6	LMCl	LMCl	Transcription factor
LGals1	+3,0	LMCm	LMCm	β -galactoside-binding protein, cell-cell and cell-matrix interactions
Pou6f1	-2,1	LMCl	Even staining	Transcription factor
Prom1	+2,1	LMCm	Even staining	Transmembrane glycoprotein
Sulf1	+5,4	LMCm	LMCm	inhibits signaling by heparin-dependent growth factors

Table 3: Candidate genes in brachial motor neurons.

10 candidate genes were chosen for an analysis of their expression patterns at E12.5 to validate the prediction of the microarray analysis. A positive FC indicates a higher expression in LMCm motor neurons, while a negative FC predicts an expression predominantly in LMCL motor neurons. Candidates highlighted in green were chosen for a more detailed analysis. Candidates highlighted in red showed no differential expression in the predicted motor neuron subpopulations.

3.1.1 RHO GTPASE ACTIVATING PROTEIN 29 - *ARHGAP29*

During axon extension, interaction of guidance cues in the surrounding mesenchyme with guidance receptors lead to turning of the growth cone. These turning events are regulated by signalling pathways via GTP binding proteins, and subsequent re-organization of the cytoskeleton within the filopodia and lamellipodia of the growth cone (Hall, 1998; Dickson, 2001; Luo, 2002). In general, GTP-binding proteins can physically interact with effector proteins in their GTP-bound active form. GTPase activating proteins (GAPs) increase the GTPase activity of small GTP binding proteins to hydrolyze the bound GTP to GDP, rendering the small GTP-binding protein inactive. *Arhgap29* contains a RhoGAP domain and is therefore in a position to inactivate Rho, a small GTP-binding protein that is also active in actin filament assembly or disassembly (Myagmar et al., 2005). Up to now, however, nothing is known about *Arhgap29* function in general, and its roles in axon elongation and promotion of dorsal-ventral guidance decisions in particular. To confirm the prediction of *Arhgap29* expression predominantly in ventrally projecting motor neurons, we performed *in situ* hybridization on cross-sections of E12.5 wildtype mouse embryos. Immunohistochemistry against forkhead box P1 (FoxP1) labels all motor neurons of the LMC (Palmesino et al., 2010). For distinction of the medial and lateral LMC we used antibody staining against *Isl1*, determining LMCm motor neurons as FoxP1⁺/*Isl1*⁺ (green dashed line in Fig. 26A), while LMCl motor neurons are characterized by FoxP1 expression in absence of *Isl1* (red dashed line in Fig. 26A). At E12.5, we found a differential expression of *Arhgap29* in motor neurons of the LMCm (arrows, green dashed line in Fig. 26A), while the LMCl showed less *Arhgap29* positive neurons (red dashed line in Fig. 26A). Furthermore, expression of the Rho-GAP was observed in the MMC (arrows in cyan dashed line in Fig. 26A). We quantified our observations by correlating the number of *Arhgap29* positive motor neurons in the two differentially projecting motor columns to the total number of FoxP1⁺/*Isl1*⁺ and FoxP1⁺/*Isl1*⁻ neurons, respectively. The quantification showed that 19,09 % +/- 1,81 SEM of LMCm motor neurons expressed *Arhgap29*, while only 4,85 % +/- 0.58 SEM of dorsally projecting motor neurons in the LMCl express the candidate gene (Fig. 26B, p≤0,001). *In situ* hybridization revealed a rather homogeneous expression of *Arhgap29* mRNA in motor neurons the ventral horn of

the spinal cord at brachial levels of E10.5 mouse embryos (Fig. 26D). However, already one day later, at E11.5, a separation of *Arhgap29* positive cells into the area of ventrally projecting motor neurons in the LMCm was observed (arrows in green dashed line in Fig. 26C, C').

Thus, our data confirm the prediction of the microarray data with a FC of +4,0 that *Arhgap29* is predominantly expressed in ventrally projecting motor neurons (Table 3), and therefore renders *Arhgap29* an interesting candidate for government of guidance decisions of ventrally projecting motor neurons of the brachial LMC.

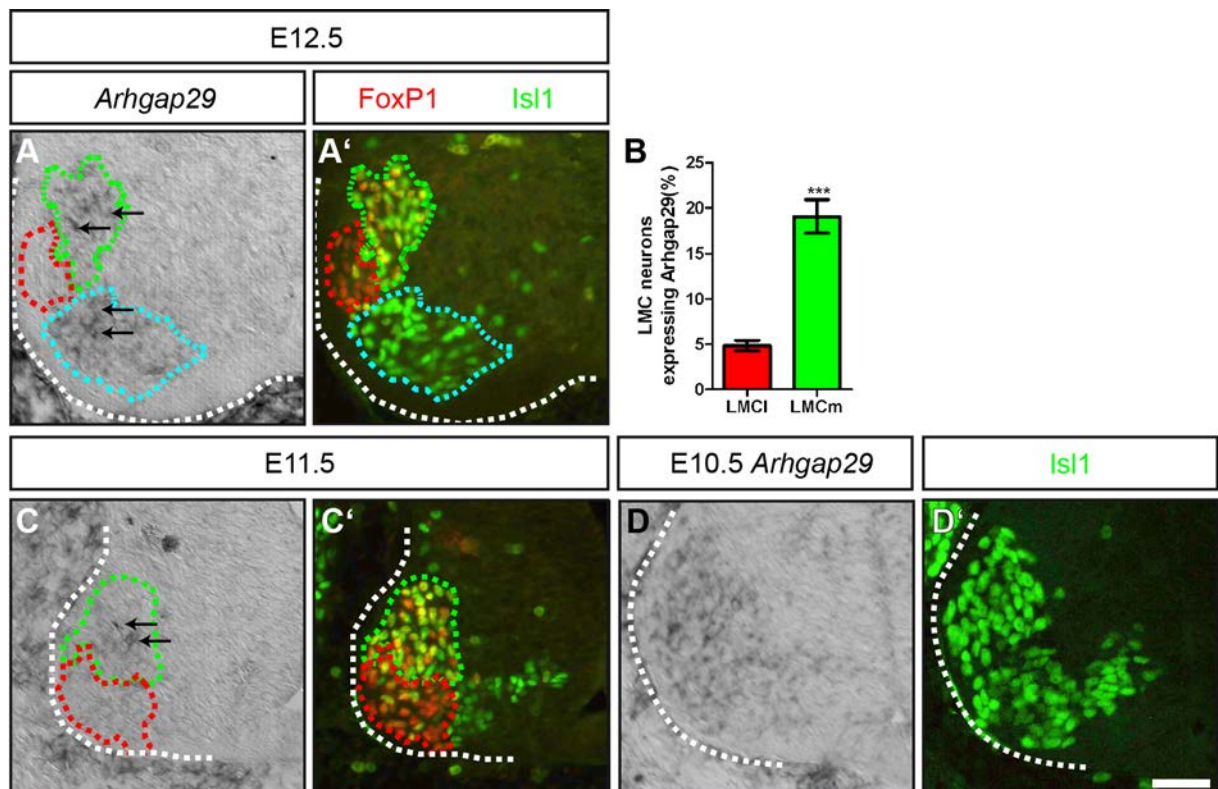


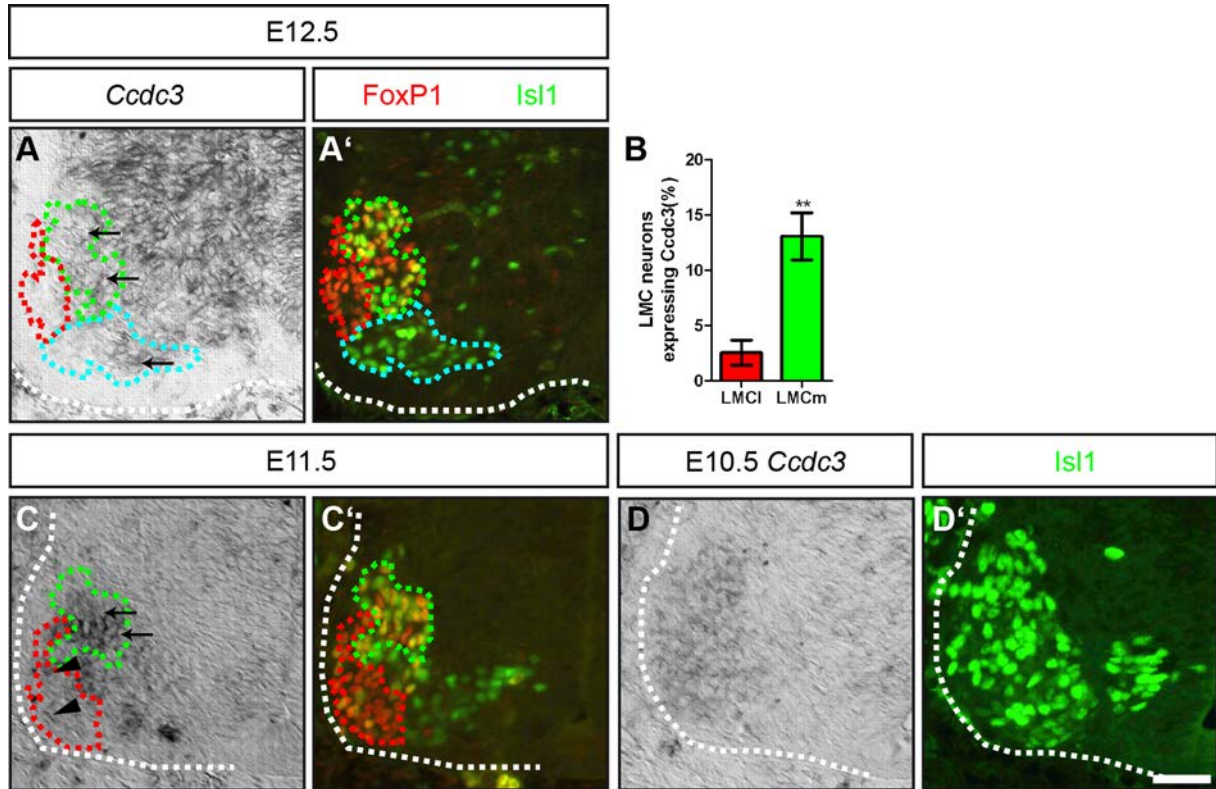
Figure 26: Expression analysis of *Arhgap29*.

(A, A') *In situ* hybridization against *Arhgap29* showed a higher expression in the FoxP1⁺/Isl1⁺ LMCm (green dashed line, arrows), than in the FoxP1⁺/Isl1⁻ LMCI (red dashed line). Furthermore, expression in subpopulations of MMC neurons were also observed (cyan dashed line, arrows). (B) Quantification of *Arhgap29* expression motor neurons in the LMCm (FoxP1⁺/Isl1⁺) and LMCI (FoxP1⁺/Isl1⁻) showed a 3,93 fold higher number of LMCm neurons expressing the Rho GTPase. (C, C') At E11.5, expression of *Arhgap29* was found predominantly in motor neurons of the LMCm, while it was virtually absent in the FoxP1⁺/Isl1⁻ LMCI neurons. (D, D') At E10.5, *Arhgap29* is expressed in LMC neurons in the ventral horn at brachial levels. Scale bar in (D') equals 50µm for (A), 40µm for (C), and 25µm for (D).

3.1.2 COILED COIL DOMAIN CONTAINING 3 – *CCDC3*

During neuronal development, guidance cues expressed by the surrounding mesenchyme, or secreted by axons themselves, are essential for correct pathfinding of motor axons. These cues can be either repulsive or attractive and interact with receptors on the growth cone at the tip of growing axons to guide them to their targets. *Ccdc3* is a novel secretory protein whose expression in endothelial cells of the vascular system and in mature adipocytes of adipose tissue is hormonally regulated by insulin or tumor necrosis factor alpha (TNF α ; Kobayashi et al., 2010). *Ccdc3* has a highly conserved coiled coil domain and is secreted through the endoplasmic reticulum-Golgi pathway, however, very little is known about its function. Coiled coil motifs are found on microtubules and other structures of the filament system of the cells, but also on motor proteins migrating along these filaments. Furthermore, coiled-coil containing proteins are involved in molecular recognition systems, and can trigger protein refolding or actin-bundling (reviewed in Burkhard et al., 2001). The microarray analysis predicted *Ccdc3* to be expressed predominantly in ventrally projecting cells of the LMCm of E12.5 embryos with a fold change of +4,3 (Table 3). When we investigated its expression pattern by *in situ* hybridization on cross-sections of E12.5 embryos, we found a prominent expression of *Ccdc3* in many neurons of the spinal cord. At brachial levels, however, within the LMC, 13,07 % +/- 2,14 SEM of all FoxP1⁺/Isl1⁺ positive neurons of the LMCm expressed *Ccdc3*, while only 2,56 % +/- 1.12 SEM of dorsally projecting neurons of the LMCl (FoxP1⁺/Isl1⁻) were found to be *Ccdc3* positive (arrows in Fig. 27A, B; p \leq 0,005). Therefore, the prediction of the microarray analysis was confirmed: in the LMCm five times more motor neurons express *Ccdc3* than motor neurons of the lateral LMC. Furthermore, we also observed *Ccdc3* expression in motor neurons of the MMC (cyan dashed line in Fig. 27A). The differential expression of *Ccdc3* in ventrally projecting motor neurons of the medial LMC was already observed at E11.5 (arrows in Fig. 27C). Very few individual neurons in the LMCl were also found to express the coiled coil containing protein (arrowheads in Fig. 27C). At E10.5, when motor axon have not yet traversed the plexus region, *Ccdc3* expression in motor neurons at brachial level is rather dispersed in all motor neurons at brachial levels (Fig. 27D).

Therefore, our quantification confirms the microarray data prediction and validates *Ccdc3* as a candidate for mediation of dorsal ventral guidance decisions of brachial motor neurons.



3.1.3 ETS DOMAIN-CONTAINING PROTEIN ELK-3

ETS family members are involved in transcriptional regulation of genes that are critical for cell differentiation and proliferation. Elk1, a close relative to Elk3 is expressed in dendrites and axon terminals and activates expression of immediate early genes like *c-fos* (Sgambato et al., 1998; Vanhoutte et al., 1999; Cesari et al., 2004) whose transcription is up-regulated in response to extracellular signals, like

growth factors or upon stimulation of axons (Kovacs, 2008). Furthermore, target derived activation of ETS gene signaling was shown to be important for the formation of distinct motor pools (Arber et al., 2000). The transcription factor *Elk3* has been predicted by the microarray screen to be predominantly expressed in ventrally projecting neurons (FC= +2,3). At E12.5, quantification of the *in situ* hybridization in the two motor columns LMCm and LMCI revealed that *Elk3* is expressed in 20,25 % \pm 1,63 SEM of FoxP1⁺/Isl1⁺ positive neurons of the LMCm, while only 6,75 % \pm 0,96 SEM of dorsally projecting LMCI neurons were found to express the transcription factor (Fig. 28A, B). Therefore, the threefold higher number of ventrally projecting motor neurons showing expression of *Elk3* in confirmed the prediction of the microarray analysis.

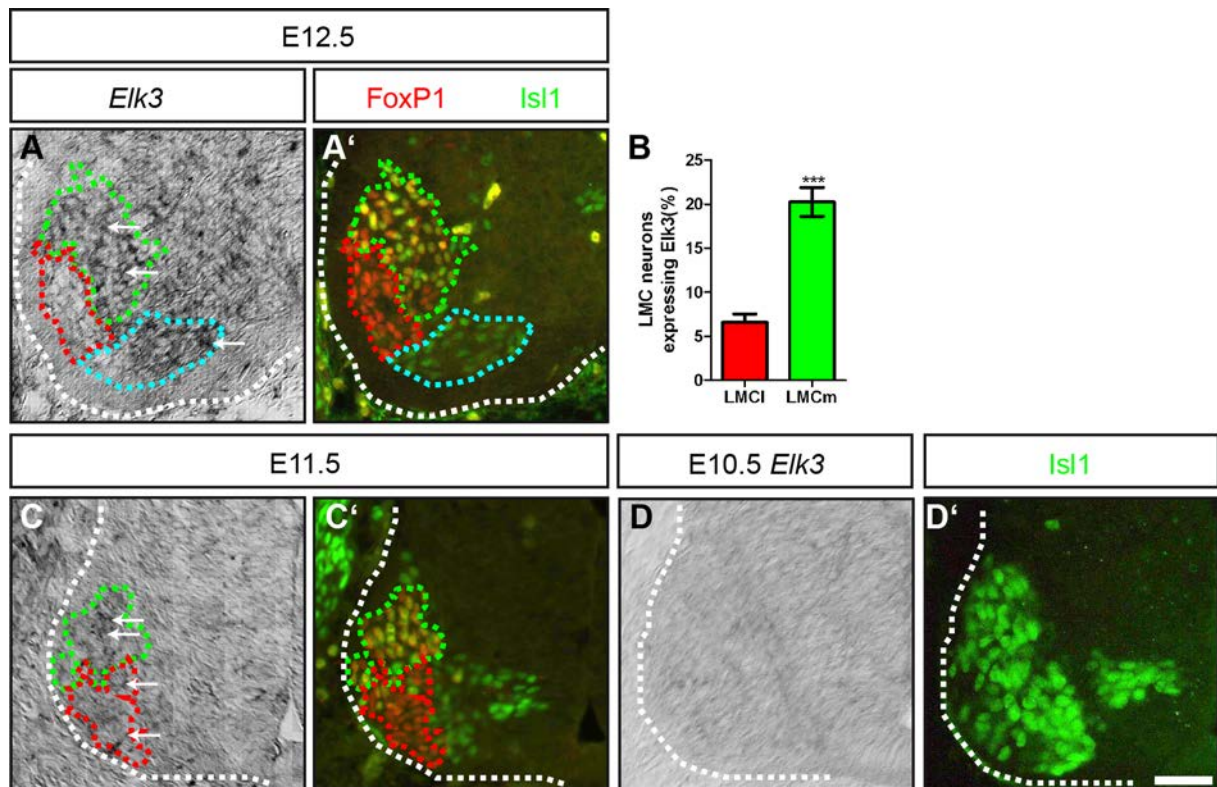


Figure 28: Expression analysis of *Elk3*.

(A, A') *In situ* hybridization against *Elk3* showed a higher expression in motor neurons of the LMCm (FoxP1⁺/Isl1⁺, green dashed line, arrows), than in dorsally projecting motor neurons of the LMCI (FoxP1⁺/Isl1⁻, red dashed line). *Ccdc3* expression was also observed in a medial subpopulation of MMC neurons (cyan dashed line, arrow) **(C, C')** At E11.5, motor neurons of the LMCm (green dashed line, arrows) and LMCI (arrowheads in red dashed line) express *Elk3*. **(D, D')** At E10.5, *Elk3* is only weakly expressed the area of the LMC in the ventral horn at brachial levels. Scale bar in **(D')** equals 50 μ m for **(A)**, 40 μ m for **(C)**, and 25 μ m for **(D)**.

At E11.5, both dorsally and ventrally projecting motor neurons appeared to express *Elk3* (arrows in Fig. 28C), while the signal in the rest of the spinal cord was

very weak or absent. At E10.5, only very weak, if any staining at all, was observed in the ventral horn of the spinal cord at brachial levels (Fig. 28D).

This expression pattern renders *Elk3* an unlikely candidate for governing dorsal-ventral guidance decisions in the plexus region. However, as also other ETS genes are activated rather late in development through target derived signalling, distinct expression of *Elk3* in LMCm motor neurons at E12.5 still could play a role for motor pool formation of motor neurons projecting their axons to the same targets in the periphery.

3.1.4 FIBROBLAST GROWTH FACTOR RECEPTOR 2 – *FGFR2*

Graded FGF-FGFR signaling along the spinal cord plays a role in the definition of the columnar identity of motor neurons within the ventral horn, among other tasks in neural induction and embryonic patterning (Dasen et al., 2003; Bottcher and Niehrs, 2005; Dasen et al., 2005). Already during very early embryonic development, *FGFR2* was found to co-localize with NCAM, a key regulator of axon growth and fasciculation, which was shown to activate downstream signaling functions of the FGF receptor (Vesterlund et al., 2011). Ablation of *FGFR2*-isoforms leads to deficits in limb bud induction and formation of the skeleton (Lizarraga et al., 1999; De Moerlooze et al., 2000; Coumoul and Deng, 2003). In the microarray screen, *FGFR2* was predicted to be expressed predominantly in ventrally projecting motor neurons (FC=+2,2). We found expression of *FGFR2* mainly and robustly in the ventricular zone (empty arrowhead in Fig. 29A), but also in the lateral regions where spinal motor neurons that innervate the distal limbs reside. When quantifying the number of *FGFR2* expressing cells in the two subdivisions of the LMC, we found that 38,29 % +/- 0,19 SEM of ventrally projecting LMCm neurons co-expressed the FGF receptor. However, we also found 28,52 % +/- 0,52 SEM of dorsally projecting neurons were positive for *FGFR2 in situ* signal. (Fig. 29B, $p \leq 0,001$). Thus, the 1.3 fold higher number of ventrally projecting motor neurons expressing *FGFR2* confirmed the microarray prediction. However, whether the relatively small difference of only 10% impacts the guidance of ventrally projecting axons needs further investigation. Its early co-expression with NCAM, which is a key player in axon sorting within the plexus region (Tang et al., 1992, Tang et al., 1994) and the fact that NCAM can

activate *FGFR2* (Vesterlund et al., 2011) implicates roles in fasciculation of axonal projections. However, whether the FGF receptor that plays such a prominent role in limb bud induction is also mediating specific axon guidance events in the motor system is unknown.

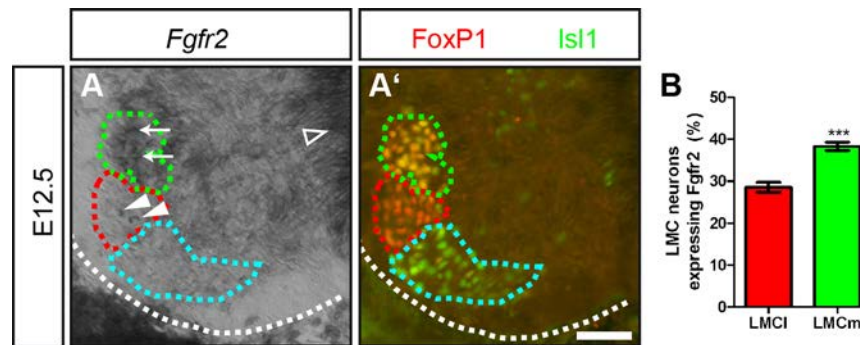


Figure 29: Expression analysis of *FGFR2*.

(A, A') *In situ* hybridization against *FGFR2* shows a higher expression in motor neurons of the LMCm (FoxP1⁺/Isl1⁺, green dashed line, arrows), than in dorsally projecting motor neurons of the LMCI (FoxP1⁺/Isl1⁻, red dashed line). **(B)** Quantification of *FGFR2* mRNA expression in motor neurons of the LMCm and LMCI showed a significantly higher number of ventrally projecting motor neurons that expressed the FGF receptor. Scale bar in **(A')** equals 50µm.

While no mouse lines are available for further investigation of *Arhgap29* and *Ccdc3* function, a conditional mouse line for *FGFR2* (Blak et al., 2007) was available at the Institute of Developmental Genetics (kindly provided by Dr. Ralf Kühn). Even though *FGFR2* shows the smallest difference in differential expression, we employed a genetic approach to conditionally ablate *FGFR2* in motor neurons of mouse embryos and Teresa Hähl investigated axon fasciculation and guidance fidelity of brachial motor axons devoid of *FGFR2* in her bachelor thesis that was supervised by me (Haehl et al., 2011).

3.1.4.1 CONDITIONAL ABLATION OF *FGFR2* IN MOTOR NEURONS DOES NOT ALTER FASCICULATION AND GROWTH PATTERNS OF MOTOR NERVES IN THE EMBRYONIC FORELIMB

To ablate *FGFR2* selectively in motor neurons, we crossed a conditional *FGFR2* line (Blak et al., 2007), in which exon 5 is flanked by loxP sites to the *Olig2-Cre* line (Dessaud et al., 2007). Deletion of exon 5 leads to a stop codon in the extracellular domain within exon 6 of *FGFR2*. To distinguish sensory from motor axons we crossed these mouse lines to the *Hb9::eGFP* line, where expression of

GFP is activated in all motor neurons (Wichterle et al., 2002). We analyzed wholemount embryo preparations stained for neurofilament (sensory axons, in the absence of GFP) and GFP (motor axons) at E12.5 to assess nerve growth deficits and impairments in fasciculation of motor axons that ablation of *FGFR2* in motor neurons might cause. Investigation of growth patterning of the four major nerve branches innervating the distal forelimb of *FGFR2^{flox/flox};Olig2-Cre⁺* mutant embryos, however, showed no obvious differences in the gross morphology of motor forelimb innervation, when compared to control embryos (Fig. 30A-D). As *FGFR2* was predicted to be differentially expressed in neurons of the LMCm, we quantified the distal advancement of the median nerve (3) into the palm of the embryonic forelimb by correlating the length of the distalmost motor nerve branch to the length of the limb. We found no significant differences in the extension of this ventrally projecting nerve when comparing the distal advancement to littermate controls (Fig. 30F, $p=0,35$). Also measurement of the individual thickness of the four major motor nerves contributing to forelimb innervation showed no alterations in fasciculation of these nerve trunks (Fig. 30E). Sensory innervation of the forelimb is not affected by ablation of *FGFR2* in motor neurons when compared to littermate controls (Fig. 30A-D).

These findings argue for an only subordinate, if any, role of *FGFR2* in motor neurons for motor axon fasciculation and patterning during embryonic development.

3.1.4.2 DORSAL-VENTRAL GUIDANCE OF MOTOR AXONS IS NORMAL IN EMBRYOS THAT LACK *FGFR2* IN MOTOR NEURONS

For the development of a functional nervous system, accurate dorsal-ventral guidance to the limb is crucial. Ablation of *FGFR2* in motor neurons does not obviously affect fasciculation and patterning of motor axons innervating the distal embryonic limb. However, guidance deficits at the dorsal-ventral choice point cannot be ruled out by intact gross morphology of motor forelimb innervation. We therefore retrogradely labeled motor neurons projecting to dorsal limb musculature by injection of dextran-coupled Rhodamine and investigated guidance fidelity of Isl1-positive motor neurons of the LMCm. We found that conditional ablation of *FGFR2* in motor neurons does not lead to a significant increase of errors in the dorsal-ventral guidance decisions when compared to wildtype littermates. In control embryos,

4,87 % +/- 0,66 SEM of dorsally backfilled motor neurons were found to be *Isl1*-positive and thus misprojecting. In *FGFR2^{flox/flox};Olig2-Cre⁺* mutant embryos, only 5,76 % +/- 0,19 SEM of neurons of the LMCm misrouted their axons to dorsal limb musculature (Fig. 30G-I).

These findings indicate no requirement for *FGFR2* in motor neurons for appropriate fasciculation and nerve patterning during innervation of the embryonic forelimb.

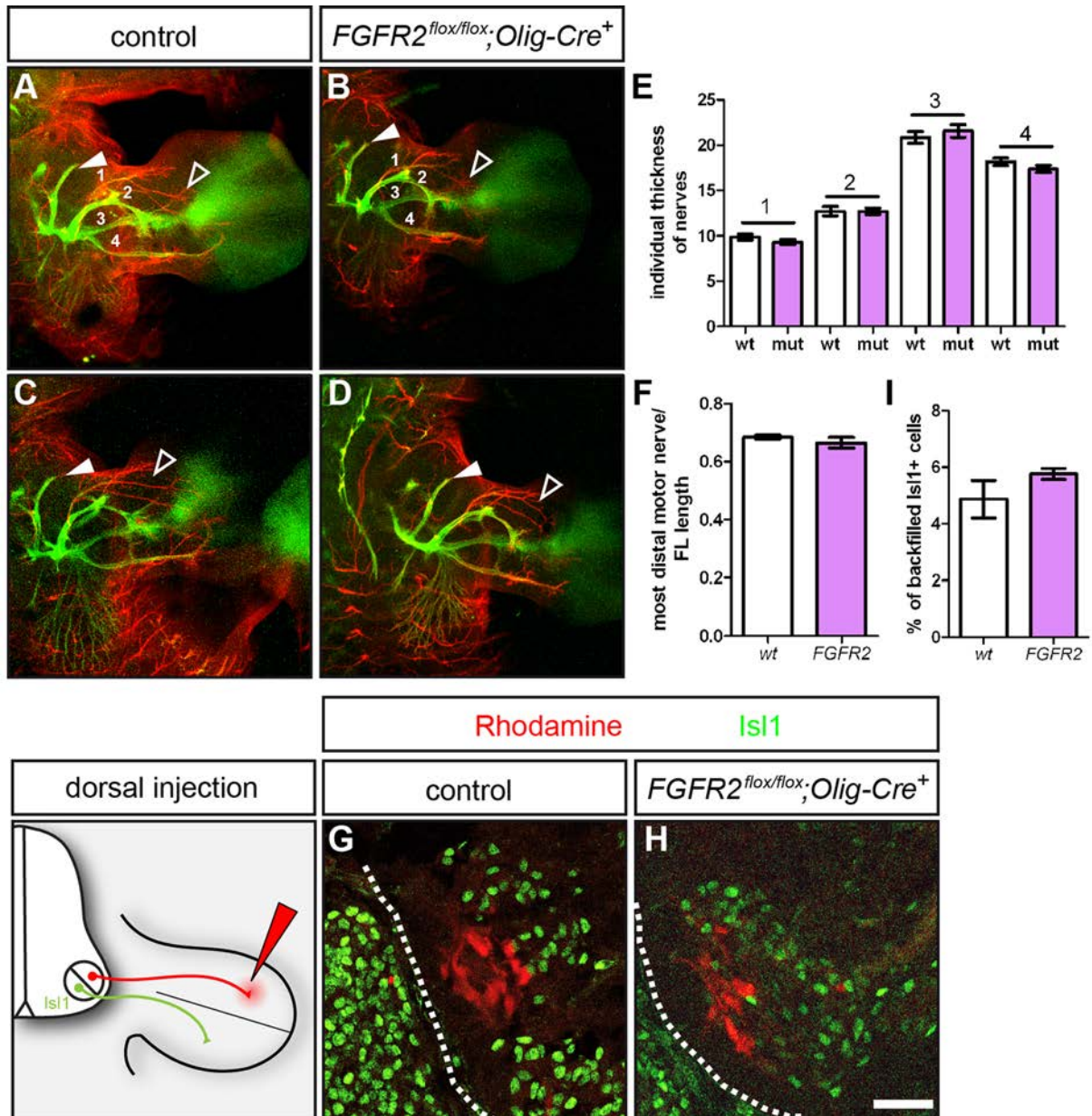


Figure 30: Conditional ablation of *FGFR2* does not affect motor axon growth, fasciculation and guidance.

Wholemout antibody staining against *Hb9::eGFP* (green, motor nerves) and neurofilament (red, motor and sensory axons). (A, C) Motor and sensory innervation of control embryo forelimbs. 1=branch of the radial nerve, 2= radial nerve, 3= median nerve, 4= ulnar nerve. (B, D) Gross

morphology of motor and sensory innervation to the forelimb is not altered in $FGFR2^{flox/flox};Olig2-Cre^+$ mutant embryos. **(E)** Quantification of the individual thickness of the 4 major motor nerves shows not significant differences in fasciculation ($p^1=0,24$, $p^2=0,99$, $p^3=0,47$, $p^4=0,19$) between control and mutant embryos. **(F)** Distal advancement of the median nerve is not impaired in $FGFR2^{flox/flox};Olig2-Cre^+$ mutant embryos. **(G, H)** Retrograde tracing from dorsal musculature showed no increase in guidance errors of LMCm neurons ($Isl1^+$) in $FGFR2^{flox/flox};Olig2-Cre^+$ mutant embryos. **(I)** Quantification of misprojecting motor neurons ($p=0,26$). Scale bar in **(H)** equals 500 μ m for **(A, B)**, 400 μ m for **(C, D)**, and 50 μ m for **(G, H)**.

3.2 VALIDATION OF CANDIDATE GENES FOR SENSORY AXON GUIDANCE

In contrast to the topographical organization of motor neurons in the LMCm and LMCI in the ventral horn of the spinal cord, sensory neurons of the DRG with targets in the dorsal or ventral limb mesenchyme are dispersed throughout the entire DRG. Before further steps to investigate roles of candidate genes in fasciculation and growth decision can be taken, the prediction of differentially expressed genes needed to be confirmed. As no markers for dorsally and ventrally projecting sensory neurons are known, we injected two different fluorescence-coupled dextrans into dorsal and ventral musculature of the forelimbs of E12.5 embryos to be able to distinguish the differentially projecting sensory neurons. The fluorescent dyes were taken up by the nerve endings and retrogradely transported to the cell bodies. This method, however, is only feasible when axons have already entered the distal limb, thus only enables us to investigate differential expression of candidate genes at E12.5 and older stages. We performed *in situ* hybridization on sections of these backfilled embryos to validate candidate genes predicted to be differentially expressed in dorsally projecting sensory neurons at brachial levels. Based on literature recherche that suggested a potential role in axon guidance and the previously mentioned selection criteria (l. 4.3.1) we chose five candidates for a more detailed investigation. Expression patterns in the embryonic DRG that were assembled in the GenePaint database (www.genepaint.org) provided additional information for the selection process. The microarray screen predicted 13 genes to be differentially expressed in dorsally or ventrally projecting sensory neurons at brachial levels. None of these genes was found among the candidate genes that were predicted to be differentially expressed in motor neurons. These findings coincide with findings, that marker genes for motor neurons, as for example *Isl1* are not differentially expressed in

sensory neurons (Sun et al., 2008). We chose five genes that might be involved in different processes regulating growth cone turning events for confirmation by *in situ* hybridization (Table 4).

Name	FC	Predicted in	Function
Cux2	-29	Dorsally projecting sensory neurons	Cut-like transcription factor
Gnb4	-31	Dorsally projecting sensory neurons	Subunit of G-protein, signal transduction
Ift172	-64,3	Dorsally projecting sensory neurons	Component of intraflagellar transport complex
Nek1	-18	Dorsally projecting sensory neurons	Kinase, ciliogenesis, cell cycle progression
PLCd4	-40	Dorsally projecting sensory neurons	Generation of second messengers

Table 4: Candidate genes in brachial sensory neurons.

Candidate genes and their corresponding FC predicted by the microarray analysis are listed and were chosen for a detailed expression analysis.

3.2.1. CUT LIKE HOMEODOMAIN TRANSCRIPTION FACTOR 2 - *CUX2*

Members of the cut-like homeodomain transcription factor family (*Cux*) were shown to regulate cell-cycle progression and development of neural progenitors. In invertebrates, *Cut* is required for external sensory organ development (Ledford et al., 2002). In vertebrates, two *Cut* homologs exist. *Cux1* plays a role in cell-cycle control (Ledford et al., 2002). *Cux2* is expressed in the olfactory epithelium, branchial arches and limb bud progress zones, roof plate, motor neurons and subsets of dorsal root ganglia (Iulianella et al., 2003; Bachy et al., 2011). The microarray screen predicted *Cux2* to be expressed predominantly in dorsally projecting sensory neurons (FC= -29). Evaluation of embryos in which dorsally and ventrally projecting sensory neurons were labeled with different fluorescently labeled dextrans showed that 53,93 % +/- 2,49 SEM of the dorsally projecting sensory neurons expressed *Cux2* (green arrows in Fig. 31A, C). In contrast, only 25,39 % +/- 4,20 SEM of ventrally projecting sensory neurons expressed the transcription factor (red arrowheads in Fig. 31A, C; $p \leq 0,005$). Thus, the number of dorsally projecting sensory neurons that show *Cux2* expression is 2,1 fold higher than that of sensory neurons that innervate targets in the ventral forelimb.

Therefore, we confirmed the microarray prediction of *Cux2* being expressed predominantly in dorsally projecting sensory neurons.

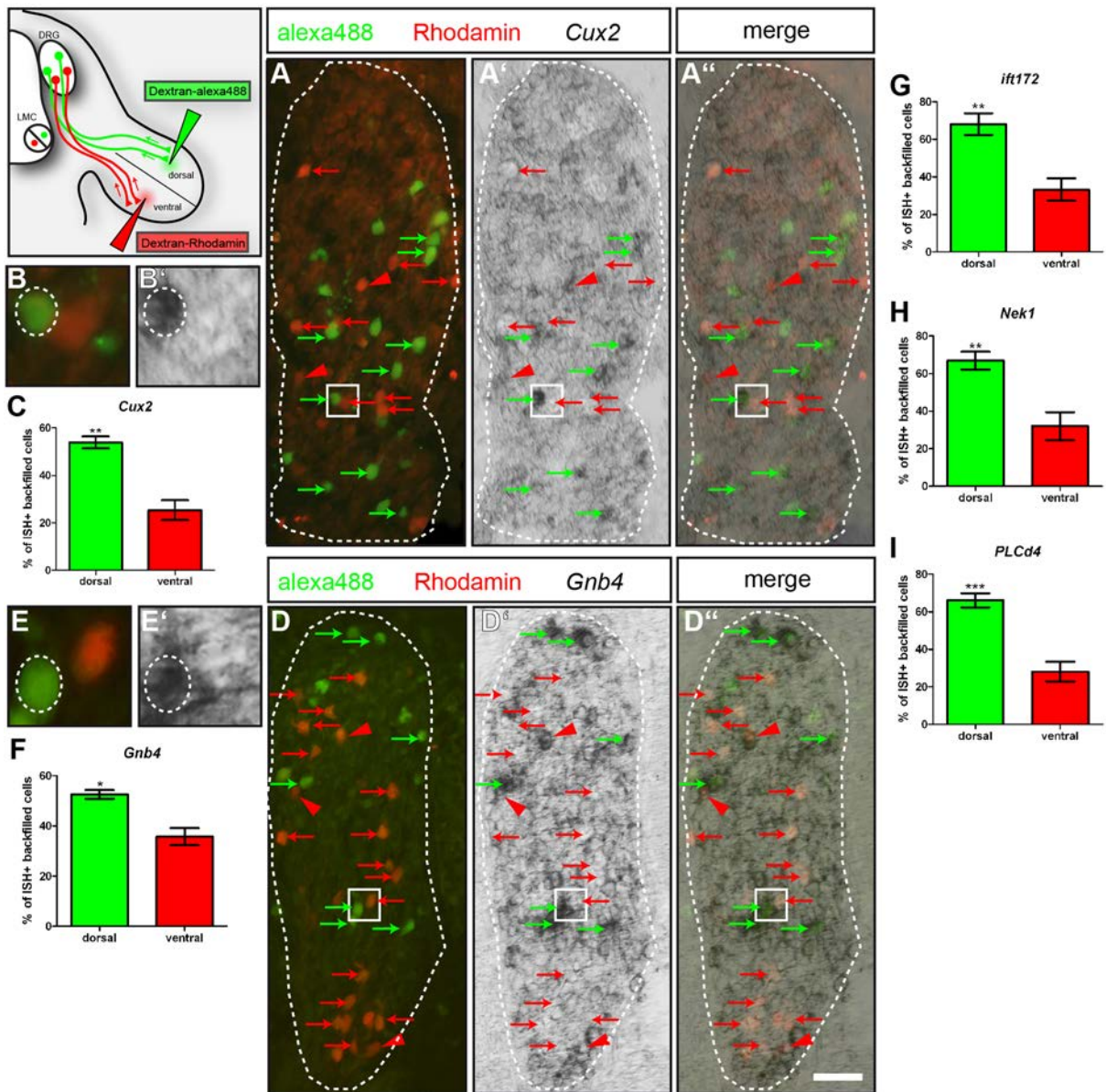


Figure 31: Validation of candidate genes for dorsal-ventral guidance of brachial sensory neurons.

(A, D) Cross sections of E12.5 embryo shows sensory neurons that were retrogradely labeled from dorsal (alexa488, green) and ventral (Rhodamine, red) limb mesenchyme. **(A')** *In situ* hybridization against *Cux2* on an adjacent slide. **(A'')** Merge of **(A)** and **(A')** showed predominant expression of *Cux2* mRNA in dorsally projecting sensory neurons (green arrows), while most ventrally projecting sensory neurons are devoid of *Cux2* expression (red arrows). **(B, B')** high magnification of the area boxed in **(A)** shows *Cux2* mRNA expression in dorsally (green), but not ventrally projecting (red) sensory neurons. **(D')** *In situ* hybridization against *Gnb4* on an adjacent slide. **(D'')** Merge of **(D)** and **(D')** showed predominant expression of *Gnb4* mRNA in dorsally projecting sensory neurons (green arrows), while only a few ventrally projecting sensory neurons are positive for *Gnb4* mRNA (red arrowheads). **(E, E')** A high magnification of the areas boxed in **(A)** shows *Gnb4* mRNA expression in dorsally, but not ventrally projecting sensory neurons. **(F)** Quantification retrogradely labeled cells with *Gnb4* mRNA expression showed a 1.47 fold higher number of dorsally projecting sensory neurons that express the guanine nucleotide binding protein. **(G)** Quantification of the *in situ* hybridization against

Ift172 on cross sections of retrogradely labeled E12.5 embryos showed a 2,04 higher expression of the intraflagellar transport protein in dorsally projecting sensory neurons when compared to sensory neurons retrogradely traced from the ventral limb. **(H)** Quantification of retrogradely labeled sensory neurons that were positive for *Nek1* mRNA expression showed a 2,1 fold higher number of dorsally projecting neurons expressing of the kinase. Only 32,01 +/- 7,42 SEM % of sensory neurons traced from the ventral limb expressed *Nek1*. **(I)** When we quantified *PLCd4* mRNA expression on cross sections of retrogradely labeled E12.5 embryos we found a 2.3 fold higher number of dorsally projecting sensory neurons that express *PLCd4*. Scale bar in **(D'')** equals 40 μ m for **(A, D)** and 10 μ m for **(B, E)**.

3.2.2. GUANINE NUCLEOTIDE BINDING PROTEIN BETA 4 – *GNB4*

Heteromeric GTP-binding proteins are coupled to cell surface receptor molecules and mediate signal transduction to intracellular downstream effectors upon activation by hydrolysis of GTP by the alpha-subunit, or activation of ion channels by beta- and gamma-subunits (Logothetis et al., 1987; Krapivinsky et al., 1995). Mice deficient in a close relative of the beta subunit-gene *Gnb4*, *Gnb1*, showed deficits in neural tube closure, neural progenitor cell proliferation and organization (Okoe and Iwakura, 2010). In the microarray screen, *Gnb4* was predicted to be expressed predominantly in dorsally projecting sensory neurons (FC= -31). We analyzed *Gnb4* expression on cross sections of E12.5 embryos in which dorsally and ventrally projecting sensory neurons were retrogradely labeled using different fluorescent tracers (Fig. 31D). Quantification of sensory neurons back labeled from dorsal limb mesenchyme showed that 52,55 % +/- 1,73 SEM of these neurons expressed *Gnb4* (green arrows in Fig. 31D, E, F). In contrast, only 35,74 % +/- 3,42 SEM of the sensory neurons retrogradely labeled from ventral limb mesenchyme expressed the beta subunit of the G protein (red arrowheads in Fig. 31D, F, p=0,018).

Thus, *Gnb4* was validated as gene that is predominantly expressed in dorsally projecting sensory neurons and might therefore be involved in dorsal-ventral guidance decisions of sensory axons.

3.2.3 INTRAFLAGELLAR TRANSPORT HOMOLOG 172 – *IFT172*

Just as cilia, axons are microtubule-based elongated structures, however, while axon-formation is confined to neuronal cells, cilia can be found on the surface of most cells, operating as antenna-like structures. Intraflagellar transport proteins (IFT) play critical roles in the assembly of microtubule precursors that form these

protrusions (Pedersen et al., 2008). Interruption of *Ift172* function, however, not only impaired cilia formation but also disrupted signaling pathways important for neural induction and embryonic patterning, resulting in impaired neural tube closure and defective patterning of the nervous system (Huangfu et al., 2003; Gorivodsky et al., 2009). These findings render *Ift172* an interesting candidate to govern also guidance decisions of axons innervating peripheral targets. In the microarray screen, *ift172* showed a fold change of -64,3 when its expression in dorsally projecting sensory neurons was correlated to the expression values in ventrally projecting neurons and was therefore predicted to be predominantly expressed in dorsally projecting sensory neurons. When we quantified expression of *Ift172* on sections of retrogradely labeled embryos according to the evaluations above, we found that 68,10 % +/- 5,79 SEM sensory neurons that were backfilled from dorsal limb mesenchyme expressed the transport protein (Fig. 31G, $p \leq 0,005$). Only 33,26 % +/- 5,98 SEM of ventrally projecting sensory neurons showed expression of *IFT172* mRNA as revealed by *in situ* hybridization.

Therefore, these findings confirm *Ift172* as a gene predominantly expressed in dorsally projecting sensory neurons as predicted by the microarray screen.

3.2.4 NEVER IN MITOSIS GENE A (NIMA) RELATED KINASE 1 – NEK1

Among other cell types, *Nek1* is expressed in postmitotic spinal sensory neurons and neurons of peripheral ganglia (Arama et al., 1998). In mice mutant for *Nek1*, checkpoint kinases during the cell cycle fail to be activated properly, which leads to growth retardation, facial dysmorphisms and neurologic abnormalities (Chen et al., 2008; White and Quarmby, 2008; Hilton et al., 2009). We analyzed *Nek1* expression on sections of retrogradely labeled embryos. The microarray analysis predicted the gene to be predominantly expressed in dorsally projecting sensory neurons (FC= -18), and indeed, we found 66,92 % +/- 4,77 SEM of sensory neurons retrogradely labeled from dorsal limb mesenchyme to express the kinase. Thus, the number of dorsally projecting sensory neurons showing *Nek1* expression was 2,1 fold higher than that of sensory neurons that innervate targets in the ventral forelimbs. (Fig. 31H, $p \leq 0,005$).

Therefore, *Nek1* was validated as candidate gene to be predominantly expressed in dorsally projecting sensory neurons as it was predicted by the microarray screen.

3.2.5 PHOSPHOLIPASE C DELTA 4 – *PLCd4*

Phospholipase C proteins generate second messengers (Rhee and Bae, 1997) that enable eukaryotic cells to induce various functions such as cell signaling, cytoskeletal re-organization, phagocytosis, membrane traffic, and ion channel activity. *PLCd4* is expressed in neuronal cells upon induction by growth factors like bradikinin, where it governs onset of DNA synthesis and cell growth (Fukami et al., 2000; Akutagawa et al., 2006). When we analyzed the expression pattern of *PLCd4* in DRG at brachial levels, we found that 28,15 % +/- 5,25 SEM of ventrally projecting sensory neurons expressed the candidate gene. The microarray analysis predicted *PLCd4* to be predominantly expressed in dorsally projecting sensory neurons (FC= -40). When we quantified dorsally projecting sensory neurons with an *PLCd4* mRNA expression, we found that 66,16 % +/- 3,77 SEM of sensory neurons back-labeled from dorsal limb mesenchyme expressed *PLCd4* (Fig. 311, $p \leq 0,001$).

Thus, we found *PLCd4* mRNA in a 2,3 times higher number of dorsally projecting sensory neurons and therefore confirmed it as a candidate gene for government of dorsal-ventral guidance decisions of sensory axon guidance.

3.2.6 OUTLOOK

Using retrograde labeling of differentially projecting sensory neurons enabled us to validate the expression patterns predicted by the microarray screen for all five sensory candidates that we chose for a closer analysis. However, even though number of dorsally projecting neurons expressing the candidate genes was about twofold higher than in sensory neurons that project to ventral targets in the limb, expression of *Cux2*, *Gnb4*, *Ift172*, *Nek1* and *PLCd4* in differentially projecting sensory neurons is not an “all or none” expression. As we also found ventrally projecting sensory neurons that showed expression of mRNAs, additional investigations are necessary to further characterize sensory neurons expressing the

candidate genes: Are these neurons nociceptors, innervating the skin, or do they project axons to targets in the musculature? Thus, is the differential expression of the candidate genes confined to TrkA- or TrkC-positive sensory neurons at brachial levels? Only then a decision can be made about a possible function as a marker gene for differentially projecting sensory neurons.

The method of retrograde tracing is only feasible when axons already have entered the limb, thus, dorsal-ventral guidance decisions have already been made. Expression analysis of the candidate genes at earlier embryonal time points, when the axons navigate the dorsal-ventral choice point in the plexus region of the limb is therefore indispensable to further elucidate a function of these candidate genes for pathfinding decisions.

IV. DISCUSSION

1. NPN-1 GOVERNS AXON-AXON INTERACTIONS DURING INNERVATION OF THE VERTEBRATE LIMB

Over the past 20 years, a number of molecular cues and corresponding receptors on the growth cones of the axons have been identified that govern axon guidance and hence contribute to the establishment of the peripheral nervous system (Tessier-Lavigne and Goodman, 1996; O'Donnell et al., 2009). Strictly regulated spatio-temporally controlled expression of these ligand-receptor systems influences growth cone behavior at distinct choice points, where nerve fibers pause, are sorted into target specific bundles, and subsequently grow to their targets in response to local cues. Axons growing into the distal limb, for example, ignore choice points of MMC axons to target axial musculature, but grow in tightly fasciculated nerve bundles into the plexus region at the base of the limb. Within this plexus region, axons from different spinal segments undergo redistribution and execute key navigational choices that will determine their further trajectories to muscular and cutaneous targets of the developing embryonal extremities (Lance-Jones and Landmesser, 1981a; Tosney and Landmesser, 1985a; Wang and Scott, 2000). The concept of pioneer axons that follow distinct pathways pre-patterned at critical positions by so called guidepost cells to their targets has been described for both invertebrate and vertebrate nervous system establishment: pioneer axons in the grasshopper leg define the pathway for motor axons to their target muscles, and pre-patterned pathways lead to correct innervation of the olfactory bulb by neurons in the murine telencephalon (Keshishian and Bentley, 1983; Sato et al., 1998; Tomioka et al., 2000; Niquille et al., 2009). The vast majority of sensory and motor fibers, however, follow these early axons that were growing into “uncharted” territories, and in order to establish precise neuronal networks, appropriate decisions when to branch off the main projection have to be made along the way. The molecular mechanisms that govern interaction between heterotypic nerve fiber tracts for

selective fasciculation and de-fasciculation, are not well understood. In this study, we investigated the role of the guidance receptor Npn-1 for coordinated growth, fasciculation and interaction between sensory and motor fiber systems during the innervation of the vertebrate limb.

1.1 FASCICULATION OF MOTOR AXONS AND THEIR ROLE IN THE ESTABLISHMENT OF PERIPHERAL SENSORY TRAJECTORIES

Motor axons from the ventral horn of the spinal cord and sensory axons from the DRG converge to spinal nerves on their way towards the plexus region at the base of the limb, and also form conjoined trajectories over wide distances to their respective peripheral targets. Whether and to what degree sensory axons depend on motor projections in the formation of their peripheral projection patterns has been controversial: Elimination of motor neurons in the embryonic chick after neural crest cells have coalesced into DRG had no obvious impact on the formation of sensory projections to limb musculature (Wang and Scott, 1999). Early surgical removal of motor neurons, however, resulted in abnormal patterning of sensory trajectories: proprioceptive sensory axons no longer projected to muscular targets but chose cutaneous pathways instead (Landmesser and Honig, 1986). Recent investigations of the establishment of epaxial projections to dorsal axial musculature showed that reverse signaling through ephrinAs expressed on sensory fibers mediates tracking of sensory axons along pre-extending epaxial motor trajectories (Wang et al., 2011).

The guidance receptor Npn-1 is expressed in motor neurons of the LMC at brachial and lumbar levels, as well as in sensory neurons of the DRG and is capable of forming homodimers or binding other cell surface molecules (Castellani, 2002; Geretti et al., 2008). Therefore, it presents itself as a plausible candidate to mediate inter-axonal interactions. When we removed *Npn-1* from motor neurons by tissue specific expression of Cre recombinase, we found a dramatic defasciculation of motor axons in and beyond the plexus region. At forelimb level, extension of motor axons into the limb is reduced in *Npn-1^{cond-/-};Olig2-Cre⁺* mutant embryos. Fasciculation and the localization of sensory nerve branches, however, were unaffected by the severe defasciculation or even missing branches of motor

trajectories. When we used a genetic approach to partially eliminate motor neurons by tissue specific activation of *diphtheria toxin fragment A* (DT-A), hardly any motor axons were sent out. Interestingly, sensory axons were able to project to the plexus region in a fasciculated manner, however, these nerve bundles were reduced in thickness and with variations in the branching frequency of sensory trajectories (Heidi Söllner, Fig. 11 in Huettl et al., 2011). Our findings therefore indicate that sensory innervation of the distal limbs depends on a minimal scaffolding that can be provided by very few motor fibers: Even though defasciculated, motor axons are still present in the proximal limb of *Npn-1^{cond-/-};Olig2-Cre⁺* mutant embryos, and might nonetheless facilitate sensory fiber growth through the plexus region by providing a permissive substrate (Landmesser and Honig, 1986). A possible explanation for the normal development of sensory nerve growth patterns in these mutants is that sensory axons still correctly present Npn-1 on their cell surfaces. Sema3A is expressed in adjacent tissues and might efficiently promote sensory axon fasciculation through a surround repulsion mechanism (Wright et al., 1995; Tessier-Lavigne and Goodman, 1996; Huber et al., 2005). Interestingly, while removal of *Npn-1* from motor neurons leads to dramatic defasciculation of motor axons in the plexus and distal limb, motor fibers remain normally fasciculated in the segment of their trajectory preceding the plexus. Additional cues presented on motor axons and interaction of these with molecules on co-extending sensory axons during growth to the plexus region might differentially regulate proximal fasciculation of spinal nerves and distal fasciculation of motor and sensory axons. Diffusion barriers preventing the exchange of specifically localized membrane proteins have been described in cultured invertebrate and mammalian neurons (Winckler et al., 1999; Katsuki et al., 2009). This intra-axonal regulation of membrane-protein exchange between proximal and distal axonal segments might govern differential sensitivities to guidance cues of growing axons during development by adjusting presence or concentration of cell surface proteins. Whether such diffusion barriers exist in extending motor axons at specific choice points such as the plexus region at the base of the limb, and whether Npn-1 localization along the axon is regulated by similar mechanisms, however, still needs to be determined.

1.2 NPN-1 GOVERNS DORSAL-VENTRAL GUIDANCE DECISIONS OF MOTOR AXONS

Complete disruption of Sema3-Npn-1 signaling by transgenic replacement of Npn-1 with a mutated receptor that is incapable of Sema3 binding (*Npn-1^{Sema-}*) not only causes defasciculation and premature ingrowth of sensory and motor axons into the distal limb, but also leads to errors in the dorsal-ventral guidance decision (Huber et al., 2005). Tissue-specific ablation of *Npn-1* in motor neurons leads to severe motor axon defasciculation, which is also accompanied by deficits in the dorsal-ventral choice of both dorsally and ventrally projecting motor neurons. The wide scattering of motor axons in the plexus area likely interferes with pre-target axon sorting within the plexus region (Imai et al., 2009) and impairs the establishment of the topographic projections of lateral LMC axons to the dorsal limb and medial LMC axons to the ventral limb. Interestingly, this phenotype is less severe compared to dorsal-ventral pathfinding errors that were observed in the *Npn-1^{Sema-}* line. Quantitative analysis of the recombinase efficiency of *Olig2-Cre* showed that Npn-1 is ablated in 70% of the motor neurons of the LMC (Fig. 7). Therefore, some motor neurons still express *Npn-1* and are able to correctly react to Sema3A expression in the surrounding limb mesenchyme, and therefore project to correct distal targets.

1.3 MAINTENANCE OF MOTOR PHENOTYPES AFTER ABLATION OF NPN-1 IN MOTOR NEURONS

Previous investigations reported corrections of aberrant projections in mice lacking the repulsive guidance cue Sema3A during late embryogenesis (E15.5; White and Behar, 2000). Since most of our analyses were done at early embryonic stages, this raises the question whether the fasciculation deficits induced by the removal of *Npn-1* in motor neurons are transient or maintained into later development or even adulthood. Unfortunately, due to poor reagent penetration and increasingly higher GFP background staining of the *Hb9::eGFP* line, an analysis of the deeper motor axons of the forelimb is not feasible at these late embryonic stages. However, we found persistent defasciculation of intercostal nerves after removal of *Npn-1* from motor axons at E15.5 (Heidi Söllner, Fig. S6 in Huettl et al., 2011). These findings

are very reminiscent of observations in mice where binding of Npn-1 to all class 3 Semaphorins was abolished (*Npn-1^{Sema-}*) and defasciculation of intercostal musculature persisted at least until E15.5. Additionally, in these mice the sciatic nerve was found to be still defasciculated at P0 (Haupt et al., 2010). Furthermore, *Npn-1^{cond-/-};Olig2-Cre⁺* mutant embryos show a carpoptosis-like phenotype and atrophied dorsal musculature in the forelimbs already at P0, which might be a result of the decreased distal advancement of motor nerves during development. Behavioural analysis of locomotor skills and electrophysiological data suggest that the deficits in motor connections to distal limb musculature persist throughout adulthood (Soellner and Huber, unpublished). These findings demonstrate that mutant phenotypes caused by loss of Npn-1 signaling are maintained at least to some degree.

1.4 NPN-1 ON SENSORY AXONS MEDIATES FASCICULATION OF SENSORY AND MOTOR AXONS

What role do sensory axons play in the establishment of motor projections to the musculature in the extremities at brachial and lumbar levels? In chicken embryos surgical removal of neural crest precursors was employed to elucidate to what extent afferent input is necessary for coordinated and spontaneous movement of the hindlimbs (Hamburger et al., 1966; Narayanan and Malloy, 1974). While these animals exhibited impairments in hatching behavior and alternate stepping due to loss of sensory afferents, non-reflexogenic movements were not affected and distribution of motor nerves innervating the hindlimb revealed a normal pattern. Temporal control of *Npn-1* expression on sensory axons seems to be crucial for spinal nerve fasciculation and coupling of sensory axon growth to pre-extended motor axons. *Ncx-Cre*-activity and thus removal of *Npn-1* after E11.5 did not result in defasciculated sensory projections, even though *Npn-1* levels were down-regulated in sensory axons (Fig. 14E). Whether late Sema3-Npn-1 signaling plays a role in late sensory innervation and final targeting of sensory nerves in the distal limbs, still needs to be addressed. Removal of *Npn-1* from sensory neurons before motor and sensory axons have joined to form spinal nerves that project to plexus region at the

base of the limb by *Ht-PA-Cre* expression caused defasciculation of sensory already before the plexus region, as well as in the distal limb. Intriguingly, the defasciculation of sensory innervation was accompanied by defasciculated motor trajectories to the fore- and hindlimbs before, in and beyond the plexus region (Figs. 15, 16, 18 and 19).

During development, blood vessels and nerve fiber tracts use similar signals and principles, and cross-talk to differentiate, grow and navigate towards their targets (Dafotakis et al., 2011). Npn-1 has been shown to play a role both in nervous system and vasculature development (Gu et al., 2003), which is also targeted by the *Ht-PA-Cre* line (Pietri et al., 2003). We found no obvious alterations in the formation of the vascular system when we investigated embryos where Npn-1 was ablated by tissue specific activation of *Ht-PA-Cre*, thus, it is unlikely that mispatterned blood vessels influence patterning of motor fibers. We also found no deficits in DRG segmentation, as it has been reported for compound mutants where *Sema3A-Npn-1* signaling and *Sema3-Npn-2* signaling was abolished simultaneously and migration of neural crest cells was impaired (Schwarz et al., 2009). Neural crest derived boundary cap cells at the ventral exit points of somatic motor projections allow somatic motor axons to exit the spinal cord, but hinder inappropriate translocation of motor neurons along their extending axons into the periphery (Vermeren et al., 2003). The Npn-2 ligands *Sema3B* and *Sema3G* were found to be secreted by boundary cap cells, preventing a subset of motor neurons from migrating out of the ventral horn of the spinal cord. Knockdown of *Npn-1* by siRNA in chicken embryos did not result in ectopically migrating motor neurons along their axons (Bron et al., 2007), suggesting that *Npn-1* plays no role in in constraining motor neurons to the ventral horn of the spinal cord. However, Npn-1 has been shown to govern migration of neural crest cells (Schwarz et al., 2009) and thus might affect positioning of boundary cap cells and motor axon outgrowth in mice. Immunohistochemical analyses showed that boundary cap cells were positioned normally at the motor exit zone (MEZ) and the DRG entry zone (DREZ) in embryos where Npn-1 was ablated in neural crest derived tissues, thus rendering an effect of mispositioned on initial motor axon fasciculation unlikely. The total loss of Schwann cells, as for example in *erbB2* deficient mice or after deletion of *Sox10* from immature Schwann cells, has been shown to cause defasciculation of the phrenic nerve, or lead to thinned and defasciculated sciatic nerve projections in the murine hindlimb (Lin et al., 2000; Finzsch et al., 2010). In *Npn-1^{cond-/-};Ht-PA-Cre⁺*

mutant mice, Schwann cells appear to migrate normally along defasciculated nerve fibers in the limb. Thus, an effect of Schwann cells on the fasciculation of motor trajectories appears unlikely, however, it cannot be completely excluded to this point. Analyses of mice where *Npn-1* is ablated specifically in Schwann cells using a Sox10-Cre line (Matsuoka et al., 2005) will help to elucidate the role of *Npn-1* for peripheral Schwann cell migration and its contribution to Schwann cell mediated fasciculation of sensory and motor projections into the developing limb.

Of particular interest for our study is the observation that sensory axons that lack Npn-1 expression take the lead in the mixed sensory-motor spinal nerve already very early during development: sensory axons in *Npn-1^{cond/-};Ht-PA-Cre⁺* mutant embryos grow ahead of motor fibers on their way to their peripheral targets (Figs. 16 and 17). This is a surprising result in the light of previous studies showing that, at least at hindlimb level, later-born sensory axons lag behind motor fibers (Tosney and Landmesser, 1985a). One possible explanation for our findings of sensory fibers overtaking motor axons might be that Npn-1 on sensory axons produces a tight coupling of these axons to leading motor fibers in wildtype animals. When *Npn-1* is removed from sensory axons, this “brake” is lifted, and sensory fibers can grow ahead of motor axons, and serve as pioneers for motor axons to follow (Fig. 28). A similar, however considerably more intense phenotype was observed when *Sema3A-Npn-1* signaling was abolished in the entire organism: Sensory axons overtake motor axons, and nerve fibers enter the limb prematurely (Huber et al., 2005). Residual expression of Npn-1 in sensory neurons (see quantification of Cre-recombinase efficiency in Fig. 7) in *Npn-1^{cond/-};Ht-PA-Cre⁺* mutant embryos might therefore explain the lack of premature ingrowth of axons into limb mesenchyme.

Alternatively, the inter-axonal, possibly ligand-independent adhesion emanating from sensory fibers together with *Sema3A*-mediated surround repulsion may force fasciculation of motor axons with sensory fibers. Upon loss of Npn-1 from sensory fibers, surround repulsion caused by *Sema3A* might no longer be sufficient to coerce motor axons into tightly fasciculated bundles, which results in defasciculated motor fibers in spite of Npn-1 still being present in motor neurons. Our observation that the phenotype of motor axon defasciculation upon the removal of Npn-1 from sensory axons is less pronounced than when *Npn-1* is ablated from motor neurons supports this explanation.

A third explanation for motor axon defasciculation after ablation of *Npn-1* from sensory axons might be provided by the neuronal co-expression of *Sema3A* and *Npn-1*. *Sema3A* expression in motor neurons has been shown to intrinsically regulate the sensitivity of motor axon growth cones to exogenous *Sema3A* exposure in the distal limbs of chicken embryos (Moret et al., 2007). Local down-regulation of the receptor at the growth cone surface by intrinsic *Sema3A* expression is used to fine-tune responsiveness of growth cones to surrounding class 3 Semaphorin expression. A similar mechanism was found for olfactory sensory neurons (OSN) innervating the olfactory epithelium where *Npn-1* and *Sema3A* are co-expressed by OSNs at various levels. Intrinsic regulation of *Npn-1* on the cell surface contributes to pre-target axon sorting and innervation of distinct region within the olfactory epithelium. Loss of *Npn-1* or *Sema3A* in OSNs, however, perturbed pre-target sorting and topographic innervation of the olfactory bulb (Imai et al., 2009). On their way to the plexus region, sensory and motor axons grow in tight spatial vicinity, and *Sema3A* is also expressed in DRG neurons (Wright et al., 1995). Therefore, it is possible that *Sema3A*, which is secreted from sensory growth cones, is not only taken up by sensory but also by motor axons. If *Npn-1* is ablated from sensory neurons, motor growth cones might be confronted with an excess of *Sema3A* and as a consequence defasciculate, very similar to the phenotype observed when *Sema3A* is overexpressed in motor neurons (Moret et al., 2007). Using cell type specific ablation of intrinsic *Sema3A* (Taniguchi et al., 1997) in sensory or motor neurons at brachial and lumbar levels will show whether *Sema3A*-mediated fine tuning of *Npn-1* levels on the surface of the growth cone contributes to axon-axon interactions and selective fasciculation of projections innervating the distal limb.

Class 3 Semaphorins constitute the most probable ligands to interact with axonally expressed *Npn-1* to mediated fasciculation. However, besides homodimerization, additional extracellular binding partners have been reported for *Npn-1*: different isoforms of vascular endothelial growth factor (VEGF) or the cell adhesion molecule L1 (Castellani, 2002; Geretti et al., 2008), which may also contribute to the formation of the sensory-motor circuitry. Intriguingly, in embryos, where *Npn-1* is ablated from sensory axons, defasciculation of both motor and sensory projections before, in, and beyond the plexus region in the distal limb are observed. These data were corroborated by genetic elimination of sensory neurons by tissue specific activation of *DT-A* expression, which caused a similar

defasciculation of motor fibers prior to the plexus. Interruption of the function of L1 at a stage when motor axons have already resorted into target-specific bundles to innervate the chick hindlimb, resulted in decreased adhesion and aberrant pathway selection of sensory axons. The pathfinding of pre-extending motor axons, however, was not affected (Honig et al., 2002). Based on these findings, our data show that inappropriate pathway selection of sensory axons and the break of the sensory-motor axon coupling *before* reaching the plexus affect the fasciculation of motor axons, while experimental defasciculation of sensory projections *after* motor axons have left this decision region has little or no effect on motor axon patterning. It is very likely that both axon-environment and axon-axon interactions are required to achieve the required accuracy of limb innervation. For the generation of the zebrafish retinotectal projection (Pittman et al., 2008) and the establishment of murine axial projections (Gallarda et al., 2008) complex combinations of different molecular mechanisms of axon co-extension and pathfinding have been reported. Therefore, while Sema3 ligands constitute the most probable environmental cues for interaction with Npn-1 on sensory and/or motor axons, communication between axons might be conferred by alternative interactions, like homophilic Npn-1 or Npn-1-L1 complexes.

1.5 ABLATION OF *NPN-1* FROM SENSORY NEURONS DOES NOT INFLUENCE THE DORSAL-VENTRAL GUIDANCE DECISION OF MOTOR AXONS

The severe defasciculation of motor nerves caused by ablation of Npn-1 in motor neurons resulted in a significant increase of errors in the dorsal-ventral guidance decision at the choice point in the plexus region at the base of the limb. In embryos, where Npn-1 is ablated from sensory neurons, both sensory and motor axons are defasciculated already before the plexus region, as well as beyond this decision point. However, motor axons are defasciculated to a less severe degree. Interestingly, the defasciculation of motor axons that we observed after ablation of Npn-1 in sensory neurons had no effect on the dorsal-ventral pathfinding decision of motor fibers. While spinal nerves are defasciculated, they still arrive at roughly appropriate positions within the plexus region, where Npn-1, which is still expressed on motor axons, can contribute to correct dorsal-ventral guidance. Whether sensory

axons are still able to correctly navigate this choice point cannot be assessed, as, up to now, no markers to distinguish dorsally from ventrally projecting sensory neurons have been identified.

1.6 CONCLUSIONS

Taken together, we have explored the potential of Npn-1 to govern fasciculation of motor and sensory projections and inter-axonal communication between these fiber systems. Whole embryo preparations revealed that removal of Npn-1 from motor neurons caused prominent defasciculation of their axons in the plexus region and further distally with a severe defect in distal axonal advancement and stereotypical dorsal-ventral pathfinding of motor axons. In contrast to early reports in chick, sensory projections to peripheral target regions developed normally. Genetic elimination of motor neurons resulted in thinned sensory trajectories to the limb, indicating that sensory axons need a minimal presence of motor fibers for establishment of correct projections. Quite unexpectedly, elimination of Npn-1 from sensory neurons caused defasciculation of both sensory and motor projections. Interestingly, defasciculation occurs not only in the plexus and the distal limb but already before the plexus. Our data therefore demonstrate that Npn-1 mediated inter-axonal communication between sensory and motor axons before the decision region at the base of the limb is required for correct peripheral nerve patterning (for a summary, see Fig. 32). These data are supported by genetic depletion of sensory neurons, which also causes defasciculation of peripheral motor projections. Our findings therefore present a novel aspect to our understanding of how complex neuronal circuits are assembled during development. While over the past years many families of guidance cues and corresponding receptors mediating environment-growth cone interactions have been identified, we now provide evidence that Npn-1 mediated inter-axonal contacts and fasciculation of sensory axons are crucial for the correct establishment of the innervation of the vertebrate limb. We show that inter-axonal communication influences the growth pattern and fasciculation of specific neuronal projections. The region where this interaction is taking place in relation to critical choice points as axons navigate to their peripheral targets seems to be of crucial significance, which raises important issues of differential sensitivities and

compartmentalization of growing axons in relation to developmental progress and will stimulate future studies in these fields.

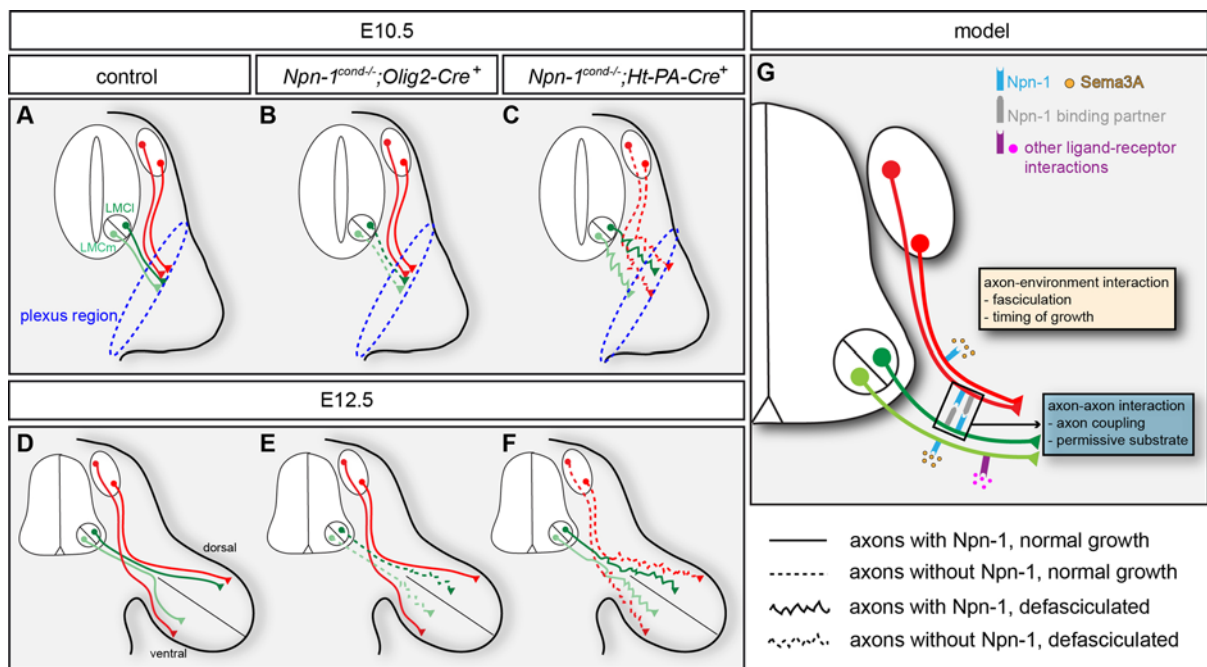


Figure 32: Npn-1 mediated axon-axon and axon-environment interactions.

(A) Schematic view of forelimb innervation at E10.5 in wildtype embryos: motor and sensory axons reach the plexus region at the base of the limb in tightly fasciculated spinal nerves. **(B)** If *Npn-1* is ablated from motor neurons (*Olig2-Cre* or *Hb9-Cre*), motor and sensory axons approach the plexus in normally fasciculated spinal nerves, however motor axons are defasciculated within the plexus. **(C)** If *Npn-1* is removed from sensory neurons (*Ht-PA-Cre*), sensory and motor axons fail to form properly fasciculated spinal nerves and are therefore defasciculated already before as well as within the plexus region. In addition, sensory neurons lead the spinal nerve projection. **(D)** Schematic view of forelimb innervation after motor and sensory axons have navigated the plexus region at E12.5. **(E)** If *Npn-1* is removed from motor neurons, motor nerves enter the limb heavily defasciculated, while sensory nerves grow fasciculated to appropriate distal positions. **(F)** If *Npn-1* is removed from sensory neurons (*Ht-PA-Cre*), both motor and sensory nerves arrive at the plexus in a defasciculated manner, and sensory nerves are heavily defasciculated in the distal limb, while motor projections show a milder defasciculation and grow in slightly inappropriate positions to each other. **(G)** Model illustrating the axon-environment and axon-axon interactions that control the initial outgrowth and joining of sensory and motor axons.

2. NPN-1 MEDIATES CRANIAL NERVE FASCICULATION AND SCHWANN CELL MIGRATION

Elimination of Sema3-Npn-1 by mutating the binding site for class 3 Semaphorins in Npn-1 (*Npn-1^{Sema-}*) was shown to cause deficits in the fasciculation and accurate guidance of axons forming spinal sensory-motor circuits that innervate the distal limbs (Huber et al., 2005). At cranial levels, defined peripheral nerves are formed from either primarily sensory, purely motor, or mixed populations of axons to innervate in precisely defined trajectories targets of the head and neck. Disruption the Sema3A-Npn-1 signaling pathway has been shown to result in defasciculation of the distal projections of the cranial trigeminal, facial, glossopharyngeal and vagus nerves (Kitsukawa et al., 1997; Taniguchi et al., 1997; Gu et al., 2003). PlexinA3 and A4, which are both signaling co-receptors of Npn-1, prevent midline crossing of facial visceromotor neurons and facilitate distal fasciculation of these projections (Schwarz et al., 2008b). Loss of the Sema3A-Npn-1 signaling pathway in the entire organism leads to mislocalization of cranial neural crest cells between facial and trigeminal ganglion along which ectopic axons are extending (Schwarz et al., 2008a). Since these projections contain both motor and sensory axons, it was unclear whether Npn-1 is required in both neuronal populations for proper distal assembly and fasciculation.

2.1 NPN-1 ON NEURAL CREST AND PLACODALLY DERIVED SENSORY TISSUES GOVERNS DISTAL FASCICULATION OF CRANIAL NERVE PROJECTIONS

In previous investigations of the involvement of Npn-1 in neural crest migration, Schwarz and colleagues used a *Wnt1-Cre* line to specifically ablate *Npn-1* from neural crest derived tissues (Danielian et al., 1998; Schwarz et al., 2008a). As this line also drives expression of Cre-recombinase in cells of the dorsal neural tube, we used the *Ht-PA-Cre* line to eliminate *Npn-1* expression from the sensory nervous system and the vasculature without affecting Npn-1 signaling pathways in possible target interneurons in the dorsal horn of the spinal cord (Pietri et al., 2003).

Consistent with previous data when Npn-1 signaling was abolished in the entire organism, specific targeting of Npn-1 by *Ht-PA-Cre* in neural crest cells leads to defasciculation of peripheral projections of trigeminal, facial, glossopharyngeal and vagus nerves. We also observed ectopic projections between the facial and trigeminal ganglia, which have previously been shown to be caused by a migration defect of neural crest cells in this region (Schwarz et al., 2008a). The distribution of neural crest-derived Sox10-positive Schwann cells appears normal along the mixed sensory-motor projections into the periphery (data not shown). Therefore, our data argues that Npn-1 expressed on sensory projections is responsible for the distal defasciculation phenotype of these cranial nerves.

2.2 NPN-1 ON SOMATIC MOTOR AXONS GOVERNS INITIAL FASCICULATION OF ABDUCENS AND HYPOGLOSSAL PROJECTIONS

While the function of Npn-1 in governing fasciculation, axon growth and cell migration in cranial sensory, branchiomotor and visceromotor trajectories has been studied before, its roles in the formation of the purely somatic motor nerves of the hindbrain have not been addressed so far. In the brainstem, three different types of motor neurons are generated in response to graded Shh signaling: Somatic motor neurons of the abducens and hypoglossal nuclei, which develop in response to similar transcription factor networks as are active in spinal motor neurons and exit the neural tube ventrally (Novitch et al., 2001), as well as branchio- and visceromotor neurons. These latter subtypes arise from the p3 domain in response to Nkx2.2 and Nkx2.9 signaling (Briscoe and Ericson, 1999; Pabst et al., 2003), their somata migrate to more dorsal positions in the neural tube, and their axons share dorsal exit points (reviewed in Guthrie, 2007). Loss of *Nkx6.1*, *Nkx6.2* and *Pax6* during somatic motor neuron development deletes abducens and hypoglossal motor neurons (Ericson et al., 1997a; Ericson et al., 1997b; Sander et al., 2000). We show that loss of *Olig2*, which is downstream of *Nkx6.1* and *Nkx6.2*, leads to a similar phenotype of specific deletion of abducens and hypoglossal motor neurons, while branchio- and visceromotor projections remain unaffected. The abducens nuclei consist of solely somatic motor neurons and innervate the lateral rectus muscle that is responsible for

lateral eye movements (Chilton and Guthrie, 2004). When we ablated *Npn-1* specifically from somatic motor neurons using the *Olig2-Cre* line, the number of somatic motor neurons was unchanged in the abducens and hypoglossal nuclei, indicating that *Npn-1* plays no role in the regulation of somatic motor neuron survival. However, we observed that the abducens nerve was markedly reduced in size after exiting the neural tube. As expected, removing *Npn-1* from sensory neurons using the *Ht-PA-Cre* line had only a very limited and transient effect on the somatic motor projection of the abducens nerve, which was completely corrected by E12.5 (data not shown). This argues for a minor, if any, role of *Npn-1* in neural crest and placodally derived cells, e.g. Schwann cells, for fasciculation of abducens fibers. Together, these data support a mode of action whereby class 3 Semaphorins expressed in neighboring tissues exert a surround repulsion on abducens fibers. Very similar to peripheral spinal projections, abducens fibers that express *Npn-1* on their surface are fasciculated to a tight bundle when they grow through a corridor formed by the repulsive ligand. Removing the axons' ability to see this inhibitory guide rail allows for fibers to wander off the fascicle and grow into adjacent tissues (Wright et al., 1995; Tessier-Lavigne and Goodman, 1996; Huber et al., 2005).

The hypoglossal nucleus is the caudal-most cranial motor nucleus within the brainstem and, like the abducens nucleus, consists exclusively of somatic motor neurons that were shown previously to express *Npn-1* (Hermanson et al., 2006). We demonstrate that in *Npn-1^{Sema-}* mutant embryos and in animals, where *Npn-1* is ablated from somatic motor neurons, initial fasciculation of the hypoglossal nerve is disturbed. This leads to elongated hypoglossal rootlets in both genotypes, that fasciculate into one nerve trunk just right before the convergence point. In embryos, where *Npn-1* was ablated in somatic motor neurons by *Olig2-Cre* we also observed a similar decrease of nerve fibers contributing to the main projection as already observed for abducens projections. This was not observed in the *Npn-1^{Sema-}* line, where only the binding site for class 3 Semaphorins is mutated, while binding of other interaction partners such as vascular endothelial growth factor (VEGF) or the cell adhesion and pathfinding molecule L1, is still possible (Castellani, 2002; Carmeliet, 2003; Geretti et al., 2008). It is therefore conceivable, that *Npn-1* serves yet other, class 3 Semaphorin-independent functions to mediate axon outgrowth and fasciculation. In mice hypomorphic for the expression of the motor neuron determinant transcription factor *Isl1*, the number of Hb9-positive motor neurons in the

spinal cord and in cranial nuclei was not altered. However, motor nerves are defasciculated and misprojecting, and hypoglossal projections are diminished in number and fail to turn rostrally (Liang et al., 2011). These findings show that low levels of *Isl1* in motor neurons interfere with proper induction of guidance mechanisms of motor axons. For the initial outgrowth of hypoglossal axons low levels of *Isl1* cause a phenotype very reminiscent of the one we observed when we ablated *Npn-1* in somatic motor neurons, thus indicating that early abolishment of motor axon pathfinding mechanisms impair both fasciculation and outgrowth of motor axons from the brainstem .

Interestingly, loss of *Sema3-Npn-1* signaling has no effect on rostral turning of the hypoglossal nerve towards the outer and inner tongue muscles. Hepatocyte growth factor (HGF) is a strong chemoattractant not only to spinal, but also to cranial motor axons (Caton et al., 2000). It is expressed in limb buds and myogenic precursor cells in the branchial arches, while the HGF receptor *Met* is expressed on subpopulations of cranial motor neurons (Ebens et al., 1996). Mice with targeted disruptions of either *Met* or HGF showed stunted growth of peripheral projections at the level of the glossopharyngeal plexus. Fasciculation of hypoglossal rootlets right after exiting the neural tube was not impaired in mice lacking HGF-*Met* signaling (Caton et al., 2000). Taken together, these data suggest an important role for *Npn-1* on somatic motor projections for fasciculation of hypoglossal projections on their way to the convergence point, while HGF-*Met* signaling facilitates general attraction towards the target fields in the tongue.

2.3 NEURAL CREST DERIVED SCHWANN CELL PROGENITORS FACILITATE INITIAL HYPOGLOSSAL NERVE FASCICULATION

Intriguingly, assembly of hypoglossal projections was also impaired after ablation of *Npn-1* from cranial neural crest and placodally derived cells. These findings were corroborated by genetic elimination of these tissues, which also impaired formation of the hypoglossal nerve. During axon guidance, axons rely on variable navigational mechanisms: mechanical features of the surrounding tissue, as for example pre-patterning of pathways by distinct cell types or selective adhesion to

a permissive substrate and detachment from non-permissive tissues (Reichardt and Tomaselli, 1991), or diffusible and cell associated cues. Pioneer axons in the grasshopper leg, or the murine telencephalon, for example, follow distinct pathways pre-patterned on critical positions by so called guidepost cells to their targets in muscles or the olfactory bulb, respectively (Keshishian and Bentley, 1983; Palka et al., 1992; Sato et al., 1998; Tomioka et al., 2000). Structures like nerve exit points, sensory ganglia, glial cells and target muscles provide essential guideposts during cranial axon elongation into the periphery (Guthrie, 2007). For the hypoglossal nerve, however, other neuronal ganglia are hardly within reach during initial outgrowth and rootlet assembly. Defective migration of future target cells as guideposts for hypoglossal nerve fasciculation due to disruption of Sema3A-Npn-1 signaling is unlikely, as hypoglossal projections are established before migration of myoblast precursors starts, which will later form the muscles of the tongue (Noden, 1983, Mackenzie et al., 1998). In chicken, circumpharyngeal neural crest cells populate the hypoglossal pathway before nervous projections are formed, and absence of these cells affects the development of glossopharyngeal, vagus and hypoglossal trajectories (Kuratani and Kirby, 1992). However, while *Ht-PA-Cre* targets all neural crest, it still needs to be assessed whether Npn-1 is important for circumpharyngeal neural crest migration.

During pathfinding of axons to their targets in the periphery, glia cells that compose a support system for the survival and functionality of neuronal connections migrate along these axons (reviewed in Nave, 2010). In primary cell cultures, Schwann cells express neuropilins and their co-receptors, and along the optic nerve, the guidance of glia cell precursors was shown to depend on the same interactions of receptors with the environment as the guidance of axons (Sugimoto et al., 2001; Ara et al., 2005). Co-expression of Npn-1 and Sema3A in somatic motor neurons therefore might provide an explanation for defective hypoglossal nerve assembly in mice lacking Npn-1 on neural crest and placodally derived tissues. This neuronal co-expression controls the sensitivity to exogenous Sema3A exposure by regulating the availability of the receptor on motor growth cones in the distal limb of chicken embryos (Moret et al., 2007). At cranial levels, Sema3A and its receptor are co-expressed in hypoglossal somatic motor neurons of chicken embryos, suggesting a similar system of fine-tuning sensitivity of hypoglossal axons to Sema3A expression in the branchial arches (Chilton and Guthrie, 2003). We found that in *Npn-1^{cond/-};Ht-*

PA-Cre⁺ mutant embryos, the number of Sox10-positive Schwann cells migrating along the initial rootlets of the hypoglossal nerve is drastically diminished. Motor growth cones of the hypoglossal nerve might be confronted with an excess of Sema3A in the branchial arches if less Sema3A is taken up by Npn-1 expressed on the surface of these glia cells. This may cause down-regulation of endogenous Npn-1 on growth cones, leading to de-sensitization to environmental Sema3A and the defasciculation of the hypoglossal nerve. The more distal growth and general guidance of hypoglossal fibers towards the tongue is facilitated by HGF-Met signaling.

Selective axon bundling is required for the establishment of proper neuronal connections over long distances. In the developing zebrafish, axons of the lateral line provide the guidance substrate for migrating glial precursor cells. Contact between migrating glia cells and axons, as well as glia-glia interactions aid in keeping a fasciculated state, while loss of glial precursors leads to defasciculation of the lateral line nerve (Gilmour et al., 2002). Accordingly, deletion of Sox10 from immature Schwann cells in mouse causes loss of myelinating cells and subsequently results in thinned and defasciculated sciatic nerve projections to the hindlimb (Finzsch et al., 2010). When we removed Npn-1 from neural crest and cells of placodal origin, fewer Schwann cells were associated with the hypoglossal roots leaving the brainstem, with some of the misprojecting rootlets completely devoid of Sox10-positive cells. In addition, these roots grew significantly longer until they fasciculated into one major nerve trunk. In *Ht-PA-Cre;DT-A^{floxed}* mutant embryos, where hypoglossal projections form aberrant loops and are decreased in number, Schwann cells are missing completely along hypoglossal projections. Final targeting of hypoglossal projections, and also migration of remaining Schwann cells along the leading axons was not perturbed by ablation of Npn-1 in cranial neural crest and placodally derived sensory cells. Whether Npn-1 directly facilitates axon-glia interactions for selective fasciculation of the hypoglossal nerve, or whether defasciculation of hypoglossal rootlets is an effect of aberrantly positioned or altogether missing Schwann cells, however, needs further investigation. While the *Ht-PA-Cre* line targets all neural crest derived tissues, using a *Sox10-Cre* line will specifically target neural crest and Schwann cells without influencing *Npn-1* expression in sensory neurons (Matsuoka et al., 2005). The conditional approach to selectively remove *Npn-1* from Schwann cells or eliminate Schwann cell progenitors by tissue specific activation of *DT-A* will

contribute to the understanding of mechanisms involved in Schwann cell migration and Schwann cell mediated axon fasciculation during embryonal development.

Intriguingly, observations of Schwann cell migration along axons in the limb of *Npn-1^{cond-/-};Ht-PA-Cre⁺* mutant revealed no obvious decrease of Sox10-positive cells. Thus, investigations of embryos where Npn-1 was ablated specifically in cells that express *Sox10-Cre* might further reveal whether migration of Schwann cells at cranial and spinal levels is differentially regulated.

2.4 CONCLUSIONS

At cranial levels, either primarily sensory, purely motor, or mixed populations of nerves project to and innervate targets of the head and neck in precisely defined trajectories. We used the system of cranial innervation to distinguish respective contributions of the different nerve types and their interactions with each other, surrounding tissues and accompanying glial cells. We specifically explored the role of Npn-1 in the assembly, guidance and fasciculation of cranial nerve projections by using tissue specific loss-of-function mutants in whole embryo preparations. Tissue specific removal of *Npn-1* from somatic motor neurons does not alter numbers of motor neurons in the abducens and hypoglossal nuclei. However, projections of the abducens nerve and fibers contributing to the hypoglossal nerve, which are both pure motor nerves, are reduced in number. In addition, the initial assembly of the hypoglossal nerve is impaired with defasciculated and elongated rootlets. After these rootlets coalesce to form the hypoglossal nerve, guidance towards the tongue proceeds normally. Ablation of Npn-1 specifically from sensory neurons caused distal defasciculation of trigeminal, facial, glossopharyngeal and vagus projections, a phenotype very reminiscent of that seen in global *Npn-1^{-/-}* and *Npn-1^{Sema-}* mutant embryos. Thus, our data demonstrates that Npn-1 is required in sensory neurons for correct fasciculation of these mixed sensory-motor nerves. Interestingly, loss of *Npn-1* from cranial neural crest and sensory tissues of placodal origin also caused defective assembly and fasciculation of the hypoglossal nerve that is constituted entirely of somatic motor fibers. The number of Schwann cell precursors that migrate along elongated hypoglossal rootlets is severely reduced, which underscores the

relevance of Schwann cells for the proper fasciculation and formation of nerve trajectories. Genetic depletion of cranial neural crest and placodally-derived sensory tissues, which leads to loss of Schwann cells, also causes deficits in hypoglossal nerve assembly and thus supports this hypothesis. Our findings present a novel aspect to the understanding of how complex circuitry is formed during development. While over the past years a variety of ligand-receptor pairs have been identified for the interaction of growth cones with their environment, we now provide evidence that Npn-1 on neural crest-derived cells is crucial for correct establishment of initial hypoglossal somatic motor projections. This work therefore raises important issues of mediation of motor axon fasciculation by neural crest derived glial components and their role for initial axon growth and selective fasciculation.

3. IDENTIFICATION OF NOVEL GUIDANCE CUES PREDICTED BY A DIFFERENTIAL MICROARRAY SCREEN

How is the precise pathfinding of motor and sensory axons to their respective targets in muscles and skin of the vertebrate extremities coordinated during development? On the one hand, intrinsic factors pre-disposition dorsal and ventral guidance decision of motor neurons innervating limb musculature: At brachial and lumbar levels in the spinal cord, the LIM homeodomain transcription factors *Isl1* and *Lim1* define medial and lateral sub-columns of the LMC, respectively (Jessell, 2000). These transcription factors confer the ability to motor neurons to select specific axonal pathways to innervate target musculature in different regions of the limb. *Lim1* expression in the lateral aspect of the LMC mediates the expression of the ephrinA receptor EphA4 receptor that mediates repulsive interaction with ephrinAs. Their expression in the ventral limb mesenchyme is controlled by the LIM homeodomain transcription factor *Lmx1b* (Kania et al., 2000). In cooperation with attractive GDNF-Ret signaling the repulsive ephrinA-EphA interactions promote a dorsal trajectory of LMCI axons (Chen et al., 1998; Helmbacher et al., 2000; Kania and Jessell, 2003; Kramer et al., 2006). Absence of *Lim1* in dorsally projecting motor neurons causes a randomized dorsal-ventral choice of LMCI axons, however, dorsal projections were not completely abolished (Kania et al., 2000). Accordingly, in the hindlimb of *EphA4*^{-/-}

mutant embryos and compound mutants where also the GDNF receptor Ret was ablated, most, but not all LMCI axons chose a ventral trajectory (Helmbacher et al., 2000; Kramer et al., 2006). The motor neuron determinant transcription factor *Isl1* is not only required for the activation of the motor neuron defining transcription factor *Hb9* (Thaler et al., 2002), but at a slightly later developmental time point also controls expression of EphB1 receptors of the surface of axons emanating from medial LMC neurons. In mice where *Isl1* was eliminated by gene targeting, no motor neurons are generated and embryos die early during development (Pfaff et al., 1996). In chicken embryos where *Isl1* expression was down-regulated by electroporation of siRNA, a higher percentage of motor axons of the LMCm chose an aberrant, dorsal trajectory (Luria et al., 2008). Accordingly, in mice hypomorphic for the expression of *Isl1*, the number of Hb9 positive motor neurons in the spinal cord and in cranial nuclei was not altered. However, motor nerves are defasciculated and misprojecting dorsal branches were observed at axial levels (Liang et al., 2011). Co-expression of EphB1 in motor neurons hypomorphic for *Isl1* rescues this phenotype in chick embryos. Thus, repulsive interaction with ephrinBs in dorsal limb mesenchyme enables LMCm axons that express EphB receptors to project correctly to ventral target musculature (Luria et al., 2008). In addition to the LIM homeodomain transcription factor mediated expression of specific guidance receptors, other guidance molecules, whose specific regulation of expression is not well understood, contribute to the establishment of topographically distinct projections into the developing limb: Sema3F is secreted in dorsal limb mesenchyme, while its receptor Npn-2 is expressed by motor neurons of the LMCm. Repulsive interaction of this ligand-receptor system guides motor axons from the LMCm towards the ventral limb: elimination of Sema3F-Npn2-signaling in mouse and chick leads to pathfinding errors of LMCm axons into dorsal limb mesenchyme (Huber et al., 2005). Netrins are expressed in a gradient along the spinal cord and act both as attractive and repulsive guidance cues by binding to different receptor molecules. Interaction with a DCC dimer confers attraction of commissural axons to the ventral midline, while binding to a DCC/Unc5 receptor activates signaling cascades, driving, for example, motor axons away from the floorplate (Kennedy et al., 2006; Williams et al., 2006). Functional elimination of LIM homeodomain transcription factors, ligand-receptor interactions (Palmesino et al., 2010), and of downstream signaling components such as members of the Src family kinases caused only about 30% of motor axons to select an aberrant trajectory at the

dorsal-ventral choice point at the base of the limb. Thus, known pathfinding mechanisms cannot explain exhaustively how correct wiring of topographic motor projections to the limbs is achieved during development.

On the other hand, extrinsically imposed factors contribute to the formation of target specific pools within the LMC and promote target innervation: Expression of ETS transcription factors like *Er81* or *PEA3* is induced upon arrival of specific nerves in the vicinity of their targets by neurotrophic factors such as GDNF and contributes to the clustering and survival of motor sharing the same muscular target. Loss of these transcription factors not only impairs organization of motor neurons in target specific pools, but also prevents final branching of nerves at their peripheral targets (Lin et al., 1998; Arber et al., 2000; Haase et al., 2002; Livet et al., 2002).

Sensory neurons show no clustered organization within the DRG that corresponds to their topographic projections in the periphery, like motor neurons in the LMC in the ventral horn. Classical surgical ablation experiments in chicken shaped the view that spinal motor fibers penetrate the developing extremities first, while sensory axons follow these established trajectories: Surgical removal of motor neurons before neural crest cells coalesced into DRG and extended axons resulted in abnormal patterning of proprioceptive sensory trajectories that now projected along cutaneous pathways (Landmesser and Honig, 1986). Elimination of motor neurons after neural crest cells formed DRG and spinal projections towards the limb did not impair peripheral patterning of sensory innervation (Wang and Scott, 1999). We found that sensory axons initially need a minimal scaffolding by motor axons to reach the plexus region, while in the periphery both cutaneous and proprioceptive sensory nerves projected to appropriate distal targets even when motor fibers were severely defasciculated or absent (Fig. 8F'). The expression of specific tyrosine receptor kinases on the different types of sensory fibers enables interaction with distinct neurotrophins, like NGF or NT-3, respectively, on the way to the target regions for promotion of axonal growth, or maintenance of neuronal cells by retrograde trophic support (Lindsay, 1996; Gallo et al., 1997; Farinas, 1999). While cues like Sema3A that mediate the fasciculation and timing of growth of sensory axons have been identified previously (Huber et al., 2005), no guidance cues governing the dorsal-ventral guidance decision of sensory axons have been identified so far.

A whole genome expression screen previously performed in the Huber Brösamle laboratory identified genes that are differentially expressed in motor and

sensory neurons projecting to the dorsal or ventral limb. We validated the predicted expression patterns of four motor and five sensory candidate genes of the brachial spinal cord by *in situ* hybridization on cross-sections of E12.5 mouse embryos. Furthermore, we investigated the role of fibroblast growth factor receptor 2 (*FGFR2*) for coordinated growth, fasciculation and guidance fidelity of brachial motor axons during innervation of the forelimbs.

3.1 *ARHGAP29* IS EXPRESSED IN VENTRALLY PROJECTING MOTOR NEURONS OF THE BRACHIAL LMC

Interaction of various classes of guidance receptors with their ligands in the periphery or on co-extending axons activates intracellular signaling cascades of small GTP-binding proteins that culminate in the reorganization of the cytoskeleton within the filopodia and lamellipodia and leads to turning of the growth cone (Huber et al., 2003). Binding of the repulsive axon guidance cue Sema3A to its Npn-1/PlexinA receptor dimer, for example, leads to increased activity of the small GTPase Rho, which results in the formation of contractile actin stress fibers, while stabilized microtubules are degraded. Down-regulation of Cdc42 and Rac1 at the same time decreases adhesion to the extracellular matrix and therefore further contributes to turning events (Kruger et al., 2005). Small GTP-binding proteins serve as molecular switches by cycling between a GTP-bound active and a GDP-bound inactive form (Carmeliet, 2003). This cycling is regulated by guanine nucleotide exchange factors (GEFs) that govern binding of GTP, and GTPase-activating proteins (GAPs), which govern hydrolysis of GTP.

Our microarray screen predicted the GTPase activating protein *Arhgap29* to be higher expressed in ventrally projecting motor neurons. Evaluation of *in situ* hybridization of E12.5 mouse embryos revealed that indeed a 4 fold higher number motor neurons of the LMCm express of *Arhgap29* when compared to motor neurons of the LMCI, and therefore confirmed the prediction of the screen. Due to technical reasons, the screen has to be performed at E12.5: At this developmental time point, motor and sensory axons have established synapses and are able to take up fluorescently labelled dextrans that have been injected into specific limb musculature. We therefore examined also earlier crucial time points: at E10.5, spinal nerves have formed a plexus at the base of the limb, but not yet traversed this

decision point. At E11.5, dorsally and ventrally projecting motor neurons are segregated in the LMCI and LMCm, respectively, and their projections have formed distinct branches towards dorsal and ventral limb musculature, following trajectories pre-patterned by pioneering axons (Rajan and Denburg, 1997). We found that *Arhgap29* shows an even expression in the entire LMC at E10.5 when the first “pioneer” motor axons start to enter the limb. The vast majority of axons innervating the distal limb follow these axons at slightly later time points. At E11.5, when the sub-columnar segregation of LMCm and LMCI neurons is established, also *Arhgap29* expression was observed predominantly in ventrally projecting motor neurons. Investigation of *Arhgap29* expression at additional intermediate time points, i.e. E10.75, E11.0, and E11.25 will further define exactly when differential expression of *Arhgap29* is established and whether this is within the right timeframe to influence dorsal-ventral guidance decisions at the base of the limb. Investigations at later stages will show whether *Arhgap29* expression is confined to distinct motor neuron pools within the LMC. In *in vitro* studies, *Arhgap29* was shown to induce cytoskeletal changes in fibroblasts, which are typical for Rho inactivation and lead to rounded-up cells (Myagmar et al., 2005). Knockdown of *Arhgap29* in human umbilical vein endothelial cells (HUVECs) by siRNA lead to increased activation of RhoA and the formation of stress fibers, while microtubules were destabilized and down-regulation of Cdc42 lead to decreased adhesion to the extracellular matrix (Xu et al., 2011). While in HUVECs these processes prohibit lumen formation of blood vessels, a very similar mechanism leads to growth cone turning of motor axons upon interaction with repulsive guidance cues (Kruger et al., 2005). Therefore, *Arhgap29* displays a very interesting candidate for further investigation of its roles in axon growth and guidance. As to date no mouse lines with mutations for the RhoGAP are available, experiments in chicken provide an avenue for a fast and efficient functional characterization. Therefore, the conservation of the *Arhgap29* expression pattern in chicken embryos (Gene ID: 424488) should be analysed first. There is ample evidence in the literature that the expression patterns of transcription factors and guidance cues are conserved between chick and mouse (Helmbacher et al., 2000; Eberhart et al., 2002; Huber et al., 2005; Moret et al., 2007). Gain-of-function experiments by electroporation of an expression vector in combination with a fluorescent marker into the spinal cord will allow to follow individual cells and their projections into the periphery. *In ovo* electroporation of siRNA that leads to

degradation of the mRNA or nucleic acid analogs (morpholino; Summerton, 1999), which block transcription can be used to knockdown *Arhgap29* function. With these methods, *Arhgap29* can be rapidly up- or downregulated in the developing chicken embryo and the consequences for axonal growth and patterning can be assessed employing wholemount embryo preparations. Furthermore, retrograde tracing of motor axons in these chicken embryos will allow for investigation of the roles of *Arhgap29* in dorsal-ventral guidance decisions during the establishment of motor projections into the peripheral limb.

3.2 THE ETS TRANSCRIPTION FACTOR *ELK3* IS EXPRESSED IN THE MEDIAL ASPECT OF THE BRACHIAL LMC

The initial expression of ETS transcription factors like PEA3 or Er81 coincides with the arrival of motor axons in the vicinity of their muscular targets. Removal of the limbs at early stages during embryonal development prevents onset of the ETS transcription factors, arguing for limb derived factors like GDNF or fibroblast growth factors (FGF) as inducers of their expression (Lin et al., 1998; Haase et al., 2002, Thisse and Thisse, 2005). In *PEA3^{-/-}* mutant embryos, on the one hand, motor axons fail to branch in their target muscle, on the other hand, cell bodies of these projections fail to cluster at a characteristic position within the LMC but are dispersed (Livet et al., 2002). Also *Er81^{-/-}* mutant mice exhibit severe coordination deficits of motor behaviour, however, the specification of motor nerves and induction of muscle spindles occurred normally. Here, proprioceptive sensory neurons that also express *Er81* fail to arborize in the ventral spinal cord and cannot provide feedback to motor neurons innervating the same muscles (Arber et al., 2000). Thus, ETS transcription factors obtain critical roles in positioning of motor neurons innervating the same targets, axonal branching and establishing sensory-motor connectivity.

The expression of the ETS transcription factor *Elk3* was found to be correlated with vasculogenesis, angiogenesis and formation of cartilage during mouse embryonal development (Ayadi et al., 2001a). Also during adulthood, *Elk3* is involved in angiogenesis and wound healing. Mice lacking *Elk3* die within 6 weeks after birth due to respiratory failure caused by compression of the lung by chylus effusions. Interestingly, these mice show also mispatterned blood and lymphatic vessels (Ayadi

et al., 2001b). *In vitro* studies that blocked *Elk3* function lead to impairments in microtubule formation (Wasylyk et al., 2008), arguing for a function of this gene during the assembly of the cytoskeleton, which might govern growth cone turning events. A close relative of *Elk3*, *Elk1* shows strong expression in neurons of the rat brain and already has been proposed to play a role in neuronal function based on its expression pattern including the soma, dendrites and axon terminals of striatal neurons (Sgambato et al., 1998). Other ETS family members, like axon steering defect 1 (*AST-1*), have been shown to be required for axon navigation, neuronal differentiation and axon outgrowth in the developing pharynx of *C. elegans* (Fukami et al., 2008).

The microarray analysis predicted *Elk3* to be expressed at higher levels in ventrally projecting motor neurons. Evaluation by *in situ* hybridization revealed that at E12.5 *Elk3* is indeed expressed predominantly in motor neurons of the LMCm. However, at E10.5, when motor axons have reached the plexus region, no expression of *Elk3* was observed in motor neurons of the LMC, and also one day later, when motor axons have traversed the choice point in the plexus region, we found no differences in expression between medial and lateral LMC. Therefore, it is unlikely that *Elk3* governs the early dorsal-ventral guidance decisions of motor axons. However, as mentioned above, ETS transcription factors that are promoting survival of motor neuron pools that project their axons to the same targets in the periphery also show a late onset of expression upon arrival of the axons at their respective target (Lin et al., 1998). FGF2 that is expressed in the limb mesenchyme and contributes to limb patterning (Thisse and Thisse, 2005) induces *Elk3* phosphorylation by Ras, which turns *Elk3* into a transcriptional activator (Wasylyk et al., 2008). Therefore, differential expression of *Elk3* in motor neurons of the LMCm might be involved in subtype specification of motor neurons. Expression analyses at later stages and retrograde tracing of motor neurons from specific muscles in the forelimb will allow for a further characterization of the motor neuron pools that express *Elk3*. Similar to *Er81*, also *Elk3* shows expression in sensory neurons of the DRG already early in embryogenesis (data not shown) into adulthood where different isoforms of the ETS transcription factor are upregulated upon nerve damage (Kerr et al., 2010). Future work will focus on the identifying the circuitry of *Elk3*-positive motor and sensory neurons and reveal whether these neurons are connected to specific muscle groups. Retrograde tracing of motor and proprioceptive sensory neurons from

specific forelimb muscles with transsynaptic viruses that express fluorescent marker proteins (Stepien et al., 2010), or transneuronally transported tracers like *cholera toxin subunit B* (Luppi et al., 1990) will allow for visualization of the connectivity within neuronal circuits. Therefore, analyses in *Elk3* deficient mice (Ayadi et al., 2001b) will enable the investigation of the roles of this ETS transcription factor in motor neuron positioning, target innervation and sensory-motor connectivity.

3.3 *CCDC3* IS EXPRESSED IN VENTRALLY PROJECTING BRACHIAL MOTOR NEURONS

During neuronal development, guidance cues expressed by the surrounding mesenchyme, or secreted by axons themselves, are essential for correct pathfinding of motor axons. Investigation of the molecular mechanisms that regulate axonal guidance is essential to understand how the different extracellular stimuli are integrated and translated into downstream signaling transduction pathways that control cytoskeletal rearrangements and hence the growth response of a given axon. During development, blood vessels and nerve fiber tracts display remarkable similarities in the use of guidance signals and principles during their establishment: specialized tip cells that lead and guide growing blood vessels share many features with growth cones at the tip of the axon. Tip cells are motile and extend filopodia that express receptors such as Neuropilins, Eph receptors or Plexins and react to molecules of the Semaphorin or ephrin families (reviewed in Adams and Eichmann, 2010). The novel secretory factor *Ccdc3* was originally detected in a screen for genes specifically expressed in the murine aorta and was found to be expressed and secreted by cells of the vascular system (Kobayashi et al., 2010).

In our screen for novel guidance cues, *Ccdc3* was predicted to be predominantly expressed in ventrally projecting motor neurons of the brachial LMC. We confirmed this prediction by *in situ* hybridization against *Ccdc3* on E12.5 mouse embryos and found 5 fold more motor neurons of the LMCm expressing the secretory factor than in motor neurons of the LMCI. At E10.5 when the first “pioneer” motor axons start to enter the limb, *Ccdc3* shows an even expression in the entire LMC. At E11.5, when the vast majority of axons innervating the distal limb has followed these axons and established dorsal and ventral motor branches in the limb, also *Ccdc3* expression was observed predominantly in ventrally projecting motor neurons.

Investigation of *Ccdc3* expression at additional time points, i.e. E10.75, E11.0, and E11.25 and later than E12.5 will further define exactly when the differential expression is established and whether it is confined to a certain subpopulation of motor neurons. As *Ccdc3* was reported to be secreted by endothelial cells of the vasculature it will be interesting to investigate whether the secretory protein plays a role in both blood vessel and motor axon extension, and whether these projections target the same regions. Unfortunately, up to now nothing is known about possible receptors for *Ccdc3* and no mice mutant for *Ccdc3* are available. The European conditional mouse mutagenesis program (EUCOMM) generated ES cells with a recombined *Ccdc3* gene for production of mutant mice. Conditional gene trapping in embryonic stem cells using a targeting vector for *Ccdc3* containing a reporter construct (β -gal) and loxP sites for specific binding of Cre recombinase will allow for the generation of a mouse model and thus enable further expression analyses and tissue specific ablation of the novel secretory gene, respectively (Testa et al., 2004). Using Cre-lines specific for motor neurons, such as the *Olig2-Cre* line (Dessaud et al., 2007), or the *Sox17-Cre* line which shows specific activity in arteries during blood vessel development (Liao et al., 2009) will allow for dissection of *Ccdc3* function in the establishment of axonal trajectories or the vascular system. Investigation of the conservation of the expression pattern of *Ccdc3* in chicken (Gene ID: 769832) will reveal whether dorsally and ventrally projecting motor neurons show differential expression of the novel secretory factor. Analyses of wholemount embryo preparations and retrograde tracing of motor axons in chicken embryos that were *in ovo* electroporated with constructs for gain- or loss-of-function will allow for investigation of the roles of *Ccdc3* in dorsal-ventral guidance decisions during the establishment of motor projections into the peripheral limb.

3.4 SPECIFIC EXPRESSION OF *FGFR2* IN VENTRALLY PROJECTING BRACHIAL MOTOR NEURONS PLAYS NO ROLE FOR MOTOR AXON GROWTH AND GUIDANCE

Tightly regulated FGF-FGFR signaling along the rostro-caudal axis plays important roles in patterning of the developing embryo and activation of defined Hox genes that designate columnar identity of motor neurons within the ventral horn of the spinal cord (Dasen et al., 2003; Bottcher and Niehrs, 2005; Dasen et al., 2005).

Already during very early embryonal development, *FGFR2* was shown to be co-localized with NCAM, a modulator of axonal growth and fasciculation in the developing brain which was observed to activate *FGFR2* signaling and its downstream pathways (Vesterlund et al., 2011). At spinal levels, interaction of NCAM on motor axons with PSA secreted by motor axons to the surrounding tissue contributes to motor axon sorting and selective fasciculation of nerves before they grow into the distal limbs (Tang et al., 1992; Tang et al., 1994). Therefore, activation of *FGFR2* signaling via NCAM might also play a role in motor axon growth and guidance. Isoforms of *FGFR2* act upstream of Shh and govern limb bud induction, development and maintenance of the limb, but also ossification and growth of the bones by interaction with FGF8 and FGF10 in the apical ectodermal ridge at the tip of the limb (Xu et al., 1998; Lizarraga et al., 1999; De Moerlooze et al., 2000; Revest et al., 2001; Coumoul and Deng, 2003). Furthermore, *FGFR2* was shown to be involved in organ development and the establishment of correct brain architecture (Hajihosseini et al., 2001; Wang et al., 2005; Aldridge et al., 2010) The role of *FGFR2* for the formation and patterning of nervous projections into the limbs, however, has not been assessed up to now.

Our microarray screen predicted *FGFR2* to be higher expressed in ventrally projecting motor neurons of the brachial LMC. We confirmed this prediction and showed that 1,3 fold more motor neurons in the LMCm expressed the FGF receptor when compared to motor neurons that project to dorsal limb musculature. Compared to the other candidate genes *Arhgap29*, *Ccdc3*, and *Elk3*, *FGFR2* shows the smallest difference in expression in dorsally and ventrally projecting motor neurons and therefore displays the weakest candidate gene. However, onset of *Elk3* expression is too late to govern initial dorsal-ventral guidance decisions, and no mouse lines are available for the most promising candidate *Arhgap29*, and the secreted protein *Ccdc3*. For *FGFR2*, a conditional mouse line (Blak et al., 2007) was available at the Institute of Developmental Genetics and kindly provided to us by Dr. Ralf Kühn. As a null mutation of the FGF receptor in the entire organism is lethal already at very early embryonal stages (Arman et al., 1998), we employed a conditional approach to selectively remove *FGFR2* from motor neurons by tissue specific activation of Cre recombinase driven by the *Olig2* promotor. We found no alterations in the general growth pattern and distal extension of motor projections into the distal limb when *FGFR2* was ablated in motor neurons. Motor nerves were fasciculated appropriately

and grew to correct distal positions. When we investigated the guidance fidelity of LMCm neurons by dorsal retrograde labeling we found no increase in errors in the dorsal-ventral guidance decision of ventrally projecting motor axons. Whether motor neurons in the LMC are still correctly positioned upon elimination of FGFR2 signaling still needs to be assessed. Using motor neuron specific markers such as *Isl1* and *Lim1* divergence of motor neurons in LMCm and LMCI can be analyzed. Graded FGF signaling along the rostro-caudal axis of the developing embryo leads to activation of different Hox genes defining the columnar identity of motor neurons within the ventral horn (Dasen et al., 2003; Bottcher and Niehrs, 2005; Dasen et al., 2005). Whether ablation of *FGFR2* in motor neurons by *Olig2-Cre* impairs clustering of motor neurons in the medial or lateral aspect of the LMC still need to be assessed. Additional expression analyses at later time points will show, whether expression of the FGF receptor is confined to specific motor pools within the LMC and thus might contribute to grouping of motor neurons projecting to the same target. FGF2, a ligand of FGFR2 (Thisse and Thisse, 2005) is expressed in the limb mesenchyme and was shown to promote the phosphorylation and thus activation of the ETS domain containing transcription factor Elk3 by the Ras-Erk signaling pathway (Wasylyk et al., 2008). Therefore, analysis of the activation of ETS transcription factors like PEA3 or ER81 might reveal whether FGF signaling from limb mesenchyme is involved in activation of genes that promote neuronal survival and formation of motor pools. Furthermore, FGF signaling was shown to upregulate GDNF and NGF mRNA in cells expressing FGFR1 and FGFR2 (Suter-Crazzolara and Unsicker, 1996; Ferhat et al., 1997). Ablation of *FGFR2* was also found to affect oligodendrocyte generation and migration in the brain (Furusho et al., 2011), and expression of the FGF receptor was also found in myelinating and non-myelinating Schwann cells in the peripheral nervous system (Furusho et al., 2009). Conditional loss of function studies using a Schwann cell specific Cre line such as *Sox10-Cre* (Matsuoka et al., 2005) might reveal whether *FGFR2* plays a role in the control of trophic support by myelinating tissues.

3.5 CUX2 IS EXPRESSED IN DORSALLY PROJECTING BRACHIAL SENSORY NEURONS

Members of the cut-like homeodomain transcription factor family (Cux) were shown to be involved in the regulation of cell-cycle progression and development of neural progenitors: *Cux1* plays a role in cell-cycle control of the nephrogenic and urogenital systems of the developing embryo (Vanden Heuvel et al., 1996; Ledford et al., 2002). *Cux2* is expressed in neuronal cells of the olfactory epithelium, in the roof plate and motor neurons of the spinal cord as well as sensory neurons in the DRG during the establishment of the vertebrate nervous system, (Iulianella et al., 2003). In the subventricular zone, *Cux2* regulates the number of layer II and III neurons, as well as dendrite branching and formation of dendritic spines (Cubelos et al., 2008; Cubelos et al., 2010).

In our microarray screen, the transcription factor was predicted to be expressed predominantly in dorsally projecting sensory neurons. We confirmed this prediction by *in situ* hybridization on backfilled embryos: 2,2 fold more dorsally projecting sensory neurons showed expression of *Cux2* when compared to ventrally projecting sensory neurons. Elimination of *Cux2* function was shown to lead increased re-entry of neuronal precursors of the subventricular zone into the cell cycle, while branching of dendrites and spine maturation was reduced (Cubelos et al., 2008; Cubelos et al., 2010). At spinal levels, *Cux2*^{-/-} mice show a reduction in the size of the spinal cord and DRG resulting from alterations in cell cycle dynamics and reduced cell cycle exit, which leads to reduced neuronal differentiation (Iulianella et al., 2008). In the DRG, *Cux2* was found to be expressed by both proprioceptive and nociceptive sensory neurons. Interestingly, onset of *Cux2* expression correlates with the generation of TrkA-positive A delta fibers and in adult mice the transcription factor was found to be expressed by 1/3 of the Type I A delta neurons (Bachy et al., 2011). While ablation of *Cux2* did not impair specification of proprioceptive projections, behavioural analysis of mutant mice showed a hypersensitivity to mechanical stimuli, which suggests miswiring of Type I A delta projections and C type TrkA positive axons. Taken together, these findings render *Cux2* a very interesting candidate for governing guidance decisions of sensory projections into the periphery. Further investigations will reveal whether specific sensory neuron subclasses express *Cux2* at relevant time points using specific markers such as IB4, Peripherin and TrpV2.

Wholemout embryo preparations of *Cux2*^{-/-} mouse embryos will allow for the investigation of the role of Cux2 for sensory axon fasciculation. Generation of a *Cux2-Cre* knock-in mouse line by homologous recombination with a suitable targeting vector in embryonic stem cells, and subsequent mating of this line with reporter strain, such as the *ROSA26R LacZ* reporter (Soriano, 1999) will contribute to elucidate whether *Cux2* is expressed predominantly in dorsally projecting sensory neurons. Investigation of homozygous mutant embryos in which sensory axons were retrogradely traced with fluorescently labeled dextrans will further show whether pathfinding of sensory axons is altered in absence of the transcription factor. These investigations thus will probably result in finding the first genetic marker for a subset of dorsally projecting sensory neurons.

3.6 A SUBSET OF DORSALLY PROJECTING BRACHIAL SENSORY NEURONS EXPRESSES

GNB4

G-protein coupled receptors and their downstream signaling cascades play important roles in a wide variety of physiological processes, including vision, olfaction, as well as in the functions of the parasympathetic and sympathetic nervous system (Simon et al., 1991). The alpha subunit of large G proteins is suggested to confer receptor and effector specificity, however, compared to the large variety of receptors, only 16 different alpha subunits have been identified (Simon et al., 1991). There is also evidence for multiple calcium, potassium, and possibly sodium channels that are responsive to G proteins (Brown and Birnbaumer, 1990), which may be activated by beta and gamma subunits of heteromeric G-proteins (Birnbaumer et al., 1990; Krapivinsky et al., 1995).

Gnb4 was predicted by our microarray screen and positively validated by *in situ* hybridization to be expressed in a higher number of dorsally projecting sensory neurons when compared to ventrally projecting sensory neurons. Mice deficient in *Gnb1*, a close relative of *Gnb4*, showed severe deficits in neural tube closure and proliferation of neural progenitor cells, as well as reduced cortical thickness which may be caused by defective phosphorylation of ERK. Furthermore, apical actin filaments were decreased in *Gnb1*^{-/-} neuronal progenitors, while at the basal side abnormal contractility was induced by low levels of S1P which induces cell

contraction by activation of RhoA and thus leads to abnormal reorganization of microtubules (Hurst et al., 2008; Okae and Iwakura, 2010). Whether Gnb4 exerts similar functions in nervous system development, and, beyond that, in axon growth and guidance, however, still has to be elucidated. Further classification of sensory neuron subtypes that express *Gnb4* will help to elucidate whether it is expressed predominantly in dorsally projecting nociceptive or proprioceptive sensory neurons. Expression analyses at earlier time points will reveal whether *Gnb4* is expressed when dorsal-ventral guidance decisions are made in the plexus region at the base of the limb. Up to now, no mouse lines with mutations in *Gnb4* are available. In chicken embryos, general mechanisms of generation of motor neuron generation, columns formation and axonal growth and guidance into the periphery that were observed in the mouse model are conserved (Helmbacher et al., 2000; Eberhart et al., 2002; Huber et al., 2005; Moret et al., 2007). Therefore, it is likely that establishment of sensory connections into the periphery also depends on similar mechanisms in both model organisms. *In ovo* electroporation of chicken embryos with a *Gnb4* (Gene ID: 424974) expression vector in combination with a fluorescent marker, which ideally contains a promoter of a gene that is active specifically during sensory neuron development, such as *Brn3a* (Dykes et al., 2011) to circumvent expression in motor neurons of the spinal cord will show whether sensory axons that express *Gnb4* chose dorsal trajectories during the establishment of limb innervation. Knock down of Gnb4 function by injection and *in ovo* electroporation of siRNA or morpholinos into the neural folds of chicken embryos or the anterior half of the somites will target neural crest derivatives or even more specifically neurons in the DRG, respectively (Martinsen et al., 2006; Chen and Krull, 2008; Kadison and Krull, 2008). These experiments will allow for an analysis of neural progenitor proliferation and axonal outgrowth in the absence of signal transduction by Gnb4.

3.7 IFT172 IS DIFFERENTIALLY EXPRESSED IN SENSORY NEURONS AT BRACHIAL LEVELS

Primary cilia are microtubule-based protrusions emanating from the surface of most quiescent cells in the vertebrate body that operate as antenna-like structures, coordinate signaling pathways which are critical during embryonic and postnatal development. Kinesin-mediated anterograde transport of intraflagellar transport

proteins (IFT) that carry the axonemal precursors α and β tubulin to the tip of the cilium is required to assemble ciliar microtubules, the axoneme. Retrograde transport of turn over products from the tip to the cell bodies is facilitated by IFT bound to dynein that migrates along microtubules (Pedersen et al., 2008). Also during axon outgrowth and dendrite formation microtubule assembly and stabilization is of critical importance for the formation of correct connections into the periphery and to other axons. Also here, kinesin and dynein mediate transport of components for microtubule assembly or disassembly (Conde and Caceres, 2009; Dent et al., 2011). In *Caenorhabditis elegans*, the *Ift172* ortholog *Osm-1* is a component of transport proteins both in cilia of chemosensory neurons and in dendrites (Signor et al., 1999). In mice mutant for the intraflagellar transport homolog 172 (*Ift172*), cilia show short axonemes with no visible microtubules (Gorivodsky et al., 2009). Furthermore, *Ift172* has been reported to be involved in different developmental signaling pathways, including Shh (Huangfu et al., 2003) or Wnt signaling (Leung et al., 2004) and influence anterior-posterior patterning of the developing embryo (Gorivodsky et al., 2009).

Our microarray screen predicted *Ift172* predominantly in dorsally projecting sensory neurons and we confirmed this prediction: indeed, 2 fold more dorsally projecting sensory neurons showed expression of *Ift172* mRNA when compared to ventrally projecting sensory neurons. Whether *Ift172* plays a role in the transport of microtubule components and therefore contributes to axon elongation and the defects in patterning after loss of *Ift172* function also impair sensory neurons and their pathfinding into the distal limbs, still needs to be elucidated. Mutation of *Osm-1* in *C.elegans* was shown to disrupt transport of fluorescent dyes into the cell bodies, and generation of a *Osm-1::GFP* fusion protein revealed that the *Ift172* ortholog is involved in both anterograde and retrograde transport along microtubules (Signor et al., 1999). Investigation of axonal transport of either fluorescent dyes or *Ift172::GFP* fusion constructs using time lapse imaging on primary cell cultures of DRG neurons of wildtype mice and mice, where *Ift172* was conditionally ablated in sensory neurons will allow for the analysis of *Ift172* function during the establishment of the axonal cytoskeleton (Howard et al., 2010). Wholemout preparations of embryos where *Ift172* was conditionally ablated in sensory neurons using the *Ht-PA-Cre* line also will reveal potential guidance deficits caused by defective microtubule assembly during the establishment of sensory projections into the periphery.

3.8 NEK1 IS EXPRESSED PREDOMINANTLY IN DORSALLY PROJECTING SENSORY NEURONS OF THE BRACHIAL DRG

Never in mitosis A (NIMA)-related kinases (Neks) are Serin/threonine kinases that have conserved roles in the regulation of microtubule structures in diverse eukaryotes, including plants, fungi and all other organisms that contain ciliated cells (Parker et al., 2007; Motose et al., 2008). Within these cells, Neks regulate mitotic spindle assembly or ciliary length by promotion of microtubule assembly or disassembly (Bradley and Quarmby, 2005). In mammalia, most Nek kinases are located to the centrosome or in cilia. Nek3, however, was found also in the cytoplasm (Tanaka and Nigg, 1999). Several Nek kinases, including *Nek3* are highly expressed in neurons of the central and peripheral nervous system (Arama et al., 1998). Ablation of Nek3 function resulted in deficits in neuronal morphology and polarity due to altered levels of α -tubulin acetylation and sprouted multiple processes instead of one axon (Chang et al., 2009).

Our microarray screen predicted *Nek1*, a close relative of *Nek3* to be predominantly expressed in dorsally projecting sensory neurons. We confirmed this prediction, showing that 2.1 fold more dorsally projecting sensory neurons express *Nek1* when compared to sensory neurons projecting to the ventral limb. In mice mutant for Nek1, checkpoint kinases fail to be activated properly during the cell cycle which leads to growth retardation, facial dysmorphisms and neurologic abnormalities (Arama et al., 1998; Chen et al., 2008). Furthermore, *in vitro* experiments showed that overexpression of *Nek1* leads to impairments, in which also microtubule assembly is defective without disrupting centrosomes, while abolishment of *Nek1* function causes loss of centrosomes and γ -tubulin which forms the base of microtubules that are assembled for cilia or axon elongation (White and Quarmby, 2008, Conde and Caceres, 2009, Dent et al., 2011). *In vitro* studies showed that *Nek1* also cycles from cilia in the cytoplasm to the nucleus, however, the signals that mediate this transit are not known (Hilton et al., 2009). Nevertheless, these findings not only show a role for *Nek1* in microtubule assembly, but also suggest functions in signal transduction. To address these two different functional mechanisms, *in vitro* studies of primary cultured sensory neurons could be employed: Investigation of primary sensory neuron cultures from mice that lack Nek1 function (Polci et al., 2004)

will show whether his kinase confers similar roles in microtubule assembly of axons as shown for ciliar formation. Disruption of the nuclear localization signal of Nek1 might further reveal whether translocation of the kinase into the nucleus transduces signals that are essential for growth cone turning events induced by extracellular cues.

3.9 *PLCD4* IS PREDOMINANTLY EXPRESSED IN DORSALLY PROJECTING SENSORY NEURONS

The hydrolysis of a minor membrane phospholipid, phosphatidylinositol 4,5-bisphosphate (PIP₂) to generate second messengers by phospholipase C (PLC) is one of the earliest key events in the regulation of various cell functions by more than 100 extracellular signaling molecules. Polypeptide growth factors like PDGF, FGFs and HGF were shown to induce PIP₂ turnover by activating PLC- γ coupled to their corresponding receptors (Rhee and Bae, 1997). HGF-Met signaling is indeed mediating axon guidance of the hypoglossal nerve and segmented growth of spinal nerves in the somites (Ebens et al., 1996; Caton et al., 2000, Kuan et al., 2004). Furthermore, expression of the growth factor in the mesenchyme of the developing limb attracts axons emanating from a subset of spinal motor neurons that express the HGF-receptor *Met* towards the plexus region at the base of the limb, and to specific targets in the dorsal and ventral limb musculature (Ebens et al., 1996). Transcription of PLC- δ isoforms, in particular *PLCd4* is activated upon treatment with growth factors such as bradykinin, lysophosphatic acid (LA) or NGF *in vitro* (Fukami et al., 2000). Bradykinin and LA have been shown to be important for neurite outgrowth and synaptic function (Hanani, 2005; Moughal et al., 2006; Sikand and Premkumar, 2007; Brogginini et al., 2010), as well as axon-glia interactions for proper myelination by interaction with ErbB (Chen et al., 2006; Britsch, 2007; Quintes et al., 2010). To which receptors PLC- δ isoforms are coupled is unclear, however, activation was also observed upon interaction with GTPases like RhoA (Homma and Emori, 1995).

Our microarray screen predicted PLCd4 to be expressed predominantly in dorsally projecting sensory neurons. We confirmed this prediction on sections of retrogradely labeled embryos and showed that 2,4 fold more sensory neurons that were retrogradely labeled from dorsal limb mesenchyme expressed PLCd4. Overexpression of PLCd4 upregulates the expression of *ErbB1* and *ErbB2*, which

leads to the activation of the ERK1/2 kinase pathway which is regulated by extracellular mitogen signals (Leung et al., 2004). Activation of this pathway in combination with signaling via small Rho GTPases has also been observed upon signaling through plexins (Kruger et al., 2005) or downstream of neurotrophin receptors like TrkA (via PLC- γ) to modulate the actin cytoskeleton (Huber et al., 2003). Blocking of PLC- δ function in rat hippocampal cells that express Trk receptors was shown to inhibit neurite formation in NGF treated cells, suggesting also a role for PLC- δ in downstream signaling of neurotrophin receptors during sensory axon outgrowth (Corbit et al., 1999). Further investigations are required to assess whether PLCd4 mediates dorsal guidance of sensory axons. Analyses of *Plcd4* deficient embryos (Fukami et al., 2001) using wholemount embryo staining techniques will reveal whether extension and fasciculated growth of sensory axons is impaired. Analysis of sensory neuron numbers and assignment of *PLCd4*-positive neurons to specific subclasses will reveal whether these neurons are nociceptive or proprioceptive sensory neurons and if target-derived neurotrophic support of subsets of sensory neurons depends on activation of downstream signaling components by PLCd4.

3.10 CONCLUSIONS

Taken together, this work contributes to the identification of molecular factors that regulate the pathfinding of motor and sensory axons towards their peripheral targets in the limb and to the establishment of sensory-motor connectivity. We confirmed the differential expression of candidate genes that was predicted by a differential microarray expression screen in motor and sensory neurons at brachial levels. Among these predicted genes we found no overlap between sensory and motor candidates, arguing for distinct guidance mechanisms for the establishment of sensory and motor fiber systems. According to the expression analyses, the most promising candidate for differential guidance of motor axons is *Arhgap29*, which was shown in blood vessel cells to mediate intracellular signaling cascades that lead to actin cytoskeleton remodeling and altered cell adhesion, resembling events that happen during growth cone turning upon repulsive interaction with guidance cues. Gain- and loss-of-function experiments in chicken will show whether cytoskeletal rearrangements upon *Arhgap29* activation or blockage affect differential motor axon

pathfinding. We found *Elk3* to be differentially expressed only at a time point when dorsal-ventral decisions are already made. As a close relative to ETS genes like *PEA3* or *Er81*, however, *Elk3* might be involved in definition of motor pools projecting the same peripheral targets. Further expression analysis and retrograde tracing of motor neurons at later stages during embryonal development will help to understand target derived induction of motor pool specification. Expression analysis of *Ccdc3* in motor neurons showed that differential expression is established between E10.5 and E11.5, thus, just at the time when the vast majority of motor axons follow pioneering axons into the distal limb. However, up to now nothing is known about the function and receptors for the secretory protein, thus extensive investigations are required to further characterize the role of *Ccdc3* during development and the establishment of motor innervation to the limb. Even though *FGFR2* showed the smallest difference in differentially projecting motor neurons, the immediate availability of a conditional mouse line at the Institute of Developmental Genetics prompted us to investigate its role in the dorsal-ventral guidance of brachial motor neurons. Analysis of embryos where this candidate was ablated in motor neurons did not show impairments in overall morphology, fasciculation and guidance fidelity of motor nerves, thus suggesting that *FGFR2* has no role in motor axon fasciculation or dorsal-ventral axon guidance.

Up to now, no markers exist to distinguish sensory neurons according to their topographic projections in the periphery. We confirmed the differential expression of five genes to be predominantly, but not exclusively expressed in dorsally projecting sensory neurons, as predicted by our microarray screen. Further investigations are required to refine this expression analysis and will reveal whether these candidates are present specifically in nociceptive or proprioceptive classes of sensory neurons. The most promising candidate in this context is *Cux2* that was shown to be expressed in a subset of TrkA-positive A-delta sensory fibers from the time point they are generated until adulthood. Behavioural analyses of *Cux2* deficient mice indicate miswiring of these fibers already during the establishment of sensory trajectories. *Gnb4* and *PLCd4* confer intracellular signaling upon stimulation from extracellular molecules that lead to cytoskeletal rearrangements, while *Nek1* promotes microtubule assembly, and also *lft172* was shown to be directly involved in microtubular transport and establishment. Based on the detailed expression analysis in sensory neuron classes, the role of these candidates in sensory axon growth and

guidance should be functionally characterized using gain- and loss-of-function approaches in mouse mutants where available or, alternatively, in chicken embryos.

During development, the establishment of sensory and motor projections to their distal targets in the extremities is achieved in a stepwise process tightly controlled in a spatial and temporal manner in response to cues in the environment or on co-extending axons. In the adult nervous system, mild injuries to peripheral projections are repaired rapidly and complete restoration of function is usually achieved. In more severe injuries, the endoneurial tubes are disrupted, and regenerating axons are no longer confined to their original sheaths, meandering into surrounding tissue and fail to innervate their respective targets. In these cases, a delay of regeneration or even unsuccessful regeneration might be caused by scar formation or destruction of endoneurial tubes composed by glia cells which provide trophic support to axons. After injuries, regenerating axons face similar challenges as axons during development: Guidance and neurotrophic factors presented by the surrounding tissues are required to ensure proper re-targeting of muscles and survival of the damaged axons and their neurons. Aberrant projections into the wrong endoneurial tubes or excessive sprouting therefore also contribute to incomplete restoration of function (reviewed in Burnett and Zager, 2004). Traumatic injuries to the brain and spinal cord of mammals were shown to induce upregulation of embryonic inhibitory or repulsive guidance cues and their receptors on the neurites, effectively preventing axons from growing into the lesion sites to re-establish connectivity within the spinal cord, and depending on the severity of the injury, also into the periphery (Mueller et al., 2006). Furthermore, diseases like *amyotrophic lateral sclerosis* (ALS) or *spinal muscular atrophy* (SMA) result in the lack of control over voluntary muscles. In ALS, both motor neurons in the brain and motor neurons in the spinal cord degenerate or die and cease to send messages to the according musculature, which atrophy, and control over voluntary movements is lost (Pradat and Dib, 2009). In SMA, degeneration of motor neurons due to a mutation in *SMN1* causes atrophy of proximal muscles of the trunk and extremities (Kostova et al., 2007). Re-establishment of drastically impaired circuitries to fully restore functionality up to now is not feasible. Cell replacement therapies to substitute defective neurons and re-generate axonal connectivity therefore are a highly interesting topic. Generation of specific motor neurons from embryonic or induced pluripotent stem cells by addition of a defined group of transcription factors (Hu et al., 2010) is only

the first step for the de-novo innervation of peripheral targets. After transplantation, these neurons have to re-integrate into sensory-motor circuits. They not only need to find their target in the periphery under more difficult conditions, as the extremities are fully developed, but also need to acquire input from sensory afferents and interneurons.

The work presented here extends our understanding of the molecular mechanisms of the formation of sensory-motor networks and has the potential to provide valuable information about the establishment of peripheral circuits during development. These findings thus might contribute to understand limitations of nerve regeneration during adulthood and provide a base for the future development of treatments to re-establish sensory-motor circuitry in case of trauma or neurological diseases.

ABBREVIATIONS

ALS	Amyotrophic lateral sclerosis
Arhgap29	Rho-GTPase activating protein 29
BCIP	5-bromo-4-chloro -3 indolyphosphate
BDNF	Brain-derived neurotrophic factor
bMN	Branchiomotor neurons
BMP	Bone morphogenic protein
<i>C. elegans</i>	<i>Caenorhabditis elegans</i>
Ccdc3	Coiled coil domain containing 3
CP	Convergence point
Cux1	Cut-like homeodomain transcription factor 1
Cux2	Cut-like homeodomain transcription factor 2
Cxcl12	Chemokine (C-X-C motif) ligand 12
Cxcr4	Chemokine (C-X-C motif) receptor 4
DIG	Digoxigenin
DMSO	Dimethyl sulfoxide
DNA	deoxyribonucleic acid
DRG	Dorsal root ganglion
<i>Drosophila</i>	<i>Drosophila melanogaster</i>
DT-A	Diphtheria toxin fragment A
EDTA	Ethylenediaminetetraacetic acid
Elk1	ETS domain-containing protein Elk1
Elk3	ETS domain-containing protein Elk3
EphA	Ephrin type-A receptor
EphB	Ephrin type-B receptor
Er81	ETS variant gene 1 (Etv1)
ErbB2	Epidermal growth factor receptor family, v-erb-b2 erythroblastic leukemia viral oncogene homolog 2
ErbB4	Epidermal growth factor receptor family, v-erb-a erythroblastic leukemia viral oncogene homolog 4
ETS	Erythroblastosis virus E26 oncogene homolog
FACS	Fluorescence activated cell sorting
FGF	Fibroblast growth factor

FGFR2	Fibroblast growth factor receptor 2
FoxP1	forkhead box P1
GAP	GTP activating protein
GDP	Guanine diphosphate
GEF	Guanine nucleotide exchange factor
GFP	Green fluorescent protein
Gnb1	guanine nucleotide binding protein (G protein), beta 1
Gnb4	guanine nucleotide binding protein (G protein), beta 4
GTP	Guanine triphosphate
Hb9	motor neuron and pancreas homeobox 1 (Mnx1)
HGF	Hepatocyte growth factor
Hox	Homeobox
Ht-PA	Human tissue plasminogen activator
HUVEC	Human umbilical vein endothelial cells
Ift172	Intraflagellar transport homolog 172
Isl1	LIM homeodomain protein Islet-1
JP	Joining point
Krox20	early growth response 2 (Egr2)
Lhx3	LIM homeobox protein 3
Lhx4	LIM homeobox protein 4
Lim1	LIM homeobox protein 1
LMC	Lateral motor column
LMCI	Lateral aspect of the LMC
LMCm	Medial aspect of the LMC
Met	Met proto-oncogene tyrosine kinase, hepatocyte growth factor receptor
Min	Minute, minutes
MMC	Medial motor column
NBT	Nitrobluetetrazolium
NCAM	Neural cell adhesion molecule
Ncx	T-cell leukemia, homeobox 2 (Tlx2)
Nek1	Never in mitosis gene a (NIMA) related kinase 1
NGF	Nerve growth factor
Nkx	NK2 transcription factor related
Npn	Neuropilin (JAX nomenclature: Nrp)
<i>Npn-1^{cond}</i>	Conditional allele of Npn-1, exon 2 is floxed
<i>Npn-1^{Sema-}</i>	Npn-1, mutated Sema-binding domain

NT-3	Neurotrophin 3
Olig2	Oligodendrocyte transcription factor 2
Pax6	Paired box gene 6
PBS	Phosphate buffered saline
PBST	Phosphate buffered saline containing 0,1% Triton X
PEA3	ETS variant gene 4 (Etv4)
PECAM	Platelet/endothelial cell adhesion molecule
PFA	Paraformaldehyde
PLCd4	Phospholipase C delta 4
pMN	Zone where motor neuron progenitors arise
PSA	Polysialic acid
Raldh2	Aldehyde dehydrogenase family 1, subfamily A2 (Aldh1a2)
Rho	Ras homolog gene family
RNA	Ribonucleic acid
Robo	Roundabout
Sema	Semaphorin
Shh	Sonic hedgehog
SMA	Spinal muscular atrophy
sMN	Somatic motor neurons
SSC	Standard saline citrate
TEA	Trietholamine
TP	Turning point
TrkA	tyrosine receptor kinase A
TrkC	tyrosine receptor kinase C
VEGF	Vascular endothelial growth factor
vMN	Visceromotor neurons
Wnt	wingless-type MMTV integration site family
X-Gal	5-bromo-4-chloro-indolyl-galactopyranoside (BCIG)

BIBLIOGRAPHY

- Adams RH, Eichmann A (2010) Axon guidance molecules in vascular patterning. *Cold Spring Harb Perspect Biol* 2:a001875.
- Akins MR, Greer CA (2006) Axon behavior in the olfactory nerve reflects the involvement of catenin-cadherin mediated adhesion. *The Journal of comparative neurology* 499:979-989.
- Akutagawa A, Fukami K, Banno Y, Takenawa T, Kannagi R, Yokoyama Y, Oda K, Nagino M, Nimura Y, Yoshida S, Tamiya-Koizumi K (2006) Disruption of phospholipase Cdelta4 gene modulates the liver regeneration in cooperation with nuclear protein kinase C. *J Biochem* 140:619-625.
- Aldridge K, Hill CA, Austin JR, Percival C, Martinez-Abadias N, Neuberger T, Wang Y, Jabs EW, Richtsmeier JT (2010) Brain phenotypes in two FGFR2 mouse models for Apert syndrome. *Developmental dynamics : an official publication of the American Association of Anatomists* 239:987-997.
- Alexander T, Nolte C, Krumlauf R (2009) Hox genes and segmentation of the hindbrain and axial skeleton. *Annu Rev Cell Dev Biol* 25:431-456.
- Ara J, Bannerman P, Shaheen F, Pleasure DE (2005) Schwann cell-autonomous role of neuropilin-2. *J Neurosci Res* 79:468-475.
- Arama E, Yanai A, Kilfin G, Bernstein A, Motro B (1998) Murine NIMA-related kinases are expressed in patterns suggesting distinct functions in gametogenesis and a role in the nervous system. *Oncogene* 16:1813-1823.
- Arber S, Han B, Mendelsohn M, Smith M, Jessell TM, Sockanathan S (1999) Requirement for the homeobox gene Hb9 in the consolidation of motor neuron identity. *Neuron* 23:659-674.
- Arber S, Ladle DR, Lin JH, Frank E, Jessell TM (2000) ETS gene Er81 controls the formation of functional connections between group Ia sensory afferents and motor neurons. *Cell* 101:485-498.
- Arman E, Haffner-Krausz R, Chen Y, Heath JK, Lonai P (1998) Targeted disruption of fibroblast growth factor (FGF) receptor 2 suggests a role for FGF signaling in pregastrulation mammalian development. *Proceedings of the National Academy of Sciences of the United States of America* 95:5082-5087.
- Ayadi A, Suelves M, Dolle P, Wasylyk B (2001a) Net, an Ets ternary complex transcription factor, is expressed in sites of vasculogenesis, angiogenesis, and chondrogenesis during mouse development. *Mech Dev* 102:205-208.
- Ayadi A, Zheng H, Sobieszczuk P, Buchwalter G, Moerman P, Alitalo K, Wasylyk B (2001b) Net-targeted mutant mice develop a vascular phenotype and up-regulate egr-1. *EMBO J* 20:5139-5152.
- Bachy I, Franck MC, Li L, Abdo H, Pattyn A, Ernfors P (2011) The transcription factor Cux2 marks development of an A-delta sublineage of TrkA sensory neurons. *Developmental biology*.
- Barnes SH, Price SR, Wentzel C, Guthrie SC (2010) Cadherin-7 and cadherin-6B differentially regulate the growth, branching and guidance of cranial motor axons. *Development* 137:805-814.
- Battye R, Stevens A, Jacobs JR (1999) Axon repulsion from the midline of the Drosophila CNS requires slit function. *Development* 126:2475-2481.
- Birnbaumer L, Yatani A, VanDongen AM, Graf R, Codina J, Okabe K, Mattera R, Brown AM (1990) G protein coupling of receptors to ionic channels and other effector systems. *British journal of clinical pharmacology* 30 Suppl 1:13S-22S.

- Bisgrove BW, Yost HJ (2006) The roles of cilia in developmental disorders and disease. *Development* 133:4131-4143.
- Blak AA, Naserke T, Saarimaki-Vire J, Peltopuro P, Giraldo-Velasquez M, Vogt Weisenhorn DM, Prakash N, Sendtner M, Partanen J, Wurst W (2007) Fgfr2 and Fgfr3 are not required for patterning and maintenance of the midbrain and anterior hindbrain. *Developmental biology* 303:231-243.
- Blochlinger K, Bodmer R, Jan LY, Jan YN (1990) Patterns of expression of cut, a protein required for external sensory organ development in wild-type and cut mutant *Drosophila* embryos. *Genes Dev* 4:1322-1331.
- Bonanomi D, Pfaff SL (2010) Motor axon pathfinding. *Cold Spring Harb Perspect Biol* 2:a001735.
- Bottcher RT, Niehrs C (2005) Fibroblast growth factor signaling during early vertebrate development. *Endocr Rev* 26:63-77.
- Bradley BA, Quarmby LM (2005) A NIMA-related kinase, Cnk2p, regulates both flagellar length and cell size in *Chlamydomonas*. *Journal of cell science* 118:3317-3326.
- Briscoe J, Ericson J (1999) The specification of neuronal identity by graded Sonic Hedgehog signalling. *Semin Cell Dev Biol* 10:353-362.
- Britsch S (2007) The neuregulin-I/ErbB signaling system in development and disease. *Advances in anatomy, embryology, and cell biology* 190:1-65.
- Brockschneider D, Pechmann Y, Sonnenberg-Riethmacher E, Riethmacher D (2006) An improved mouse line for Cre-induced cell ablation due to diphtheria toxin A, expressed from the Rosa26 locus. *Genesis* 44:322-327.
- Broggini T, Nitsch R, Savaskan NE (2010) Plasticity-related gene 5 (PRG5) induces filopodia and neurite growth and impedes lysophosphatidic acid- and nogo-A-mediated axonal retraction. *Molecular biology of the cell* 21:521-537.
- Bron R, Vermeren M, Kokot N, Andrews W, Little GE, Mitchell KJ, Cohen J (2007) Boundary cap cells constrain spinal motor neuron somal migration at motor exit points by a semaphorin-plexin mechanism. *Neural development* 2:21.
- Bronner-Fraser M (1994) Neural crest cell formation and migration in the developing embryo. *The FASEB journal : official publication of the Federation of American Societies for Experimental Biology* 8:699-706.
- Brown AM, Birnbaumer L (1990) Ionic channels and their regulation by G protein subunits. *Annual review of physiology* 52:197-213.
- Buchwalter G, Gross C, Wasylyk B (2005) The ternary complex factor Net regulates cell migration through inhibition of PAI-1 expression. *Mol Cell Biol* 25:10853-10862.
- Burgess RW, Jucius TJ, Ackerman SL (2006) Motor axon guidance of the mammalian trochlear and phrenic nerves: dependence on the netrin receptor *Unc5c* and modifier loci. *The Journal of neuroscience : the official journal of the Society for Neuroscience* 26:5756-5766.
- Burkhard P, Stetefeld J, Strelkov SV (2001) Coiled coils: a highly versatile protein folding motif. *Trends in cell biology* 11:82-88.
- Burnett MG, Zager EL (2004) Pathophysiology of peripheral nerve injury: a brief review. *Neurosurgical focus* 16:E1.
- Carmeliet P (2003) Blood vessels and nerves: common signals, pathways and diseases. *Nature reviews Genetics* 4:710-720.
- Castellani V (2002) The function of neuropilin/L1 complex. *Advances in experimental medicine and biology* 515:91-102.
- Caton A, Hacker A, Naeem A, Livet J, Maina F, Bladt F, Klein R, Birchmeier C, Guthrie S (2000) The branchial arches and HGF are growth-promoting and chemoattractant for cranial motor axons. *Development* 127:1751-1766.
- Cesari F, Brecht S, Vintersten K, Vuong LG, Hofmann M, Klingel K, Schnorr JJ, Arsenian S, Schild H, Herdegen T, Wiebel FF, Nordheim A (2004) Mice deficient for the ets transcription factor *elk-1*

- show normal immune responses and mildly impaired neuronal gene activation. *Mol Cell Biol* 24:294-305.
- Chang J, Baloh RH, Milbrandt J (2009) The NIMA-family kinase Nek3 regulates microtubule acetylation in neurons. *Journal of cell science* 122:2274-2282.
- Chen H, Bagri A, Zupicich JA, Zou Y, Stoeckli E, Pleasure SJ, Lowenstein DH, Skarnes WC, Chedotal A, Tessier-Lavigne M (2000) Neuropilin-2 regulates the development of selective cranial and sensory nerves and hippocampal mossy fiber projections. *Neuron* 25:43-56.
- Chen H, Lun Y, Ovchinnikov D, Kokubo H, Oberg KC, Pepicelli CV, Gan L, Lee B, Johnson RL (1998) Limb and kidney defects in Lmx1b mutant mice suggest an involvement of LMX1B in human nail patella syndrome. *Nature genetics* 19:51-55.
- Chen S, Velardez MO, Warot X, Yu ZX, Miller SJ, Cros D, Corfas G (2006) Neuregulin 1-erbB signaling is necessary for normal myelination and sensory function. *The Journal of neuroscience : the official journal of the Society for Neuroscience* 26:3079-3086.
- Chen WP, Chang YC, Hsieh ST (1999) Trophic interactions between sensory nerves and their targets. *Journal of biomedical science* 6:79-85.
- Chen Y, Chen PL, Chen CF, Jiang X, Riley DJ (2008) Never-in-mitosis related kinase 1 functions in DNA damage response and checkpoint control. *Cell Cycle* 7:3194-3201.
- Chen YX, Krull CE (2008) Using in ovo electroporation to transfect cells in avian somites. *CSH protocols* 2008:pdb prot4924.
- Chilton JK, Guthrie S (2003) Cranial expression of class 3 secreted semaphorins and their neuropilin receptors. *Developmental dynamics : an official publication of the American Association of Anatomists* 228:726-733.
- Chilton JK, Guthrie S (2004) Development of oculomotor axon projections in the chick embryo. *The Journal of comparative neurology* 472:308-317.
- Cirulli V, Yebra M (2007) Netrins: beyond the brain. *Nature reviews Molecular cell biology* 8:296-306.
- Cleaver O, Krieg PA (2001) Notochord patterning of the endoderm. *Developmental biology* 234:1-12.
- Conde C, Caceres A (2009) Microtubule assembly, organization and dynamics in axons and dendrites. *Nature reviews Neuroscience* 10:319-332.
- Corbit KC, Foster DA, Rosner MR (1999) Protein kinase Cdelta mediates neurogenic but not mitogenic activation of mitogen-activated protein kinase in neuronal cells. *Mol Cell Biol* 19:4209-4218.
- Cordes SP (2001) Molecular genetics of cranial nerve development in mouse. *Nature reviews Neuroscience* 2:611-623.
- Coumoul X, Deng CX (2003) Roles of FGF receptors in mammalian development and congenital diseases. *Birth Defects Res C Embryo Today* 69:286-304.
- Cubelos B, Sebastian-Serrano A, Beccari L, Calcagnotto ME, Cisneros E, Kim S, Dopazo A, Alvarez-Dolado M, Redondo JM, Bovolenta P, Walsh CA, Nieto M (2010) Cux1 and Cux2 regulate dendritic branching, spine morphology, and synapses of the upper layer neurons of the cortex. *Neuron* 66:523-535.
- Cubelos B, Sebastian-Serrano A, Kim S, Moreno-Ortiz C, Redondo JM, Walsh CA, Nieto M (2008) Cux-2 controls the proliferation of neuronal intermediate precursors of the cortical subventricular zone. *Cereb Cortex* 18:1758-1770.
- Culotti JG, Kolodkin AL (1996) Functions of netrins and semaphorins in axon guidance. *Current opinion in neurobiology* 6:81-88.
- Dafotakis M, Schiefer J, Wiesmann M, Muhlenbruch G (2011) [Bilateral wrist drop - central or peripheral lesion?]. *Fortschritte der Neurologie-Psychiatrie* 79:304-306.
- Danielian PS, Muccino D, Rowitch DH, Michael SK, McMahon AP (1998) Modification of gene activity in mouse embryos in utero by a tamoxifen-inducible form of Cre recombinase. *Curr Biol* 8:1323-1326.
- Dasen JS, Liu JP, Jessell TM (2003) Motor neuron columnar fate imposed by sequential phases of Hox-c activity. *Nature* 425:926-933.

- Dasen JS, Tice BC, Brenner-Morton S, Jessell TM (2005) A Hox regulatory network establishes motor neuron pool identity and target-muscle connectivity. *Cell* 123:477-491.
- De Moerlooze L, Spencer-Dene B, Revest JM, Hajihosseini M, Rosewell I, Dickson C (2000) An important role for the IIIb isoform of fibroblast growth factor receptor 2 (FGFR2) in mesenchymal-epithelial signalling during mouse organogenesis. *Development* 127:483-492.
- Deiner MS, Kennedy TE, Fazeli A, Serafini T, Tessier-Lavigne M, Sretavan DW (1997) Netrin-1 and DCC mediate axon guidance locally at the optic disc: loss of function leads to optic nerve hypoplasia. *Neuron* 19:575-589.
- Dent EW, Gupton SL, Gertler FB (2011) The growth cone cytoskeleton in axon outgrowth and guidance. *Cold Spring Harb Perspect Biol* 3.
- Dessaud E, Yang LL, Hill K, Cox B, Ulloa F, Ribeiro A, Mynett A, Novitsch BG, Briscoe J (2007) Interpretation of the sonic hedgehog morphogen gradient by a temporal adaptation mechanism. *Nature* 450:717-720.
- Dickson BJ (2001) Rho GTPases in growth cone guidance. *Current opinion in neurobiology* 11:103-110.
- Donoghue PC, Graham A, Kelsh RN (2008) The origin and evolution of the neural crest. *BioEssays : news and reviews in molecular, cellular and developmental biology* 30:530-541.
- Dykes IM, Tempest L, Lee SI, Turner EE (2011) Brn3a and Islet1 act epistatically to regulate the gene expression program of sensory differentiation. *The Journal of neuroscience : the official journal of the Society for Neuroscience* 31:9789-9799.
- Ebens A, Brose K, Leonardo ED, Hanson MG, Jr., Bladt F, Birchmeier C, Barres BA, Tessier-Lavigne M (1996) Hepatocyte growth factor/scatter factor is an axonal chemoattractant and a neurotrophic factor for spinal motor neurons. *Neuron* 17:1157-1172.
- Eberhart J, Swartz ME, Koblar SA, Pasquale EB, Krull CE (2002) EphA4 constitutes a population-specific guidance cue for motor neurons. *Developmental biology* 247:89-101.
- Ericson J, Briscoe J, Rashbass P, van Heyningen V, Jessell TM (1997a) Graded sonic hedgehog signaling and the specification of cell fate in the ventral neural tube. *Cold Spring Harb Symp Quant Biol* 62:451-466.
- Ericson J, Rashbass P, Schedl A, Brenner-Morton S, Kawakami A, van Heyningen V, Jessell TM, Briscoe J (1997b) Pax6 controls progenitor cell identity and neuronal fate in response to graded Shh signaling. *Cell* 90:169-180.
- Farinas I (1999) Neurotrophin actions during the development of the peripheral nervous system. *Microscopy research and technique* 45:233-242.
- Fazeli A, Dickinson SL, Hermiston ML, Tighe RV, Steen RG, Small CG, Stoeckli ET, Keino-Masu K, Masu M, Rayburn H, Simons J, Bronson RT, Gordon JI, Tessier-Lavigne M, Weinberg RA (1997) Phenotype of mice lacking functional Deleted in colorectal cancer (Dcc) gene. *Nature* 386:796-804.
- Ferhat L, Represa A, Zouaoui-Aggoun D, Ferhat W, Ben-Ari Y, Khrestchatsky M (1997) FGF-2 induces nerve growth factor expression in cultured rat hippocampal neurons. *The European journal of neuroscience* 9:1282-1289.
- Finzsch M, Schreiner S, Kichko T, Reeh P, Tamm ER, Bosl MR, Meijer D, Wegner M (2010) Sox10 is required for Schwann cell identity and progression beyond the immature Schwann cell stage. *J Cell Biol* 189:701-712.
- Fritzsch B, Northcutt RG (1993) Cranial and spinal nerve organization in amphioxus and lampreys: evidence for an ancestral craniate pattern. *Acta anatomica* 148:96-109.
- Fu SY, Sharma K, Luo Y, Raper JA, Frank E (2000) SEMA3A regulates developing sensory projections in the chicken spinal cord. *Journal of neurobiology* 45:227-236.
- Fujisawa H, Kitsukawa T, Kawakami A, Takagi S, Shimizu M, Hirata T (1997) Roles of a neuronal cell-surface molecule, neuropilin, in nerve fiber fasciculation and guidance. *Cell and tissue research* 290:465-470.

- Fukami K, Ichinohe M, Hirata M, Nakamura Y (2008) Physiological functions of phospholipase C delta-type. *Advances in enzyme regulation* 48:261-273.
- Fukami K, Nakao K, Inoue T, Kataoka Y, Kurokawa M, Fissore RA, Nakamura K, Katsuki M, Mikoshiba K, Yoshida N, Takenawa T (2001) Requirement of phospholipase Cdelta4 for the zona pellucida-induced acrosome reaction. *Science* 292:920-923.
- Fukami K, Takenaka K, Nagano K, Takenawa T (2000) Growth factor-induced promoter activation of murine phospholipase C delta4 gene. *European journal of biochemistry / FEBS* 267:28-36.
- Fukami K, Yoshida M, Inoue T, Kurokawa M, Fissore RA, Yoshida N, Mikoshiba K, Takenawa T (2003) Phospholipase Cdelta4 is required for Ca²⁺ mobilization essential for acrosome reaction in sperm. *J Cell Biol* 161:79-88.
- Furusho M, Dupree JL, Bryant M, Bansal R (2009) Disruption of fibroblast growth factor receptor signaling in nonmyelinating Schwann cells causes sensory axonal neuropathy and impairment of thermal pain sensitivity. *The Journal of neuroscience : the official journal of the Society for Neuroscience* 29:1608-1614.
- Furusho M, Kaga Y, Ishii A, Hebert JM, Bansal R (2011) Fibroblast growth factor signaling is required for the generation of oligodendrocyte progenitors from the embryonic forebrain. *The Journal of neuroscience : the official journal of the Society for Neuroscience* 31:5055-5066.
- Gallarda BW, Bonanomi D, Muller D, Brown A, Alaynick WA, Andrews SE, Lemke G, Pfaff SL, Marquardt T (2008) Segregation of axial motor and sensory pathways via heterotypic trans-axonal signaling. *Science* 320:233-236.
- Gallo G, Lefcort FB, Letourneau PC (1997) The trkA receptor mediates growth cone turning toward a localized source of nerve growth factor. *The Journal of neuroscience : the official journal of the Society for Neuroscience* 17:5445-5454.
- Gammill LS, Gonzalez C, Bronner-Fraser M (2007) Neuropilin 2/semaphorin 3F signaling is essential for cranial neural crest migration and trigeminal ganglion condensation. *Developmental neurobiology* 67:47-56.
- Gaufo GO, Thomas KR, Capecchi MR (2003) Hox3 genes coordinate mechanisms of genetic suppression and activation in the generation of branchial and somatic motoneurons. *Development* 130:5191-5201.
- Geretti E, Shimizu A, Klagsbrun M (2008) Neuropilin structure governs VEGF and semaphorin binding and regulates angiogenesis. *Angiogenesis* 11:31-39.
- Gilmour DT, Maischein HM, Nusslein-Volhard C (2002) Migration and function of a glial subtype in the vertebrate peripheral nervous system. *Neuron* 34:577-588.
- Gorivodsky M, Mukhopadhyay M, Wilsch-Braeuninger M, Phillips M, Teufel A, Kim C, Malik N, Huttner W, Westphal H (2009) Intraflagellar transport protein 172 is essential for primary cilia formation and plays a vital role in patterning the mammalian brain. *Developmental biology* 325:24-32.
- Gu C, Rodriguez ER, Reimert DV, Shu T, Fritzsche B, Richards LJ, Kolodkin AL, Ginty DD (2003) Neuropilin-1 conveys semaphorin and VEGF signaling during neural and cardiovascular development. *Developmental cell* 5:45-57.
- Guthrie S (2007) Patterning and axon guidance of cranial motor neurons. *Nature reviews Neuroscience* 8:859-871.
- Haase G, Dessaud E, Garces A, de Bovis B, Birling M, Filippi P, Schmalbruch H, Arber S, deLapeyriere O (2002) GDNF acts through PEA3 to regulate cell body positioning and muscle innervation of specific motor neuron pools. *Neuron* 35:893-905.
- Haehl T, Huettl RE, Huber AB (2011) Analysis of candidate genes for motor axon guidance in the spinal cord (Bachelor thesis).
- Hajihosseini MK, Wilson S, De Moerlooze L, Dickson C (2001) A splicing switch and gain-of-function mutation in FgfR2-IIIc hemizygotes causes Apert/Pfeiffer-syndrome-like phenotypes. *Proceedings of the National Academy of Sciences of the United States of America* 98:3855-3860.

- Hall A (1998) Rho GTPases and the actin cytoskeleton. *Science* 279:509-514.
- Hamburger V, Wenger E, Oppenheim R (1966) Motility in the chick embryo in the absence of sensory input. *Journal of Experimental Zoology* 162:133-159.
- Hammond R, Vivancos V, Naeem A, Chilton J, Mambetisaeva E, Andrews W, Sundaresan V, Guthrie S (2005) Slit-mediated repulsion is a key regulator of motor axon pathfinding in the hindbrain. *Development* 132:4483-4495.
- Hanani M (2005) Satellite glial cells in sensory ganglia: from form to function. *Brain research Brain research reviews* 48:457-476.
- Harland R (2000) Neural induction. *Current opinion in genetics & development* 10:357-362.
- Harris R, Sabatelli LM, Seeger MA (1996) Guidance cues at the Drosophila CNS midline: identification and characterization of two Drosophila Netrin/UNC-6 homologs. *Neuron* 17:217-228.
- Hatano M, Iitsuka Y, Yamamoto H, Dezawa M, Yusa S, Kohno Y, Tokuhisa T (1997) Ncx, a Hox11 related gene, is expressed in a variety of tissues derived from neural crest cells. *Anatomy and embryology* 195:419-425.
- Haupt C, Kloos K, Faus-Kessler T, Huber AB (2010) Semaphorin 3A-Neuropilin-1 signaling regulates peripheral axon fasciculation and pathfinding but not developmental cell death patterns. *The European journal of neuroscience* 31:1164-1172.
- He Z, Tessier-Lavigne M (1997) Neuropilin is a receptor for the axonal chemorepellent Semaphorin III. *Cell* 90:739-751.
- He Z, Wang KC, Koprivica V, Ming G, Song HJ (2002) Knowing how to navigate: mechanisms of semaphorin signaling in the nervous system. *Science's STKE : signal transduction knowledge environment* 2002:re1.
- Helmbacher F, Schneider-Maunoury S, Topilko P, Tiret L, Charnay P (2000) Targeting of the EphA4 tyrosine kinase receptor affects dorsal/ventral pathfinding of limb motor axons. *Development* 127:3313-3324.
- Hieberger T, Gourley E, Erickson A, Koulen P, Ward CJ, Masyuk TV, Larusso NF, Harris PC, Igarashi P (2006) Proteolytic cleavage and nuclear translocation of .brocystin is regulated by intracellular Ca²⁺ and activation of protein kinase C. *J.Biol.Chem.* 281: 34357 -34364
- Hilton LK, White MC, Quarumby LM (2009) The NIMA-related kinase NEK1 cycles through the nucleus. *Biochem Biophys Res Commun* 389:52-56.
- Hollyday M, Jacobson RD (1990) Location of motor pools innervating chick wing. *The Journal of comparative neurology* 302:575-588.
- Homma Y, Emori Y (1995) A dual functional signal mediator showing RhoGAP and phospholipase C-delta stimulating activities. *EMBO J* 14:286-291.
- Honig MG, Camilli SJ, Xue QS (2002) Effects of L1 blockade on sensory axon outgrowth and pathfinding in the chick hindlimb. *Developmental biology* 243:137-154.
- Howard PW, Howard TL, Maurer RA (2010) Generation of mice with a conditional allele for Ift172. *Transgenic Res* 19:121-126.
- Howard PW, Maurer RA (2000) Identification of a conserved protein that interacts with specific LIM homeodomain transcription factors. *J Biol Chem* 275:13336-13342.
- Hu BY, Weick JP, Yu J, Ma LX, Zhang XQ, Thomson JA, Zhang SC (2010) Neural differentiation of human induced pluripotent stem cells follows developmental principles but with variable potency. *Proceedings of the National Academy of Sciences of the United States of America* 107:4335-4340.
- Huang EJ, Reichardt LF (2001) Neurotrophins: roles in neuronal development and function. *Annual review of neuroscience* 24:677-736.
- Huang X, Saint-Jeannet JP (2004) Induction of the neural crest and the opportunities of life on the edge. *Developmental biology* 275:1-11.
- Huangfu D, Liu A, Rakeman AS, Murcia NS, Niswander L, Anderson KV (2003) Hedgehog signalling in the mouse requires intraflagellar transport proteins. *Nature* 426:83-87.

- Huber AB, Kania A, Tran TS, Gu C, De Marco Garcia N, Lieberam I, Johnson D, Jessell TM, Ginty DD, Kolodkin AL (2005) Distinct roles for secreted semaphorin signaling in spinal motor axon guidance. *Neuron* 48:949-964.
- Huber AB, Kolodkin AL, Ginty DD, Cloutier JF (2003) Signaling at the growth cone: ligand-receptor complexes and the control of axon growth and guidance. *Annual review of neuroscience* 26:509-563.
- Huettl RE, Huber AB (2011) Cranial nerve fasciculation and Schwann cell migration are impaired after loss of Npn-1. *Developmental biology*.
- Huettl RE, Soellner H, Bianchi E, Novitsch BG, Huber AB (2011) Npn-1 contributes to axon-axon interactions that differentially control sensory and motor innervation of the limb. *PLoS biology* 9:e1001020.
- Hunt P, Wilkinson D, Krumlauf R (1991) Patterning the vertebrate head: murine Hox 2 genes mark distinct subpopulations of premigratory and migrating cranial neural crest. *Development* 112:43-50.
- Hurst JH, Mumaw J, Machacek DW, Sturkie C, Callihan P, Stice SL, Hooks SB (2008) Human neural progenitors express functional lysophospholipid receptors that regulate cell growth and morphology. *BMC neuroscience* 9:118.
- Imai T, Yamazaki T, Kobayakawa R, Kobayakawa K, Abe T, Suzuki M, Sakano H (2009) Pre-target axon sorting establishes the neural map topography. *Science* 325:585-590.
- Iulianella A, Sharma M, Durnin M, Vanden Heuvel GB, Trainor PA (2008) Cux2 (Cutl2) integrates neural progenitor development with cell-cycle progression during spinal cord neurogenesis. *Development* 135:729-741.
- Iulianella A, Vanden Heuvel G, Trainor P (2003) Dynamic expression of murine Cux2 in craniofacial, limb, urogenital and neuronal primordia. *Gene Expr Patterns* 3:571-577.
- Jessell TM (2000) Neuronal specification in the spinal cord: inductive signals and transcriptional codes. *Nature reviews Genetics* 1:20-29.
- Jungbluth S, Bell E, Lumsden A (1999) Specification of distinct motor neuron identities by the singular activities of individual Hox genes. *Development* 126:2751-2758.
- Kadison SR, Krull CE (2008) Transfecting neural crest cells in avian embryos using in ovo electroporation. *CSH protocols* 2008:pdb prot4925.
- Kania A, Jessell TM (2003) Topographic motor projections in the limb imposed by LIM homeodomain protein regulation of ephrin-A:EphA interactions. *Neuron* 38:581-596.
- Kania A, Johnson RL, Jessell TM (2000) Coordinate roles for LIM homeobox genes in directing the dorsoventral trajectory of motor axons in the vertebrate limb. *Cell* 102:161-173.
- Kao TJ, Kania A (2011) Ephrin-mediated cis-attenuation of Eph receptor signaling is essential for spinal motor axon guidance. *Neuron* 71:76-91.
- Kao TJ, Palmesino E, Kania A (2009) SRC family kinases are required for limb trajectory selection by spinal motor axons. *The Journal of neuroscience : the official journal of the Society for Neuroscience* 29:5690-5700.
- Katsuki T, Ailani D, Hiramoto M, Hiromi Y (2009) Intra-axonal patterning: intrinsic compartmentalization of the axonal membrane in *Drosophila* neurons. *Neuron* 64:188-199.
- Kawakami A, Kitsukawa T, Takagi S, Fujisawa H (1996) Developmentally regulated expression of a cell surface protein, neuropilin, in the mouse nervous system. *Journal of neurobiology* 29:1-17.
- Kennedy TE, Wang H, Marshall W, Tessier-Lavigne M (2006) Axon guidance by diffusible chemoattractants: a gradient of netrin protein in the developing spinal cord. *The Journal of neuroscience : the official journal of the Society for Neuroscience* 26:8866-8874.
- Kerr N, Pintzas A, Holmes F, Hobson SA, Pope R, Wallace M, Wasylyk C, Wasylyk B, Wynick D (2010) The expression of ELK transcription factors in adult DRG: Novel isoforms, antisense transcripts and upregulation by nerve damage. *Mol Cell Neurosci* 44:165-177.

- Keshishian H, Bentley D (1983) Embryogenesis of peripheral nerve pathways in grasshopper legs. III. Development without pioneer neurons. *Developmental biology* 96:116-124.
- Ketschek A, Gallo G (2010) Nerve growth factor induces axonal filopodia through localized microdomains of phosphoinositide 3-kinase activity that drive the formation of cytoskeletal precursors to filopodia. *The Journal of neuroscience : the official journal of the Society for Neuroscience* 30:12185-12197.
- Keynes R, Krumlauf R (1994) Hox genes and regionalization of the nervous system. *Annual review of neuroscience* 17:109-132.
- Kidd T, Bland KS, Goodman CS (1999) Slit is the midline repellent for the robo receptor in *Drosophila*. *Cell* 96:785-794.
- Kitsukawa T, Shimizu M, Sanbo M, Hirata T, Taniguchi M, Bekku Y, Yagi T, Fujisawa H (1997) Neuropilin-semaphorin III/D-mediated chemorepulsive signals play a crucial role in peripheral nerve projection in mice. *Neuron* 19:995-1005.
- Kobayashi S, Fukuhara A, Taguchi T, Matsuda M, Tochino Y, Otsuki M, Shimomura I (2010) Identification of a new secretory factor, CCDC3/Favine, in adipocytes and endothelial cells. *Biochem Biophys Res Commun* 392:29-35.
- Kolodkin AL, Levengood DV, Rowe EG, Tai YT, Giger RJ, Ginty DD (1997) Neuropilin is a semaphorin III receptor. *Cell* 90:753-762.
- Kostova FV, Williams VC, Heemskerk J, Iannaccone S, Didonato C, Swoboda K, Maria BL (2007) Spinal muscular atrophy: classification, diagnosis, management, pathogenesis, and future research directions. *Journal of child neurology* 22:926-945.
- Kovacs KJ (2008) Measurement of immediate-early gene activation- c-fos and beyond. *Journal of neuroendocrinology* 20:665-672.
- Kramer ER, Knott L, Su F, Dessaud E, Krull CE, Helmbacher F, Klein R (2006) Cooperation between GDNF/Ret and ephrinA/EphA4 signals for motor-axon pathway selection in the limb. *Neuron* 50:35-47.
- Kramer SG, Kidd T, Simpson JH, Goodman CS (2001) Switching repulsion to attraction: changing responses to slit during transition in mesoderm migration. *Science* 292:737-740.
- Krapivinsky G, Krapivinsky L, Wickman K, Clapham DE (1995) G beta gamma binds directly to the G protein-gated K⁺ channel, IKACH. *J Biol Chem* 270:29059-29062.
- Kruger RP, Aurandt J, Guan KL (2005) Semaphorins command cells to move. *Nature reviews Molecular cell biology* 6:789-800.
- Kuan CY, Tannahill D, Cook GM, Keynes RJ (2004) Somite polarity and segmental patterning of the peripheral nervous system. *Mech Dev* 121:1055-1068.
- Kulaga HM, Leitch CC, Eichers ER, Badano JL, Lesemann A, Hoskins BE, Lupski JR, Beales PL, Reed RR, Katsanis N (2004) Loss of BBS proteins causes anosmia in humans and defects in olfactory cilia structure and function in the mouse. *Nature genetics* 36:994-998.
- Kuratani SC, Kirby ML (1992) Migration and distribution of circumpharyngeal crest cells in the chick embryo. Formation of the circumpharyngeal ridge and E/C8⁺ crest cells in the vertebrate head region. *Anat Rec* 234:263-280.
- LaMora A, Voigt MM (2009) Cranial sensory ganglia neurons require intrinsic N-cadherin function for guidance of afferent fibers to their final targets. *Neuroscience* 159:1175-1184.
- Lance-Jones C, Landmesser L (1981a) Pathway selection by chick lumbosacral motoneurons during normal development. *Proc R Soc Lond B Biol Sci* 214:1-18.
- Lance-Jones C, Landmesser L (1981b) Pathway selection by embryonic chick motoneurons in an experimentally altered environment. *Proc R Soc Lond B Biol Sci* 214:19-52.
- Landmesser L, Honig MG (1986) Altered sensory projections in the chick hind limb following the early removal of motoneurons. *Developmental biology* 118:511-531.
- Le Douarin NM (2004) The avian embryo as a model to study the development of the neural crest: a long and still ongoing story. *Mech Dev* 121:1089-1102.

- Ledford AW, Brantley JG, Kemeny G, Foreman TL, Quaggin SE, Igarashi P, Oberhaus SM, Rodova M, Calvet JP, Vanden Heuvel GB (2002) Deregulated expression of the homeobox gene *Cux-1* in transgenic mice results in downregulation of p27(kip1) expression during nephrogenesis, glomerular abnormalities, and multiorgan hyperplasia. *Developmental biology* 245:157-171.
- Lee SK, Pfaff SL (2001) Transcriptional networks regulating neuronal identity in the developing spinal cord. *Nature neuroscience* 4 Suppl:1183-1191.
- Leung DW, Tompkins C, Brewer J, Ball A, Coon M, Morris V, Waggoner D, Singer JW (2004) Phospholipase C delta-4 overexpression upregulates ErbB1/2 expression, Erk signaling pathway, and proliferation in MCF-7 cells. *Molecular cancer* 3:15.
- Liang X, Song MR, Xu Z, Lanuza GM, Liu Y, Zhuang T, Chen Y, Pfaff SL, Evans SM, Sun Y (2011) *Isl1* is required for multiple aspects of motor neuron development. *Mol Cell Neurosci*.
- Liao WP, Uetzmann L, Burtscher I, Lickert H (2009) Generation of a mouse line expressing Sox17-driven Cre recombinase with specific activity in arteries. *Genesis* 47:476-483.
- Lieberam I, Agalliu D, Nagasawa T, Ericson J, Jessell TM (2005) A Cxcl12-CXCR4 chemokine signaling pathway defines the initial trajectory of mammalian motor axons. *Neuron* 47:667-679.
- Lin JH, Saito T, Anderson DJ, Lance-Jones C, Jessell TM, Arber S (1998) Functionally related motor neuron pool and muscle sensory afferent subtypes defined by coordinate ETS gene expression. *Cell* 95:393-407.
- Lin W, Sanchez HB, Deerinck T, Morris JK, Ellisman M, Lee KF (2000) Aberrant development of motor axons and neuromuscular synapses in *erbB2*-deficient mice. *Proceedings of the National Academy of Sciences of the United States of America* 97:1299-1304.
- Lindsay RM (1996) Role of neurotrophins and trk receptors in the development and maintenance of sensory neurons: an overview. *Philosophical transactions of the Royal Society of London Series B, Biological sciences* 351:365-373.
- Livet J, Sigrist M, Stroebel S, De Paola V, Price SR, Henderson CE, Jessell TM, Arber S (2002) ETS gene *Pea3* controls the central position and terminal arborization of specific motor neuron pools. *Neuron* 35:877-892.
- Lizarraga G, Ferrari D, Kalinowski M, Ohuchi H, Noji S, Kosher RA, Dealy CN (1999) FGFR2 signaling in normal and limbless chick limb buds. *Dev Genet* 25:331-338.
- Logothetis DE, Kurachi Y, Galper J, Neer EJ, Clapham DE (1987) The beta gamma subunits of GTP-binding proteins activate the muscarinic K⁺ channel in heart. *Nature* 325:321-326.
- Lu QR, Sun T, Zhu Z, Ma N, Garcia M, Stiles CD, Rowitch DH (2002) Common developmental requirement for Olig function indicates a motor neuron/oligodendrocyte connection. *Cell* 109:75-86.
- Luo L (2002) Actin cytoskeleton regulation in neuronal morphogenesis and structural plasticity. *Annu Rev Cell Dev Biol* 18:601-635.
- Luppi PH, Fort P, Jouviet M (1990) Iontophoretic application of unconjugated cholera toxin B subunit (CTb) combined with immunohistochemistry of neurochemical substances: a method for transmitter identification of retrogradely labeled neurons. *Brain research* 534:209-224.
- Luria V, Krawchuk D, Jessell TM, Laufer E, Kania A (2008) Specification of motor axon trajectory by ephrin-B:EphB signaling: symmetrical control of axonal patterning in the developing limb. *Neuron* 60:1039-1053.
- Mackenzie S, Walsh FS, Graham A (1998) Migration of hypoglossal myoblast precursors. *Developmental dynamics : an official publication of the American Association of Anatomists* 213:349-358.
- Manzanares M, Cordes S, Ariza-McNaughton L, Sadl V, Maruthainar K, Barsh G, Krumlauf R (1999) Conserved and distinct roles of *kreisler* in regulation of the paralogous *Hoxa3* and *Hoxb3* genes. *Development* 126:759-769.
- Manzanares M, Cordes S, Kwan CT, Sham MH, Barsh GS, Krumlauf R (1997) Segmental regulation of *Hoxb-3* by *kreisler*. *Nature* 387:191-195.

- Martinsen BJ, Neumann AN, Frasier AJ, Baker CV, Krull CE, Lohr JL (2006) PINCH-1 expression during early avian embryogenesis: implications for neural crest and heart development. *Developmental dynamics : an official publication of the American Association of Anatomists* 235:152-162.
- Masuda T, Yaginuma H, Sakuma C, Ono K (2009) Netrin-1 signaling for sensory axons: Involvement in sensory axonal development and regeneration. *Cell adhesion & migration* 3:171-173.
- Matsuoka T, Ahlberg PE, Kessar N, Iannarelli P, Dennehy U, Richardson WD, McMahon AP, Koentges G (2005) Neural crest origins of the neck and shoulder. *Nature* 436:347-355.
- McCabe KL, Bronner-Fraser M (2009) Molecular and tissue interactions governing induction of cranial ectodermal placodes. *Developmental biology* 332:189-195.
- Meulemans D, Bronner-Fraser M (2004) Gene-regulatory interactions in neural crest evolution and development. *Developmental cell* 7:291-299.
- Ming G, Song H, Berninger B, Inagaki N, Tessier-Lavigne M, Poo M (1999) Phospholipase C-gamma and phosphoinositide 3-kinase mediate cytoplasmic signaling in nerve growth cone guidance. *Neuron* 23:139-148.
- Mitchell KJ, Doyle JL, Serafini T, Kennedy TE, Tessier-Lavigne M, Goodman CS, Dickson BJ (1996) Genetic analysis of Netrin genes in *Drosophila*: Netrins guide CNS commissural axons and peripheral motor axons. *Neuron* 17:203-215.
- Moret F, Renaudot C, Bozon M, Castellani V (2007) Semaphorin and neuropilin co-expression in motoneurons sets axon sensitivity to environmental semaphorin sources during motor axon pathfinding. *Development* 134:4491-4501.
- Motose H, Tominaga R, Wada T, Sugiyama M, Watanabe Y (2008) A NIMA-related protein kinase suppresses ectopic outgrowth of epidermal cells through its kinase activity and the association with microtubules. *The Plant journal : for cell and molecular biology* 54:829-844.
- Moughal NA, Waters CM, Valentine WJ, Connell M, Richardson JC, Tigyi G, Pyne S, Pyne NJ (2006) Protean agonism of the lysophosphatidic acid receptor-1 with Ki16425 reduces nerve growth factor-induced neurite outgrowth in pheochromocytoma 12 cells. *J Neurochem* 98:1920-1929.
- Mueller BK, Yamashita T, Schaffar G, Mueller R (2006) The role of repulsive guidance molecules in the embryonic and adult vertebrate central nervous system. *Philosophical transactions of the Royal Society of London Series B, Biological sciences* 361:1513-1529.
- Muhr J, Graziano E, Wilson S, Jessell TM, Edlund T (1999) Convergent inductive signals specify midbrain, hindbrain, and spinal cord identity in gastrula stage chick embryos. *Neuron* 23:689-702.
- Myagmar BE, Umikawa M, Asato T, Taira K, Oshiro M, Hino A, Takei K, Uezato H, Kariya K (2005) PARG1, a protein-tyrosine phosphatase-associated RhoGAP, as a putative Rap2 effector. *Biochem Biophys Res Commun* 329:1046-1052.
- Narayanan CH, Malloy RB (1974) Deafferentation studies on motor activity in the chick. I. Activity pattern of hindlimbs. *J Exp Zool* 189:163-176.
- Nave KA (2010) Myelination and support of axonal integrity by glia. *Nature* 468:244-252.
- Niederreither K, McCaffery P, Drager UC, Chambon P, Dolle P (1997) Restricted expression and retinoic acid-induced downregulation of the retinaldehyde dehydrogenase type 2 (RALDH-2) gene during mouse development. *Mech Dev* 62:67-78.
- Niquille M, Garel S, Mann F, Hornung JP, Otsmane B, Chevalley S, Parras C, Guillemot F, Gaspar P, Yanagawa Y, Lebrand C (2009) Transient neuronal populations are required to guide callosal axons: a role for semaphorin 3C. *PLoS biology* 7:e1000230.
- Noden DM (1983) The embryonic origins of avian cephalic and cervical muscles and associated connective tissues. *Am J Anat* 168:257-276.
- Novitsch BG, Chen AI, Jessell TM (2001) Coordinate regulation of motor neuron subtype identity and pan-neuronal properties by the bHLH repressor Olig2. *Neuron* 31:773-789.

- Nusser N, Gosmanova E, Zheng Y, Tigyi G (2002) Nerve growth factor signals through TrkA, phosphatidylinositol 3-kinase, and Rac1 to inactivate RhoA during the initiation of neuronal differentiation of PC12 cells. *J Biol Chem* 277:35840-35846.
- O'Donnell M, Chance RK, Bashaw GJ (2009) Axon growth and guidance: receptor regulation and signal transduction. *Annual review of neuroscience* 32:383-412.
- Okae H, Iwakura Y (2010) Neural tube defects and impaired neural progenitor cell proliferation in Gbeta1-deficient mice. *Developmental dynamics : an official publication of the American Association of Anatomists* 239:1089-1101.
- Pabst O, Rummelies J, Winter B, Arnold HH (2003) Targeted disruption of the homeobox gene Nkx2.9 reveals a role in development of the spinal accessory nerve. *Development* 130:1193-1202.
- Palka J, Whitlock KE, Murray MA (1992) Guidepost cells. *Current opinion in neurobiology* 2:48-54.
- Palmesino E, Rousso DL, Kao TJ, Klar A, Laufer E, Uemura O, Okamoto H, Novitsch BG, Kania A (2010) Foxp1 and Ihx1 coordinate motor neuron migration with axon trajectory choice by gating Reelin signalling. *PLoS biology* 8:e1000446.
- Pan J, Wang Q, Snell WJ (2005) Cilium-generated signaling and cilia-related disorders. *Laboratory investigation; a journal of technical methods and pathology* 85:452-463.
- Parker JD, Bradley BA, Mooers AO, Quarmby LM (2007) Phylogenetic analysis of the Neks reveals early diversification of ciliary-cell cycle kinases. *PLoS one* 2:e1076.
- Pedersen LB, Veland IR, Schroder JM, Christensen ST (2008) Assembly of primary cilia. *Developmental dynamics : an official publication of the American Association of Anatomists* 237:1993-2006.
- Pfaff SL, Mendelsohn M, Stewart CL, Edlund T, Jessell TM (1996) Requirement for LIM homeobox gene *Isl1* in motor neuron generation reveals a motor neuron-dependent step in interneuron differentiation. *Cell* 84:309-320.
- Pietri T, Eder O, Blanche M, Thiery JP, Dufour S (2003) The human tissue plasminogen activator-Cre mouse: a new tool for targeting specifically neural crest cells and their derivatives in vivo. *Developmental biology* 259:176-187.
- Pittman AJ, Law MY, Chien CB (2008) Pathfinding in a large vertebrate axon tract: isotypic interactions guide retinotectal axons at multiple choice points. *Development* 135:2865-2871.
- Polci R, Peng A, Chen PL, Riley DJ, Chen Y (2004) NIMA-related protein kinase 1 is involved early in the ionizing radiation-induced DNA damage response. *Cancer Res* 64:8800-8803.
- Pradat PF, Dib M (2009) Biomarkers in amyotrophic lateral sclerosis: facts and future horizons. *Molecular diagnosis & therapy* 13:115-125.
- Price SR, De Marco Garcia NV, Ranscht B, Jessell TM (2002) Regulation of motor neuron pool sorting by differential expression of type II cadherins. *Cell* 109:205-216.
- Prince V, Lumsden A (1994) *Hoxa-2* expression in normal and transposed rhombomeres: independent regulation in the neural tube and neural crest. *Development* 120:911-923.
- Quintes S, Goebbels S, Saher G, Schwab MH, Nave KA (2010) Neuron-glia signaling and the protection of axon function by Schwann cells. *Journal of the peripheral nervous system : JPNS* 15:10-16.
- Rajan I, Denburg JL (1997) Mesodermal guidance of pioneer axon growth. *Developmental biology* 190:214-228.
- Raper JA, Bastiani MJ, Goodman CS (1983) Guidance of neuronal growth cones: selective fasciculation in the grasshopper embryo. *Cold Spring Harb Symp Quant Biol* 48 Pt 2:587-598.
- Reichardt LF, Tomaselli KJ (1991) Extracellular matrix molecules and their receptors: functions in neural development. *Annual review of neuroscience* 14:531-570.
- Revest JM, Spencer-Dene B, Kerr K, De Moerlooze L, Rosewell I, Dickson C (2001) Fibroblast growth factor receptor 2-IIIb acts upstream of Shh and Fgf4 and is required for limb bud maintenance but not for the induction of Fgf8, Fgf10, Msx1, or Bmp4. *Developmental biology* 231:47-62.
- Rhee SG, Bae YS (1997) Regulation of phosphoinositide-specific phospholipase C isozymes. *J Biol Chem* 272:15045-15048.

- Rickmann M, Fawcett JW, Keynes RJ (1985) The migration of neural crest cells and the growth of motor axons through the rostral half of the chick somite. *Journal of embryology and experimental morphology* 90:437-455.
- Rowitch DH, Lu QR, Kessler N, Richardson WD (2002) An 'oligarchy' rules neural development. *Trends in neurosciences* 25:417-422.
- Ruiz i Altaba A (1993) Induction and axial patterning of the neural plate: planar and vertical signals. *Journal of neurobiology* 24:1276-1304.
- Sander M, Paydar S, Ericson J, Briscoe J, Berber E, German M, Jessell TM, Rubenstein JL (2000) Ventral neural patterning by Nkx homeobox genes: Nkx6.1 controls somatic motor neuron and ventral interneuron fates. *Genes Dev* 14:2134-2139.
- Sato Y, Hirata T, Ogawa M, Fujisawa H (1998) Requirement for early-generated neurons recognized by monoclonal antibody lot1 in the formation of lateral olfactory tract. *The Journal of neuroscience : the official journal of the Society for Neuroscience* 18:7800-7810.
- Schwarz Q, Maden CH, Davidson K, Ruhrberg C (2009) Neuropilin-mediated neural crest cell guidance is essential to organise sensory neurons into segmented dorsal root ganglia. *Development* 136:1785-1789.
- Schwarz Q, Vieira JM, Howard B, Eickholt BJ, Ruhrberg C (2008a) Neuropilin 1 and 2 control cranial gangliogenesis and axon guidance through neural crest cells. *Development* 135:1605-1613.
- Schwarz Q, Waimey KE, Golding M, Takamatsu H, Kumanogoh A, Fujisawa H, Cheng HJ, Ruhrberg C (2008b) Plexin A3 and plexin A4 convey semaphorin signals during facial nerve development. *Developmental biology* 324:1-9.
- Serafini T, Colamarino SA, Leonardo ED, Wang H, Beddington R, Skarnes WC, Tessier-Lavigne M (1996) Netrin-1 is required for commissural axon guidance in the developing vertebrate nervous system. *Cell* 87:1001-1014.
- Sgambato V, Vanhoutte P, Pages C, Rogard M, Hipskind R, Besson MJ, Caboche J (1998) In vivo expression and regulation of Elk-1, a target of the extracellular-regulated kinase signaling pathway, in the adult rat brain. *The Journal of neuroscience : the official journal of the Society for Neuroscience* 18:214-226.
- Sharma K, Sheng HZ, Lettieri K, Li H, Karavanov A, Potter S, Westphal H, Pfaff SL (1998) LIM homeodomain factors Lhx3 and Lhx4 assign subtype identities for motor neurons. *Cell* 95:817-828.
- Shirasawa S, Yunker AM, Roth KA, Brown GA, Horning S, Korsmeyer SJ (1997) Enx (Hox11L1)-deficient mice develop myenteric neuronal hyperplasia and megacolon. *Nature medicine* 3:646-650.
- Signor D, Wedaman KP, Orozco JT, Dwyer ND, Bargmann CI, Rose LS, Scholey JM (1999) Role of a class DHC1b dynein in retrograde transport of IFT motors and IFT raft particles along cilia, but not dendrites, in chemosensory neurons of living *Caenorhabditis elegans*. *J Cell Biol* 147:519-530.
- Sikand P, Premkumar LS (2007) Potentiation of glutamatergic synaptic transmission by protein kinase C-mediated sensitization of TRPV1 at the first sensory synapse. *The Journal of physiology* 581:631-647.
- Simon MI, Strathmann MP, Gautam N (1991) Diversity of G proteins in signal transduction. *Science* 252:802-808.
- Smith JL, Schoenwolf GC (1997) Neurulation: coming to closure. *Trends in neurosciences* 20:510-517.
- Soriano P (1999) Generalized lacZ expression with the ROSA26 Cre reporter strain. *Nature genetics* 21:70-71.
- Srinivas S, Watanabe T, Lin CS, Williams CM, Tanabe Y, Jessell TM, Costantini F (2001) Cre reporter strains produced by targeted insertion of EYFP and ECFP into the ROSA26 locus. *BMC developmental biology* 1:4.

- Stepien AE, Tripodi M, Arber S (2010) Monosynaptic rabies virus reveals premotor network organization and synaptic specificity of cholinergic partition cells. *Neuron* 68:456-472.
- Sugimoto Y, Taniguchi M, Yagi T, Akagi Y, Nojyo Y, Tamamaki N (2001) Guidance of glial precursor cell migration by secreted cues in the developing optic nerve. *Development* 128:3321-3330.
- Sullivan G (1962) Anatomy and embryology of the Wing Musculature of the domestic fowl (*Gallus*). *Australian Journal of Zoology* 10:458-518.
- Summerton J (1999) Morpholino antisense oligomers: the case for an RNase H-independent structural type. *Biochimica et biophysica acta* 1489:141-158.
- Sun Y, Dykes IM, Liang X, Eng SR, Evans SM, Turner EE (2008) A central role for *Islet1* in sensory neuron development linking sensory and spinal gene regulatory programs. *Nature neuroscience* 11:1283-1293.
- Suter-Crazzolara C, Unsicker K (1996) GDNF mRNA levels are induced by FGF-2 in rat C6 glioblastoma cells. *Brain research Molecular brain research* 41:175-182.
- Tanaka K, Nigg EA (1999) Cloning and characterization of the murine *Nek3* protein kinase, a novel member of the NIMA family of putative cell cycle regulators. *J Biol Chem* 274:13491-13497.
- Tang J, Landmesser L, Rutishauser U (1992) Polysialic acid influences specific pathfinding by avian motoneurons. *Neuron* 8:1031-1044.
- Tang J, Rutishauser U, Landmesser L (1994) Polysialic acid regulates growth cone behavior during sorting of motor axons in the plexus region. *Neuron* 13:405-414.
- Taniguchi M, Yuasa S, Fujisawa H, Naruse I, Saga S, Mishina M, Yagi T (1997) Disruption of semaphorin III/D gene causes severe abnormality in peripheral nerve projection. *Neuron* 19:519-530.
- Terauchi A, Johnson-Venkatesh EM, Toth AB, Javed D, Sutton MA, Umemori H (2010) Distinct FGFs promote differentiation of excitatory and inhibitory synapses. *Nature* 465:783-787.
- Tessier-Lavigne M, Goodman CS (1996) The molecular biology of axon guidance. *Science* 274:1123-1133.
- Testa G, Schaft J, van der Hoeven F, Glaser S, Anastassiadis K, Zhang Y, Hermann T, Stremmel W, Stewart AF (2004) A reliable lacZ expression reporter cassette for multipurpose, knockout-first alleles. *Genesis* 38:151-158.
- Thaler JP, Lee SK, Jurata LW, Gill GN, Pfaff SL (2002) LIM factor *Lhx3* contributes to the specification of motor neuron and interneuron identity through cell-type-specific protein-protein interactions. *Cell* 110:237-249.
- Thisse B, Thisse C (2005) Functions and regulations of fibroblast growth factor signaling during embryonic development. *Developmental biology* 287:390-402.
- Tomioka N, Osumi N, Sato Y, Inoue T, Nakamura S, Fujisawa H, Hirata T (2000) Neocortical origin and tangential migration of guidepost neurons in the lateral olfactory tract. *The Journal of neuroscience : the official journal of the Society for Neuroscience* 20:5802-5812.
- Tosney KW, Landmesser LT (1985a) Development of the major pathways for neurite outgrowth in the chick hindlimb. *Developmental biology* 109:193-214.
- Tosney KW, Landmesser LT (1985b) Growth cone morphology and trajectory in the lumbosacral region of the chick embryo. *The Journal of neuroscience : the official journal of the Society for Neuroscience* 5:2345-2358.
- Vanden Heuvel GB, Quaggin SE, Igarashi P (1996) A unique variant of a homeobox gene related to *Drosophila cut* is expressed in mouse testis. *Biol Reprod* 55:731-739.
- Vanhoutte P, Barnier JV, Guibert B, Pages C, Besson MJ, Hipskind RA, Caboche J (1999) Glutamate induces phosphorylation of Elk-1 and CREB, along with c-fos activation, via an extracellular signal-regulated kinase-dependent pathway in brain slices. *Mol Cell Biol* 19:136-146.
- Vermeren M, Maro GS, Bron R, McGonnell IM, Charnay P, Topilko P, Cohen J (2003) Integrity of developing spinal motor columns is regulated by neural crest derivatives at motor exit points. *Neuron* 37:403-415.

- Vesterlund L, Tohonen V, Hovatta O, Kere J (2011) Co-localization of neural cell adhesion molecule and fibroblast growth factor receptor 2 in early embryo development. *The International journal of developmental biology* 55:313-319.
- von Bartheld CS, Fritsch B (2006) Comparative analysis of neurotrophin receptors and ligands in vertebrate neurons: tools for evolutionary stability or changes in neural circuits? *Brain, behavior and evolution* 68:157-172.
- Wang G, Scott SA (1999) Independent development of sensory and motor innervation patterns in embryonic chick hindlimbs. *Developmental biology* 208:324-336.
- Wang G, Scott SA (2000) The "waiting period" of sensory and motor axons in early chick hindlimb: its role in axon pathfinding and neuronal maturation. *The Journal of neuroscience : the official journal of the Society for Neuroscience* 20:5358-5366.
- Wang KH, Brose K, Arnott D, Kidd T, Goodman CS, Henzel W, Tessier-Lavigne M (1999) Biochemical purification of a mammalian slit protein as a positive regulator of sensory axon elongation and branching. *Cell* 96:771-784.
- Wang L, Klein R, Zheng B, Marquardt T (2011) Anatomical coupling of sensory and motor nerve trajectory via axon tracking. *Neuron* 71:263-277.
- Wang Y, Xiao R, Yang F, Karim BO, Iacovelli AJ, Cai J, Lerner CP, Richtsmeier JT, Leszl JM, Hill CA, Yu K, Ornitz DM, Elisseff J, Huso DL, Jabs EW (2005) Abnormalities in cartilage and bone development in the Apert syndrome FGFR2(+S252W) mouse. *Development* 132:3537-3548.
- Wasylyk C, Zheng H, Castell C, Debussche L, Multon MC, Wasylyk B (2008) Inhibition of the Ras-Net (Elk-3) pathway by a novel pyrazole that affects microtubules. *Cancer Res* 68:1275-1283.
- White FA, Behar O (2000) The development and subsequent elimination of aberrant peripheral axon projections in Semaphorin3A null mutant mice. *Developmental biology* 225:79-86.
- White MC, Quarmby LM (2008) The NIMA-family kinase, Nek1 affects the stability of centrosomes and ciliogenesis. *BMC Cell Biol* 9:29.
- Wichterle H, Lieberam I, Porter JA, Jessell TM (2002) Directed differentiation of embryonic stem cells into motor neurons. *Cell* 110:385-397.
- Williams ME, Lu X, McKenna WL, Washington R, Boyette A, Strickland P, Dillon A, Kaprielian Z, Tessier-Lavigne M, Hinck L (2006) UNC5A promotes neuronal apoptosis during spinal cord development independent of netrin-1. *Nature neuroscience* 9:996-998.
- Wilson L, Maden M (2005) The mechanisms of dorsoventral patterning in the vertebrate neural tube. *Developmental biology* 282:1-13.
- Winckler B, Forscher P, Mellman I (1999) A diffusion barrier maintains distribution of membrane proteins in polarized neurons. *Nature* 397:698-701.
- Wright DE, White FA, Gerfen RW, Silos-Santiago I, Snider WD (1995) The guidance molecule semaphorin III is expressed in regions of spinal cord and periphery avoided by growing sensory axons. *The Journal of comparative neurology* 361:321-333.
- Xu K, Sacharidou A, Fu S, Chong DC, Skaug B, Chen ZJ, Davis GE, Cleaver O (2011) Blood vessel tubulogenesis requires Rasip1 regulation of GTPase signaling. *Developmental cell* 20:526-539.
- Xu X, Weinstein M, Li C, Naski M, Cohen RI, Ornitz DM, Leder P, Deng C (1998) Fibroblast growth factor receptor 2 (FGFR2)-mediated reciprocal regulation loop between FGF8 and FGF10 is essential for limb induction. *Development* 125:753-765.
- Yamashita T, Tucker KL, Barde YA (1999) Neurotrophin binding to the p75 receptor modulates Rho activity and axonal outgrowth. *Neuron* 24:585-593.
- Yazdani U, Terman JR (2006) The semaphorins. *Genome biology* 7:211.

ACKNOWLEDGEMENTS

Finally, I want to thank all the people who contributed in so many different ways to the realization of this work and who made my time at the Institute of Developmental Genetics unique and unforgettable. In particular I want to mention:

***Prof. Dr. Wolfgang Wurst**, who gave me the opportunity to work in his Institute, for his direct and indirect support and interest in my work;*

***Dr. Andrea Huber Brösamle**, for giving me the possibility to work on the fascinating topic of sensory-motor circuit formation, for encouraging me and constantly contributing to my understanding of developmental neurobiology. I want to thank Andrea for being a source of impulses, advice and support with so many great ideas, not only as a supervisor and member of my Thesis committee, but also for our daily life in the lab. I hope our future work together will reveal many other thrilling results.*

***Prof. Dr. Harald Luksch (WZW, Zoology)** and **Prof. Dr. Chichung Lie (FAU, Erlangen)**, members of my Thesis committee, for scientific suggestions, discussions and questions that contributed to accomplish my doctoral work.*

***Prof. Dr. Alex L. Kolodkin**, **Prof. Dr. Thomas M. Jessell**, **Prof. Dr. Lou F. Reichardt**, **Prof. Dr. Magdalena Götz**, **r. Bennet G. Novitch** and **Dr. Ralf Kühn** for providing research material.*

***Prof. Dr. Laure Bally-Cuif (CNRS)**, **Prof. Dr. Jochen Graw**, and **Prof. Dr. Reinhard Köster (TU Braunschweig)** for providing research material, making available laboratory equipment and supporting me with excellent discussions.*

***ENINET - Network of European Neuroscience Institutes** and the **TUM Graduate School** for providing me with the resources to attend international conferences.*

***Frau Fieder**, **Clarinda**, **Manuela**, **Monika** and **Regina**, for their technical assistance and care in the animal facilities.*

*Our secretaries, **Elisabeth, Karin and Angie**, for taking care of all of us, helping with many bureaucratic tasks or when the printer won't work (... again...).*

*All current and former members of the "AHB group": **Georg, Corinna, Heidi, Micha, Elisa, Jana, Daniela, Ruth, Janice, Julia, Nikola, Stefan, Laura, Teresa, Tobi, Anna, Anja, Karina, Sandra, José** (and sorry if I forgot someone...), for your help whenever I needed a helping hand, but also for making work enjoyable and fun by just being there. Many and sincere THANKS!*

*And last but not least... my **friends**, my **parents** and my **family**, for helping and supporting me, for distracting me whenever necessary; **Korbinian**, just for being as sweet as you are, and giving me the first nickname I actually like; and **Lars** – you are the best purring hot-water bottle ever.*

Dipl. Biol., Rosa-Eva Hüttl

Adresse: Innerthann 2
83104 Tuntenhausen
Geburtsdatum/ -ort: 30.10.1982 in Rosenheim
Nationalität: deutsch
E-Mail: REHuettl@web.de
rosa-eva.huettl@helmholtz-muenchen.de

Ab 01/2012 **Dr. Andrea Huber Brösamle**
Postdoc-Position

Seit 07/2008 **Doktorarbeit: Prof. Dr. Wolfgang Wurst/ Dr. Andrea Huber Brösamle**
Institut für Entwicklungsgenetik,
Helmholtz Zentrum München, Neuherberg
Thema: „Untersuchung molekularer Mechanismen, die zur Bildung sensorisch-motorischer Netzwerke beitragen.“

Schul- und Hochschulausbildung

11/2007 – 06/2008 **Diplomarbeit: Dr. Andrea Huber Brösamle**
Institut für Entwicklungsgenetik
Helmholtz Zentrum München, Neuherberg
Thema: „Wie man das Nervensystem verkabelt – Die Rolle von Neuropilin-1 während der Bildung peripherer Netzwerke und die genomweite Suche nach neuen Wegfindungsmolekülen“

03/2005 – 06/2008 **Hauptstudium der Biologie an der Technischen Universität München**
Schwerpunkt: Genetik, Humangenetik, Immunologie
Abschluss: Diplom (1,2)

10/2003 – 03/2005 **Grundstudium der Biologie an der Technischen Universität München**
Abschluss: Vordiplom

09/1993 – 06/2002 **Gymnasium Bad Aibling**
Abschluss: Allgemeine Hochschulreife/ Abitur (1,9)

Veröffentlichungen:

Publikationen:

Huettl, R.E., Soellner, H., Bianchi, E., Novitch, B.G., Huber, A.B., **2011**. Npn-1 contributes to axon-axon interactions that differentially control sensory and motor innervation of the limb. PLoS biology 9, e1001020.

Huettl, R.E., Huber, A.B., **2011**. Cranial nerve fasciculation and Schwann cell migration are impaired after loss of Npn-1. Developmental biology.

Artikel:

Rosa-Eva Hüttl und Andrea Huber Brösamle: Durch Kommunikation ans Ziel – Nervenfaserverbindungen während der Embryonalentwicklung. Deutsche Zeitschrift für Klinische Forschung (Erscheinungstermin 18.01.2012).

Konferenzbeiträge:

Neuroscience 2010 SfN 40th Annual Meeting in San Diego, USA; 13.-17. November 2010
R.E.Huettl, H. Soellner, E. Bianchi, B.G. Novitch, A.B. Huber: "Npn-1 mediated axon-axon interactions differentially control sensory and motor innervation of the limb". (Poster)

Munich interact 2010, 23.März 2010

R.E.Huettl, H. Soellner, E. Bianchi, T.M. JESSELL, B.G. Novitch, A.B. Huber: "Npn-1 mediated axon-axon interactions differentially control sensory and motor innervation of the limb". (Poster)

Final 2009 ENINET Meeting in Crete, 19.-23. Mai 2009

R.E.Huettl, H. Soellner, E. Bianchi, T.M. JESSELL, B.G. Novitch, A.B. Huber: "Who is leading whom? – The role of Neuropilin-1 in the development of the sensory-motor circuit". (Poster)

Munich interact 2009, 2. April 2009

R.E.Huettl, H. Soellner, E. Bianchi, T.M. JESSELL, B.G. Novitch, A.B. Huber: "Who is leading whom? – The role of Neuropilin-1 in the development of the sensory-motor circuit". (Poster)

ENINET 2008 Minisymposium, 19. -20. Oktober 2008

R.E.Huettl, H. Soellner, E. Bianchi, T.M. JESSELL, B.G. Novitch, A.B. Huber: "Who is leading whom? – The role of Neuropilin-1 in the development of the sensory-motor circuit". (Poster)

